

Control of Cell Fate using Self-Organized Honeycomb-Patterned Films

Masaru Tanaka¹, Sadaaki Yamamoto² & Masatsugu Shimomura¹

¹ *Institute of Multidisciplinary Research for Advanced Materials (IMRAM),
Tohoku University, Sendai, Japan*

² *Creative Research Initiative "Sousei", Hokkaido University, Sapporo, Japan*

INTRODUCTION: The design of nano- and microstructures based on self-organization is a key area of research in the search for new biomaterials and biodevices, and such structures have a variety of potential applications in tissue engineering scaffolds and medical implants. 3D scaffolds of appropriate pore size and porosities and with interconnected pores are required to facilitate cell adhesion, proliferation, differentiation, and eventual tissue regeneration in a natural manner. We have reported a honeycomb-patterned polymer film (honeycomb film) with regular pores that is formed by self-organization. The honeycomb films exerted a strong influence on cell morphology, proliferation, cytoskeleton, focal adhesion, and ECM production profiles [1-4]. In neural tissue engineering, preparation of neural stem / progenitor cells (NSCs) is required for a potential therapy for diseases of the nervous systems. Neural stem / progenitor cells (NSCs) are self-renewing, immature, undifferentiated, and multipotent. This research studied the influence of the pore size of the honeycomb films on the proliferation and differentiation of NSCs.

METHODS: The honeycomb film from poly(ϵ -caprolactone) (PCL) was prepared on a glass substrate by employing a previously described method. The flat film was prepared by a spin coater in dry condition. NSCs were derived from the cerebral cortex of embryonic 14 day mice. The NSCs were seeded on the films at a density of 2×10^4 cells/cm². NSCs were cultured in serum medium (Opti-MEM, 10 % Fetal Bovine Serum, 55 μ M 2-mercaptoethanol) for 24 hr. After that, NSCs were cultured in serum-free medium. The morphologies of neurons were examined by a scanning electron microscope (SEM) and a confocal laser scanning microscope. NSCs were immunostained for Nestin and BrdU. Cell number was estimated by measuring of DNA concentration from the extracted samples

RESULTS & DISCUSSION: NSCs differentiated into neurons in round shape and their neurites extended randomly on the flat film. The morphology of cells on the honeycomb films was dependent on the pore size (Fig. 1). On the film with a pore size of 1.5 μ m, the cell bodies showed flat shape. Their neurites extended randomly and jumped over the pore of the film. On the film with a pore size of 10 μ m, the cell bodies with round morphology adhered on the rims of the films. Their neurites extended

along the rims forming simple network. The honeycomb film acted as a positive cue to support neurite extension. The morphology similar to that on the films with pore size of 10 μ m was also observed on the films with pore size of 5 and 8 μ m. Interestingly, on the honeycomb film of with pore size of 3 μ m, several large spheroids were observed. The neurites gathered to form large bundles which radiated out from the periphery of the spheroids. NSCs formed spheroids in the diameter of 30-90 μ m. This phenomenon was specific for NSCs on the honeycomb film with pore size of 3 μ m and was not associated with NSCs cells on neither the honeycomb films (pore size of 1.5, 5, 8, and 10 μ m), nor the flat film. The immunostaining for Nestin and BrdU labeling identified the spheroids as aggregates of self-renewed NSCs. The diameter of spheroids was increased with culture time. These results implied that the honeycomb films with the subcellular sized pore promoted NSC proliferation, while preventing their differentiation. We found that the number of total neural cells was increased after 3 days due to maintain of undifferentiation and proliferation of NSCs. Our studies demonstrated that the NSCs morphology, proliferation, and differentiation are controlled by the pore size of the honeycomb film. It is expected that the honeycomb films will have great potentials as biomaterials for neural tissue regeneration in a growth factor free proliferation process of neural stem cells.

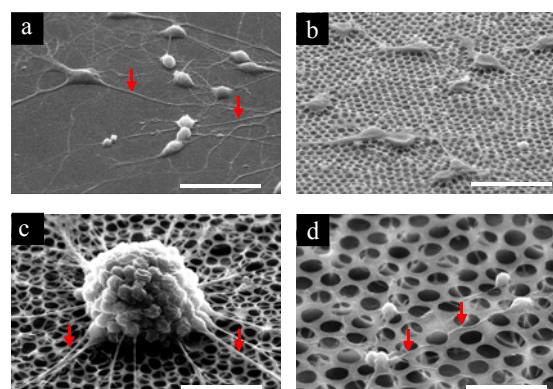


Fig. 1: SEM images of cell morphologies derived from embryonic 14 day mice cerebral cortex after culturing for 5 days on the Flat film (a), Honeycomb film with pore size of 1.5 μ m (b), 3 μ m (c), and 10 μ m (d). Bar; 30 μ m

REFERENCES: ¹ M. Tanaka et al (2007) *J. Nanosci. Nanotech*, 7, 763-772. ² M. Tanaka et al (2008) *Colloids Surf A*, 313-314, 515-519. ³ S. Yamamoto et al (2007) *Langmuir*, 23, 8114-8120. ⁴ J. R. Mcmillan et al (2007) *Tissue Engineering*, 13, 789-798.

Flux, Floods & Tiny Pores: The Problems with Nutrient-Perfused Cells

[Joshua O. Eniwumide](#), Ansgar Petersen, and Georg N Duda

Julius Wolff institute and Centre for Musculoskeletal Surgery, Berlin-Brandenburg Centre for Regenerative Therapy, Charité, 13353 Berlin, Germany

INTRODUCTION: Diffusion of oxygen and nutrients to the centre of tissue-engineered constructs does not maintain cell viability and proliferation indefinitely. GAG and mineralised matrix produced by chondrocytes and osteoblasts curtailed approximately 400 μ m and 240 μ m from the surface of the 3D constructs [1]. Yet, despite improving nutrient supply, perfusion bioreactors are still associated with cellular viability issues within tissue-engineered constructs [2]

Using a range of perfusion strategies, and monitoring their associated pressures and strains, the present study aims to produce a tissue-engineered construct, homogenous in cellular viability and functions.

METHODS: Articular chondrocytes harvested from skeletally mature merino mixed ewes were cultured in 4% (w/v) agarose at 20×10^6 cells per ml in DMEM+10% FCS for up to 12 days. The cells were either cultured in free-swelling conditions, or perfused at different flow rates using a bioreactor. Biochemical assays and histological staining were performed to measure cell proliferation and matrix synthesis

RESULTS: The cells produced sufficient matrix proteins, forming colonies with neighbouring cells by day 12. The extent and sizes of these colonies were greatly reduced at the centre-most region of the free-swelling cultures (fig 1), while the perfused cultures contained such colonies throughout, or at least without a notable difference at their central cores, irrespective of flow rates. Molecular transport into the 3D constructs was improved with perfusion. Over a prolonged period, an enhanced proliferation and matrix accumulation ensued at the central core. Despite this, solute concentration was not homogeneous within the constructs, thus a gap still existed between the core and peripheral margins (fig 2).

Cellular functions at the constructs centre increased with perfusion flow rate. However, compaction, and often breakages were observed at the edges. The pressures associated with perfusion flow were typically below 1kPa, for flow rates of up to 0.64 mm⁷hr. At 1.27 mm/hr the pressure rose to 10kPa. This was often accompanied by construct damage.

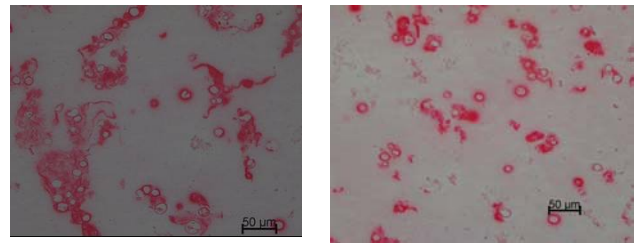


Fig. 1: Representative micrograph, showing production and accumulation of type II collagen by the articular chondrocytes at the periphery (left) and center (right) of cylindrical agarose constructs

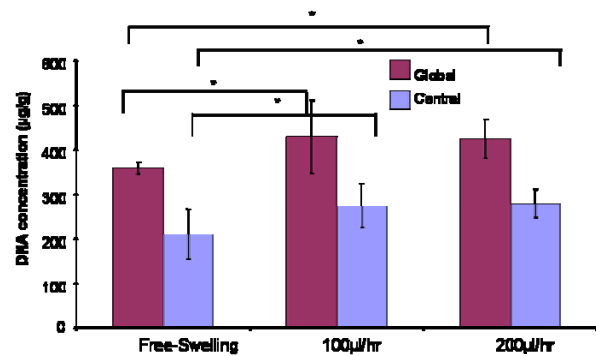


Fig. 2: DNA concentrations after 12 days culture in either free-swelling or with media perfusion. Measurements were made at the constructs centres and globally, at all other regions.

DISCUSSION & CONCLUSIONS: The observed pressures and those of other flow rates are being applied hydrostatically to the cell-seeded constructs, using the bioreactor. In doing so, the direct contribution of pressure in media perfusion will be better understood.

REFERENCES: [1] I. Martin, D. Wendt and M. Heberer, The role of bioreactors in tissue engineering, *Trends in biotechnology*, **22** (2004), 80-86.

[2] T. Davisson, R.L. Sah and A. Ratcliffe, Perfusion increases cell content and matrix synthesis in chondrocyte three-dimensional cultures, *Tissue engineering*, **8** (2002), 807-816.

ACKNOWLEDGEMENTS: This work is funded by the Marie Curie Intra European Fellowship programme, for which, JE is very thankful.

Elucidating the mechanisms of cellular uptake of rod shaped semiconductor nanocrystals: a tunable interaction

C Tortiglione¹, M Malvindi^{1,2}, A Quarta², A Tino¹, T Pellegrino²

¹ Istituto di Cibernetica "E. Caianiello" CNR, Pozzuoli, Italy ² National Nanotechnology Laboratory of CNR-INFM, Unità di ricerca IIT and Scuola Superiore ISUFI, Lecce, Italy

INTRODUCTION: The successful use in biology and medicine of functional nanoparticles and nanodevices based on innovative biomaterials, (gold, cadmium telluride, cadmium selenide, iron oxide) with unique chemico-physical properties, has recently raised new issues on the interactions of such novel materials with cell membranes. Presentation of chemical information at the same size scale as that of cell surface receptor may potentially interfere with cellular processes, eliciting undesired responses[1], such as cell uptake, sequestration in endosomal/lysosomal compartments, or activation of signalling cascade pathways. Here we show that the cell uptake of fluorescent CdSe/CdS quantum rods (QRs) by *Hydra vulgaris*, a simple model organism at the base of metazoan evolution, can be tuned by modifying nanoparticle surface charge by means of pH. Moreover, by a functional assay, we identified the molecular factors underlying this interaction

METHODS: CdSe/CdS nanorods were prepared by seeded growth approach as recently reported [1, 2]. *Hydra vulgaris* were asexually cultured in physiological solution (SolHy: 1mM CaCl₂, 0.1mM NaHCO₃, pH=7 or pH 4) and in vivo experiment performed as reported [1].

RESULTS: In our previous works, challenging living *Hydra vulgaris* at neutral pH with CdSe/CdS QRs, did not result in nanocrystal internalization into Hydra. Here, living animals were challenged with different QRs at both acidic and neutral pH and the internalization was monitored at various times post-incubation. Results showed that QR cellular uptake occurred only at acidic pH, in a calcium independent way and only for QR showing positive surface charge (figure 1). Among four different QR type analysed, only those showing positive zeta potential values, at pH4, were internalized, while those presenting negative values did not. In an attempt to identify the molecular targets underlying QR internalization at acidic pH, we tested the involvement of annexin B12 (ANX), a hydra protein belonging to the annexins superfamily which pH dependent behaviour could possibly account for nanoparticle uptake. As Hydra treatment with anti-ANX antibody prevents QR uptake, we show the involvement of ANX in the QR uptake at acidic

pH, and provide a first functional role for Hydra ANX in vivo.

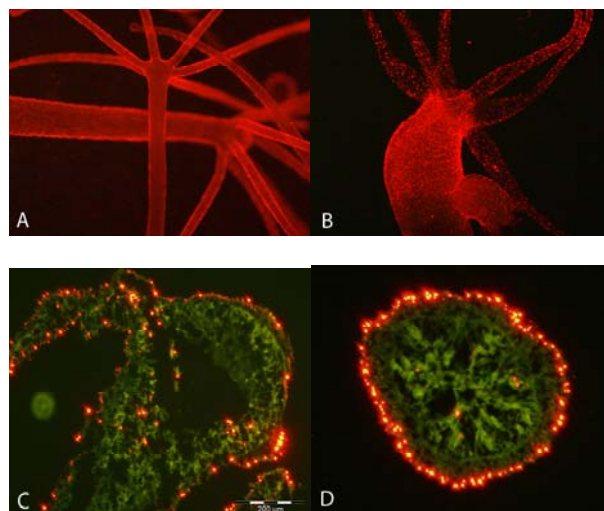


Fig 1: In vivo fluorescence imaging of *Hydra vulgaris* exposed to QRs for different times A) 30 minutes p.i. QR red fluorescence labels uniformly all body regions B) 2 hr post incubation fluorescence staining is compacted into granular structures C) longitudinal and D) cross sections of fixed specimens 24 hr p.i.: QRs are located on both epithelial layers

DISCUSSION & CONCLUSIONS:

We were able to selectively control specific interactions between cell membrane and nanoparticles: the combined effect of pH dependent factors (QR positive charge and ANX membrane insertion) resulted in the active internalization of QRs in specific cell types and according to a precise temporal dynamic. As the uptake of nutrients and all communication among cells and between cells and their environment occurs through the plasma membrane, we provide new clues to understand the processes evoked at this interface by nanoscale objects which is a priority when designing nanodevices for biomedical purposes.

¹ M. Malvindi, L. Carbone, A. Quarta et al., Small, 2008, 4(10): p. 1747-55.

² L. Carbone, C. Nobile, M. De Giorgi, et al., Nano Lett, 2007, 7(10): p. 2942-50.

Nanotopography as a Tool for Controlling Skeletal Stem Cell Differentiation

RJ McMurray¹, N Gadegaard², ROC Oreffo³ & MJ Dalby¹

¹ Centre for Cell Engineering, Faculty of Biomedical and Life Sciences, Joseph Black Building, University of Glasgow, Glasgow, G12 8QQ, UK ² Centre for Cell Engineering, Department of Electronic and Electrical Engineering, Rankine building, University of Glasgow, Glasgow, G12 8QQ, UK ³ Bone and Joint Research Group, University of Southampton, Southampton, SO16 6YD, UK

INTRODUCTION: Topography has previously been well documented to affect a number of cellular responses including cell adhesion, apoptosis and more recently, differentiation. It is the ability to control the differentiation of stem cells using specific topographical cues, in the absence of defined media which holds particularly exciting potential within the field of regenerative medicine. In the present study, bone mineral formation *in vitro* was examined at successive time points following skeletal stem cell culture on substrates with controlled disordered nanopits to produce the first temporal profile of skeletal stem cell differentiation when cultured on nanopit substrates.¹

METHODS: Stro-1 enriched skeletal stem cells were maintained in basal medium (10% FCS/ α MEM, Life Technologies, UK) at 37°C with 5% CO₂ in humid conditions. To detect either stem cell retention or osteoprogession towards committed bone cells immunofluorescence detection of two stem cell markers, Stro-1 and ALCAM along with two bone cell markers, osteopontin and osteocalcin were used. Nickel shims were used to emboss the disordered nanopits (100 nm depth, 120 nm diameter, 300 nm pitch, with a disorder of ± 50 nm from centre) into PMMA. The nanopit substrate was compared to skeletal stem cells cultured on control planar PMMA substrates and control planar PMMA substrates treated with dexamethasone and ascorbic acid to induce osteogenic differentiation. No additional supplements were added to the media of the cells cultured on the test topography.

RESULTS: The focus of this study was to observe the temporal differentiation of skeletal populations on 100 nm depth, 120 nm diameter, 300 nm pitch, with a disorder of ± 50 nm from centre nanopits, a novel topography. Our results show that skeletal stem cells cultured on the NSQ50 nanotopography underwent osteogenic differentiation and displayed a normal growth profile over time, in contrast to cells cultured on control topographies with osteogenic medium.

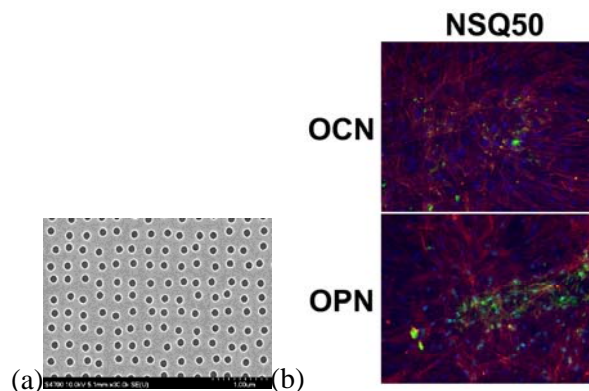


Fig 1. (a) SEM image of NSQ50 topography, (b) OCN and OPN immunofluorescent staining of skeletal stem cells after 28 days of culture on NSQ50 nanopit substrate in the absence of osteogenic media. Red=actin, Blue=nucleus, Green=OCN/OPN.

DISCUSSION & CONCLUSIONS: The NSQ50 nanopit topography has previously been shown to produce bone mineral formation *in vitro* comparable to that of cells treated with osteogenic media.² The results presented here provide evidence that nanotopography alone may offer a valuable new approach for stimulating the osteogenic differentiation of skeletal stem cells over that of defined media.

REFERENCES:

- McMurray R.J., Gadegaard N., Oreffo R.O.C., Dalby M.J. A Temporal Study of Skeletal Stem Cell Differentiation following Culture on Substrates Patterned With a Novel Nanopattern Containing Controlled Disorder. (2009) *Submitted*.
- Dalby M.J., Gadegaard N., Tare R., Andar A., Riehle M.O., Herzyk P., Wilkinson C.D.W., Oreffo R.O.C. The Control of Mesenchymal Stem Cell Differentiation Using Nanoscale Symmetry and Disorder. (2007) *Nature Mat.*

ACKNOWLEDGEMENTS: RJM is funded by a Lord Kelvin/Adam Smith Scholarship. MJD, ROCO and NG are funded by the BBSRC, EPSRC and EU. We also thank Dr Rahul Tare for providing the skeletal stem cells.

MICROFLUIDIC DEVICE TO TEST NANOPARTICLE TOXICITY

Abhay Andar¹, Sher Ahmed¹, Nikolaj Gadegaard¹, Melanie Favre², Philippe Neiderman², Martha Liley² and Mathis O. Riehle¹

1. Centre for Cell Engineering, Institute of Biomedical and Life Sciences, University of Glasgow 2. CSEM, Centre Suisse d'Electronique et de Microtechnique SA, Neuchâtel, Switzerland

INTRODUCTION: Recent years have seen a growth in the manufacturing of nanoparticles in industry which has given rise to concerns regarding their impact on public health and the environment. One route of entry into the human body is through the lung epithelium. This paper reports the development of a microfluidic device to test the toxicity of nanoparticles on Calu-3 (Cancer lung epithelia) cells. These cells form tight monolayers, which can be assessed measuring TEER (Trans Epithelial Electrical Resistance). TEER is a very routine method to analyze the integrity and restrictiveness of the cell monolayer.^[1-3] Our aim was to create an integrated multiplexed microfluidic device allowing the analysis and monitoring of Calu-3 function and nanoparticle translocation. Another motivation was to reduce the need for in-vivo test models.

METHODS: Our device is a multilayered microfluidic setup. The transverse section of the device (figure 1) shows 1) the top layer micro channel, (concentration gradient generator) fabricated in poly-di-methyl siloxane using photolithography and polymer casting 2) the middle is a silicon wafer with a 500nm thick microporous (2µm, 5% area fill, hex symmetry) silicon nitride layer, and 3) the bottom layer micro channel. The electrodes are used to measure TEER. The silicon wells were fabricated using photolithography and wet etch, the pores in the membrane by photolithography followed by dry etch.

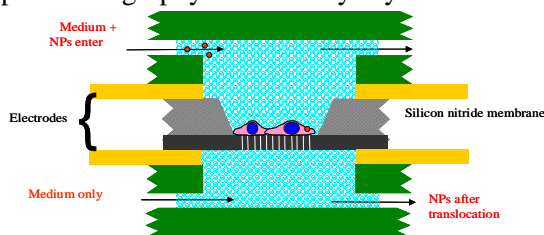


Figure 1: Shows a schematic of a working device.

RESULTS: Calu-3 cells were seeded onto the porous silicon nitride membranes and observed for 3 days inside the device. The Christmas-tree type concentration gradient generator^[4] provides the 5

wells with a range of different solute concentrations on the top, whereas the bottom is sub fused by “clean” media. Individual well devices allowed TEER measurements on Calu-3 monolayers. After optimisation of the growth condition Calu-3 proliferated on the nitride membranes and after 7-8 days inside the device they are seen to form a confluent monolayers.

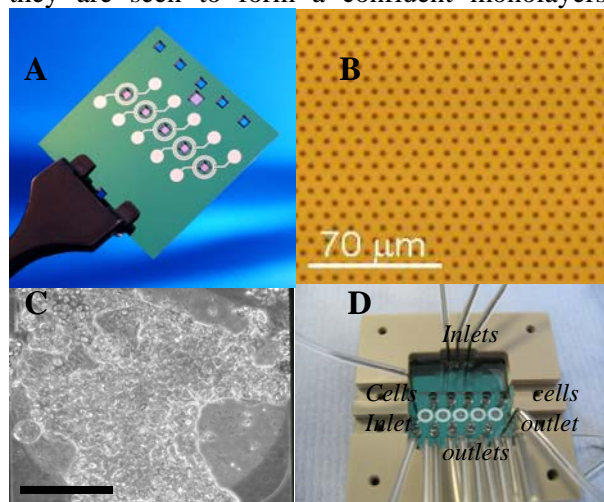


Figure 2 A) Silicon chip showing the concentric electrodes and the 5 silicon nitride membrane. B) Silicon nitride membrane C) Calu-3 cell layer observed after day 3 in the device. (scale 500µm) D) Final fully automated diagnostic device.

DISCUSSION & CONCLUSIONS: This device is in the final stages of optimisation. The cell monolayers have shown to produce competent and tight monolayers under static (no-fluid-flow) conditions and flow conditions. The advantage of such a device is that we are able to perform five experiments in parallel with different solute concentrations. The next step will be to analyse known harmful nanoparticles.

REFERENCES: ¹ K. Donaldson, V. Stone et al (2004) *Occupational and Environmental Medicine*, **61**: 727 ² A. Nemmar, P. H. Hoet, et al. (2002a) *Circulation*, **105**: 411. ³ Bogdan I. Florea, Maria L. Cassara (2003) *Journal of Controlled Release*, **87**: 131. ⁴ N. L. Jeon, Dertinger et al, (2000) *Langmuir*, **16**, 8311-8316

ACKNOWLEDGEMENTS: Nanosafe2 project (contract no. NMP2-CT-2005-515843)

ANALYTE RESPONSIVE PLGA NANOFIBRE SCAFFOLDS

H.Chesters, FRAJ Rose, Y Reinwald L. Buttery, J.Aylott

School of Pharmacy, University of Nottingham, UK.

INTRODUCTION: An electrospun poly(lactico-glycolic acid) (PLGA) nanofibre scaffold incorporating analyte responsive, optical nanosensors has been prepared for tissue engineering applications. The electrospun nanofibrous structure is formed in a high-voltage electrostatic field. The resulting non-woven, porous, biocompatible structure has morphological similarities to the extracellular matrix of natural tissue and is capable of supporting cell attachment and proliferation. The optical nanosensors incorporated into the scaffold can be utilised to assess the transport of analytes through the matrix and can aid in the preparation of more effective scaffolds. In addition nanosensors can be delivered to cells growing upon the scaffold, where they can be utilised to monitor intracellular analyte concentrations.

METHODS: Nanosensors are incorporated into the scaffold at the time of electrospinning. The nanosensors consist of a biocompatible sol-gel matrix to which two fluorophores, an analyte responsive fluorophore and a reference fluorophore are incorporated, enabling a ratiometric response. Fluorophores used for pH measurements include 5'-carboxyfluorescein (FAM) and 5-carboxytetramethylrhodamine (TAMRA) that are pH responsive and non-pH responsive respectively. Oxygen measurements have been performed using a ruthenium complex ($\text{Ru}(\text{phen})_3$) as the oxygen responsive component and Oregon Green Dextran as the reference dye.¹ A commercially available liposomal transfection agent was utilized to deliver the nanosensors to 3T3 fibroblasts cultured upon the scaffold. Real-time observation of nanosensors located in 3T3s was carried out using Confocal Laser Scanning Microscopy (CLSM).

RESULTS: Confocal and Scanning Electron Microscopy show that the nanosensors have been immobilised in the PLGA scaffold (Fig.1). and that nanosensors have been delivered to 3T3s cultured upon PLGA scaffolds (Fig.2). The nanosensors remain optically active and responsive to changes in pH and oxygen enabling real-time measurements of the analyte of interest (Fig. 3).

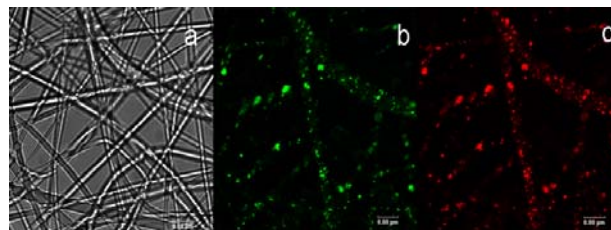


Fig.1: Confocal images of nanosensors incorporated into PLGA scaffold (a)transmission (b)FAM (c)TAMRA

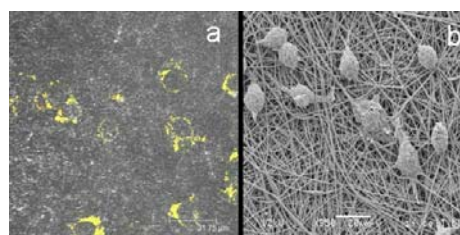


Fig.2: Microscopy images of 3T3s transfected with nanosensors cultured upon PLGA scaffold. (a)colocalisation of Oregon green and ($\text{Ru}(\text{phen})_3$) (b)SEM

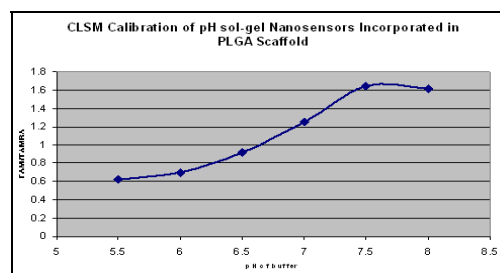


Fig.3: Calibration of pH Nanosensors incorporated in PLGA scaffold

DISCUSSION & CONCLUSIONS: The analyte responsive scaffold has applications for tissue engineering as it can be utilised to evaluate cellular response to the local environment during the development of 3-dimensional tissue constructs.

REFERENCES: ¹ H. Xu, J. W. Aylott, R. Kopelman, T. J. Miller and M. A. Philbert, *Analytical Chemistry*, 2001, **73**, 4124-4133.

ACKNOWLEDGEMENTS: The author would like to acknowledge the BBSRC for financial support.

Astrocyte alignment in 3D collagen gels increases neurite outgrowth; implications for improving spinal cord repair

E. East, D. Blum de Oliveira, J. P. Golding and J. B. Phillips.

The Open University, Department of Life Sciences, Walton Hall, Milton Keynes, MK7 6AA.

INTRODUCTION: A major impediment to tissue engineered repair of CNS damage is the glial scar that forms around implanted graft devices and creates an inhibitory environment for axon growth out of the repair site¹. The glial scar is composed of a 3-dimensional (3D) meshwork of astrocytes which become reactive in response to damage stimuli. Previous studies have shown that longitudinal alignment of astrocytes growing in monolayer is sufficient to direct and enhance the growth of neurites over their surface^{2,3}. The aim of this work therefore was to develop a 3D culture system in which the effect of astrocyte alignment on neurite growth could be modelled in a spatially relevant environment.

METHODS: Rectangular tethered collagen gels⁴ (Fig 1) were made by co-culturing primary rat astrocytes (950K), neural fibroblasts (50K) and DRGs (4 dissociated) in 0.5 ml (2 mg/ml) type I rat tail collagen per mould. After setting, gels were maintained in culture to align for 3 days at 37°C. In this system the cells generate forces that contract the restrained gels, forming a central region in which cells align with the axis of principal strain. The gels have unaligned control areas (delta zones), which are stress-shielded regions with no single axis of principal strain. Gels were fixed with 4%PFA and stained for GFAP, β III-tubulin and hoechst (astrocytes, neurons and nuclei). Astrocyte alignment (aspect ratio) and neurite length were measured using Volocity and Openlab image analysis software (Improvision) and mapped according to gel region (Fig 1C).

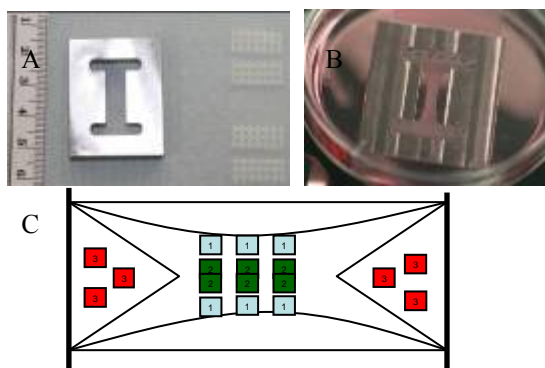


Figure 1. A. Mould and tethering bars. B. Contracted gel. C. Schematic of gel areas for analysis, 1=gel edges, 2=gel middle, 3=delta zones.

RESULTS: Astrocyte alignment was significantly greater at the edges and middle of gels ($P < 0.01$ and

$P < 0.05$ respectively) when compared to delta zones. Neurites in aligned regions grew in an orientated manner compared to neurites growing in all directions in delta zones (Fig 2 A & B). Furthermore, neurites in aligned regions were significantly longer than those in delta zones (Fig 2C). In gels without astrocytes (fibroblast and DRG only) neurites were of similar lengths in all regions (Fig 2D), suggesting a key role of aligned astrocytes in enhancing axon outgrowth.

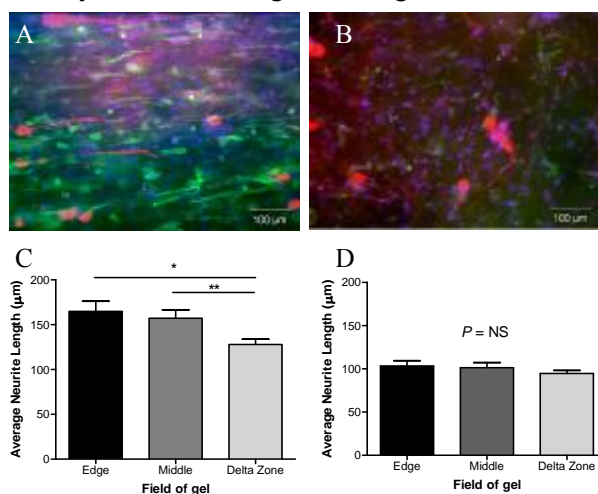


Figure 2. Staining for GFAP, β III tubulin and hoescht in gel edge (A) and delta (B) zones. Neurite length in gels with (C) and without (D) astrocytes, $n=6$ gels.

DISCUSSION & CONCLUSIONS: This model provides a system whereby astrocyte/neuronal interactions can be investigated in a more realistic spatial arrangement than that offered by 2D culture. Alignment of astrocytes in a 3D matrix is sufficient to enhance the growth and directionality of neurites. This could provide a useful basis to improve the design of implantable devices for the treatment of CNS injury, and suggests reactive astrocytes per se are amenable to manipulations that may make them favourable substrates for regenerating axons.

¹ H.M. Geller & J.W. Fawcett (2002) *Exp Neurol* **174**:125-136. ² R. Biran, M.D. Noble & P.A. Tresco (2003) *Exp Neurol* **184**:141-152. ³ J.K. Alexander, B. Fuss & R.J. Colello (2006) *Neuron Glia Biol* **2**:93-103. ⁴ J.B. Phillips *et al.* (2005) *Tissue Eng* **11**:1611-1617. Funded by the Wellcome Trust.

MODELLING THE EFFECTS OF INTERLEUKIN-6 USING A NOVEL ORGANOTYPIC CULTURE MODEL

E. L. Smith, R. Baruah, S. Y. Taylor, R. J. Waddington, X. Wei & A. J. Sloan

Tissue Engineering & Reparative Dentistry, School of Dentistry, Cardiff University

INTRODUCTION: Inflammatory bone destruction is central to the pathogenesis of diseases such as periodontitis and rheumatoid arthritis. Current models of periodontitis include restricted *in vitro* cell culture systems, and *in vivo* models which can be expensive and difficult to obtain clear data from. *Ex vivo* models represent a promising alternative. We have developed a murine mandible slice culture system to model inflammatory mediated bone destruction during periodontitis, and have demonstrated that LPS downregulates the matrix protein BSP, and stimulates osteoclastogenesis via TLR4 signalling within the model¹. In this study we investigated the effects of interleukin-6 (IL-6), known to act as both a pro- and anti-inflammatory cytokine, on osteoclastogenesis, bone matrix, and inflammation within the model.

METHODS: Hemi-mandibles dissected from 10-12 week old male CD1 mice were sliced into 1mm thick transverse sections using a diamond-edged bone saw. Slices were cultured using Trowel type techniques for 0 to 14 days in either the presence of absence of 10ng/ml IL-6. Following culture slices were fixed, demineralised and embedded in paraffin wax before sectioning. Slice viability was confirmed using counts of periodontal ligament cell nuclei. The resident osteoclastic response to stimulation was measured by quantifying the number of TRAP positive cells following IL-6 treatment. Sections were also immunolabelled for a marker of bone matrix (BSP) and for expression of the pro-inflammatory cytokine IL-1 β , visualisation was via a FITC-conjugated secondary antibody and nuclei were counterstained using bisbenzimidazole. To develop local bone resorption within the model, preosteoclast cell suspensions labelled with cell tracer were microinjected into the periodontal ligament (PDL) prior to culture.

RESULTS: Tissue histomorphometry was maintained during culture and following stimulation with IL-6. Treatment with IL-6 did not significantly alter numbers of PDL cell nuclei, or of TRAP positive osteoclasts within the model system, but did increase expression of BSP within the matrix. Expression of IL-1 β , a destructive cytokine upregulated during periodontitis, was observed within unstimulated control cultures, but was significantly downregulated following IL-6

treatment. Tracer fluorescence indicated that microinjected preosteoclasts remained at the injection site, while slice histomorphometry and PDL nuclei numbers were maintained.

Fig. 1: Maintenance of tissue histomorphometry (left) and osteoclast number (right) following IL-6 treatment.

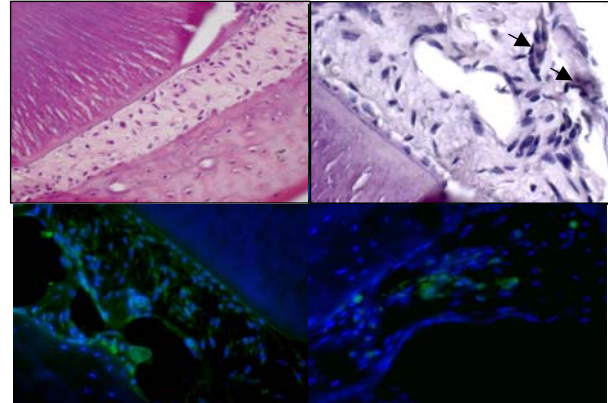


Fig. 2: IL-6 stimulation increased BSP expression within the matrix (top right) but decreased IL-1 β expression (bottom right) compared with unstimulated controls (top left and bottom left).

DISCUSSION & CONCLUSIONS: This method may provide a viable model for the study of bone pathophysiology. Data suggests that IL-6 may increase expression of BSP, or affect its localisation within the PDL matrix of mandible slices. Microinjection of preosteoclasts may provide a viable model for generating a localised inflammatory response.

REFERENCES: ¹S.Y. Taylor et al, *J Dent Res* 87 (Spec Iss C):0302, 2008 (www.dentalresearch.org)

ACKNOWLEDGEMENTS: Supported by NC3Rs Research Grant No. 77844.

Engineering Angiogenesis by Hypoxia-Induced Signaling: Adopting a Physiological Approach

E.Hadjipanayi, R.A. Brown, V.Mudera, U.Cheema

UCL, Tissue Repair and Engineering Centre, Division of Surgical and Interventional Sciences, Institute of Orthopaedics and Musculoskeletal Sciences, London, HA7 4LP, UK

INTRODUCTION: Successful engineering of tissues with clinically relevant size and complexity critically depends on their *in vitro* pre-vascularization which can promote cell survival, differentiation and rapid vascularization post-implantation. However, mimicking *in vitro* the physiological complexity of a vascular network currently presents major obstacles¹. In this study we tested the hypothesis that a hypoxia-induced signaling (HIS) - cell population can generate the complete angiogenic cascade necessary for inducing endothelial cell sprouting and tubule formation within a 3D construct.

METHODS: HUVECs and human-dermal-fibroblasts (HDFs) were co-cultured in 3D spiral or flat collagen constructs² for 1 or 2 weeks, with no direct contact between the two cell types. HDFs were seeded at high density (23×10^6 cells/ml) or low density (1×10^6 cells/ml) in spiral and flat constructs, respectively. HUVEC-only constructs served as controls. Constructs were cultured in the presence or absence of anti-VEGF neutralizing antibody. O₂ tension within constructs was monitored using an optical fibre-based system³. ELISA was used to quantify HIF-1 α and VEGF in 5 and 10 day cultures.

RESULTS: Cell O₂ consumption in high-HDF-density co-cultures resulted in hypoxic O₂ levels (<3%) in the HDF region's core, within 24hrs. In high-HDF-density co-cultures HUVECs formed CD31 and von-Willebrand factor positive capillary-like structures (CLS) with lumens and invaded the HDF region at 1 week. There was a significant increase in the number of sprouts from 1 to 2 weeks which correlated with a reduction in the number of endothelial-cell clusters. No CLS formation was observed in HUVEC-only cultures or in low-HDF-density co-cultures (no hypoxic stimulus). HIF-1 α was present in high-HDF-density co-cultures at 5 and 10 days, while VEGF levels increased by 7 fold from 5 to 10 days. No HIF-1 α or VEGF were detected in HUVEC-only cultures.

Anti-VEGF neutralizing antibody reduced sprout length by 50% in high-HDF-density co-cultures.

DISCUSSION & CONCLUSIONS:

While it is widely accepted that long-term exposure of cells to hypoxia can be detrimental to cell viability, the results of this study indicate that hypoxia can be employed as a physiological signal for inducing an angiogenic response within a 3D tissue construct. Here we show that the angiogenic response was accompanied by up-regulation of two critical, hypoxia-inducible angiogenic factors, HIF-1 α and VEGF. However, the use of hypoxia as the primary angiogenic signal would be expected to trigger the complete angiogenic cascade required for a physiological angiogenic response. The ability to spatially localize the hypoxic signal within a 3D tissue construct could be an invaluable tool for engineering angiogenesis *in vitro* or for pre-conditioning constructs prior to implantation.

We propose that a HIS - cell population could rapidly and physiologically induce an angiogenic response within a 3D tissue construct.

REFERENCES:¹N.C.Rivron, J.Liu, J. Rouwkema, J. de Boer, C.A. van Blitterswijk (2008) Engineering vascularised tissues in vitro. *European cells and Materials* **15**, 27-40. ²R.A.Brown, M.Wiseman, C.B.Chuo, U.Cheema, S.N.Nazhat (2005) Ultrarapid engineering of biomimetic materials and tissues: Fabrication of nano- and microstructures by plastic compression. *Advanced Functional Materials* **15**, 1762-1770. ³U.Cheema, R.A.Brown, B.Alp, A.J.MacRobert (2008) Spatially defined oxygen gradients and vascular endothelial growth factor expression in an engineered 3D cell model. *Cell Mol.Life Sci.* **65**, 177-186.

ACKNOWLEDGEMENTS: This work was funded by BBSRC and EPSRC. Umber Cheema is a BBSRC David Phillips Fellow and is funded through this route.

Mechanical responses of bone tissue formation in 3D engineered constructs via primary cilia.

A. Sittichokechaiwut¹, C.R. Jacobs², G.C. Reilly¹

¹ Tissue Engineering Group, Department of Engineering Materials, University of Sheffield, U.K.

² Department of Biomedical Engineering, Columbia University, U.S.A.

INTRODUCTION: Tissue engineered bone requires mechanical stimulation for adequate matrix production. Previously, we have shown that 2 hour bouts of dynamic cyclic compressive loading induce matrix production by osteoblasts [1]. However, the mechanisms by which cells transduce mechanical signals are poorly understood. Interestingly, primary cilia, which are known mechanical sensing organelles of kidney cells, have recently been shown to be potential mechanosensors in bone [2]. We have shown that fluid shear stress increases bone matrix production by MLO-A5 cells (late-stage osteoblasts), with intact primary cilia in 2-D but that the response is reduced when the primary cilia is removed. The aims of the present study are to investigate whether the primary cilia may also be involved in mechanosensation by MLO-A5 cells cultured in a porous 3D environment and subjected to dynamic compressive loading.

METHODS: Polyurethane scaffolds were cut into cylinders of 10 mm diameter and 10 mm height. Scaffolds were seeded with MLO-A5 cells at densities of 2.5×10^5 per scaffold. Cell-seeded scaffolds were dynamically loaded in compression at 1Hz, 5% strain in a biodynamic chamber (BOSE, ELF3200). To remove primary cilia from cells, cell-seeded scaffolds were incubated with 4 mM chloral hydrate for 24 hr prior to loading. Dynamic compressive loading was applied for 2 hours on day 10. Gene expression of OPN and COL1 were measured 12 hrs after a single bout of loading or control treatment.

RESULTS: Confocal microscopy verified that primary cilia were present on MLO-A5 cells cultured in 3D (Fig.1) and were removed by chloral hydrate treatment. Loaded scaffolds containing cells with primary cilia present) showed higher levels of COL1 and OPN mRNA (about 2 fold), as measured by band density relative to GAPDH, compared with non-loaded controls. Loaded cells that had been treated with chloral hydrate to remove the primary cilia had reduced levels of these matrix protein mRNAs (Fig. 2).

CONCLUSIONS: The primary cilium may mediate the matrix-forming response of bone cells to mechanical loading in 3D, either by sensing matrix deformation or fluid flow through porous scaffolds. This has implications for mechanical conditioning in bone tissue engineering.

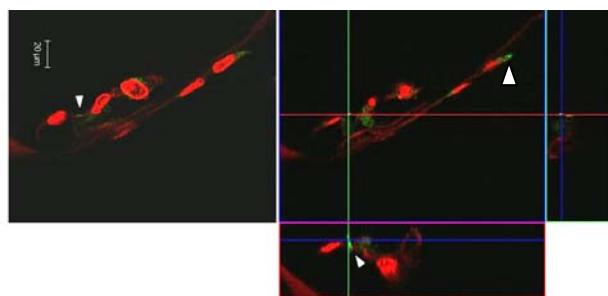


Fig. 1: Primary cilia of MLO-A5 cells on a 3D PU scaffold shown in green (arrow head). Cells also were stained with PI (red) The scaffold struts autofluoresce in red.

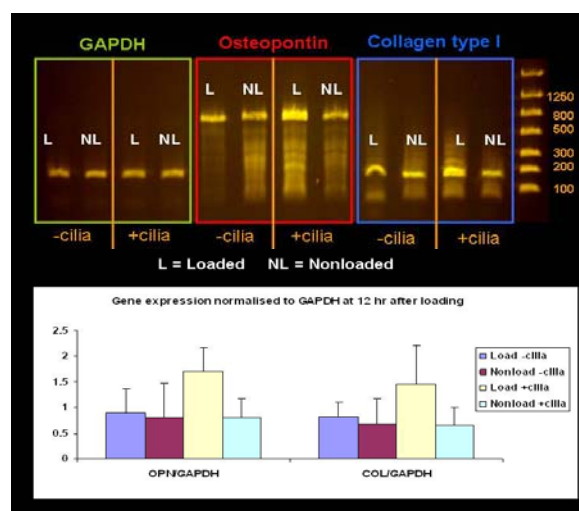


Fig. 2: mRNA expression of OPN and COL1 at 12 hrs after a single bout loading '+ cilia' = non treated cells with primary cilia intact '- cilia' = cells after chloral hydrate treatment'

REFERENCES: ¹ Sittichokechaiwut, A et al. (2009) Bone, **44**: 822-829 ² Malone, A.M., et al. (2007) Proc Natl Acad Sci. **104**: 13325-30.

ACKNOWLEDGEMENTS: MLO-A5 cells were donated by L. Bonewald, U. of Missouri Kansas City. AS was funded by the Royal Thai Gov.

Combined Treatment of Biomatrices with Nisin and Pulsed Electric Fields as a Potential Decontamination Method?

S. Griffiths^{1,2}, M. Maclean², S.J. MacGregor², J.G. Anderson², M.H Grant¹

¹ [Bioengineering Unit](#), ² [The Robertson Trust Laboratory for Electronic Sterilisation Technologies \(ROLEST\)](#), University of Strathclyde, Wolfson Building, 106 Rottenrow, Glasgow, UK.

INTRODUCTION: Pulsed electric field (PEF) treatment has been shown to achieve bacterial inactivation in collagen gels whilst retaining the ability of the collagen to function as a biomaterial [1, 2]. Nisin, an antimicrobial peptide, has been used widely as a food preservative and has shown bactericidal action against a number of Gram-positive bacteria [3]. The potential of nisin to increase the efficacy of PEF disinfection of collagen gels to be used for tissue engineering applications was investigated.

METHODS: Collagen gels, produced using type I collagen, were seeded with *Staphylococcus epidermidis* at concentrations of approximately 10³ CFU/ml. Firstly, seeded collagen gels were subjected to PEF treatment (45 kV/cm, 100 pulses, each of 1µs duration) using a static test chamber. Next, collagen gels, seeded with *S. epidermidis*, were produced containing either 500 or 3000 IU/ml of nisin and used to test the effect of nisin with and without PEF treatment on *S. epidermidis*. The surviving bacteria were enumerated as CFU counts after plating samples onto Brain Heart Infusion agar and incubating at 37 °C for 18-24 h. All treatments were repeated in triplicate and the level of inactivation determined.

The viability of mammalian cells cultured on collagen gels containing nisin was also assessed. Collagen gels were produced containing a range of nisin concentrations (0-3000 IU/ml) and then seeded (10⁴ cells/cm²) with 3T3 cells. After 3 days of culturing their viability was assessed by carboxyfluorescein diacetate/ethidium bromide staining and observed under a Carl Zeiss AxioImager fluorescence microscope.

RESULTS: Treatment with nisin alone at 500 IU/ml caused no significant reduction in the *S. epidermidis* cell population. At 3000 IU/ml a similar level of inactivation to PEF treatment alone was achieved (see Table 1). The greatest microbial inactivation was achieved with a combined treatment of nisin and PEF. These combined treatments achieved inactivation values greater than 3 log₁₀ CFU/ml.

No change to 3T3 cell viability or morphology was

observed when cultured on collagen gel containing nisin (see Figure 1).

*Table 1. Inactivation of S. epidermidis in collagen gel after exposure to nisin or PEF treatment alone and in combination. Results are mean ± SD, n=3. * P<0.05, compared with treatment with PEF or nisin alone, ANOVA with Dunnett's comparison.*

Collagen gel treatment	Inactivation (Log ₁₀ CFU/ml)
PEF alone	0.66 ± 0.09
Nisin level at 500 IU/ml:	
Nisin alone	0.01 ± 0.03
PEF + nisin	3.40 ± 0.23 *
Nisin level at 3000 IU/ml:	
Nisin alone	0.61 ± 0.21
PEF + nisin	3.29 ± 0.08 *

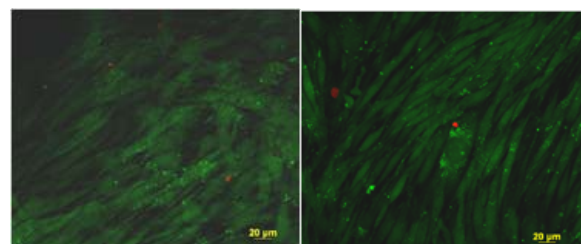


Fig. 1: 3T3 cells cultured for 3 days on native collagen gel (left) and on collagen gel containing 3000 IU/ml of nisin (right), stained with Ethidium bromide and CFDA

DISCUSSION & CONCLUSIONS: The incorporation of nisin into collagen gel greatly enhanced the lethal effects of PEF treatment. Further development may offer a safe compatible decontamination method for tissue engineering matrices.

REFERENCES: ¹ S. Smith, S. Griffiths, S.J. Macgregor, et al. (2008) *J Biomed Mater Res A*. DOI 10.1002/jbm.a.32150. ² S. Griffiths, S. Smith, S.J. Macgregor, et al. (2008). *J Appl Microbiol*. 105(4): p. 963-969. ³ C.K. Bower, J.E. Parker, A.Z. Higgins, et al. (2002). *Colloids and Surfaces B: Biointerfaces*. 25: p. 81-90.

ACKNOWLEDGEMENTS: EPSRC studentship, Doctoral Training Centre in Medical Devices- S.G.

Towards a Physiologically Informed Bioreactor: Engineering Challenges & Compromises

[M. W. Naing](#), Y. Liu, and D. J. Williams

*Healthcare Engineering Research Group, Centre for Biological Engineering, Loughborough University,
Loughborough, LE11 3TU, UK*

INTRODUCTION: The presence of mechanical stimulus has been shown to instigate tissue differentiation. It can also be used to prevent de-differentiation of cells. However, inappropriately applied stimulus may cause cells to go down an undesirable lineage. The current generation of bioreactors usually apply a single component of stimulus. These do not accurately reflect physiological conditions. We therefore chose to develop a bioreactor that more closely mimics the *in vivo* conditions experienced by the intervertebral disc, our tissue of interest. Realising such systems is challenging.

METHODS: In collaboration with Bose Electroforce Test Instruments a multi-axial bioreactor was designed and developed to deliver the following dynamic mechanical stimulation conditions: hydrostatic pressure, pulsatile perfusion flow and uniaxial compression. This mechanical arrangement allows triaxial stimulation of samples. The system can accommodate up to four samples simultaneously in separate sample mounts which allow perfusion of media through the scaffolds. The samples are housed in a hydrostatic chamber which can apply up to 0.3 MPa of pressure. Different combinations of compressive stresses, and pulsatile flow can be dynamically and concurrently administered to the samples.

Real-time data capture of the changes in mechanical properties of the samples can be achieved through a specially-designed software package. The software allows the user to apply a sequence of differing conditions dynamically during the experiment including adapting to the changing properties of the scaffolds. Real-time images can be recorded via a viewing window to the hydrostatic chamber or novel optics. This complex system affords the opportunity to investigate the effect of different combinations of mechanical stimulus on various scaffold and cell types.

OPTIMISATION: While the “first generation” system delivered by the supplier is state-of-the-art technology, continual detailed improvements in design and operational protocols are necessary to

achieve robust experimental procedures and realize the original intent. Mechanical stimulation parameters being optimised include: closed loop control of hydrostatic pressure, media flow rate into the samples, balancing external hydrostatic and the internal sample pressure, and pulsatile flow rate. With multiple interconnected components, maintaining the sterility of the system for the extended duration of experiments is a challenge.



Fig. 1: The Tri-axial Bioreactor system and incubator at Loughborough University

DISCUSSION & CONCLUSIONS: As bioreactors attempt to more closely replicate physiological conditions, trade-offs are required between our bio-mimetic aspirations and the practical limitations of engineering, both design and machine building. The construction of demonstrator systems allows the definition of both common ground and key problem areas.

ACKNOWLEDGEMENTS: Acknowledgements go to David Dingmann, Aaron Owens, Dr Sandy Williams and Dr Darren Burke from Bose Corporation.

Investigation of the biological activity of TGF- β 1 during Re-epithelialisation Using a Computational Modelling Approach

T Sun¹, S Adra², R Smallwood², M Holcombe², S MacNeil¹

¹ Department of Engineering Materials, ² Department of Computer Science, Sheffield University, Kroto Research Institute, Broad Lane, Sheffield, S3 7HQ, UK

INTRODUCTION: The functions of TGF- β 1 in epidermal wound healing appear paradoxical based on the results from *in vitro* and *in vivo* studies [1-2]. As most biological models have limitations which do not reflect the complexity of wound healing *in vivo* we suggest a computational model might be a useful complementary approach to understanding the range of functions of TGF- β 1 in re-epithelialisation. The aim of this research is to develop a 3D user friendly model to simulate wound healing in skin and the actions of TGF- β 1 in wound healing.

METHODS: An agent-based keratinocyte colony formation model [3] was extended to include biological rules governing wound healing in skin epithelia. It was then integrated with a COPASI (COMplex Pathway SIMulator) [4-5] model of the subcellular mechanisms of TGF- β 1. The integrated model was first validated by comparison of the *in virtuo* simulation of the multicellular behaviour of keratinocytes in re-epithelialisation at the cellular level and of the TGF- β 1 mechanisms at the subcellular level with the extensive literature for TGF- β 1. This was then used to investigate the relationship between cell migration and proliferation during epidermal wound healing at the cellular level and the functions of TGF- β 1 on different keratinocyte populations at the subcellular level.

RESULTS: 1. After verification and validation, the integrated model successfully simulated aspects of the re-epithelialisation process of an epidermal wound at both the cellular and some sub-cellular aspects (Figure 1a-d).

2. *In virtuo* investigations indicated that both cell proliferation and migration are crucial for reepithelialisation. Further model analysis predicted there must be mechanisms coordinating the behaviour of the proliferating and migrating keratinocyte populations.

3. The model was then used to investigate the expression and regulation of TGF- β 1 in the various keratinocyte populations. It was found that TGF- β 1 played a positive role in epidermal wound healing by coordinating the behaviour of these keratinocyte populations –reducing proliferation in some cells and stimulating migration -and that

these actions of TGF- β 1 were not contradictory when their temporal-spatial functions were considered (Figure 1a-c).

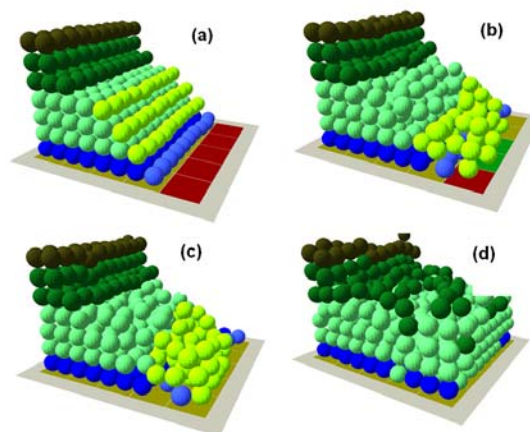


Fig. 1: Appearance of (a) a freshly created (b-c) healing and (d) re-epithelialised epidermal wound simulated by an integrated agent and COPASI based model. The cells that are influenced by TGF- β 1 are labelled as yellow.

DISCUSSION & CONCLUSIONS: Our research demonstrates that a computational modelling approach can be an effective additional tool to aid our understanding of the different behaviours of keratinocyte populations and the functions of TGF- β 1 during epidermal wound healing at both cellular and subcellular levels. Specifically, model analysis indicates that TGF- β 1 plays important roles in balancing the proliferation and migration of keratinocytes for normal wound healing. The model offers a new approach to ask “what if” questions of how epithelial cells self regulate during wound healing which will be useful for looking looking at many aspects of normal and abnormal skin biology.

REFERENCES: ¹Zambruno *et al*, *The Journal of Cell Biology*, 129: 853-865, 1995. ²Gerard *et al*, *The New England Journal of Medicine*, 342: 1350-1358, 2000. ³Sun *et al*, *Journal of the Royal Society Interface*, 4: 1107-1117, 2007. ⁴Hoops *et al*, *Bioinformatics*, 22: 3067-74, 2006. ⁵Vilar *et al*, *PLoS Computational Biology*, 2(1):e3, 2006.

ACKNOWLEDGEMENTS: We gratefully acknowledge financial support from EPSRC (UK) for this research.

Influence of Cell Number and Collagen Concentration on the Mechanical Behaviour of Collagen Hydrogel Constructs

M Ahearne¹, SL Wilson¹, KK Liu¹, AJ El Haj¹, S Rauz², & Y Yang¹

¹Institute for Science and Technology in Medicine, School of Medicine, Keele University, UK.

²Academic Unit of Ophthalmology, School of Immunity & Infection; Birmingham University, UK.

INTRODUCTION: Collagen hydrogels have been under investigation for use in developing constructs for tissue engineering. Optimisation of initial cells seeding and collagen concentrations are important factors in successfully developing an engineered tissue. We have examined the effect of different collagen and cell concentrations on the elastic modulus of collagen hydrogels seeded with corneal fibroblasts and examined how the modulus changes over time in culture.

METHODS: Rat-tail collagen type 1 (BD Bioscience) and human corneal fibroblasts were used to make hydrogel constructs [1]. Hydrogels with collagen concentrations of 2.5, 3.5 and 4.5 mg/ml and 5×10^5 cells per gel were manufactured. Hydrogels with cell concentrations of 5×10^5 , 3×10^5 and 1×10^5 cells per gel with 3.5mg/ml collagen concentration were also manufactured. The hydrogels were cultured at 37°C 5% CO₂ over several weeks.

The elastic modulus of hydrogels was measured using a non-destructive spherical indentation technique [1]. Hydrogels were suspended around their outer edge and a ball was placed on top of them causing them to deform. An image acquisition system (Fig. 1), consisting of a long working distance objective microscope linked to a CCD camera, recorded the deformation profile. A theoretical model was used to calculate the elastic modulus of the hydrogels from their deformation every 3 to 4 days.

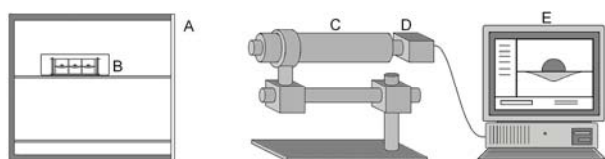


Fig. 1: Schematic of instrument system: (A) incubator at 37°C; (B) sample holder and balls; (C) long working distance microscope; (D) CCD camera; (E) image analysis system.

RESULTS: Hydrogels with lower initial collagen concentrations increased in modulus faster than those with higher collagen concentrations (Fig. 2A). These hydrogels contracted and became thinner more quickly than those with a higher collagen concentration. As hydrogels became

thinner they increased the ratio of cells to total volume. Hydrogels with 5×10^5 cells increased in modulus more quickly than those with lower cell concentrations (Fig. 2B).

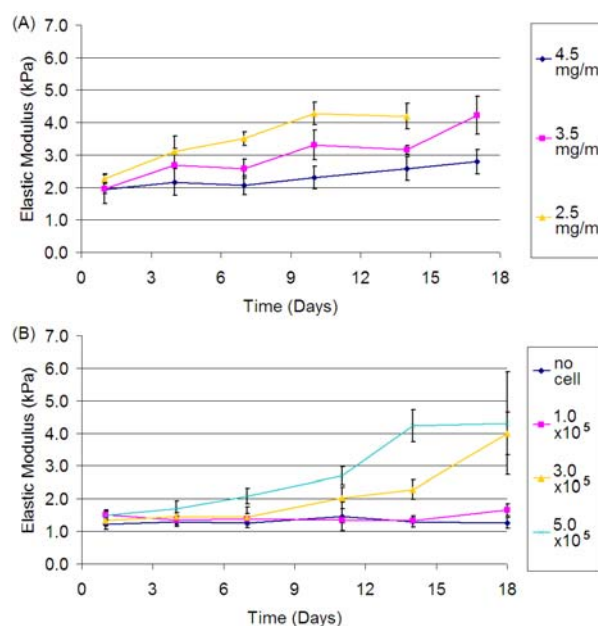


Fig. 2: Elastic modulus of collagen hydrogels with (A) different initial collagen concentrations and (B) different initial cell seeding concentrations.

DISCUSSION & CONCLUSIONS: The influence of collagen and cell concentration on the mechanical behaviour of collagen hydrogels has been demonstrated. Fibroblasts formed an integral part of the structure of these hydrogels and were able to manipulate the hydrogels overall mechanical properties. By using the spherical indentation technique, the effect of collagen and cell concentration can be optimized for tissue engineering applications.

REFERENCES: M. Ahearne, Y. Yang, K.Y. Then et al (2008) *Br J Ophthalmol* 92:268-71.

ACKNOWLEDGEMENTS: This research was funded by BBSRC (BB/F002866/1)

Stem Cells are "Touch-Feely": A Role for Extracellular Matrix in Differentiation and Disease

Wilda Helen¹, Jean E. Schwarzbauer², & Adam J. Engler¹

¹*Department of Bioengineering, University of California, San Diego; La Jolla, CA USA 92093*

²*Department of Molecular Biology, Princeton University; Princeton, NJ USA 08544*

INTRODUCTION: Fibronectin (FN), a major extracellular matrix component that assembles into a fibrillar network, plays a significant role in the development and maintenance of most tissues as well as directing the initial fate choices in the mouse embryonic stem cells (ESCs) as we show here.

METHODS: Self-renewing mouse ESCs were maintained on gelatin-coated plates in DMEM containing 2mM L-glutamine, 1mM sodium pyruvate, 0.5mM penicillin and streptomycin, 1mM non-essential amino acids, 10% fetal bovine serum for ES, 1-thioglycerol and 10³ units/ml leukemia inhibitory factor (LIF). To induce differentiation in the absence of any specific growth factors, cells were cultured either as non-adherent multicellular embryoid bodies or as adherent monolayers on various substrates containing fibronectin: FN-coated surface prepared with 10µg/ml human plasma FN incubated for 1 hour at 37°C or a fibrillar FN matrix prepared from NIH3T3 cells, which were subsequently removed using an established protocol¹ prior to ESC plating. Immunostaining, polymerase chain reaction (RT-PCR), and Western blotting were used to evaluate the differentiation of the ES cells into endoderm lineage.

RESULTS: Over 8 days in culture, ES cells differentiating as multicellular embryoid bodies (EBs) exhibit a 10-fold drop in expression of Nanog, a self-renewal marker, concurrent with a 3-fold upregulation in FN production as well as the onset of differentiation markers. However, FN and GATA4, an endoderm-specific marker, appear to be temporally and spatially correlated within the EB while FN and Nanog are inversely correlated with each other. To probe how intrinsic FN matrix properties, such as structure and stiffness, could specifically regulate endoderm development, ESCs were grown in monolayer culture on FN-coated surfaces, soft fibrillar FN matrices ($E \sim 0.4$ kPa), and crosslinked fibrillar FN matrix ($E \sim 4.5$ kPa). Confocal microscopy indicates that cells can remodel FN-coated surfaces and make fibrils, though these coated substrates did not recapitulate the structure of the fibrillar matrix. As such, immunofluorescent staining of GATA4, an endoderm marker, indicates higher expression for

ESCs on fibrillar substrate (Figure 1). To provide a broader picture of lineage specification, a quantitative PCR screen of 78 genes was performed after 7 and 14 days of culture. ESCs cultured on soft fibrillar matrix upregulate predominantly endoderm makers 8-fold versus self-renewing ESCs and are comparable to positive controls (embryoid bodies), while FN coatings and crosslinked fibrillar matrices exhibit a less specific and intense increase in differentiation markers. Moreover, crosslinked fibrillar FN matrix does not show as significant an increase in endoderm markers. Intrinsic matrix parameter sensing appears to be dependent on $\alpha 5\beta 1$ integrins, which has greater activation on fibrillar substrates compared to matrix coatings. Both substrates, however, have significant activation compared with ESCs cultured in self-renewing conditions.

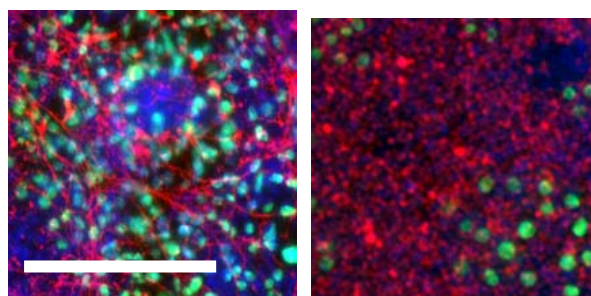


Figure 1: Fibrillar FN (left; red) induced more nuclear expression of GATA4 (green) than FN-coated substrates (right). DAPI stained nuclei (blue) indicate the total number of cells.

DISCUSSION & CONCLUSIONS: When taken together, our data suggests that optimal intrinsic properties, i.e. a soft, fibrillar matrix, are necessary for specific induction of endoderm.

REFERENCES: ¹Y. Mao, J. E. Schwarzbauer, *J. Cell Sci.* **118**, 4427 (Oct 1, 2005).

ACKNOWLEDGEMENTS: The authors would like to thank Dr. Ihor Lemischka for providing ESCs for these studies as well as acknowledge funding from the National Institutes of Health (to JES) and the American Heart Association (to AJE).

Adipose-derived stem cells (ASCs) for peripheral nerve repair

¹R Kaewkhaw, ²AM Scutt & ¹JW Haycock

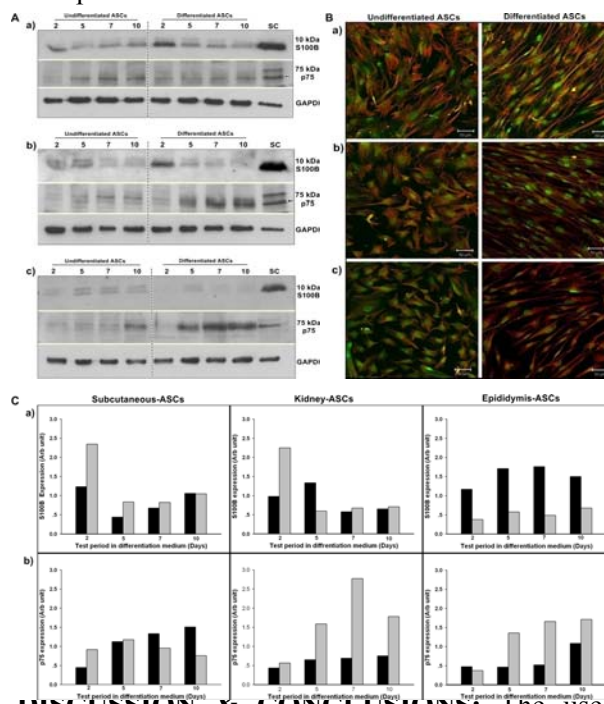
Departments of ¹Engineering Materials & ²Medicine, University of Sheffield, UK.

INTRODUCTION: When peripheral nerves are injured due to acute trauma, axonal damage is often too significant for reinnervation to take place without surgical intervention. The use of nerve guidance conduits (NGCs) as devices for enabling repair are being favoured together with the co-delivery of Schwann cells, as potential approaches. NGCs are hollow tubular devices that bridge the gap between proximal and distal nerve stumps, and experimentally are made from a variety of degradable materials. Schwann cells have a central role in stimulating axonal regrowth, and it is known that when delivered within an NGC the extent of nerve regeneration is significantly increased in comparison with the NGC alone (1). However, their use clinically is questionable, as healthy nerves are required for autologous preparation, and culture times *in vitro* are slow. The aim of the present study was therefore to investigate the potential of adipose-derived stem cells (ASCs) from three anatomical sites for differentiation in to a glial cell phenotype.

METHODS: Stem cells were isolated from: i) subcutaneous; ii) kidney adipose and iii) epididymis adipose tissue of adult male Wistar rats according to the method of Bjornorp *et al* (2). Tissue was finely minced and cells liberated from the tissue by collagenase digestion. Stem cells were separated from tissue debris, mature adipocytes and blood cells by sieving, centrifugation and adherence to tissue culture plastic. Cells were then cultured according to an experimental differentiation protocol using β -mercaptoethanol, retinoic acid, forskolin, bFGF, PDGF and HRG1- β 1. Multipotent differentiation potential was confirmed along osteogenic and adipogenic lineages before investigation of the glial lineage. Incubation times in glial differentiation medium were studied at 2, 5, 7 and 10 days in culture. The protein markers S100 β and p75 and GFAP were studied by Western blotting and immunofluorescence microscopy. Cellular phenotypic changes in length and width were also characterized.

RESULTS: Positive staining for calcium, alkaline phosphatase, collagen and lipid droplets were identified for all three adipose-derived stem cell sources, confirming the multipotent potential of each source prior to investigating glial cell differentiation. An increase in S100 β and p75 expression varied with incubation time for each ASC source, with maximum expression of both markers in subcutaneous cells arising after 2 days. In contrast kidney-derived cells

expressed S100 β maximally after 2 days, but only expressed p75 between 5 and 10 days. Epididymis-derived cells expressed p75 at high levels from 5-10 days, but did not show elevated levels of S100 at any time points.



DISCUSSION & CONCLUSIONS: The use of

Figure 1. Differentiation of adipose-derived stem cells (ASCs) into Schwann cells. A. Western Blotting for S100 β and p75 protein after 2, 5, 7 and 10 days culture in glial differentiation medium, a) subcutaneous, b) kidney and c) epididymis-ASCs.

B. Immunocytochemistry (at day2) for S100 β (green) and GFAP (red) shows Schwann cell-like morphology, a) epididymis, b) kidney and c) subcutaneous-ASCs. Scale bar: 50 μ m. C. Bar graphs (black: undifferentiated-ASCs, grey: differentiated ASCs) illustrating densitometry of a) S100 β and b) p75 bands. Values shown are as a ratio of GAPDH

adipose-derived stem cells as an alternative to Schwann cells for peripheral nerve repair shows tremendous potential. The exact source of ASCs varies in potential for expression of the glial markers S100 and p75. However, subcutaneous cells appear to demonstrate an early expression profile of both markers. This will form a basis for extending work in to the use of NGCs and injury models *in vivo*.

REFERENCES: 1. A. Mosahebi *et al Tissue Engineering* 7, 525 (2001). 2. P. Bjornorp *et al, Journal of Lipid Research*, 19, 316-324 (1978).

ACKNOWLEDGEMENTS: SFR Scholarship programme Thailand, for financial support.

A NOVEL AND RAPID ISOLATE METHOD OF HUMAN MUSCLE DERIVED SUBPOPULATIONS

K Carlqvist, PM Brett, MP Lewis

Division of Biomaterial and Tissue Engineering, UCL Eastman Dental Institute

INTRODUCTION: There have been several reports regarding the differential plasticity of cells within muscle, including the potential to differentiate down both the myogenic and the osteogenic lineage.¹ Muscle is a complex tissue and cells derived from muscle (MDCs) consists of two major groups of cells, muscle precursor cells and a heterogeneous population of interstitial cells.² We have in this project used differential adhesion to different substrates to isolate the various subpopulations, and investigate their plasticity to differentiate down the myogenic and osteogenic lineage.

METHODS: Subpopulations of MDCs (n=3) were isolated by differential adhesion to fibronectin (Fn), gelatin(Gel), or tissue culture plastic (Pl).

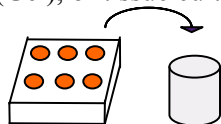


Fig.1: Differential plating for 20min.³ Plates had previously been coated with Fn, Gel, or left uncoated.

The morphological differences between various subpopulations were studied by phase contrast microscopy. Differential media, osteogenic or myogenic, were added to the cells when they reached confluency. The subpopulations' expression of Alkaline Phosphatase (ALP), an early osteogenic marker, was quantified. Myotube forming cells were first identified by phase contrast microscopy and thereafter stained for the myogenic markers desmin and α -sarcomeric actin, and DAPI, a nuclei stain. Quantification of myogenicity of the subpopulations was performed by assessing the ratio of both desmin expressing as well as myotube forming cells was assessed.

RESULTS: The results demonstrated that substrate could be used to isolate various MDC subpopulations. The subpopulations were morphological different; the MDCs^{Gel} were clearly larger than MDCs^{Fn}. The MDCs^{Fn} were also the subpopulation that consequently expressed higher levels of ALP compared with the other subpopulations. Gel adherent cells formed easily myotubes, in stark contrast to Fn adherent cells that appeared unable to fuse to myotubes. The

phase contrasts results were confirmed by the immunostaining .

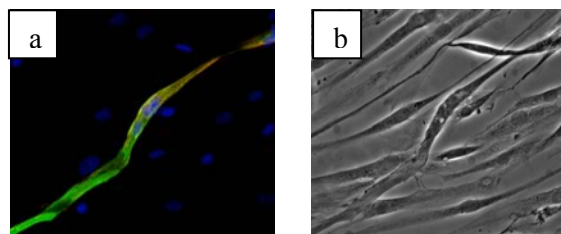


Fig.2: ^{20min}MDCs^{Gel} after 3 days in myogenic media. Myotube a) expressing desmin (green), α -sarcomeric actin (red), and is nuclei stained by DAPI (blue) b) in bright field.(x40)

DISCUSSION & CONCLUSIONS: These results clearly demonstrated that MDCs consists of several subpopulations. It also appears as the more osteogenic population can rapidly be isolated by adhesion for 20 min to Fn, whilst the more myogenic population is isolated after 20 min on Gel. These results could be of great importance for the understanding of both muscle regeneration and the plasticity of MDCs.

REFERENCES: ¹ C.B. Gates, T. Karthikeyan, F. Fu, J. Huard (2008), *J Am Acad Orthop Surg* **16**:68-76 ² A.C.M. Sinanan, J.R. Machell, G.T. Wynne-Hughes, N.P. Hunt, M.P. Lewis (2008) *Biol Cell.* **100**(8):465-77 ³ G.P.Dowthwaite, J.C. Bishop, S.N. Redman, I.M Khan, P. Rooney, D.J. Evans, L. Haughton, Z. Bayram, S. Boyer, B. Thomsom, M.S Wolfe, C.W. Archer (2004) The surface of articular cartilage contains a progenitor cell population, *J Cell Sci* **29**(117): 889-97

ACKNOWLEDGEMENTS: This project has been sponsored by Engineering and Physical Sciences Research Council (EPSRC), Eastman foundation for oral research and training (EFFORT), and Straumann AG.

Differentiation Enhancement of ADSC in Scaffolds with IGF-1 Gene Impregnation under Dynamic Microenvironment

Y Zhu,^{1,2} T Liu,¹ X Ma,¹ & Z Cui²

¹ Dalian R&D Center for Stem Cell and Tissue Engineering, [School of Chemical Engineering, Dalian University of Technology, Dalian, 116024, China](#)

² Oxford Centre for Tissue Engineering and Bioprocessing, [Department of Engineering Science, Oxford University, Oxford OX1 3PJ, UK](#)

INTRODUCTION: Biochemical and mechanical signals enabling cardiac regeneration can be elucidated by using *in vitro* tissue engineering models [1,2]. We hypothesized that insulin-like growth factor-I (IGF-I) and three dimensional dynamic microenvironment could act independently and interactively to enhance the survival and differentiation of adipose tissue-derived stem cells (ADSCs) and hence the construction of engineered cardiac grafts, IGF-I could be expressed by the ADSCs through genetic modification, which can be conveniently done by incorporating the relevant genes into the three dimensional scaffold.

METHODS: ADSCs were cultured on three dimensional porous scaffolds with or without plasmid DNA PIRES2-IGF-I in cardiac media, and in a spinner flask bioreactor. Cell viability, formation of cardiac like structure, expression of functional proteins, and gene expressions were testified with the cultured constructs on culture day 14. A comparative study was made with the static culture as well (without the stirring action).

RESULTS: The results showed that dynamic microenvironment enhanced release of plasmid DNA; DNA PIRES2-IGF-I in scaffold, after the release, can transfect the ADSCs; IGF-I had beneficial effects on the cellular viability and the increase of total protein; and it also increased the expressions of cardiac specific proteins and genes in the grafts (figure 2). It was also demonstrated that dynamic stirring environment could promote the proliferation of ADSCs.

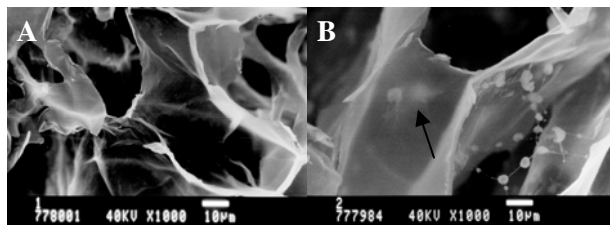


Fig. 1: Surface structure of scaffold-plasmid DNA complex was observed by SEM.

A: Collagen/chitosan scaffold without plasmid DNA as control, Surface of pores was smooth; B:

Some beads were shown on the surface of scaffold-plasmid DNA complex, some even in the scaffold (black arrow).

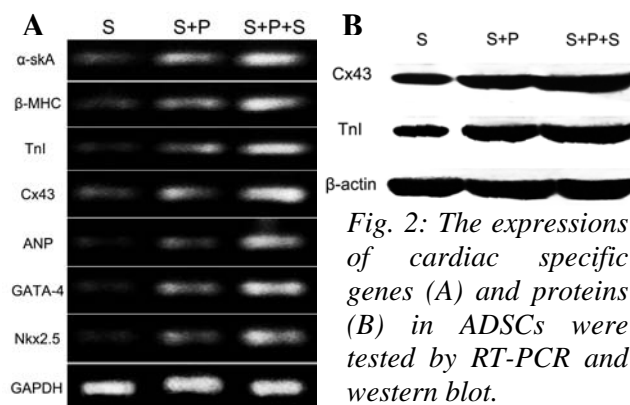


Fig. 2: The expressions of cardiac specific genes (A) and proteins (B) in ADSCs were tested by RT-PCR and western blot.

DISCUSSION & CONCLUSIONS: IGF-I, expressed by ADSCs transfected by DNA PIRES2-IGF-I incorporated into scaffold, and hydrodynamic microenvironment can independently and interactively increase cellular viability, and interactively increased the expressions of cardiac specific proteins and genes in the grafts. Our findings demonstrate that multifactorial stimulation of tissue engineered cardiac grafts by IGF-I and dynamic microenvironment resulted in independent and interactive effects on ADSC survival and differentiation into cardiomyocyte, which would be useful for developing tissue engineered grafts for myocardial repair.

REFERENCES: ¹ O. Caspi, A. Lesman, Y. Basevitch, et al. (2007) *Circ Res* **100**: 263-70. ² M. Cheng, M. Moretti, G. Engelmayr Jr, et al. (2008) *Tissue Engineering* **14**: 1-9.

ACKNOWLEDGEMENTS: This work was supported by The National Natural Sciences Foundation of China (30670525) and China Scholarship Council.

THE EFFECT OF SKELETAL STEM CELLS, HYDROXYAPATITE COATED STEM CELLS AND COLLAGEN COATED ALLOGRAFT ON THE BIOMECHANICAL PROPERTIES OF IMPACTED BONE GRAFT

A.M.H.Jones¹, T.S.Foong¹, AM New¹, B.J.R.F Bolland¹, J.C.Pound¹, SA Davies², S Mann², D.G.Dunlop¹, R.O.C. Oreffo¹.

¹ Bone & Joint Research Group, Centre for Human Development, Stem Cells and Regeneration, Developmental Origins of Health and Disease, University of Southampton.

²Mann Centre for Organised Matter Chemistry, School of Chemistry, University of Bristol.

INTRODUCTION: Impaction bone grafting (IBG) of morcellised fresh frozen allograft remains the current gold standard for replacing bone stock in revision hip surgery. The ability of the graft bed to resist shear and go on to form a new living bony construct is a critical factor in the long-term success of the revision implant. Here, we analyze the effects of skeletal stem cells, Hydroxyapatite nanoparticle (HAp) coated stem cells and allograft coated with type I collagen on the potential for biomechanical enhancement of impaction bone grafting

METHODS: An in vitro model was developed to replicate the femoral IBG process, all samples were cultured for 2 weeks. Plain allograft was used as the control. For the effects of cellular concentration, human bone marrow stromal cells (HBMSCs) were seeded at a density of 5×10^3 , 5×10^4 and 2×10^5 cells per cc of graft. For the effects of Collagen coating of allograft and HA coating of HBMSCs, seeding density was kept constant at 5×10^4 cells per cc and standard basal cultured HBMSCs used for controls. Following mechanical shear testing (n=12) the shear strength and interparticulate cohesion were calculated using the Mohr Coulomb failure equation. The samples were also measured for DNA content and Osteogenic activity.

RESULTS:

Table 1. The effect of increasing HBMSC cell concentration (cells/cc allograft) on Shear strength(τ) and Interparticulate cohesion(c)

Cell Concentration	Shear Strength kPa	Cohesion c kPa
0	245.5	55.8
5×10^3	248.9	61.3
5×10^4	272.2	75.6
2×10^5	284.9	95.7

Cell seeding density had a critical effect on the mechanical properties of the impacted allograft construct (Table 1). The difference compared to

the control plain allograft was approaching significance at 5×10^4 cells/cc with $p=0.065$, and highly significant at the 2×10^5 level with $p=0.001$.

Table 2. The effect of HAp coated cells and Collagen coated allograft on Shear strength (τ) and Interparticulate cohesion(c)

5×10^4 Cells/cc Allograft	Shear Strength kPa	Cohesion c kPa
Basal Control	272.2	75.6
HAp	309.0	89.4
Collagen	302.3	113.3

Furthermore, Collagen coating of the allograft and HAp nanocoating of the osteoprogenitors significantly improved Shear strength further at the lower seeding density (5×10^4) (Table 2) with $p=0.04$ and $p=0.03$ respectively compared to the basal control. Osteogenic differentiation was significantly higher in both Collagen and HAp groups ($p=0.001$) compared to the basal control.

DISCUSSION & CONCLUSIONS: Skeletal stem cell number has a critical effect on the allografts biomechanical properties. HAp coated osteoprogenitors and collagen coated allograft enhanced mechanical properties of adhesion and shear strength still further, and resulted in enhanced osteogenic differentiation. The translation of these facile techniques within a theatre setting is proposed and augers well for regenerative protocols in orthopaedics and a step change in clinical strategies in impaction bone grafting.

ACKNOWLEDGEMENTS: Southampton University Hospitals Trust, Biotechnology and Biological Sciences Research Council.

Bioactive Sugar Gels For Liver Tissue EngineeringR.F. Ambury¹, R.V. Ulijn², C. Merry¹¹ School of Materials, University of Manchester, Manchester, UK.² WESTCHEM, University of Strathclyde, Glasgow, UK

INTRODUCTION: The primary objective of this study was to identify, develop and characterise a novel bioactive hydrogel capable of evaluating hepatocyte behaviour on a tissue realistic mimic. The materials were selected to mimic the native liver tissue with β -galactose moieties to control cellular adhesion via the specific asialoglycoprotein receptors (ASGP-R) found on hepatocytes [1].

METHODS: The gels were created by modifying a commercially available block co-polymer of polyethylene glycol and acrylamide, (PEGA) with galactose moieties found in lactobionic acid (LA), producing a unique bioactive sugar-based gel. A control sugar, D-glucuronic acid (GA), was used for comparative reasons.

Monomers used were mono- and bis-acryloamido PEG ($M_w=1900 \text{ gmol}^{-1}$), and dimethylacrylamide. The pendant PEGA amine groups were used as ligands to which the sugars attach. Sugar modified PEGA was spin coated onto epoxy-functionalised glass substrates and cured by exposing the material to a 365 nm UV light source [2].

The resultant gels were characterised using FT-IR, water contact angle analysis, protein adsorption and dansyl chloride labeling prior to cellular evaluation. The biocompatibility of the surfaces was evaluated with a hepatic cell line looking at degree of attachment, proliferation, and morphology using light microscopy, Alamar Blue and DNA assays, immunochemical staining and PCR.

RESULTS: FT-IR analysis of LA exhibits a broad OH absorption occurring in the region between 3500 and 2800 cm^{-1} , and a distinctive band at approximately 1740 cm^{-1} corresponds to carbonyl stretching (C=O) of carboxylic acid. This unique peak disappears as the galactose moieties within the LA are incorporated into the PEGA gel. A similar trend was also observed with the control GA sugar within the PEGA gel, confirming that the sugars had been integrated into the material. Protein adsorption onto the surfaces illustrated no significant difference in the amount of total protein adsorbed over the course of 24 hours between the PEGA and sugar PEGA surfaces, confirming the non fouling nature of PEGA, table 1.

Sample	Protein Adsorption ($\mu\text{g}/\text{mm}^2$) \pm S.D.
Epoxy Glass	0.0689 (0.003)
PEGA	0.0240 (0.001)
PEGA+LA	0.0233 (0.005)
PEGA+GA	0.0238 (0.005)

Table 1: Total protein adsorption $\mu\text{g}/\text{mm}^2$ in over 24 hours \pm standard deviation (S.D).

Cellular experiments showed that hepatocytes attached preferentially to the sugar surfaces, with few cells seen on the PEGA surfaces. It was observed that cells on the PEGA with LA surface were more metabolically active and proliferated to a monolayer by day 7 in culture. Immunochemical staining of the cells for actin, vinculin and phosphorylated focal adhesion kinase (pFAK) illustrated morphology differences between the surfaces, fig 1.

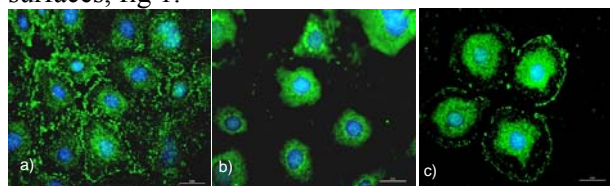


Fig 1: pFAK staining of hepatocytes on a) Tissue Culture Plastic, b) PEGA+LA and c) PEGA+GA.

Internalisation of pFAK and vinculin by the cells on the PEGA with LA surface is consistent with previous work conducted, in which attachment to the surface of the material has been mediated by ASGP-R [1].

DISCUSSION & CONCLUSIONS: LA and GA sugars have been successfully immobilised onto the pendant amine of PEGA which has been verified by FT-IR, water contact angle measurements, total protein adsorption and dansyl chloride staining. The surfaces are biocompatible with good cellular attachment, potentially mediated by ASGP-R, and proliferation observed.

REFERENCES: 1) C.S. Cho, T.Hoshiba, I. Harada, T. Akaike. *Reactive & Functional Polymers*, 2007, 67, 1301-1310 2) M. Zourob, J.E. Gough, R.V. Ulijn. *Adv. Mater.*, 2006, 18, 655-659

DIFFERENTIAL EFFECT OF SUBSTRATE STIFFNESS AND ADSORBED FIBRONECTIN DENSITY ON VASCULAR SMOOTH MUSCLE MIGRATION RATE

A. Whitton¹ D. J. Flint² & R. A. Black¹

¹Bioengineering Unit, University of Strathclyde, Glasgow, UK

²Strathclyde Institute of Pharmacy and Biomedical Sciences, University of Strathclyde, Glasgow, UK

INTRODUCTION: Current surgical approaches to the treatment of patients with cardiovascular disease include the implantation of devices that aim to restore and maintain the flow of blood; however, the patency of such devices in the long term is limited by a physiological process called intimal hyperplasia (IH) or restenosis: the thickening of the vessel wall in response to injury. This study aims to investigate the effect of both the stiffness of the implanted material and the concentration of adsorbed proteins from the blood onto the material surface on the migration of the cells resident in the vessel wall; an important early stage in the progression of IH.

METHODS: Films of polyurethane (PU) Z1A1 and Z3A1 (Biomer Technology Ltd., Runcorn, Cheshire, UK) were cast from solution (10% in DMF). The polymers have a nominal tensile modulus of 3.1 and 10.6MPa respectively. Solutions of fibronectin of differing concentration were deposited onto discs of these PU films and left for 1 hour to allow the protein to adsorb onto the membrane surface, followed by washing in PBS. A 1% albumin (BSA) solution was subsequently applied to the surfaces to block any further protein adsorption. The amount of fibronectin that had adsorbed on each surface was quantified using the ELISA method.

For the purpose of measuring migration rates a variation of the fence migration assay¹ was used. Briefly, human Aortic Smooth Muscle Cells (hASMCs, Lonza) were grown to confluence behind barriers created on the surface of each membrane. The barriers were then removed and the cells were observed for periods of up to five days as they traversed the barrier and populated the cell-free area. Phase-contrast images were acquired at regular intervals throughout this period using an AxioImager Z1 microscope (Zeiss), from which the average migration rate of the cells was determined.

RESULTS: ELISA results showed a correlation between concentration of fibronectin in solution and the surface density of adsorbed protein up to a saturation level. Figure 1 shows the migratory rates of hASMCs on the two grades of polyurethane as a function of the amount of adsorbed fibronectin, expressed as a percentage of saturation. It was found that a migration rate was maximal at certain

adsorbed protein densities, and the density at which this peak occurred differed for the two polymers, the peak for the more compliant PU occurring at a higher protein density than the stiffer PU.

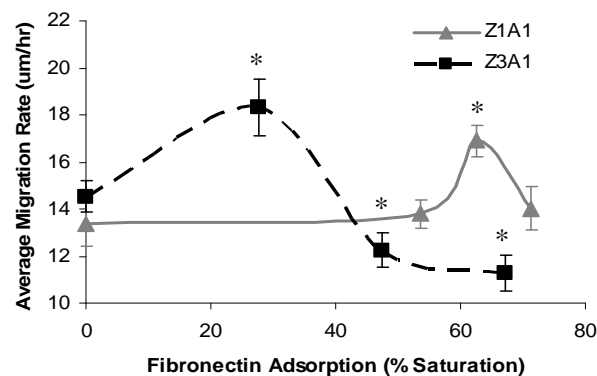


Fig. 1: Migration rate of hASMCs on PU vs. adsorbed fibronectin density (measured as percentage of full saturation). * denotes statistically significant result ($p < 0.05$; $N = 16$) with respect to control samples (no fibronectin).

DISCUSSION & CONCLUSIONS: Many cell types have been found to have maximal migration rates on surfaces to which they adhere at intermediate adhesion strengths.² Furthermore, both substrate stiffness and the density of surface-bound cell-adhesion sites have an effect with an increase in either producing an increase in the strength of cell attachment to fibronectin-treated hydrogels.³ The results of the present study are consistent with these observations in that the maximum migration rate of hASMCs occurs at higher densities of adsorbed adhesion molecules on the softer substrate than on a stiffer PU substrate. These results have important implications for the design of implanted devices irrespective of whether or not migration of cells from the surrounding tissue may be the desired outcome.

REFERENCES: ¹Pratt, B. M.; et al., *J. A. Am. J. Pathol.*, 1984 **117** (3), 349-354. ²DiMilla, P. A et al., *J. Cell Biol.*, 1993 **122**, 3, 729-737. ³Peyton, S. R, Putnam, A. *J. Cell. Physiol.* 2005**204**,198–209

Self-organising clay-based gels for tissue engineering

J.I. Dawson¹, J.M. Kanczler¹, G.A. Attard², R.O.C. Oreffo¹

¹ *Institute of Developmental Sciences, University of Southampton, UK*

² *School of Chemistry, University of Southampton, UK*

INTRODUCTION: The dynamic physical properties of hydrogels and their high permeability for water-soluble metabolites suggest their potential as tissue engineering matrices. However, the essential hydrophilicity of hydrogels present challenges for the retention, in space and time, of growth factors encapsulated within the gel network [1].

Certain clays are well-known for their ability both to self-organise into colloidal gel networks *and* to adsorb biological molecules, owing to the large and highly charged specific surface area of the nano/micro-sized clay particles. Laponite is a thixotropic clay FDA approved for use in the cosmetics and pharmaceutical industry.

METHODS: Laponite suspensions were added drop-wise to cell culture media. Protein diffusion and uptake of Laponite capsules was assessed by assaying supernatant using the Bradford assay and the alkaline phosphatase dose response of C2C12 cells to BMP2. Laponite was also added dropwise to solutions of fluorescein isothiocyanate (FITC) labelled BSA and Lysozyme for analysis by confocal microscopy. To assess chondrogenesis in Laponite, Human Bone Marrow Stromal Cells (HBMSCs) were encapsulated in Laponite and cultured in the presence of TGF β -3, followed by histological examination after 28 days. To assess *in vivo* potential, Laponite was added dropwise into media containing VEGF and implanted subcutaneously in immunocompromised mice.

RESULTS: Upon addition to physiological saline, rapid self-organisation of free-flowing laponite suspensions into stiff gels was observed. Remarkably, whilst negligible diffusion of BSA, lysozyme and BMP2 out of the capsule was observed over 48 hours, extensive protein uptake from the media was observed in the presence of Laponite capsules (Fig. 1).

To assess Laponite's facility as a tissue engineering matrix, HBMSCs were encapsulated in Laponite and cultured in chondrogenic media. After 28 days, Sox-9 expressing cells were observed throughout the cross section of the 50 μ l capsule embedded in areas of proteoglycan-rich matrix immunologically positive for Type-II collagen. To further assess the bioavailability of

encapsulated factors, Laponite was added dropwise into media containing VEGF and implanted subcutaneously in nu/nu mice. After 28 days extensive neo-vascularisation was observed only in capsules added to VEGF containing media.

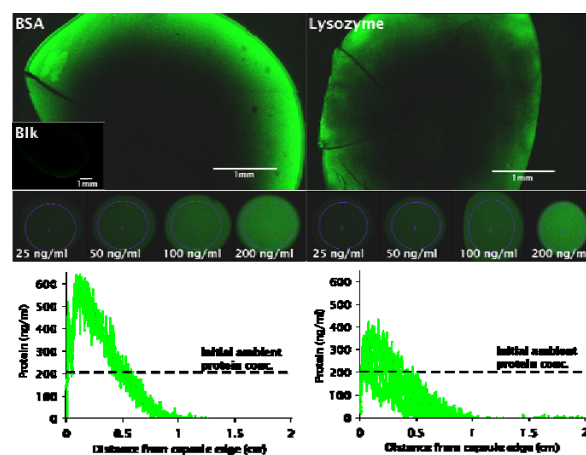


Fig. 1: Sorbed protein distribution. Laponite was added dropwise to media containing 200ng/ml FITC- labelled BSA or lysozyme. After 2hrs capsules were washed three times (2x10 mins, 1x12hrs). Standard curve indicates 2-3 fold concentration of protein within Laponite compared to the initial ambient concentration.

DISCUSSION & CONCLUSIONS: The ability of low viscosity Laponite suspensions to self-organise via both thixotropic means and rapidly in response to an ambient saline medium indicates potential facility for minimally invasive cell delivery and *in situ* 3D support. This, together with the observed ability to host chondrogenic differentiation of HBMSCs and induce vascularisation *in vivo* through the localisation and retention of exogenously applied growth factors could offer new cell and protein delivery options for bone and cartilage engineering.

REFERENCES: ¹ J.L. Drury and D.J. Mooney (2003) *Biomaterials* **24**:4337-4351.

ACKNOWLEDGEMENTS: The authors thank David Johnson and Joanna Greengough for technical support and the BBSRC for funding.

INTRODUCING CHEMICAL FUNCTIONALITY IN FMOC-PEPTIDE GELS FOR CELL CULTURE

V. Jayawarna¹, S. M. Richardson², A. Saiani³, J.E. Gough³, R.V. Ulijn¹.

¹WestCHEM, Department of Pure & Applied Chemistry, The University of Strathclyde, 295 Cathedral Street, Glasgow G1 1XL. ² Faculty of Life Sciences, Stopford Building, The University of Manchester, Oxford Road, Manchester M13 9PT, UK. ³ Materials Science Centre, The University of Manchester, Grosvenor Street, Manchester M1 7HS, UK

INTRODUCTION: Aromatic short peptide derivatives provide suitable building blocks for development of cell culture matrices [1, 2]. It is well known that cell adhesion and proliferation of various cell types can be enhanced (or reduced) by modification of hydrogel surfaces with simple chemical functionality, including amine (NH₂), carboxyl (COOH), and hydroxyl (OH) [3,4]. In this paper we aim to investigate how Fmoc-F₂ (Fluorenylmethoxycarbonyl-diphenylalanine) based hydrogels of building blocks with chemical functionality can be matched with the requirements of specific cell types including bovine chondrocytes, 3T3 fibroblasts and human dermal fibroblasts.

METHODS: Fmoc-F₂ and the three composition gels Fmoc-F₂/Fmoc-X (where X = lysine (K), serine (S), glutamic acid (D)) were prepared by suspending the powders to a concentration of 20 mmol l⁻¹ in sterile H₂O and dissolved using 0.5 M sterile NaOH. Solutions were transferred to culture inserts in 12-well plates carrying culture media. Upon gel formation, structural (using Cryo-SEM, AFM, FTIR) and mechanical (using rheology) characteristics of the hydrogel matrices and cell behaviour in 2D and 3D culture (live/dead staining, LDH assay, F-actin staining and PCR) were studied.

RESULTS: All four solutions formed gels at a physiological pH between 7.5 and 8 within 1 h and had a water content of over 99% (w/w). All compositions produced fibrous scaffolds with fibre diameters in the range of 32–65 nm and structures adopt a predominantly antiparallel β -sheet conformation. Oscillatory rheology confirmed mechanical profiles of soft viscoelastic materials with elastic moduli dependent on the chemical composition, ranging from 502 Pa (Fmoc-F₂/D) to 21.2 KPa (Fmoc-F₂).

All gels support 2D culture of chondrocytes at around 100% viability after 48 h with no obvious difference in cell morphology. Fmoc-F₂/S and Fmoc-F₂/D gels also supported higher HDF cell, while Fmoc-F₂/S gels supported 3T3 cell viability over the 48 h time course (at around 91% for 3T3).

Fmoc-F₂/S also support retention of chondrocyte morphology in 3D culture and express high quality RNA as confirmed by real time Q-PCR.

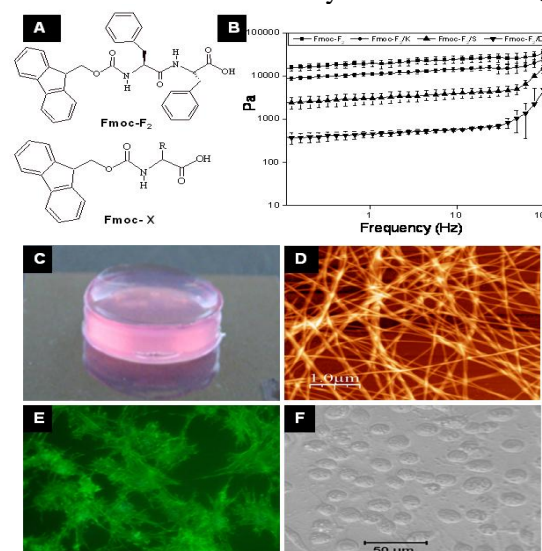


Fig. 1: A: Chemical structure of Fmoc-F₂ and Fmoc amino acid; B: Linear viscoelastic spectra for the four peptide gels; C: Hydrogel; D: AFM image of hydrogel; E: Fluorescence microscopy image showing the organisation of F-actin filaments; F: chondrocytes retain rounded morphology on gel by optical microscopy.

DISCUSSION & CONCLUSIONS: Although these results do not provide confirmatory results to disentangle the relative importance of mechanical properties and chemical functionalities on controlling cell behaviour in Fmoc-peptide gels, it is clear that both are important and can be varied by formulation. These results provide a further step towards development of Fmoc-peptide gels as 3D in vitro cell culture systems.

REFERENCES: ¹ V. Jayawarna, et al., (2006) *Adv Mater* 18:611-4. ² A. Mahler, et al., (2006) *Adv Mater* 18:1365-70. ³ H.K. Pokharna, et al., (1990) *J Bioact Compat Polym* 5: 42-52. ⁴ S. Rimmer, et al., (2007) *Biomaterials* 28:319-31.

ACKNOWLEDGEMENTS: The authors like to thank the Leverhulme Trust and EPSRC for financial support.

Nano-domain detection in Poly (vinyl pyrrolidinone) hydrogels.

M.V. Flores-Merino^{1,2}, G.C. Reilly¹, A.J. Engler² & G Battaglia¹

¹The Biomaterials and Tissue Engineering Research Group. [Department of Engineering Materials University of Sheffield.](#) ²Stem Cell Biology and Bioengineering Lab. [Department of Bioengineering. University of California.](#)

INTRODUCTION: The mechanical properties of hydrogels has been shown to be a useful predictor of cell behavior,¹ especially as stem cell differentiation has been shown to be related to the stiffness of the cell's substrate.² Poly (vinyl pyrrolidinone) (PVP) hydrogels are thought to be a suitable cell substrate for tissue engineering applications, and in this work we studied local variations in the stiffness by atomic force microscopy (AFM) to determine its mechanical suitability for cells.

METHODS: Preparation of (PVP) hydrogels: 1-vinyl-2-pyrrolidinone (Sigma-Aldrich, UK) was mixed with Di-ethylene glycol bis-allyl carbonate (0.25, 0.5, 1, 1.5 and 1.75%) (Greyhound chromatography, UK) and 2,2-Azobis (2-methylpropionitrile) (Molekula, UK) under dry nitrogen. Polymerization was carried out for 24hrs at 50° C. Hydrogels were immersed in a solution of PBS until water equilibrium content was reached. AFM measurements: Samples of PVP were attached to a glass slide and placed on an Asylum MFP-3D-BIO AFM (Asylum Research; Santa Barbara, CA). Hydrogel samples immersed in PBS and tested using AC and Force mode with a SiN cantilever (Asylum Research; Santa Barbara, CA) having a spring constant of 90 pN/nm and tip radius of < 50nm. A scan area of 5µm was used for both the imaging and force spectroscopy measurements. Force curves of hydrogels were fit to the Hertz cone model.

RESULTS: It was found that the Young's Modulus of PVP hydrogels ranges from 4.5 ± 0.48 kPa (0.25%) to 40.8 ± 1.89 kPa (1.75%) (Table 1). Within a given sample however, force spectroscopy mapping shows that PVP hydrogels present regions with higher and lower stiffness on their surface, resulting in well-defined domains of gel characterized as within ~15% of E_{max} or E_{min} for each sample (Figure 1). Domain area was found to be in the nanometer size range though it was dependant on the crosslinker with a sharp transition between 1 and 1.5% crosslinking (Table 1). On the other hand, surface roughness did not substantially change as a function of crosslinking.

The same study performed on poly (acrylamide) hydrogels with 0.225% crosslinker did not exhibit

such spatially-dependent behaviour, though their Young's modulus were consistent with previously reported values.²

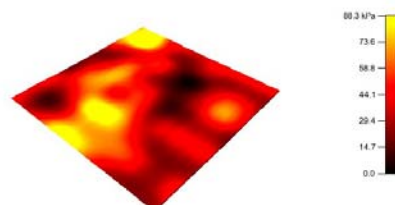


Fig. 1. Example of Force Mapping Spectroscopy of 1.75% PVP hydrogel (width of field 5µm)

Table 1. Young's Modulus values and nanodomain size of PVP Hydrogels.

% Crosslinker of PVP	Young's Modulus (kPa)	Nanodomain size (nm ²)
0.25	4.5 ± 0.48	264.6 ± 0.11
0.5	6.9 ± 0.16	201.1 ± 0.03
1.0	13.7 ± 1.89	198.7 ± 0.06
1.5	31.0 ± 0.80	511.2 ± 0.19
1.75	40.8 ± 1.89	554.7 ± 0.13

DISCUSSION & CONCLUSIONS: PVP hydrogels present nanodomains with different Young's modulus values, which are likely related to the polymerization process and the crosslinker density. PVP hydrogels with nanodomains may be useful to study the relationship between the nano-patterned substrate stiffness and the differentiation of stem cells.

REFERENCES: ¹ J. Drury, D. Mooney. Biomaterials (2003) **24**: 4337-4351. ² A.J. Engler, S. Sen, H.L. Sweeney, and D.E. Discher (2006) Cell **126**(4): 677-89.

ACKNOWLEDGEMENTS: The authors gratefully acknowledge the financial support provided by CONACyT, The University of Sheffield Excellent Exchange scheme and the UK-US Foreign and Commonwealth office Stem Cell Collaboration Development Award.

Enhancement of human primary osteoblast adhesion and function by plasma surface modification of PEEK

A.H.C. Poulsson¹ & R.G. Richards^{1,2}

¹ AO Research Institute, AO Foundation, CH. ² Cardiff School of Biosciences, Cardiff University, UK.

INTRODUCTION: Polyetheretherketone (PEEK) has come into the spotlight as a replacement for metals in devices such as spine cages and patient specific CMF implants due to its radiolucency, good strength and wear properties. Many polymers such as PEEK have an intrinsic low surface energy which can limit cellular adhesion and this can in turn lead to implant loosening as a result of fibrous encapsulation. Surfaces with higher energy are known to promote rapid cellular adhesion and spreading, in contrast to surfaces with lower energy^{2,3}. To improve cellular adhesion the surface energy of PEEK can be increased by plasma surface treatment. The present study aims to investigate the effect of oxygen plasma treatment of PEEK on the adhesion and functionality of primary human osteoblast-like cells (HOB).

METHODS: Discs (13mm diameter) of injection moulded PEEK Optima™ discs (Invibio), Thermanox (THX) (Nunc) and standard medical grade titanium (cpTi, ISO 5832/2) (Synthes) were used in this study. PEEK samples were exposed to an oxygen plasma for varying treatment times using an EMITECH RF plasma treater. Surface chemical compositions were characterised by XPS, wettability by contact angle and changes in topography by AFM and SEM. HOB cells isolated from human femoral heads removed during total joint replacement operations were grown to 70-80% confluence in DMEM (10% FCS in 5% CO₂ at 37°C), and plated at 10³ cells/cm². Alpha-MEM (0.1µM dexamethasone and 10mM β-glycerophosphate) was used as mineralisation media over the 28d experiments. Cell functionality was assessed by alkaline phosphatase activity (ALP), phenotypic gene expression by qPCR, mineralisation by Alizarin red S (ARS) staining, cell attachment by SEM and cell density through the alamarBlue™ (AB) assay. Sampling was performed at 1, 7, 14, 21 and 28d.

RESULTS: Surface characterisation by XPS of the untreated PEEK discs showed 10-12 atom % surface oxygen, confirming that these surfaces are relatively hydrophobic in character⁴. Analysis of the plasma treated PEEK showed the surface oxygen to increase with longer treatment times to ~16 atomic% after 30min treatment, demonstrating an increase in surface energy. High resolution C1s

spectra showed a greater increase in C-OR type functional groups than C=O and O-C=O with increasing treatment times. Surface roughness measured by AFM was affected after treatment times longer than 20min where changes in the surface micro- and nano-structure were observed. The HOB cells were found by SEM to attach more readily to the treated surfaces than to the untreated PEEK surfaces, and higher densities were also measured on the treated surfaces by 7d with the AB assay (Fig 1). From 14d onwards the cells on all the modified PEEK surfaces were shown to have similar cell densities to cpTi. Nodule formation quantified by ARS staining was found to be greater on the treated PEEK surfaces than on the THX surfaces from 14d onward, and the treated PEEK surfaces had similar levels to the cpTi surfaces throughout the 28d experiments.

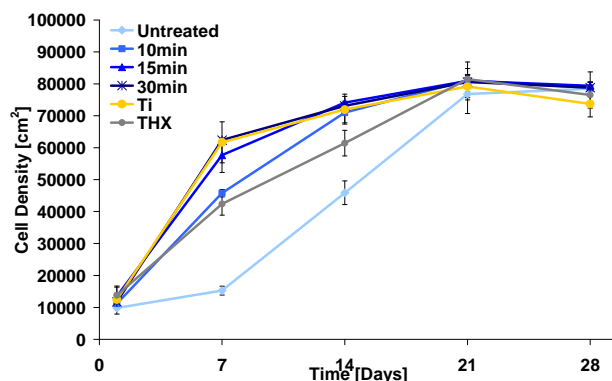


Fig. 1: HOB cell adhesion on treated and untreated PEEK compared to standard Ti and THX surfaces.

DISCUSSION & CONCLUSIONS: Oxygen plasma treatment of PEEK can be used to increase the surface energy and thereby aid the adhesion of HOB cells. This surface modification has led to more characteristic osteoblast behaviour, indicating that these treated surfaces are likely to improve bony integration to PEEK implants.

REFERENCES: ¹Kurtz, S.M. and Devine, J.N. *Biom.*, 28, 4845, 2007. ²Lopez, G.P., Ratner, B.D., et al. *J Biom. Res.*, 26, 415, 1992. ³Kasemo, B. *Surf. Sci.* 500, 656, 2002. ⁴Comyn, J., Mascia, L., and Xiao, G. *Int J Adhesion & Adhesives*, 16, 97, 1996.

ACKNOWLEDGEMENTS: Financial contribution and PEEK discs were kindly supplied by Invibio Ltd.

VASCULAR NETWORK WITHIN BIOACTIVE GLASS SCAFFOLDS:

O Tsigkou,¹ S Lin,¹ MM Stevens,¹ JR Jones¹

¹Imperial College London, London, UK

INTRODUCTION: Bone engineering offers an alternative to repair bone defects with viable and functional substitutes. In a large graft, the core is under hypoxic conditions that lead to cell death. We hypothesised that an engineered functional three-dimensional (3D) vascular network within the graft will support and induce formation of superior bone to be used for permanent repair of orthopaedic defects. The objective of this study is to demonstrate that endothelial cells (ECs) combined with bone marrow-derived mesenchymal stem cells (MSCs), as a source of smooth muscle cells or pericytes, can form a vascular network within the sol gel derived bioactive glass scaffold; this engineered network will inosculate with the host vasculature upon implantation and reduce the time required for a true functional graft vasculature to form.

METHODS: MSCs were purchased from Lonza. HUVECs were purchased from ATCC and cultured on gelatin (0.1%) coated plates and expanded in EGM-2 complete medium (CAMBREX).

3D porous 70S30C (70 mol% SiO₂ and 30 mol% CaO) bioactive glass scaffolds were fabricated as previously described¹.

For vascular network formation, HUVECs and MSCs were combined in a fibronectin containing collagen gel prepared as previously described² and infused into the interconnected porous network of the scaffolds.

Vascularised bone constructs were developed by firstly seeding the scaffolds with MSCs followed the next day by addition of ECs/MSCs containing collagen gel. Culture conditions optimal for bone formation and vascular network organization were determined. Osteogenic differentiation of MSCs was assessed by alkaline phosphatase enzymatic activity (ALPase) and bone formation by collagen formation, and calcium deposition. Vascular network formation within the 3D scaffold was assessed by fluorescent microscopy and immunohistochemical staining.

RESULTS: MSCs seeded on the 70S30C scaffolds for 21 days in the absence of ascorbic acid, β -glycerol phosphate and dexamethasone, resulted in higher amounts of ALPase compared to MSCs cultured with these supplements (Fig 1).

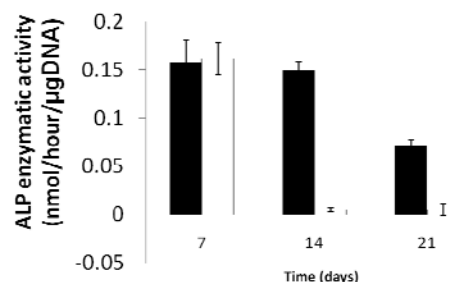


Fig 1: ALPase of MSCs cultured on 70S30Ca scaffolds in the absence (black bars) and in the presence (white bars) of osteogenic supplements. (* $p < 0.001$). Scale bar 1000 μ m

Fluorescent microscopy (Fig 2) demonstrated the formation of a strong capillary-like network connecting through the scaffold pore network via the pore interconnects lasting for up to 21 days.

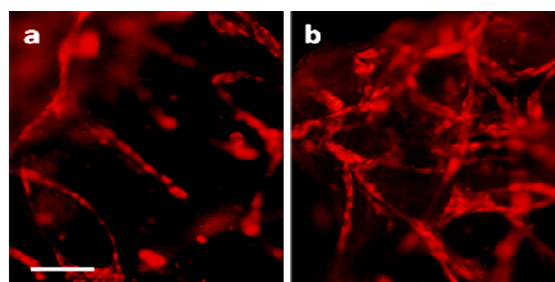


Fig 2: Fluorescence image of the formation of the vascular network within the 70S30C scaffold after 5 days (a) and 13 days (b) *in vitro*. Red: HUVECs. Scale bar 100 μ m.

Masson's trichrome staining demonstrated collagen formation in the absence of osteogenic supplements.

CONCLUSION: 3D 70S30C bioactive glass scaffolds enhance the formation of bone and support the formation of a vascular network *in vitro*. Further investigation of the angiogenic potential of HUVECs and the *in vivo* formation of vascularised bone is also being investigated.

REFERENCES: 1. Jones, J. R. et.al., *Biomaterials*, 2006; 27: 964-973.
2. Wang Z.Z, et.al, *Nat. Biotechnol* 25, 317, 2007

ACKNOWLEDGEMENTS: This work was funded by EPSRC. JR Jones is a Royal Academy of Engineering and EPSRC Research Fellow.

Mechanotransduction in Response to a Topographical Mechanostimulus: Chromosome, mRNA, Protein and Whole-Cell Analyses

McNamara, L.E.^{1,2}, Burchmore, R.², Riehle, M.O.¹ and Dalby, M.J.¹

1. Centre for Cell Engineering, Faculty of Biomedical and Life Sciences, University of Glasgow, Glasgow, G12 8QQ

2. Sir Henry Wellcome Functional Genomics Facility, Division of Molecular and Cellular Biology, University of Glasgow, Glasgow, G12 8QQ

INTRODUCTION: Mechanotransduction is the means by which cells respond to mechanical stimuli (e.g. cell stretch and surface topography) by signalling cascades, or via direct physical tugging of the cytoskeleton on the nucleus. The resulting gene- and protein-level changes mediate the overall response to the mechanostimulus. Topographic substrates have great potential for use as non-invasive mechanostimuli for probing cell-material interactions and mechanotransduction.

METHODS: Human fibroblasts were cultured for 24h on quartz microgrooves (2.5 μm depth x 25 μm pitch) or planar quartz controls. At this timepoint, RNA was extracted for a microarray study, and protein was prepared for Fluorescence 2D-Difference Gel Electrophoresis (2D-DiGE) analysis (discussed in [1]). Differentially regulated proteins were identified using DeCyder v5.0 (GE Healthcare) and mass spectrometry. Microarray and 2D-DiGE data were submitted for Ingenuity Pathways Analysis (IPA) to identify cellular pathways likely to be affected by the gene- and protein changes. Confocal microscopy was used to optically section immunostained cells for 3D reconstruction, and chromosomal territories were examined using FISH (Fluorescence *In situ* Hybridisation) with whole-chromosome probes.

RESULTS: Microgrooved structures provided a non-invasive means of investigating cellular mechanotransduction by influencing cell morphology. This was assessed by 2- and 3D microscopy, with evidence of alignment of actin, tubulin and vimentin in the direction of the grooves, and effects on the nuclear lamina. The 3D shape and arrangement of nucleoli was also affected, with evidence of alignment induced by the topography. Over 200 genes were differentially expressed, with evidence of involvement in important cellular pathways. Several proteins were identified as differentially regulated, with functions in DNA replication, cytoskeletal remodelling, and protein translation, roles that were concordant with the changes at the gene- and whole-cell levels. FISH was used to investigate direct mechanotransduction at the chromosomal level, with rational selection of the

chromosomes studied, based on the microarray data.

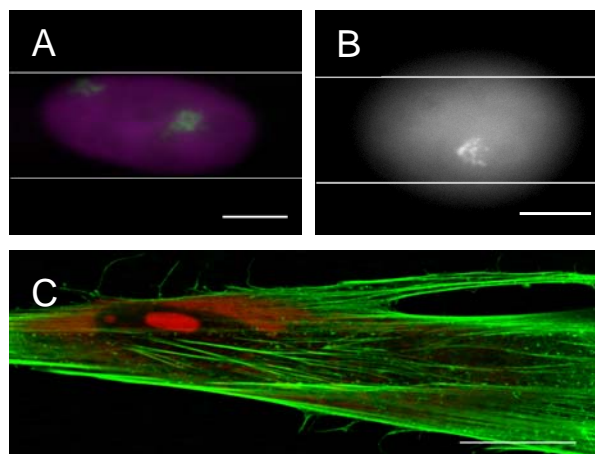


Fig. 1. A, B) Chromosome territories of Chromosome 3 (A) and 1 (B) in the nuclei of cells on the topography, detected by FISH. Bars: 5 μm . Green/White: FISH signal, Purple: DNA. C) Confinement of nucleoli by topography-induced cytoskeletal arrangement. Bar: 20 μm . Red: RNA/DNA, Green: Actin.

DISCUSSION & CONCLUSIONS: The topographical mechanostimulus resulted in morphological changes in cyto- and nucleoskeletal elements, nuclei and nuclear components. These physical changes are very likely to have contributed to the gene- and protein-level effects observed using transcriptomics and proteomics. This work should enhance our understanding of mechanotransduction and cell-material interactions, and inform future efforts to develop new-generation biomaterials for the direction of cellular responses.

REFERENCE: ¹ L.E. McNamara, M.J. Dalby, M.O. Riehle, R. Burchmore (2009). Submitted.

ACKNOWLEDGEMENTS: LEM is funded by BBSRC Doctoral Training Grant BB/D526329/1. The authors would like to thank Ms. F. Kantawong, Dr. K. Jayawardena, Dr. N. Klauke, Ms. S. McFarlane, Ms. J. Wang, Dr. P. Herzyk, and all in CCE, SHWFGF and MBSU for their assistance and helpful discussion.

DEVELOPMENT OF INTERVERTEBRAL DISC REGENERATION STRATEGIES USING MESENCHYMAL STEM CELL-SEEDED HYDROGELS

[SM Richardson](#)¹, R Ulijn², AJ Freemont¹ & JA Hoyland¹

¹ [Tissue Injury and Repair](#), University of Manchester, Manchester, M13 9PT, UK

² Laboratory for Biomolecular Nanotechnology, The University of Strathclyde, G1 1XL, UK

INTRODUCTION: During intervertebral disc (IVD) degeneration the nucleus pulposus (NP) is damaged, leading to spinal instability and low back pain. Current clinical interventions cannot repair the IVD matrix; therefore our aim is to use a tissue engineering approach to regenerate the NP. Due to changes in their behaviour NP cells cannot be used, therefore we have focussed on the use of human mesenchymal stem cells (MSCs) for our IVD tissue engineering strategies. However, in order to develop a successful strategy a number of issues must be considered. This includes the identification and efficacy testing of an ideal biomaterial and the optimisation of conditions for differentiation of MSCs into NP-like cells. Importantly, any implanted cells must be capable of surviving within the harsh physiochemical environment of the degenerate IVD and we have developed an *in vitro* loading bioreactor in order to test MSC survival, differentiation and matrix formation under conditions similar to those experienced within the human IVD.

METHODS: Human MSCs were seeded in a range of biomaterials to test their ability to maintain MSC viability, allow or support lineage-specific differentiation to NP-like cells and permit or promote matrix synthesis and deposition. These biomaterials included chitosan/glycerophosphate (C/Gp) hydrogels, type I collagen hydrogels and self-assembling dipeptide hydrogels, which are all capable of gelation *in vivo* following implantation into the IVD. A range of variables were also tested, including cell density, culture media, and oxygen concentration and application of mechanical load. Following culture phenotype was assessed using real-time quantitative PCR and matrix synthesis assessed using histological staining, immunohistochemistry, and DMMB and Sircol assays for proteoglycans and collagens respectively.

RESULTS: C/Gp hydrogels demonstrated MSC differentiation in standard medium and increasing cell density from 1×10^6 to 4×10^6 /ml (equivalent to *in vivo* NP cell density) improved PG production over collagen and importantly was more influential than the addition of growth factors. MSCs cultured in type I collagen gels demonstrated more rapid differentiation when cultured in hypoxic conditions and exposed to daily mechanical (compressive) loading. Notably, these cells failed to demonstrate either hypertrophic or osteoblastic marker genes when cultured under hypoxic loaded conditions. When MSCs were cultured in self-assembling peptide hydrogels they rapidly differentiated into NP-like cells without the need for differentiating medium and varying the peptide composition of these hydrogels altered the gene expression profiles of the differentiated cells.

DISCUSSION & CONCLUSIONS: We have analysed a number of biomaterials and combined this with studies into the effects of cell seeding density and humoral environment to ascertain the optimal conditions for MSC differentiation and appropriate matrix formation. The results demonstrate the importance of identifying the correct biomaterial and conditions for MSC differentiation to NP-like cells if a successful tissue engineering strategy is to be identified for regeneration of the degenerate human IVD.

ACKNOWLEDGEMENTS: This work was funded through grants from the ARC, BBSRC, MRC, EPSRC, NWDA and RCUK.

DESIGNING SYNTHETIC SCAFFOLDS TO TAKE THE PLACE OF HUMAN DERMIS FOR SOFT TISSUE RECONSTRUCTION

Professor Sheila MacNeil

*Tissue Engineering Group, The Kroto Research Institute, University of Sheffield,
Broad Lane, Sheffield, S3 7HQ*

INTRODUCTION: Since 1992 our group has been developing tissue engineered skin based on human dermis from which we have removed all cells, sterilised and then reconstituted with the cultured keratinocytes and fibroblasts of the patient (1). Early stage clinical evaluation of this tissue engineered skin for contracture release following burns injuries revealed a major problem was that of delayed neovascularisation of tissue engineered skin resulting in loss of some tissue engineered grafts (2). Subsequent studies using tissue engineered oral mucosa to replace scarred tissue in the urethra in substitution urethroplasties (3,4) showed excellent take of tissue engineered oral mucosa based on natural dermis on this very well vascularised bed.

AIM: Against this background why bother developing synthetic scaffolds to replace the human dermis? The motivation comes from wanting to reduce risk in translating tissue engineered materials to the clinic. If we can avoid the use of donor skin this would be viewed as advantageous and would increase its uptake by many clinicians who are currently uneasy about using donor skin on patients. Another practical issue is that of availability. The development of a synthetic dermal alternative will ensure an off the shelf replacement available at any time. Further, if one is going to design a synthetic scaffold to take the place of human dermis then one can introduce features into it – the use of a biodegradable scaffold with a deliberately open weave to promote angiogenesis and the incorporation of an anti-inflammatory to aid initial take of skin cells on the wound bed as desirable attributes.

METHODS AND RESULTS: Initially working with PLA and PGA electrospun scaffolds, we established that the rate of biodegradation of the scaffolds *in vivo* can be tuned by varying the ratio of polyglycolic acid to polylactic acid, as anticipated. Scaffolds composed of microfibers (2-3µm) with more than 95% porosity proved excellent substrates for cell and vascular ingrowth *in vivo*. Degradation of these scaffolds was associated with vigorous macrophage activity but no appreciable activation of any inflammatory response in a rat model. The scaffolds *in vitro* supported the attachment and cellular organisation of keratinocytes and fibroblasts (5).

For clinical use however scaffolds must also be sterilized and their properties must approximate to those of the native tissue to be replaced. Recent studies looking at the sterilisation of the scaffolds with a range of protocols –gamma irradiation, ethylene oxide, peracetic acid and ethanol identified peracetic acid as

clear front runner method . These studies also revealed that all wetting and sterilisation methods reduce the initial mechanical strength of the scaffolds (compared to assessment when dry) but introduction of cells improves the elasticity of scaffolds.

Improved strength of scaffolds can be achieved by heat annealing or vapor pressure annealing of several layers of scaffold. Thus it is possible to predict what mechanical strength and elasticity of scaffold one needs to start from in order to end up with a cell impregnated scaffold which has the approximate physical characteristics of the desired epithelial tissue.

Finally introducing Ibuprofen to electrospun PLGA scaffolds led to an attenuation of the inflammatory response in adjacent skin cells while the scaffolds promote cell attachment and migration. Ibuprofen also accelerated the breakdown of the scaffolds.

DISCUSSION AND CONCLUSIONS: In summary our work of the last 4 years or so tells us that it will be possible to produce tissue engineered electrospun scaffolds for a range of soft tissues which will have predictable biodegradation and mimic the mechanical strength and elasticity of the native tissues for clinical use. Further these scaffolds can be designed to release Ibuprofen to assist in the initial clinical grafting of tissue engineered constructs *in vivo* when there can be an initial inflammatory reaction from the host which can threaten tissue engraftment.

REFERENCES:

1. MacNeil S, Progress and Opportunities in Tissue Engineering of Skin. (2007) Nature Insights. Nature 445, 874-880
2. Sahota, PS, Burn, JL, Heaton, M, Freedlander, Suvarna, SK, Brown, NJ and MacNeil, S. (2003) Development of a reconstructed human skin model for Angiogenesis. Wound Repair and Regeneration 11, 275-284.
3. Bhargava S, Chappell,CR, Bullock AJ, Layton C and MacNeil S (2004).Tissue-engineered buccal mucosa for substitution urethroplasty. British Journal of Urology 93,807-811.
4. Bhargava S, Patterson J, Inman RD, MacNeil S, Chapple CR. (2008) Tissue engineered buccal mucosa urethroplasty - clinical outcomes. European Urology 53(6):1263-1271
5. Blackwood K, McKean R, Canton I, Freeman C, Franklin K, Cole D, Brook I, Farthing P, Rimmer S, Haycock JW, Ryan AJ, MacNeil. (2008) Development of biodegradable electrospun scaffolds for dermal replacement. Biomaterials 29(21):3091-104

Development of a Functional Model of the Glomerular Filtration Barrier Using Electrospun Collagen Nanofibres in a Bioartificial Composite Basement Membrane

S Slater,¹ V Beachley², X Wen², T Hayes³, B Su³, M Saleem¹, P Mathieson¹ and S Satchell¹.

¹Academic Renal Unit, Bristol University, Bristol, United Kingdom, ²Department of Bioengineering, Clemson University, Charleston, United States and ³Biomaterials Engineering Group, Bristol University, United Kingdom.

INTRODUCTION: The glomerular filtration barrier (GFB) comprised of glomerular endothelial cells (GEnC), glomerular basement membrane (GBM) and podocytes, functions as a whole to filter the blood. We have previously generated unique conditionally immortalised (ci) human GEnC [1] and podocytes (ciPod) [2] cell lines. Utilising these cell lines we have developed models of the human GFB, with cells seeded on either side of a membrane, to study its barrier properties and cross-talk (in particular by VEGF) between cellular components. The initial model consists of cells cultured on opposite side of tissue culture inserts, with the GBM represented by the synthetic porous support. However this support is much thicker than the GBM in vivo. Therefore the second part of this work identifies a suitable biocompatible material to replace the porous support to produce a model more closely mimicking the in vivo GFB.

METHODS: Conditionally immortalised cell lines were used; at 33°C cells proliferate, at 37°C they become quiescent. Cells were cultured on opposite sides of tissue culture inserts in the presence or absence of VEGF receptor blocking chimeras. Barrier properties were measured after 1 and 2 weeks incubation using an Endohm 12 electrode. Cells were also seeded onto a number of matrices to identify a suitable material to represent the GBM, including collagen type I, Matrigel, peptide hydrogel, Cellagen; nanofibre matrices of collagen type I or collagen I/chitosan made by electrospinning, nickel mesh, or a combination of matrix and mesh. Monolayer formation after 1 week incubation at 33°C was visualised using immunofluorescence (IF) for actin and light or electron microscopy (EM).

RESULTS: GEnC and podocytes were successfully cultured on opposite sides of tissue culture inserts. Measurement of transendothelial electrical resistance (TEER) demonstrated formation of cell monolayers, which was confirmed by IF and EM. Disruption of crosstalk between the cell layers, by blocking VEGF receptors resulted in a decrease in TEER. ciGEnC

and ciPod seeded onto gelatin, collagen type I, and matrigel gels did not form a confluent monolayer. Subsequently we used electrospinning, to produce nanofibre membranes of collagen type I/chitosan or type I collagen. Both cell types adhered to and proliferated on nanofibre membranes made of collagen I or a collagen I/chitosan mix, however a confluent monolayer was only formed on the collagen I membrane.

DISCUSSION & CONCLUSIONS: We have developed two models of the GFB. The first using a tissue culture insert, from which we have been able to assess barrier function across the cell layers, and the effect of cross-talk between the cellular components. In particular, blocking the action of VEGF lead to a decrease in barrier function. This suggests the cell layers have become more permeable and is in agreement with in vivo data demonstrating a loss of VEGF leads to a disruption of barrier function in the GFB [3]. We have subsequently optimised this model to develop a model containing a more biologically relevant GBM. We have identified electrospun type I collagen nanofibre membrane as a suitable material to act as the GBM. Both ciGEnC and ciPod will adhere to, proliferate, and form a confluent monolayer on this material. This membrane can now be used to produce a more physiological model of the GFB, enabling more representative studies of its function. In particular, selective permeability of the GFB to protein in health and disease, and also the clearance of drugs can be studied.

REFERENCES: ¹Satchell, S.C., et al *Kidney International* 69:1633-40 2006. ²Saleem, M.A., et al *J Am Soc Nephrol* 13 630-8 2002. ³Eremina, V. et al *N Engl J Med* 2008.

ACKNOWLEDGEMENTS: This work is funded by the BBSRC.

Characterization of Fluid and Protein Transport Properties in Hollow Fibre Membrane Scaffolds

RJ Shipley^{1,2} & MJ Ellis³

¹Christ Church and ²[Oxford Centre for Industrial and Applied Mathematics](#), University of Oxford

³Department of Chemical Engineering, University of Bath

INTRODUCTION: Membranes fabricated from cyclic esters such as PLGA must allow permeation of protein solutions to effectively perform their role as scaffolds for cell culture in tissue engineering applications. For a PGLA hollow fibre membrane bioreactor, preliminary work is required to ensure proteins can indeed permeate the porous walls, and to determine operating conditions at which this function is optimised. We present a mathematical model that describes the transport of the culture media components through the fibre, the wall, and the extra-capillary space, and highlight the dependence of protein permeation on the underlying pH, ionic strength, fluid flow regime, and protein and membrane properties. Finally, we demonstrate how to integrate the mathematical models with experimental data for the specific case of IgG to quantify the impact of fouling, and propose optimal operating conditions for the bioreactor.

METHODS: A schematic of the setup is shown in Figure 1. Fluid flow in the lumen and ECS were described by the Navier-Stokes' equations for an incompressible fluid of constant viscosity. Flow in the membrane is described using Darcy's law for an isotropic porous structure with constant permeability. We prescribe continuity of fluid flux and pressure on the lumen and membrane walls, together with a slip condition (applicable when a fluid flows over a permeable boundary). We prescribe pressure and velocity distributions that capture the outlet, together with the lumen outlet pressure (experimentally measured) and a global conservation of mass equation. Protein transport is described throughout using advection-diffusion equations; advection is through the fluid velocity, the diffusivity is constant in the lumen and ECS, and we employ an experimentally motivated time-dependent diffusivity in the membrane to capture fouling.

RESULTS: Experimentally known parameter values are summarized in Table 1. A typical inlet flow velocity is $U=0.133$ m/s; therefore, the Reynolds number based on the fibre length L is $Re=UL/\nu \approx 1.3 \times 10^4$. Defining the aspect ratio of the fibre, $\epsilon=d/2L=4 \times 10^{-3}$, the reduced Reynolds number $\epsilon^2 Re \ll 1$. Lubrication theory is employed

to exploit the geometry of the system to simplify the associated systems. The determination of the membrane permeability and Beaver slip coefficient will be presented based on integration of the model outputs with experimental data. Analytic expressions for the protein concentration at the lumen and ECS outlet are compared against permeation studies to infer the importance of fouling.

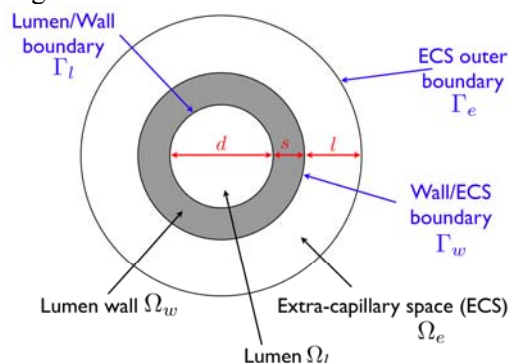


Fig.1: Schematic of a radial cross-section through a single module

Table 1. Typical parameter values

Parameter	Description	Value
d	Diameter of lumen	400 μm
s	Width of lumen wall	200 μm
l	Width of ECS	600 μm
L	Length of fibre	10 cm
Q	Typical inlet flow rate	1-4 ml/min
ν	Kinematic viscosity	$1 \times 10^{-6} \text{ m}^2\text{s}^{-1}$

DISCUSSION & CONCLUSIONS: Predictions of the experimentally-parameterised models permit a set of operating conditions to be identified under which IgG permeates the membrane under physiological conditions (pH 7.0, 37°C and an ionic strength of 0.15 M NaCl). These operating conditions are employed, and data confirming IgG permeation will be presented.

ACKNOWLEDGEMENTS: Work funded by Christ Church, University of Oxford and EU Marie Curie Fellowships in Early Stage Research Training; with thanks to Fernando Acosta for technical assistance in the lab.

OPTIMISATION OF CULTURE CONDITIONS FOR AN IN-VITRO PULMONARY MODEL FOR NANOTOXICITY TESTING

S.Ahmed¹, A. Andar¹, N Gadegaard¹, M Liley² & M Riehle¹

1. Centre for Cell Engineering, Institute of Biomedical and Life Sciences, University of Glasgow

2. CSEM, Centre Suisse d'Electronique et de Microtechnique SA, Neuchâtel, Switzerland

INTRODUCTION: Nanoparticles can be defined as nano-structured materials of less than 100nm in diameter¹. In recent years there has been a huge increase in the use of these nanoparticles and they can be found in places such as sunscreens, toothpastes, diesel car emissions and the food we eat. Due to the huge increase in surface area exhibited by nanoparticles; there can be a huge difference in the physico-chemical properties in comparison to a bulk material¹. It has been seen that these nanoparticle can translocate into circulation and reach other parts of the body. Our study aims to optimize the proliferation of lung epithelial cell monolayers on both silicon nitride and polyester membranes transwell supports for translocation studies *in vitro*.

METHODS: Human bronchial epithelial cells (Calu-3) were seeded onto silicon nitride and Transwell polyester inserts with either collagen, fibronectin or a collagen/fibronectin mixture and percentage confluence was measured each day. Trans epithelial electrical resistance (TEER) measurements were taken on the Transwell inserts using an Evom multimeter using STX electrodes (World precision instruments Ltd.) to measure the integrity of the monolayer formed. Translocations experiments were performed using 2000KDa, 500KDa, 70KDa and 4KDa FITC-dextran (Sigma). The percentage of dextrans that diffused from the apical to the basal sides of the membrane was measured using a spectrophotometer (Envision).

RESULTS: When a growth medium containing 15% foetal bovine serum was used the cells were seen to form a good tight monolayer of cells reaching confluence by day 7. TEER measurements were taken on Transwell polyester inserts. Collagen coating had no effect on TEER value. A TEER value of approximately 600Ω.cm² was achieved on both 3.0µm and 0.4µm pore diameter membranes. Translocation studies through 3.0µm pore diameter Transwell membranes showed that percentage translocation decreased as particle size increased through a cell monolayer. Translocations through the 0.4µm Transwell membranes showed minimal translocation through a cell monolayer. A preliminary result of a 2% translocation through a

cell monolayer on silicon nitride membranes was seen.

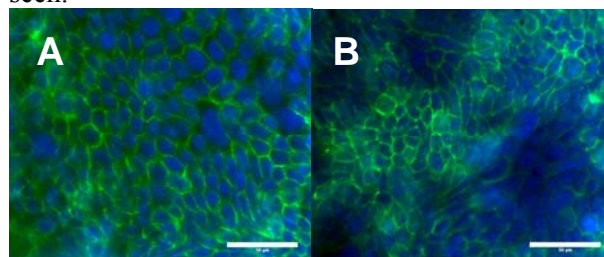


Fig1.0 shows staining for tight junction proteins ZO-1(A) and Occludin (B) in green and nuclear staining in blue on Transwell polyester inserts.

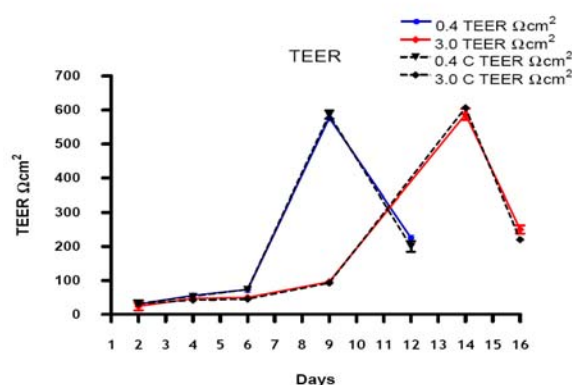


Fig2. Shows TEER values against number of days for collagen and non-collagen coated Transwell polyester inserts.

DISCUSSION & CONCLUSIONS: Excellent TEER values were obtained on both pore sizes with minimal standard deviation. Good comparative results were achieved for translocations through conventional polyester membranes and the silicon nitride membranes. These silicon nitride membranes are widely being used in miniaturized in-vitro systems² and it would be useful to see how certain cells adapt to these surfaces.

REFERENCES: 1 Geys, J., Hoet, P. H. et al (2006) *Toxicol Lett.* **160**, 218-226. 2 Sarina Harris Ma, Lori A. Lepak (2005) *Lab Chip* **5**, 74-85

ACKNOWLEDGEMENTS: I would like to thank the Faculty of biomedical sciences, University of Glasgow and the Nanosafe2 project (contract no. NMP2-CT-2005-515843)

NOVEL BIODEGRADABLE THERMORESPONSIVE DISPERSIONS FOR CELL DELIVERY

R.Cheikh Al Ghanami¹, W.Wang¹, L.Hamilton¹, M.Fraylich², B.Saunders², K.M.Shakesheff¹, C.Alexander¹

School of Pharmacy, The University of Nottingham, University Park, Nottingham NG7 2RD (UK)¹, Manchester Materials Science Centre, School of Materials, The University of Manchester, Manchester M1 7HS (UK)²

INTRODUCTION: Direct injection of cell suspensions is inefficient and generates poor starting conditions for tissue regeneration[1] Thermally-induced colloid aggregation has been employed to create a self assembling material in which the colloidal mixture of cells and biodegradable microparticles is injectable at room temperature, but aggregates *in-situ* into a porous scaffold that protect the cells and subsequently promote tissue regeneration. The particles are designed to be sterically stabilized by the surface thermoresponsive polymer, which when at a critical temperature collapses leading to particles aggregation (Fig.1).

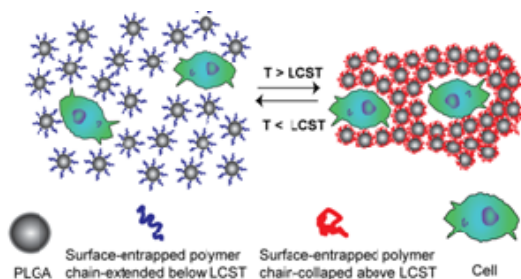


Fig 1: Thermogelling cell-particles dispersions

METHODS: The thermoresponsive copolymer poly(ethylene glycol methyl ether methacrylate)-co- poly (propylene glycol methacrylate) (PEGMA-co-PPGMA) was prepared by free radical polymerisation (GPC and NMR characterisation and LCST determined, 34-36 °C). The PLGA microparticles (2-5µm) coated with PEGMA-co-PPGMA were prepared by an emulsion-diffusion-evaporation technique, where PEGMA-co-PPGMA was used as the emulsion stabiliser. Resulting particles were characterised by SEM and Coulter Sizer. Suspensions injectability was assessed using Texture Analyzer TA HDPlus. Tube inversion was used to assess gelation behaviour of the particles suspensions. The attachment, viability and proliferation of murine C₂C₁₂ cells on and within the gels were investigated.

RESULTS and DISCUSSION:

The thermogelling particles dispersion is injectable (Fig.2). Dispersion of C₂C₁₂ cells with Particles at RT, followed by incubation at 37 °C results in cells encapsulation inside the biodegradable polymer scaffold. The cells remained viable in the gel-matrix for extended times (Fig.3)

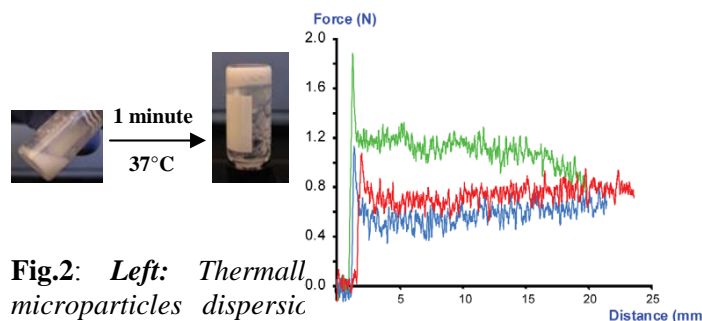
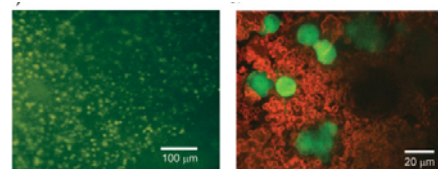


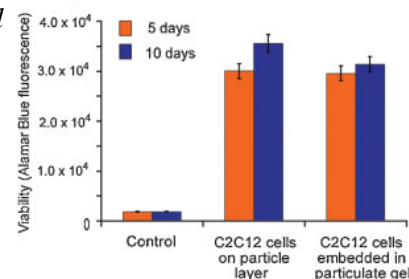
Fig.2: *Left:* Thermal aggregation of microparticles (dispersed in culture media). *Right:* The force required to inject dispersions of particles (60 % w/v in PBS) (at RT) (green line) varied only slightly from buffer solution (blue lines) and movement of the empty syringe barrel (red line).

Fig.3

A. Live-dead stain confirms the encapsulation of live cells (green) and scaffold formation (red).



B. Encapsulated cell viability proved with Alamar blue assay.



CONCLUSIONS: The surface-engineered microparticles, showing thermoresponsive behaviour are promising for biomedical applications, being composed of biocompatible PEG and PPG segments with a biodegradable core. Cells could be successfully encapsulated within the particles matrix [2], which can incorporate actives, such as small-molecule drugs and biomolecules such as growth factors or others.

REFERENCES:[1] Vacanti *et al.* Transplantation of cells in matrices for tissue regeneration. *Adv Drug Deliv Rev* **33**, 165-182 (1998) [2] W. Wang *et al.*, *Advanced Materials*. 2009, 21, 1-5

ACKNOWLEDGEMENTS: Funding from EPSRC, Algerian Government

Osteogenesis within muscle: craniofacial vs. limb muscle cellsAlqahtani K, Buxton, P, Parkar, M, Wall, IB¹. & Lewis MP*Division of Biomaterials and Tissue Engineering, UCL Eastman Dental Institute*¹*Regenerative Medicine Bioprocessing Unit, UCL Advanced Center for Biochemical Engineering*

INTRODUCTION: Ectopic bone formation in skeletal muscle has been observed as a result of pathological and experimental conditions¹. These observations have led researchers to investigate the existence of osteoprogenitor cells within skeletal muscles². Most of the work in this field has described cells isolated from non-craniofacial muscle. However, the involvement of neural crest cells (NCC) in the development of craniofacial skeletal muscles (CSkM; masseter) may have an effect on the multipotentiality of the cells isolated from these muscles. It is therefore hypothesized that CSkM contains a more highly active multipotential cell population than non-craniofacial muscles. Therefore, the aim of this study is to investigate and compare the osteogenic differentiation abilities of cells isolated from craniofacial and limb muscles.

METHODS: Cells derived from mouse masseter (CSkM) and hind-limb (LM) muscles were isolated by enzymatic digestion, then serially plated based on their adhesion properties (PP1 being cells that adhered within 1 hour, PP2 cells that adhered between 1 and 48 hours and PP3 being cells that adhered after 48 hours). Cells were differentiated along the osteogenic and myogenic lineages using osteogenic medium (OS), or myogenic medium (MM). Osteogenic differentiation was assessed by Alkaline Phosphatase (ALP) activity, and calcium deposits. Myogenic differentiation was assessed by the presence of multinucleate myotubes.

RESULTS: The growth dynamics of the PP1 fraction of cells (both CSkM and LM) demonstrated an initial rapid growth rate compared to the other fractions. PCR identification of relevant mRNA transcripts showed that the PP1 fraction was Nanog⁺, Sca-1⁺, CD34⁺, Desmin⁻; whilst the PP3 fraction was Nanog^{+/-}, Sca-1⁺, CD34⁻, Desmin⁺. The myogenic differentiation abilities were also different among different pre-plates. More myotubes were observed in late adhered cells (PP3) compared to early-adhered ones (PP1 and PP2) (Figure 1). Cells from CSkM and LM were examined for their mineralisation capabilities after treatment with OS medium for 21 and 28 days. All cells showed increased mineralisation compare to the positive control mouse osteoblast (MOB). Generally, early adhered cells from both CSkM and LM showed greater mineralisation than late adhered cells.

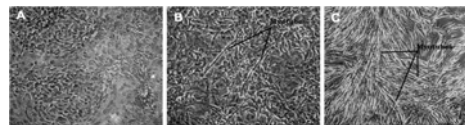


Fig1: Phase contrast images of myotube formed by CSkM after day 21 (A) PP1 (B) PP2 (C) PP3

In order to investigate the effect of cell age on differentiation potentials, cells from craniofacial muscle at passages 1 and 14, were exposed to OS, MM, and standard growth media for one week. After one week, RNA was extracted and RT-PCR was performed to examine the expression of osteogenic (Runx-2 and ALP) and myogenic (MyoD and Desmin) genes. In general, osteogenic genes were expressed in early-adhered cells and myogenic genes were expressed in late adhered cells. In passage 14 cells, early adhered cells continue to express osteogenic genes. On the other hand, the expression of myogenic genes in late adhered cells decreased compared to the same cells at early passage number. Finally, ALP expression was observed in PP1 and PP2 in both control and differentiated cells.

DISCUSSION & CONCLUSIONS: Different populations of cells that may have different osteogenic and myogenic differentiation abilities were isolated from CSkM and LM based on their adhesion properties. Early isolated cells (PP1 and PP2) from both muscles showed higher osteogenic and lower myogenic differentiation abilities compared to the late preplate (PP3). There are some differences in gene expression between early and late adhered cells. Early adhered cells are Nanog⁺, Sca-1⁺, CD34⁺, Desmin⁻. Where as the late adhered cells are Nanog^{+/-}, Sca-1⁺, CD34^{+/-}, Desmin⁺. There are no clear differences in osteogenic differentiation abilities between cells isolated from both muscles.

REFERENCES: ¹Urist MR, *et al.* Clin Orthop Relat Res. 196 Jul Aug;59:59-96. ²Bosch P, *et al.* Orthop Res. 2000 Nov;18 (6):933-4.

MICROFLUIDICS AS A TOOL TO STUDY EPITHELIAL CELL RESPONSE TO *P. aeruginosa*Sultan M. Al-Sharif¹, Abhay Andar¹, Nikolaj Gadegaard¹, Susan Rosser² and Mathis O. Riehle¹

1. Centre for Cell Engineering, Institute of Biomedical and Life Sciences, University of Glasgow

2. Environmental Biotechnology, Plant science, Institute of Biomedical and Life Sciences, University of Glasgow

INTRODUCTION: This project presents a microfluidic gradient generator for the cultivation of epithelial cell lines to investigate their response to pathogenic bacteria. This could offer a quick and high throughput academic study of pathogens to test their interactions with human cells. Many studies have proposed mechanisms for how *Pseudomonas aeruginosa* infect epithelial cells and how they manage to remain in the epithelia¹. One of the abilities of *P. aeruginosa* is adherence to epithelial cells via flagella and pili which disrupt some cell-cell and cell-surface interactions^[1-2].

METHODS: The device masters were fabricated on silicon substrates using an SU-8 photoresist and photolithography techniques in a clean room. The devices were prepared in PDMS (polydimethylsiloxane) elastomer and bonded to a glass coverslip. The microfluidic channel consists of a Christmas-tree-type concentration gradient generator that separates the solutes (in this case antibiotic) from 0 – 100%. Each cell culture well would then have a different concentration of solute and the cells would grow under different conditions inside the same chip.

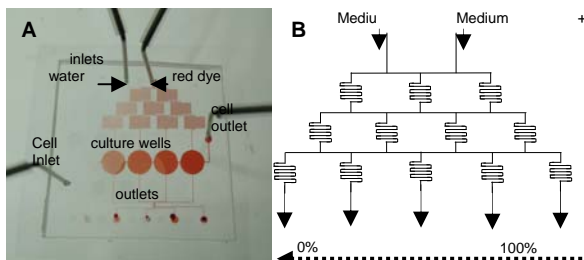


Figure 1: (A) Concentration gradient created in the device using red dye and water. (B) schematic of a working device.

RESULTS: MDCK (Madin-Darby Canine Kidney) cells were cultured in these devices. Preliminary results seem to show shrinkage of cell monolayers in response to bacterial infection.

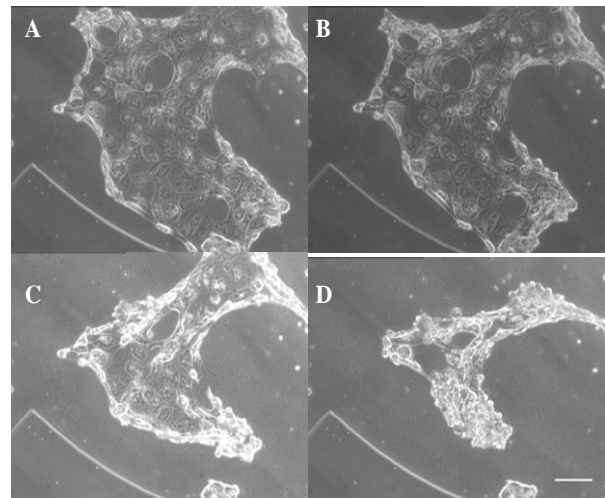


Figure 2: (A) to (D) Shows how the MDCK cell monolayer inside the device seems to shrink over time after being infected with the *P. aeruginosa*.

DISCUSSION & CONCLUSIONS:

Microfluidics allows us to manipulate very small amounts of fluids (in microlitres) within micrometer scale channels. One of the fundamental concepts of microfluidics is to reduce consumption of solutes^[3-4]. Future directions would be to study effects of the bacterial biofilm on cell monolayers and epithelial resistance of monolayers under the influence of different antibiotic concentrations in microfluidic devices.

REFERENCES: 1. Jacob *et al*, (2002) *Infection and Immunity*. 6399-6408; 2. Kerchov and Elimelech, (2007) *American Chemical Society*. **24**., 3392- 3399. 3. Swanson, B (2002).

Microbiological Methods. 361-366. 4. N. L. Jeon, Dertinger *et al*,(2000) *Langmuir*, 16, 8311-8316

ACKNOWLEDGEMENTS: I would like to thank the Faculty of Biomedical and Life Sciences, University of Glasgow.

Hypoxia-mimicking Materials for Bone and Cartilage Tissue Engineering

M Azevedo^{1,2}, G Jell^{1,2}, R Hill¹ & M M Stevens^{1,2}

¹ Department of Materials, *Imperial College London*, London U.K.

² Institute for Biomedical Engineering *Imperial College London*, London U.K.

INTRODUCTION: During cartilage and bone formation or regeneration, cells respond to changes in the oxygen pressure through a hypoxia-sensing pathway^{1,2}. This pathway then activates numerous genes involved in progenitor cell recruitment, cell proliferation and differentiation^{2,3}. These fundamental processes necessary for normal bone and cartilage development and repair could be critical for many bone and cartilage tissue engineering (TE) strategies. The current project aims to develop a new generation of hypoxia stimulating materials for use in cartilage and bone TE. Novel resorbable bioactive glasses (BG) were chosen as the delivery systems for hypoxia stimulating ions (Co²⁺ ions) due to their controllable ion release profiles, long shelf life and low manufacturing cost.

METHODS: Two series of melt-derived BG with increasing concentrations of Co²⁺ were synthesized. Their chemical composition was tailored to specific applications (cartilage or bone) by the addition of magnesium and zinc. A number of different techniques, including XRD, DSC, ²⁹Si NMR and ICP-OES, were used to understand how Co²⁺ ions affect the glass structure and to determine the ion release profiles. To study the effect of the BG in cell viability and in the hypoxia pathway, SaOs2 cells (an osteosarcoma-derived cell line) were treated with the dissolution products of the glasses prepared. Total DNA content, lactate dehydrogenase (LDH), HIF-1 α (hypoxia inducible factor-1 α) levels and VEGF (vascular endothelial growth factor) expression were measured.

RESULTS: Cobalt-containing BG were successfully developed. A strong correlation between the position of the silicon peak in ²⁹Si NMR and the network connectivity calculated considering Co²⁺ as a network modifier was found, indicating Co²⁺ acts as a network modifier in the glass structure. Moreover, the addition of Co²⁺ to the glass was shown to decrease the glass transition temperature (T_g), suggesting that Co²⁺ makes the glass structure more easily disrupted. This data is in accordance with the ICP results that showed silicon release increases with addition of Co²⁺ to the BG. A controlled release of Co²⁺ within the biologically active concentration range was also achieved with the BG produced. The dissolution products of these BG significantly increased HIF-

1 α levels (Fig.1) and induced the production of the potent angiogenic factor VEGF in a concentration-dependent way. Total DNA content and LDH results showed no significant effect of the BG in cell viability on the first 48h. However, one week later, a considerable decrease in cell number was observed with the highest Co²⁺ concentration tested.

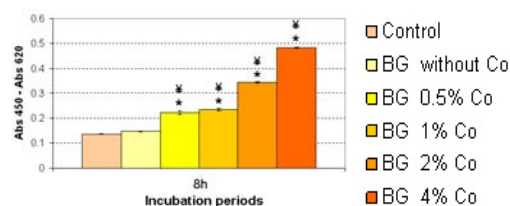


Fig. 1: HIF-1 α levels: a concentration-dependent increase in the levels of the transcription factor responsible for the activation of the hypoxia pathway (HIF-1 α) with Co²⁺ BG was observed.

DISCUSSION & CONCLUSIONS: A series of cobalt-containing BGs was produced and Co²⁺ was shown to act as a network modifier in the glass structure. A controlled release of ions within a biologically active concentration range was achieved and shown to be essential to maintain cell viability. The increase in HIF-1 α levels and VEGF expression strongly demonstrate the activation of the hypoxia pathway and the posterior cellular responses using the Co²⁺ BG. The data presented here strongly suggests the potential of hypoxia-mimicking materials in tissue engineering applications.

REFERENCES: ¹ J. C. Utting, et al. (2006) *Exp Cell Res.* **312**:1693-702 ² P. J. Emans (2007) *Bone* **40**:409-18 ³ J. Malda, et al (2007) *Tissue Eng* **13**:2153-62.

ACKNOWLEDGEMENTS: This work was supported by EPSRC and FCT grant SFRH / BD / 36864 / 2007.

AN OVERVIEW ON CRYOGEL POLYMERIC SCAFFOLDS WITH SPECIAL APPROACH TO CARTILAGE TISSUE ENGINEERING

Sumrita Bhat¹, Deepti Singh¹, Kevin Shakesheff² and Ashok Kumar^{1*}

¹Department of Biological Science and Bioengineering, Indian Institute of technology Kanpur, 208016-Kapur, INDIA and ²Centre for Biomolecular Sciences, University of Nottingham, University Park, NG7 2RD, Nottingham, UK

INTRODUCTION: A paradigm shift is taking place in medicine from using synthetic implants and tissue grafts to a tissue engineering approach that uses degradable porous material scaffolds integrated with biological cells or molecules to regenerate tissues. The techniques involve the use of three-dimensional (3-D) scaffolds characterized according to the types of application. Materials and fabrication technologies are critically important for tissue engineering in designing temporary artificial extracellular matrices (scaffolds). We have recently developed and utilized various polymeric cryogel scaffolds for biomedical and bioengineering applications synthesized using cryogelation method. At present, cryogels are being used in various biomedical and biotechnology field including use as chromatographic matrices, carriers for the immobilization of molecules and cells, matrices for cell separations, and tissue engineering which includes using scaffold for skin, bone, cartilage, cardiac and liver tissues. These are blends of natural and synthetic polymers like agarose, gelatin, hydroxy ethyl methacrylate, and chitosan were used for preparing scaffold for cartilage tissue engineering. These scaffolds show good elastic and mechanical characteristics and well controlled pore architecture with high porosity.

METHODS: These matrices are synthesized at sub zero temperature resulting in formation of interconnected networks. These scaffolds were seeded with the primary goat chondrocytes and co culture with mesenchymal stem cells. Various immuno chemical and biochemical assays were performed to assess the proliferation and extra cellular matrix synthesis on these scaffolds. For other tissue engineering applications respective cell lines were cultured on these matrices. Cell-matrices interaction was examined further by biochemical assays.

RESULTS: Biochemical analysis like Glycosaminoglycans (GAG) and collagen exhibited the synthesis of extra cellular matrix on these scaffolds which was further confirmed by SEM micrographs. Imaging techniques like fluorescent and confocal microscopy were utilized to check proliferation of these cells on scaffolds by staining them with DAPI and PI.

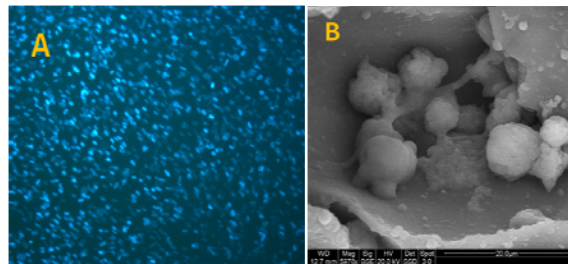


Fig. 1 Chondrocytes on scaffold stained with (A) DAPI and (B) SEM image of two weeks chondrocyte culture.

DISCUSSION & CONCLUSIONS: These cryogels did not show any failure during stress and strain procedure and their capacity to retain shapes after drying makes these cryogels more effective and easy for handling. Cell-matrix interaction observed while co-culturing primary chondrocytes with mesenchymal stem cells and primary goat chondrocytes showed good cell attachment, proliferation and secretion of extra cellular matrix (ECM) in cryogels proving their potential for tissue engineering applications particularly for cartilage regeneration.

REFERENCES: 1) Kathuria, N., Tripathi, A., Kar, K. K. and Kumar, A. (2009). Elastic and Macroporous Chitosan-Gelatin Cryogels: A New Material for Tissue Engineering. *Acta Biomaterialia* 5, 406- 418. 2) Tripathi A, Kathuria N, Kumar A (2009). Elastic and macroporous agarose-gelatin cryogels with isotropic and anisotropic porosity for tissue engineering. *JBMR Part A*: DOI: 10.1002/jbm.a.32127. 3) Dainiak, M., Kumar, A., Galaev, I. Yu. and Mattiasson, B. (2006). Detachment of affinity captured bioparticles by elastic deformation of macroporous hydrogel. *Proc. Nat. Acad. Sci. (PNAS) -USA* 103, 849-854.

ACKNOWLEDGEMENTS:

Authors would like to acknowledge the funding agencies like DST-UKIERI award, DBT (INDIA) and UK- India Science Bridge Programme.

*Corresponding author: ashokkum@iitk.ac.in

Single Unconfined Compression of Cellular Dense Collagen Scaffolds for Cartilage and Bone Tissue Engineering

A Bohr¹, K Memarzadeh¹, B Alp², R Brown² & V Salih³

¹UCL Dept. of Mechanical Engineering; ²UCL Tissue Regeneration & Engineering Centre, Institute of Orthopaedics, HA7 4LP, UK; ³UCL Eastman Dental Institute, 256 Gray's Inn Rd., London, WC1X 8LD, UK.

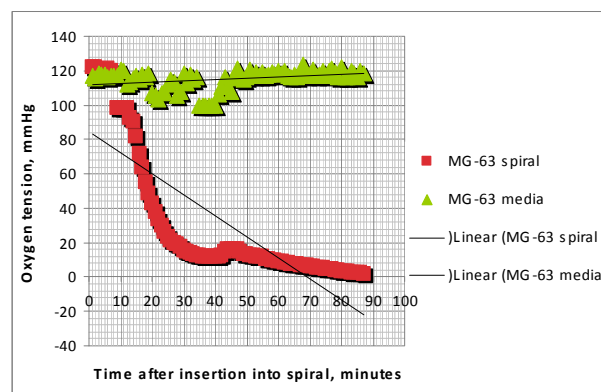
INTRODUCTION: Cell seeded collagen matrix scaffolds have been extensively evaluated recently as potential systems for *de-novo* tissue regeneration and repair for a variety of tissue types. While collagen gels are biologically excellent as starting point scaffold materials, their use is limited by the lack of cohesive structure and inherently weak mechanical properties due to a high liquid content (>99%). An ingenious method of combining unconfined plastic compression (PC) with capillary action has shown that these scaffolds can be rapidly processed into tissue like structures, which can be immediately implanted into the host^[1]. It has been shown that the rapid increase in fibrillar collagen density dramatically enhanced the mechanical properties of such scaffolds thus potentially eliminating the need for long term cellular action. This simple project investigated the effect of single unconfined compression on cartilage-cell seeded collagen matrices in terms of cell viability, proliferation and oxygen consumption.

METHODS: *Scaffold preparation:* Neutralized collagen gels (2ml) were prepared in rectangular moulds (10mmx30mm). Cellular constructs were produced by single compression (SC). Unconfined compressive load of 1.5 KPa for 5 min was initially applied to produce collagen sheets, which were rolled to give cylinder scaffolds of ~2 mm diameter. Collagen content using SC and DC was measured gravimetrically after freeze drying. MG63 bone cells and ATDC-5 cartilage cells were incorporated between neutralization and setting/multiple compaction at a pre-compression density of 5×10^5 cell/ml. Acellular scaffolds were used as controls.

Assessment of Cell Viability: Samples were fixed in formalin at days 1, 5 and 10 and wax embedded. 5µm histology sections were obtained and labeled with DAB conjugated TUNEL based cell apoptosis detection kit. A minimum of 1000 cells were counted in random light microscope fields (x20 objective), evaluated for TUNEL reactivity and morphological signs of cell necrosis, and a cell death index was obtained. *Proliferation:* at days 1, 3, 7 and 10 samples were subjected to Alamar Blue proliferation assay – a non-destructive assay that may be used on the same samples over time.

Oxygen Monitoring: Fibre optic oxygen probes (Oxford Optronix, Oxford, UK) were inserted into the centre of SC constructs and oxygen levels in the centre of cell-seeded constructs were measured over 5 days.

RESULTS: COL-I protein content averaged 12%, and for SC processed scaffolds. Despite the evidence of cell death (approx. 13 % of the total cell count) after 24 h in culture, no significant increase in the number of dead cells occurred as a function of time in the SC processed scaffolds for either cell type. Cell proliferation within the collagen sheets was confirmed for both cell types, and reached levels expected for the numbers of cells seeded within the scaffolds after 10 days in vitro. Oxygen levels in the core of such constructs were significantly low, showing depletion of oxygen by MG63 cells (*Fig. 1*).



CONCLUSION: SC collagen scaffolds maintained integrity and considerable MG63 and ADTC cell viability up to 10 days in culture and should be therefore further investigated as potential scaffolds for hard-tissue engineering. We have established a method for the monitoring of oxygen in the model PC collagen cultures and shown that the high density PC collagen material allows good perfusion of oxygen.

REFERENCE: [1] RA Brown, M Wiseman, C-B Chuo, U Cheema, SN Nazhat. *Advanced Functional Materials* 15, (2005) 1762.

An *in vitro* model for spinal cord injury

S Boomkamp¹, L Ross², M Riehle², S Barnett¹

¹ Glasgow Biomedical Research Centre, University of Glasgow, G12 8QQ, UK

² Centre for Cell Engineering, University of Glasgow, G12 8QQ, UK

INTRODUCTION: Damage to the central nervous system (CNS) severely impacts the ability of nerves to communicate and often leads to loss of neuronal function with the formation of an astrocytic scar. Currently there are few *in vitro* models to evaluate the pathological consequences of CNS injury, and most research in this field is based on lengthy, involved, and severe animal studies. Despite this, research into the repair of spinal cord injury (SCI) has seen significant progress, and it is now believed a combination of treatments (drugs, cells and scaffolds) may be sufficient to promote functional regeneration. The number of potential combinations of treatments (drug cocktails and cell transplantation) makes a reliable *in vitro* model for SCI highly desirable. We aim to develop an *in vitro* model of SCI using a previously developed CNS culture system in combination with microfabricated devices. These cultures produce a carpet of spinal cord axons when plated on a monolayer of neurosphere-derived astrocytes (NsAs) which become myelinated by oligodendrocytes. Our aim is to confine the cell bodies, align the axons on topographies and after myelination, cut these in a defined way, and follow axonal outgrowth and remyelination over time. Following establishment of the base-line repair status, a combination of reagents will be introduced to assess the most beneficial repair strategy.

METHODS: Spinal cord cells (from E15 SD rat embryo's) were cultured on a monolayer of neurosphere-derived astrocytes (obtained from the striatum of 1 day-old rat pups), on poly-L-lysine coated coverslips¹ for 22 days, the time required for myelination to occur. The CNS cultures were axotomised using a scalpel blade and the cells were allowed to recover for up to 15 days prior to immunofluorescence studies.

Multilayer structures for confinement and alignment are prepared in SU8 using photolithography.

RESULTS: Preliminary data show that, despite the cultures remained viable, detectable areas of demyelination and axon damage could be observed immunofluorescence, possibly affecting glial/axonal interactions and inducing apoptosis. Following recovery of the axotomised cells for a minimum of 5 days, large GFAP positive cells

(glial fibrillary acidic protein, an astrocyte marker) could be visualised within the induced lesions, suggesting an astrocytic response, and the formation of features typical of a glial scar (Fig. 1). In order to achieve a more organized morphology allowing easier measurement of axonal outgrowth, three-dimensional, micro-engineered constructs are currently being developed to align axons prior to axotomy, so as to allow the measurement of the effects of potential therapeutics on axonal outgrowth and repair (Fig. 2).

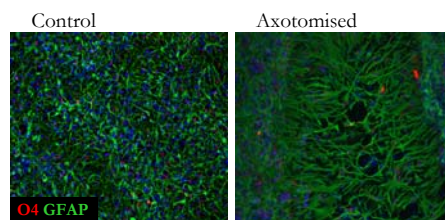


Fig. 1 Mixed CNS cultures (left) and when axotomised (right) and recovered for 5 days, stained for the presence of O4 (oligodendrocytes-red) and GFAP (astrocytes-green).

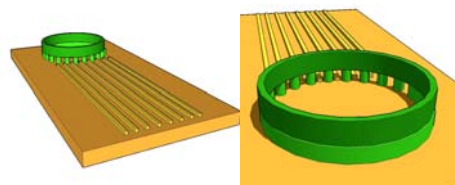


Fig. 2. The 3D-topography which will allow measurement of axonal outgrowth.

DISCUSSION & CONCLUSIONS: This *in vitro* model for CNS injury makes it possible to assess the pathological changes occurring during neuronal degeneration and will allow for combinatorial therapeutic approaches to be evaluated *in vitro*.

REFERENCES: ¹ A. Sørensen, K. Moffat, C Thomson, S.C. Barnett (2008) *Glia* **56**: 750-763.

ACKNOWLEDGEMENTS: We would like to thank the NC3Rs for support of this work, and EPSRC for funding of LR as part of the DTC in Proteomics and Cell Technologies.

An Injectable *In Situ* Solidifying Osteoinductive Scaffold for Bone Tissue Engineering

A Boussahel¹ & K Shakesheff¹

¹ *Tissue Engineering Group, School of Pharmacy, University of Nottingham.*

INTRODUCTION: The current aging population and the rise in the incidence of age related fractures pose a huge burden on the health services. Current therapies including the use of allografts and autografts are limited. An injectable *in situ* solidifying polymer based scaffold, which can be injected into cavities of irregular shape and size in a minimally invasive manner could offer a superior alternative. The scaffold could be designed to release BMP₂ *in situ*, while degrading and allowing the regeneration of bone tissues. The aim of this project was to develop an injectable scaffold formulation that could easily be injected at room temperature and hardened at body temperature, producing a scaffold with sufficient mechanical properties to withstand *in vivo* loading. The entrapment of protein molecules into PLGA [Poly(lactic-co-glycolic) acid] microspheres was also optimised. These particles were then used to prepare injectable scaffolds and the release of protein was determined over time.

METHODS: An *in situ* solidifying injectable scaffold was developed by changing the glass transition temperature of PLGA to 37° C, through the addition of Poly(ethylene glycol) (PEG). The PLGA/PEG microparticles were prepared by melt blending of PLGA with PEG and grinding. The particles were then mixed with saline to form a paste at room temperature, the injectability of which was investigated by controlling the particle size, shape and paste ratio. Additives such as Carboxymethylcellulose (CMC) were also considered. To mimic body conditions, the pastes were sintered at 37 °C, and the effect of particle size, paste ratio and sintering time on the compressive strength and the young's modulus of the scaffolds was determined. In addition to the adhesive PLGA/PEG particles, PLGA microspheres encapsulating three model proteins Lysozyme, HRP (horse radish peroxidase) and BSA (bovine serum albumin) were prepared using optimised water in oil in water emulsion (W/O/W) and solid in oil dispersion (S/O/W) methods. The injectable scaffolds were fabricated using either a combination of PLGA/PEG particles with PLGA microspheres encapsulating a protein or PLGA/PEG particles with plain PLGA microspheres.

These powder mixes were added to plain saline and saline containing a protein respectively and sintered at 37°C. For protein release studies, the formed scaffolds were placed at 37 °C in saline and the release monitored for three months.

RESULTS: The injectability studies revealed an important role of the factors investigated. For optimal injectability, spherical particles in the size range 100-400 µm should be used in a 1:1 paste with 0.5 % CMC. The resulting scaffolds sintered at 37 °C possessed mechanical properties close to human trabecular bone. The young's modulus of the scaffolds was found to increase with decreasing particle size and increasing PLGA/PEG particles content. It was also noted that after 24 hours of sintering, the scaffolds changed their behaviour and adopted a more elastic than a brittle structure. Protein encapsulation was optimised by investigating the role of multiple process parameters. Using W/O/W method the Polyvinylalcohol (PVA) concentration and additives such as sucrose were found to improve the encapsulation efficiency (EE%). On the other hand, the micronisation of proteins was considered to be the controlling factor for encapsulation using S/O/W. This was affected by freezing conditions and PEG molecular weight. The three investigated proteins were encapsulated to relatively high efficiencies; (65-85 %) and (35-55 %) using W/O/W and S/O/W methods respectively. The release of protein from scaffolds demonstrated a burst release at day 1 followed by a lag phase for 20 days, this was then followed by variable release kinetics.

DISCUSSION & CONCLUSIONS: Using PLGA/PEG particles and PLGA microspheres, an injectable formulation that hardened at body temperature forming a scaffold with optimal mechanical properties for bone tissue engineering was developed. Proteins could be encapsulated into PLGA microspheres to a high efficiency using both methods. Incorporating the protein in either the saline phase or the microspheres resulted in the same release pattern.

Differentiated MSCs Seeded in a Highly Dense Collagenous Matrix Produce Novel Biphasic Osteochondral Constructs

M. Brady^{1,2}, S. Sivanathan², P. Warnke² & V. Mudera¹

¹ UCL Tissue Repair & Engineering Centre, IOMS, Middlesex, HA7 4LP, United Kingdom

² Dept. of Oral and Maxillofacial Surgery, University of Kiel, 24105 Kiel, Germany

INTRODUCTION: Structural damage to both the articular cartilage and subchondral bone results in pain and disability for millions of people worldwide, representing a major clinical challenge. Being a hybrid of both bone and cartilage, requirements for osteochondral tissue engineering are more complex than previously investigated single tissue types. Novel methods of integrating bone and cartilage tissue constructs need to be explored. In this study, two hyper-hydrated collagen gels, containing osteogenic and chondrogenic cells, were integrated to create a biphasic osteochondral construct.

METHODS: Primary human MSCs, harvested from bone marrow of patients undergoing reconstructive surgery, were preconditioned in osteogenic (Ascorbic Acid, β -glycerophosphate, dexamethazone) and chondrogenic (TGF- β , ITS) media. These cells were then suspended in two separate collagen gels and integrated by partial setting. Upon complete setting, the resulting single gel was plastic compressed to produce a highly dense collagen sheet and spiralled (Brown *et al.*, 2005). The biphasic construct was then cultured for 7 days under static conditions. Cell labelling was used to track the osteogenic and chondrogenic cells. Von Kossa and Alcian Blue stains were performed to assess bone and cartilage matrix deposition. RT-PCR was used to assess gene expression of specific markers of bone and cartilage.

RESULTS: After 7 days in culture, cell tracking (osteogenic cells: green; chondrogenic cells: red) revealed no cell migration across the osteochondral boundary. Von kossa Staining revealed matrix mineralization by the osteogenic cells. Furthermore, GAG deposition by the chondrogenic cells was indicated by alcian blue staining. RT-PCR results showed that markers of bone (ALP, BSP, RUNX2) and cartilage (Aggrecan and SOX9) were expressed within the relative sections of the biphasic constructs.

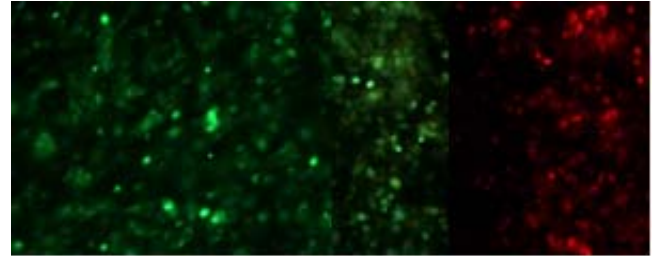


Fig. 1: Osteogenic cells (green) and chondrogenic cells (red) were tracked over 7 days and no migration over the osteochondral boundary was evident. Verifying two distinct 'bone' and 'cartilage' zones within the single biphasic construct.

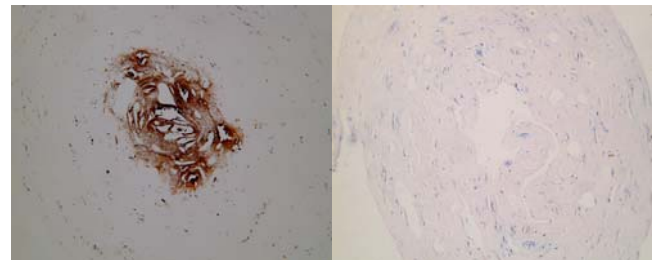


Fig.2: Von Kossa stain (left) showed evidence of matrix mineralization by the osteogenic cells and Alcian Blue stain indicated GAG deposition by the differentiated chondrocytes (right).

DISCUSSION & CONCLUSIONS: The aim of this study was to tissue engineer a biphasic osteochondral plug by integrating two cell phenotypes within a highly dense collagen matrix. Using bone (Von Kossa, ALP, BSP, RUNX2) and cartilage (Alcian blue, aggrecan and SOX9) markers, we have successfully demonstrated the formation of two distinct 'bone-like' and 'cartilage-like' zones to create a novel integrated osteochondral plug for clinical application.

REFERENCES: ¹ Brown RA, Wiseman M, Chuo CB, Cheema U and Nazhat SN. Ultrarapid Engineering of Biomimetic Materials and Tissues. *Adv. Funct. Mater.*, 2005, 15, 1762.

ACKNOWLEDGEMENTS: This research was funded by the EU within the framework of the MyJoint Project (FP-6 NEST 028861).

Osteogenic differentiation of human mesenchymal stem cells within a perfused bioreactor system.

JJ Campbell, E Maeda, SJ Ye, W Wang & DA Lee

School of Engineering and Material Sciences, Queen Mary University of London. Mile End Road, London E1 4NS

INTRODUCTION: Fluid flow induced shear stresses within long-bones provide an important mechanoregulatory signal to osteocyte and osteoblast cell populations as well as inducing osteogenic differentiation in mesenchymal stem cells (MSCs) [1-2]. A growing number of studies report the pro-osteogenic nature of oscillatory fluid flows on bone marrow progenitors maintained in monolayer cultures, typically within parallel plate flow chambers [3]. However, few studies have applied varying flow modalities and flow rates within 3D cultures more analogous to the *in vivo* microenvironment. This study utilized porous glass substrates to investigate the effects of continuous or oscillatory flow on human MSCs.

METHODS: Grade 1 porous glass (PG) was obtained pre-cut to cylindrical dimensions (9mm diameter, 2.5mm height) in order to fit 13mm Swinnex (Millipore) filter canisters. PG internal dimensions were analysed by μ CT and mercury porosimetry. Fluid flow within assembled PG-filter canisters was modelled using Fluent 6.2 software (Ansys UK Ltd, Sheffield UK) assuming a continuous flow rate of 100 mL/day. Passage 5 human mesenchymal stem cells (hMSCs, Cambrex BioSciences, UK) were seeded within acid washed sterilized PG and cultured for 24hrs prior to bioreactor assembly. A perfusion bioreactor was assembled from commercially available components comprising filter canisters perfused by individual syringe reservoirs mounted on a programmable syringe driver (PHD2000 series, Harvard apparatus, MA, USA) via gas-permeable silicon tubing (Fig 1). Osteogenic media, DMEM + 10%FCS, 10mM β -glycerophosphate, 10nM dexamethasone was used for all experiments. Applied flow rates comprised either a continuous flow (1mL/24hr), dynamic (0.5Hz) fluid flows at rates of 10mL/24hr or 1L/24hr, superimposed on the continuous flow, or a static control for a total duration of 4 and 8 days (Fig 2). Cell metabolism was analyzed before and after flow exposure by alamar blue reduction. Gene expression was assessed by real-time qPCR for osteogenic genes, osteocalcin, osteopontin, runx-2 and alkaline phosphatase. Genome-wide microarray analysis was performed using the Illumina human ref-6 expression system.

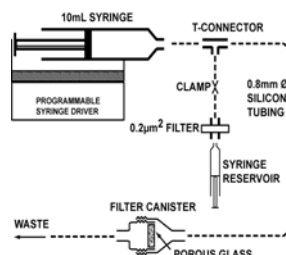


Fig 1. Schematic of fluid flow bioreactor system

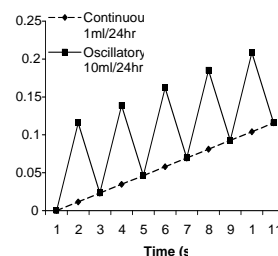


Fig 2. Volumetric media delivery with time.

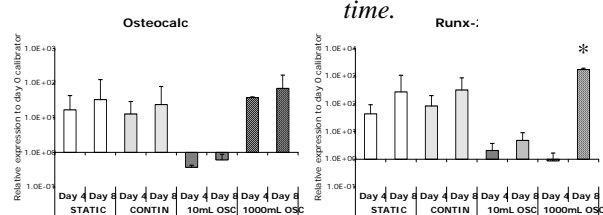


Fig 3. Temporal expression of indicated genes under static, continuous and oscillatory flow regimes. * indicates $p < 0.05$.

RESULTS & DISCUSSION hMSCs exposed to oscillatory fluid flows of 10mL/24hr and 1000mL/24hr (0.5Hz) exhibited a reduction in cell metabolism compared to cells exposed to either static or continuous flow regimes. Monotonic increases in all osteogenic genes were evident throughout the 8 day analysis period under all flow conditions. By day 8, runx-2 expression was significantly elevated under high (1000mL/24hr) oscillatory flows, equivalent to 1.3 dyne/cm² at the flow-exposed PG interface (Fig 3). Microarray analysis revealed that continuous and oscillatory fluid-flow environments applied to hMSCs results in significant alterations in differentiation-associated genes and various metabolic pathways when compared to static flow conditions. These experiments demonstrate a pro-osteogenic influence for oscillatory fluid flow applied within a robust well-characterized 3D environment that is suitable for long-term studies of this type.

REFERENCES: ¹J. Klein-Nulend, et al (2005) FASEB J, **9** 441-5. ²N. Datta, et al (2006) Proc Nat Acad Sci **103** 2488-93. ³N.N. Batra, et al (2005) J Biomech, **38** 1909-17.

ACKNOWLEDGEMENTS: BBSRC.

Sourcing Cells For Intestinal Tissue Engineering – Differentiating Embryonic Stem Cells To The Intestinal Precursor Fate

D A Carter¹, L Buttery¹, V Sottile² & FRAJ Rose¹

¹ *Division of Drug Delivery & Tissue Engineering, School of Pharmacy.*

² *School of Clinical Sciences.*

^{1,2} *Centre for Biomolecular Sciences, University of Nottingham, NG7 2RD.*

INTRODUCTION: To differentiate embryonic stem (ES) cells towards the intestinal precursor fate *in vitro* the signals that cells are exposed to during *in vivo* development must be mimicked. The growth factor Activin-A (Act-A) has been shown to selectively differentiate ES cells towards the endodermal germ layer from which the visceral organs, including the intestine, arise [1, 2, 3]. Co-culture of ES cells with appropriate early stage embryonic tissue, where inducing signals are present, has also been shown to promote differentiation towards a particular fate [4, 5, 6].

METHODS: The purpose of this study was to direct the differentiation of murine ES (mES) cells using a dual approach. Firstly mES cells were directed towards the (definitive) endoderm fate by *in vitro* treatment with Act-A in culture. The cells were then further differentiated towards the intestinal epithelial stem cell (ISC) fate by *ex vivo* co-culture with day 6 embryonic chick gut tissue explants. For the initial phase of the treatment, we compared the efficiency of several culture conditions to promote the expression of selected endodermal markers including *FoxA2* & *Sox17*. GAPDH was included as a ubiquitously expressed control. In the 2nd phase the expression of the ISC markers *Lgr5* [7] & *Mushashi-1* (*Msi-1*) [8] was examined following co-culture with embryonic chick tissue as was the expression of CD133, a marker associated with adult stem cell populations.

RESULTS: The strongest expression of *FoxA2* & *Sox17* was detected in ES cells cultured in monolayer for 2 days, as Embryoid Bodies for 3 days & in monolayer for a further 9 days with Act-A present throughout (Fig 1). A population of undifferentiated cells remained in all conditions.

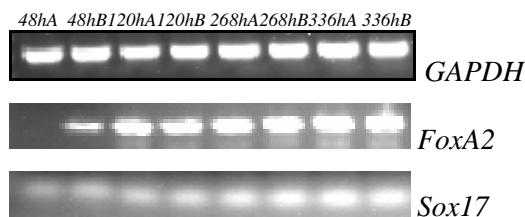


Fig. 1: Expression of markers of (definitive) endoderm through the course of *in vitro* treatment with Act-A evaluated by RT-PCR.

The expression of the selected markers has also been observed at the protein level following immunohistochemical analysis (data not shown). Furthermore, expression of *Lgr5*, CD133 & *Mushashi-1* was observed at the RNA level following the 7 day co-culture phase with embryonic chick gut tissue. A small population of cells remained undifferentiated.

Control Co-culture

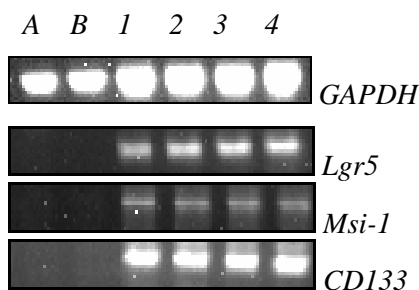


Fig. 2: Expression of markers of ISC following 7 days co-culture with embryonic chick gut tissue evaluated by RT-PCR.

DISCUSSION & CONCLUSIONS: Expression of *FoxA2* & *Sox17* in the treated cells indicated differentiation towards the (definitive) endoderm fate [2, 3].

The expression of *Lgr5*, *Msi-1* & CD133 in the cells post co-culture indicated that a population of ISC-like cells was being produced.

REFERENCES: 1 Kubo (2004) *Development* 131:1651-62. 2 Yasunaga (2005) *Nature Biotechnology* 23(12):1542-50. 3 D'Amour (2005) *Nature Biotechnology* 23(12):1534-41. 4 Van Vranken (2005) *Tissue Engineering* 11:1177-87. 5 Fair (2003) *Surgery* 134:189-96. 6 Sugie (2005) *Biochemical & Biophysical research communications* 332:241-7. 7 Barker (2007) *Nature* 449:1003-8. 8 Potten (2003) *Differentiation* 71: 28-41.

ACKNOWLEDGEMENTS: Thankyou to the BBSRC for funding this work.

Microstructure and nanomechanical characterization of tissue engineered bone deposited on titanium alloy scaffolds

J. Chen^{1,3}, M.A. Birch², S.J. Bull¹, S. Roy¹

¹ School of Chemical Engineering and Advanced Materials, Newcastle University, UK

² Institute of Cellular Medicine, The Medical School, Newcastle University, UK

³ School of Engineering and Materials Science, Queen Mary University of London, London UK

INTRODUCTION: The clinical success of an orthopaedic implant is strongly related to its osseointegration which depends on several factors including surface characteristics. Electropolishing is a cost effective approach to modify the surface of metals such as titanium and our work has identified how TiAl6V4 modified in this way can influence osteoblast differentiation and bone formation. In this study, we investigate the microstructure and nanomechanical response of bone formed *in vitro* on unmodified and electropolished Ti alloy.

METHODS: Sprague-Dawley rat osteoblasts were isolated by sequential enzymatic digestion. Cells were plated onto the surface of the titanium alloy (untreated and electropolished at 9v in 3M sulphuric acid in methanol for 30s) and cultured for up to 35 days. Throughout the course of the experiments the cultures were fed every three days with osteogenic media (containing β -glycerophosphate, L-ascorbic acid and dexamethasone). The morphology and microstructure of the bone was characterized by environmental scanning electron microscopy (ESEM) and atomic force microscopy (AFM). Chemical composition was analyzed by energy dispersive X-ray (EDX). The nanoindenter with *in-situ* AFM was used to assess the nanomechanical response of the mineralized matrix.

RESULTS: ESEM analysis of the surfaces (Fig.1) reveals characteristics of the bone-like matrix that was formed. Rose-like microstructures were observed in the mineralised matrix formed on electropolished Ti alloy (Fig.1a), which provides clear evidence of woven bone. The agglomeration of crystal structures with average diameter \sim 800nm (so-called calcospherulites [1]) on both surfaces was also observed in AFM images. The calcospherulite is regarded as a representative element of the bone. EDX analysis of the deposited matrix revealed high concentrations of Ca and P which indicate that mineralization has taken place. The ratio of Ca/P for bone grown on electropolished surface was higher.

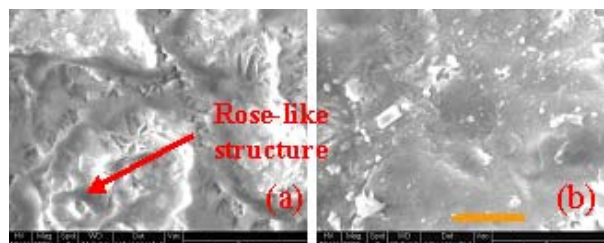


Fig. 1: ESEM image of bone on (a) treated and (b) untreated surface. Scar bar is 5 μ m.

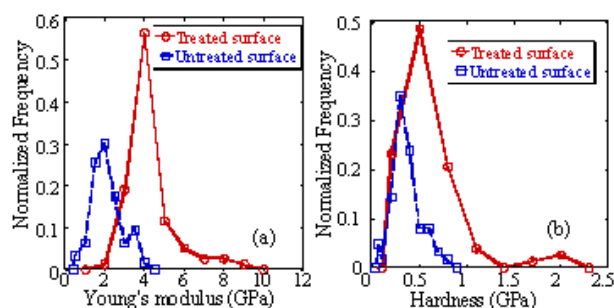


Fig. 2: The statistical distribution of the (a) Young's modulus and (b) hardness for the tissue engineered bone.

Nanomechanical characterisation of the mineralised matrix showed that the average values of Young's modulus and hardness increase on the electropolished surface compared to the untreated Ti alloy (Fig.2).

DISCUSSION & CONCLUSIONS: The measured Young's modulus and hardness values are reasonable compared to those in the literature [2-3]. The electropolished surface enhances the mineralization and adhesion between bone and the scaffold, therefore, the mechanical properties of the bone improves. This study also demonstrates that nanoindentation with *in-situ* AFM imaging is very useful to identify and characterize small features (such as calcospherulite) which is not easily achievable by other techniques.

REFERENCES: ¹ R. J. Midura et al (2007) *Bone* **41**:1005. ²A. Chiou et al (2005) *Journal of Bone and Mineral Research* **20**: 2002. ³ B. Chaudhry et al (2009) *J Mater Sci: Mater Med* **20**:257.

Role of surface nickel content on human cell cytoskeleton formation on Nitinol

W. Chrzanowski¹, J. Szade², A.D. Hart³, D.A. Armitage⁴, M.J. Dalby³, and J.C. Knowles⁵

¹*Mech. Eng. Dep., James Watt South Building, University of Glasgow, Glasgow G12 8QQ*

²*University of Silesia, Institute of Physics, ul.Uniwersytecka 4,40-007 Katowice, PL*

³*Centre for Cell Engineering, Joseph Black Building, University of Glasgow, Glasgow G12 8QQ*

⁴*De Montfort University, Leicester School of Pharmacy, The Gateway, Leicester, LE1 9BH, UK*

⁵*UCL Eastman Dental Institute, 256 Gray's Inn Road, London WC1X8LD*

INTRODUCTION: Cell activity on an implant surface can be modulated by cues such as topography, chemistry or stiffness^(1,2). For Ni-Ti alloy this is achieved mainly by alteration in chemistry. However, high nickel concentrations may be a concern in the use Nitinol on a larger scale. Current reports on Nitinol bring contradictory data⁽³⁻⁵⁾ suggesting that high nickel content is not particularly dangerous and nickel-titanium alloys are safe to be used. On the other hand it was shown that nickel has a toxic effects on cells⁽⁶⁾. Nevertheless, shape memory effects and pseudo-elasticity could support different treatments (e.g. scoliosis) and currently, Nitinol is used to produce porous foams and coatings (Actipore™), pins, clamps and intramedullary nails. In this paper authors investigated a role for nickel surface concentration on influencing cell behaviour e.g. cytoskeleton formation and organization *in vitro*.

METHODS: NiTi samples were ground on SiC paper to a mirror finish and washed. Three groups of samples were prepared: thermally oxidised at 400°C in air for 1 h (TO); alkali treated in 10M NaOH (24 h, 80°C), then heat treated at 600°C in air for 1 h (BNT); and plasma cleaned for 1 h (PC). To assess chemical composition the XPS analysis were conducted. To investigate role of the nickel (high vs. low surface content) on formation and organization of the cytoskeleton samples were cultured with primary human cells (osteoblasts) for 3 days and stained for actin, tubulin and nuclei.

RESULTS: Surface chemistry tests showed that TO samples had surfaces composed of TiO₂ and nickel oxides – *Table 1*. The chemical treatment resulted in significant increase in Ni concentration on the top layer, and drop in Ti content. Both elements were oxide forms. Relatively high level of carbon contamination (28%) was observed after the chemical treatment. Plasma cleaning resulted in similar content of Ni and Ti that was observed for TO samples and both elements were observed in oxide states. Fluorescent staining showed that the cells cytoskeleton was well developed on all tested samples. Actin stress fibers were formed primarily in the cell periphery (Fig. 1). For TO samples dense actin stress fibre network was also observed

in the cytoplasm region. Tubulin appeared well organized, forming radiating fibres out from the organizing centre beside the nucleus. No significant difference in cell spreading was observed for all tested samples.

Table 1. Nickel and titanium content (XPS).

	Ni (wt. %)	Ti (wt. %)
TO	6.12±3.01	20.07±0.28
BNT	20.23±0.46	1.37±0.1
PC	7.60±0.57	17.36±0.14

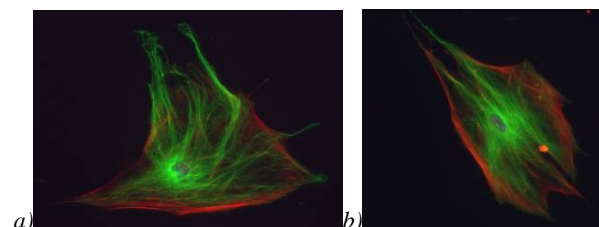


Fig. 1 Fluorescence images of actin (red) and tubulin (green) cytoskeleton: a) 400, b) BNT.

DISCUSSION & CONCLUSIONS:

Concentration of nickel causes the main concern for wider applications of Nitinol in medicine. The present study showed that high nickel content and different types of oxide layers on Nitinol do not alter cytoskeletal formation and organisation. This suggested that cell behaviours on Nitinol are not directly linked to the nickel surface content or its release, which was different for the tested samples⁽⁵⁾. Furthermore, prolonged test are currently undergoing to confirm the findings.

REFERENCES: ¹Dalby MJ. Medical Engineering & Physics 2005; 27(9):730-42. ²AJ Engler, S Sen, et. al. Cell 2006; 126(4):677-689. ³MF Chen, XJ Yang, et al. Mat. Sc. & Eng:C 2004;(24 (4)):497-502. ⁴W Chrzanowski, EAA Neel, DA Armitage, JC Knowles. A. Biomaterialia 2008; 4(6):1969-84. ⁵S Shabalovskaya, J Anderegg, et.al. A. Biomaterialia 2008; 4(3):447-67. ⁶VC Dinca, S Soare, A Barbalat, et.al Applied Surface Science 2006; 252:4619-4624.

Advances in micro-fabrication: from 2D to 3D PDMS scaffolds for tissue engineering applications

B Cortese¹, M Riehle², Stefania D'Amone, and Giuseppe Gigli

¹ National Nanotechnology Laboratories of CNR-INFN, Distretto Tecnologico, [NNL](#), Università del Salento, Italy

² [Centre for Cell Engineering](#), Institute of Biomedical and Life Sciences, University of Glasgow, U.K.

INTRODUCTION: One of the principal challenges facing the field of tissue engineering is the creation of three dimensional scaffolds resembling a natural tissue environment [1]. While many surfaces used in biological systems are formed in two dimensions, 3D structures will increase the complexity of the constructs, bringing them closer to mimicking the complexity found in nature. The present work describes the progress made in developing polydimethylsiloxane (PDMS) constructs to control cell motility from 2D surfaces to a third dimension.

METHODS: Substrates were fabricated by simply replicating patterned SU-8 masters with a mixture of PDMS 10:1, (Sylgard 184 Silicone Elastomer Kit, Dow Corning, Midland, MI), which was cured at 80° for 1 h, and subsequently easily peeled off the mould. The 2D PDMS substrates were obtained by combining a 50:1, soft membrane with micro-patterned stiffer substrates; while three dimensional (3D) tubular scaffolds comprising multiple levels of pore-textured grooves were obtained straightforwardly by simply rolling the micro-structured sheet without mechanical aid due to the elasticity of PDMS.

RESULTS: The 2D structure was obtained as previously described [2]. A thin soft membrane was bonded on a patterned substrate enabling a gradient rigidity while presenting uniform substrates without physical or chemical limitations, as shown in Figure 1.

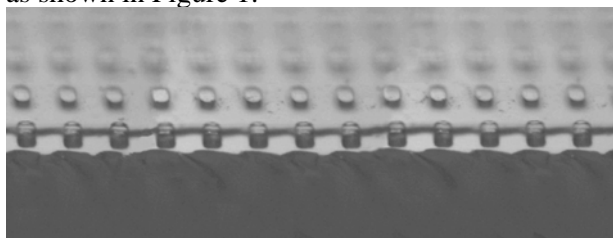


Fig. 1: Optical image of 2D PDMS structure made of a thin soft membrane bonded to a patterned substrate.

The 3D scaffold was achieved by simply spin coating uncured PDMS on a three level SU-8 photoresist master (of 10, and 60 μm lines, of different heights), which once cured was subsequently rolled in a tubular form.

DISCUSSION & CONCLUSIONS: It is known that cellular response to environmental cues is complex. Within 2D substrates, physical changes due to gradient rigidity played an important role in cell motility and functionality, with a net migration of cells towards stiffer regions, represented by the underlying patterns [2]. This work presents the progress in the development of a PDMS structure for the control of cell environment. The need to control cell motility while mimicking the cellular environment has brought to the development of a 3D multi-layered micro and nano structure which can direct cell adhesion and proliferation, and can increase the functionality and engraftment capacity.

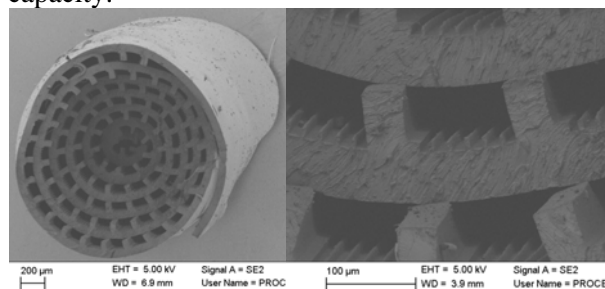


Fig. 2: Sem image of 3D PDMS multilayered structure made of a rolled up multi-structure .

The novel multi-layered structure combines micro features on different levels for simultaneous control and direction of cells. In addition to a precise, controlled, and reproducible micro-structure, the flexibility and elasticity of PDMS texture may provide the scaffold with an even higher degree of stimulation for tissue engineering. Besides, the manufacturing technique used in this study will facilitate and improve the development of 3D structures for other applications and functionalities such as guiding nerve regeneration.

REFERENCES: ¹ K. Seunarine, D.O. Meredith, M.O. Riehle, et al (2008) *Microelectronic Engineering* **85**:1350-54. ² Cortese, B, Riehle M, Cingolani Roberto et al (2008) *European Cells and Materials* **16**:44.

ENGINEERING BIO-SURFACES FOR CELL ADHESION.C. Cuestas-Ayllón¹, A. Glidle³, G. McPhee³, V. Grazi¹, M. Riehle⁴ and J. M. de la Fuente¹, H. Yin³¹Instituto de Nanociencia de Aragón, Universidad de Zaragoza, Zaragoza, Spain³Electronics & Electrical Engineering, University of Glasgow, UK⁴Centre for Cell Engineering, University of Glasgow, UK.

INTRODUCTION: In natural habitats, the chemistry of the matrix surrounding cells is heterogeneous, with well-designed nanometric arrangements of different motifs that play a role in cell recognition processes. These include “RGD” peptide sequences and the carbohydrates in glycosamino-glycans. Understanding the influence of these arrangements on cell function will have a profound impact in developing biomaterials that induce desired cellular responses.

Convergence of advances in chemistry and microengineering has made possible the micro- and nanoscale definition of specific surface chemistries. In this work, we exploit the robust “click chemistry” (Cu (I) catalyzed Azide-Alkyne reaction¹) and photo-lithography to develop a patterned surface with generic bioactive motifs. Ultimately, this will enable the generation of defined RGD and carbohydrate microstructures for cellular studies.

METHODS: To generate azide terminated surfaces, plain or micropatterned glass substrates were treated with 2% of 3-glycidoxypropyl-trimethoxysilane solution in anhydrous toluene for 2h, followed by immersion in 10 mM O-(2-Aminoethyl)-O’-(2-azidoethyl)heptaethylene glycol in DI water for 2h. After rinsing and stripping off the photoresist pattern with acetone, the surface was modified with various alkyne derivatised molecules (fluorescein, RGD and mannose) by performing a “click reaction” in 0.1M NaCl solution (20min)².

RESULTS: The reactive epoxy groups were utilised for two purposes: generation of azide bearing motifs prior to the click reaction, and conjugation with commonly used non-adhesive linkers (e.g. amino-terminated PEG) to prevent cell adhesion in the “non-click” modified areas.

To evaluate the actual functionality of surfaces following these reactions, C (1s) and N (1s) XPS measurements were performed. These show that the epoxy, PEG, azide and alkyne motifs were successfully attached on the glass surface at different stages. For example, the success of the azide modification is shown in Fig. 1, in which peaks corresponding to partially charged nitrogen

centres in the azide surface shift in binding energy following the click cyclisation reaction.

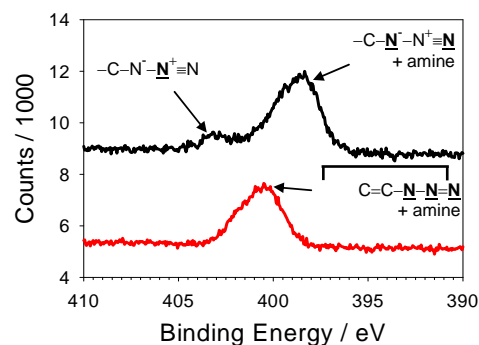


Fig. 1: N (1s) XPS spectra for azide-terminated surface (black trace) and then after “click reaction” with alkyne derivatised fluorescein (red trace).

Fluorescence images (Fig.2) of micropatterned surfaces further demonstrate the reactivity and uniformity of the click generated alkyne fluorescein surface.

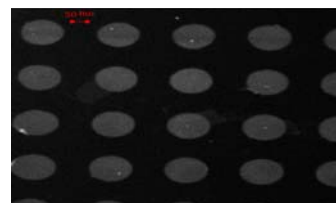


Fig.2: Fluorescence image of micropatterned azide surface after click reaction with alkyne-fluorescein.

Initial cell culture experiments show that 3T3 fibroblasts have minimal attachment on PEG and azide surfaces but spread well on others.

DISCUSSION & CONCLUSIONS: Micro-structured surfaces for quantitative and selective attachment of biomolecules has been developed using “click chemistry” in conjunction with microfabrication. Initial cellular evaluations show that the method is highly efficient in generating patterns of different surface chemistries that might modulate cell attachment and proliferation.

REFERENCES: ¹ H.C. Kolb et al., *Angew. Chem. Int. Ed.* 2001, 40, 2004. ² R.Kumar et al., *J. AM.Chem. Soc.* 2007, 129, 6859-6864.

ACKNOWLEDGEMENTS: This work has been supported by MEC and ARAID. HY is supported by the Royal Society of Edinburgh.

A Novel Technology to Concentrate Therapeutic Cells from Bone Marrow Aspirates

JN Ridgway¹, A Horner¹, A Butcher¹, JT Watson², SJ Curran¹

¹ Smith & Nephew Biologics and Spine, York Science Park, Heslington, York. ² St Louis University, Dept. of Orthopaedic Surgery, St Louis, MO, USA

INTRODUCTION: Bone marrow is rich in osteogenic progenitor cells with potential to enhance bone healing. However, clinical use of BMA has highly variable outcomes as aspiration techniques yield marrow diluted with peripheral blood. To address this issue Hernigou et al (2005) performed clinical studies using concentrated BMA, demonstrating that reliable healing occurs when osteoprogenitor cells exceed 1000 colony forming units per ml. Currently BMA concentration depends upon centrifugation or cell capture onto graft material, requiring capital equipment or limiting application to open grafting procedures. To address these issues we have developed a stand alone, single use, disposable automated filtration device allowing rapid concentration and recovery of nucleated cells from BMA.

METHODS: Our BMA concentrator utilizes controlled vacuum pressure and acoustics to maintain steady state filtration. Volumes of Human BMA (Lonza, Rockville MD) ranging from 5ml to 45ml were processed through the device. Nucleated cell number was determined using a Coulter Counter, cell viability using a Guava EasyCyte and osteoprogenitor and stem cell number by CFU assays.

RESULTS: The time for each run, irrespective of starting volume was under 15 minutes. There was a linear relationship between BMA volume reduction and total nucleated cell (TNC) concentration, up to 8 fold volume reduction. Samples with >4 fold volume reduction (our target clinical minimum) showed a mean recovery of 93.2% TNC. The linear relationship between volume reduction and TNC concentration was lost at >9 fold volume reduction with recovery of TNC falling to 69%. TNC viability in all samples remained in excess of 95% irrespective of volume reduction. The number of CFU-f and CFU-ob/ml of aspirate increased linearly versus volume reduction. Interestingly, CFU/CFUOb recovery remained above 90% at >9 fold volume reduction, the point where TNC recovery was seen to fall.



Fig 1 BMA filtration prototype pre (left) and post (right) use

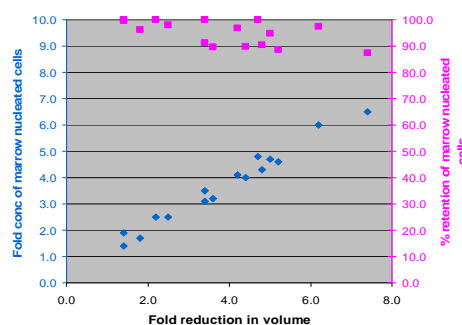


Fig 2 BMA concentration and TNC concentration

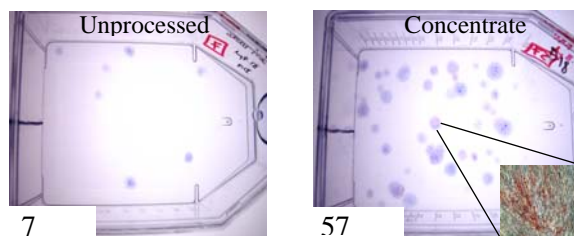


Fig 3 CFU assay before and after processing

DISCUSSION & CONCLUSIONS: The data show our device rapidly and consistently concentrates the therapeutic cell containing TNC fraction of BMA. Rapid processing times and automated functioning are key features for intra-operative application of this device to enhance bone healing.

REFERENCES: Hernigou P, et al. Percutaneous autologous bone-marrow grafting for nonunions. Influence of the number and concentration of progenitor cells. J Bone Joint Surg 2005; 87-A (7):1430-1437.

Distinct responses of stem cells to BMP12 and BMP13 during in vitro tenogenesis

T. Dale¹, N. Maffulli², A.E. Haj¹ & N.R. Forsyth¹

¹ *Guy Hilton Research Centre, Keele University Medical School, Stoke-On-Trent ST4 7QB, UK*

² *Barts and The London School of Medicine and Dentistry, London E1 4DG, UK*

INTRODUCTION: There are approximately 2 million Achilles tendon sports-related injuries each year worldwide. Of these, over 250,000 require surgical intervention and prolonged rehabilitation. The poor repair of the tendon is a direct consequence of its limited blood supply and poor cell content. To overcome this limitation, direct strategies are required to provide alternative clinical remedies. We have examined whether non-specialized human stem cells (embryonic and marrow stromal) can be induced into becoming specialized tendon-like cells through growth factor supplementation (BMP12 and BMP13) and oxygen tension modulation.

METHODS: Primary tenocytes, marrow stromal cells (MSC) (1st or 2nd passage), and embryonic stem cells (SHEF1 and SHEF2) of human origin were maintained in appropriate basal media in either standard hyperoxic (21% O₂, 7% CO₂) or normoxic (2% O₂, 7% CO₂) conditions (RS Biotech, Irvine, UK). Growth factor induction (BMP12, BMP13, and BMP12/BMP13) was performed triplicate in 96-well plate formats where 0, 3, 10, and 30 ng/ml concentrations were used on cells plated at either High (1-2X10⁴) or Low (1-2X10³) densities. Cells were fixed at Days 0, 1, 5, 10, 20 and 40 and examined histologically using either Alcian Blue (proteoglycans) or Masson's Trichrome (collagen, elastin). Normalised image analysis of wells was performed using Image J (NIH). Statistical analysis was performed using Excel.

RESULTS: Quantification of histological staining revealed that all cell types displayed distinct growth factor-induced profiles (Figure 1 and Table 1). This profile was entirely oxygen-reliant. Tenocytes underwent differentiation with either BMP13 (21% O₂, Low Density) or BMP12/BMP13 (2% O₂, High/Low Density). MSC were responsive to all growth factors in 2% O₂ when plated at high density but non-responsive in 21% O₂. hESC displayed a more varied response profile. All growth factors induced differentiation in 21% O₂ High Density but only BMP12/BMP13 induced a response in 2% O₂.

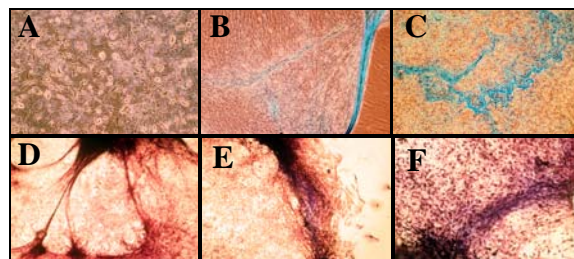


Fig. 1: Representative images of Tenocyte (A), MSC (B), and hESC (C) stained with Alcian Blue or Masson's Trichrome (D-F all hESC) after 40 days differentiation.

Table 1. Overview of Tenogenic Differentiation.

Cell Type	O ₂	Density	BMP12	BMP13	BMP12+ BMP13
Teno cytes	21	High	-	-/+	-
		Low	-	+	-
	2	High	-	-	+
		Low	-	-	+
MSC	21	High	-	-	-
		Low	-	-	-
	2	High	+	+	+
		Low	-	-	-
hESC	21	High	+	+	+
		Low	-	-	-
	2	High	-	-	+
		Low	-	-	-

DISCUSSION & CONCLUSIONS: The signalling pathways required for in vivo tenogenic differentiation are complex. In addition the biochemical cues required for in vitro tenogenesis are poorly defined. Here we have demonstrated that 1) tenocytes can be induced to terminally differentiate with growth factors (BMP12 and/or BMP13), that 2) MSC are histologically non-responsive to either BMP12 or BMP13 in standard conditions, and that 3) for the first time hESC are responsive to BMP12 and BMP13 induction. The natures of these histological changes remain to be determined by further molecular analysis. This research will ultimately improve our understanding of the conditions required for tenogenesis.

ACKNOWLEDGEMENTS: We wish to acknowledge RS Biotech, AOFAS and the North Staffordshire Medical Institute for their support in performing this research.

The Influence of Penetratin and/or Magnetic Field on Magnetic Nanoparticle Uptake *in vitro*

T Dejardin, C-A Smith and C C Berry

Centre for Cell Engineering, Department of Micro Cell Biology, University of Glasgow UK.

INTRODUCTION: One of the more commonly researched types of nanoparticles with regards to bioapplications is magnetic nanoparticles (mnps), which are commonly used in MRI and more recently targeted magnetic drug delivery and cell transfection (magnetofection) [1, 2]. In this study we investigate the uptake of commercially available mnps against those derivatised with a cell penetrating peptide (penetratin; derived from the homeodomain of Antennapedia protein) [3] both in the presence and absence of an 8mT magnetic field.

METHODS: Fluorescent iron oxide particles (Chemicell, 500nm) were functionalised with penetratin and prepared at an experimental concentration of 0.01mg/ml. Infinity telomerase primary human fibroblasts (h-TERT BJ1, Clontech Labs. USA) are seeded onto 13mm diameter coverslips at a density of 1×10^4 cells per discs in 1ml of complete medium. In all experiments cells were incubated with plain & penetratin derivatised nps \pm magnetic field (8mT).

Cell Viability: Cell viability was assessed using calcein AM and ethidium homodimer, with cells observed using fluorescence microscopy. **Cellular Uptake:** Cells were fixed, observed by fluorescence microscopy, and Image J used to determine the best incubation time for further experiments. **SEM:** Cells were fixed and processed for SEM. **Cell Immunofluorescence:** Cells were fixed and immunostained for F-actin & anti-clathrin or anti-caveolin for uptake mechanisms. The samples were viewed by fluorescence microscopy and intensities determined via Image J. **Western Blots:** Samples were then freeze/thawed to lyse cells and run Western blot for both clathrin and caveolin.

RESULTS: No toxicity effects were observed at any concentrations. Over the hour incubation time course without the magnetic field, penetratin nps clearly indicated uptake after 1 minute incubation, steadily increasing with time, however plain np uptake was minimal. The magnetic field significantly increased uptake of both nps compared to no field. In this case plain np uptake was totally random, with nps spread all over the coverslip surface; conversely penetratin np uptake

was cell specific with nps appearing clustered in the perinuclear area. SEM images indicated clear cell membrane response to all np treatments, with F-actin blebbing (fig. 1) and many filopodia as compared to control cells. With regards uptake mechanisms, both caveolin and clathrin appeared increased with penetratin np uptake, both \pm magnetic field, suggesting both were involved. With almost no uptake observed without a field for plain nps, under the field, minimal uptake was noted and appeared co-localised with clathrin as opposed to caveolin.

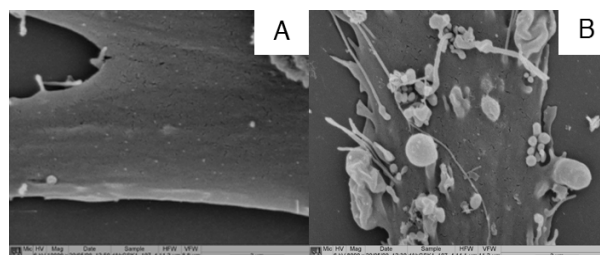


*Fig.1. H-tert cells incubated 5min 37°C, 5%CO2
A: Control B: with Penetratin-mNPs*

DISCUSSION & CONCLUSIONS: Application of an 8mT magnetic field produced a strong influence on uptake, particularly on plain nps, without which uptake was almost non-existent. Penetratin clearly enhanced cell specific uptake, both \pm magnetic field. Interestingly, uptake appeared to be dependent on both clathrin and caveolin. Results clearly indicated that whilst magnetic fields do pull nps into cells, the uptake is random. Results further showed that the use of a cell penetrating peptide such as penetratin effectively enhanced cell specific uptake with no effect on cell viability. It is thus suggested that the use of such peptides should be adopted in future magnetic targeting and magnetofection bioapplications [4].

1. Berry CC. & Curtis ASG. *J Phy D: Appd Phy* 36; 198-206 (2003).
2. Lubbe AS. *et al. J Surg Res* 95; 200-6 (2001).
3. Lundberg P. & Langel U. *J Mol Recognit* 16; 227-33 (2003).
4. Berry CC. *Nanomed* 3; 357-365 (2008)

ACKNOWLEDGEMENTS: I thank the team of the CCE, particularly Andy Hart, for their kindness and their collaboration to this project.

Smart culture of mouse embryonic stem cells on thermo-responsive polymers

Sabrina Dey¹, Morgan Alexander², Barrie Kellam³, Cameron Alexander¹, and Felicity RAJ Rose¹

¹ Division of Drug Delivery and Tissue Engineering, ²Laboratory of Biophysics and Surface Analysis, ³Division of Medicinal Chemistry and Structural Biology. School of Pharmacy, The University of Nottingham, University Park, Nottingham, NG7 2RD, UK.

INTRODUCTION: Current cell culture methods of mammalian cells use trypsin as means to detach them from the culture surface. This inflicts damage to cell membrane receptors (mainly integrins)¹ as well as the potential of contamination if cells were to be used for clinical applications e.g. mouse embryonic stem cells (mESCs). The application of thermo-responsive surfaces² for controllable attachment/detachment of mouse ESCs using 2-(2'-methoxyethoxy) ethyl methacrylate-co-oligo(ethyleneglycol) methacrylate (poly (MEO₂MA-co-OEGMA)), for a potential method to manipulate embryonic stem cells in culture without the use of enzymes and feeder layers (Figure1).

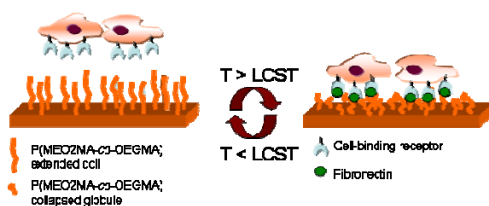


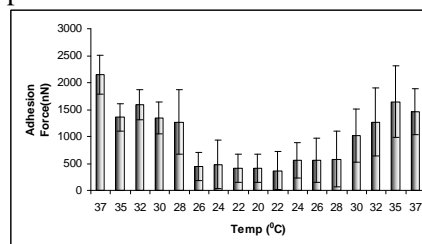
Fig. 1: Use of thermo-responsive surfaces to culture mammalian cells.

METHODS:

Polymer grafting of thermo-responsive polymers: poly (allyl-alcohol) plasma coated glass cover slips were treated with 2-bromoisobutyryl bromide in the presence of THF and triethylamine anhydrous. (Atom Transfer Radical Polymerisation; ATRP) was carried overnight. Cover slips were then washed with THF and cold water prior to surface analysis or cell culture. **Cell response on the thermo-responsive surfaces:** Prior to mouse embryonic stem cell culture, the surfaces were incubated with 5ug/ml fibronectin at 37°C overnight. Feeder free mES cells (E14Tg2A Line) were cultured on these surfaces in DMEM containing 15% FCS and 100 uL/ml LIF, at 37°C, 5% CO₂ in air.

RESULTS and DISCUSSION: WCA measurements and adhesion force-curve measurements using AFM below and above the lower critical solution temperatures (LCST) indicated that poly (MEO₂MA-co-OEGMA), grafted brushes had a reversible temperature switching behaviour from hydrophobic at 37°C to

hydrophilic at 20°C and revealed that switching is reversible influencing the wettability of the surface. mESC were cultured on fibronectin coated surfaces at 37°C and were observed to adopt a similar morphology as seen on gelatine treated tissue culture polystyrene (control). Cells detached from the thermo-responsive grafted surfaces when the temperature was lowered to 10°C.



CONCLUSIONS: We have shown that Poly (MEO₂MA-co-OEGMA) was grafted successfully

Fig. 2: Adhesion force-curve of the surface studied at different temperatures (Above and below LCST).

Embryoid bodies formation Attachment (37°C) Detachment (10°C)



Fig. 3: Feeder free mouse embryonic stem cell response on poly (MEO₂MA-co-OEGMA). 1. Formation of Embryoid bodies on poly (MEO₂MA-co-OEGMA). 2. mESCs attachment to the surface after treatment with fibronectin at 37°C. 3. Detachment from Poly (MEO₂MA-co-OEGMA) grafted surfaces below LCST. (bars: 100µm)

from the surface. 3T3 fibroblasts and mESCs adhered, spread at 37°C and detached when the temperature was lowered to below LCST. These attachment-detachment cycles could be performed at least three times and hence this could be used as a passaging tool for stem cells.

REFERENCES: ¹Charity Waymouth. *In vitro*.1974;10;97-111. ²Teruo Okano *et al.* *Makromol. Chem., Rapid Commun.*1990; 11, 571-576. ³Lutz, J.F. and A. Hoth, *Macromolecules*, **2006**, 39(2), 893.

ACKNOWLEDGEMENTS: This work is funded by the Algerian Government.

DEVELOPING A 3-DIMENSIONAL BIODEGRADABLE CONSTRUCT FOR THE TREATMENT OF SPINAL CORD INJURY

P. Donoghue*, R. Lamond*, T. Lammel, N. Gadegaard, M. Riehle & S.C Barnett

University of Glasgow.

INTRODUCTION: Following disease or injury, the central nervous system fails to regenerate competently, resulting in functional deficits. In particular, spinal cord injury (SCI) leads to the formation of a glial scar, which is inhibitory to axonal outgrowth, presenting a physical and molecular barrier to regeneration. One strategy to enhance repair is cell transplantation which promotes the in-growth of many axons but these are unaligned and infrequently exit the graft. Previous studies have shown that 2D biodegradable constructs with micro grooves can be used to provide a suitable growth substrate allowing axons to align *in vitro* (Sorensen et al., 2007). We aim to modify these constructs into biocompatible 3D scaffolds (Seunarine et al., 2006), with aligned pores to aid diffusion of trophic factors for transplantation *in vivo*. Initially we will develop optimal parameters of depth, pore, and topography *in vitro* using a culture system of glia and axons to mimic the intact CNS.

METHODS: *Preparation of flat poly-ε-caprolactone (PCL) constructs:* PCL sheeting was hot embossed using quartz templates etched with multiple parallel microgrooves with various widths (100µm, 50µm, 25µm, 12.5µm). The microgroove patterns were either 5µm or 10µm deep.

Preparation of the PCL constructs for investigating the effect of pores upon axonal alignment: Constructs were prepared by spin coating 25% PCL dissolved in chloroform on a blank or pillared silicon wafer to produce non-porous and porous membranes respectively. Each membrane was hot embossed with an aligned topography, before being transferred to 13mm diameter Minusheets.

Rat spinal cord cultures: A mixed cell population was taken from embryonic day 15 (E15) rat spinal cord and cultured *in vitro* for up to 30 days, allowing the formation of a carpet of axons and differentiation of myelinating oligodendrocytes. Immunocytochemistry was used to visualise glial cells, myelin sheaths and axons (Figure 1A).

RESULTS: It has previously been shown that axonal alignment, survival and myelination were enhanced by culturing a mixed E15 spinal cord population onto a 2D PCL non-porous construct in the presence of an astrocyte monolayer. Altering the width of the grooves suggested that widths of

12-25µm were optimum for axonal alignment (Sorensen et al., 2007). It is hypothesised that further manipulation of the topography may alter axonal alignment and myelination. Therefore, our initial experiments were focused on altering groove depth and examining the effects of the pores on alignment.

DISCUSSION & CONCLUSIONS: The next stage of this work is the generation of a 3D scaffold to be used for culturing spinal cord neurones in an *in vitro* environment similar to spinal cord that may ultimately be used *in vivo* as part of a therapeutic treatment for SCI (Figure 1B). As such, the effects of altering the dimensions of the microgroove pattern and inserting pores throughout upon the alignment of axons is of great significance for the development of the 3D system.

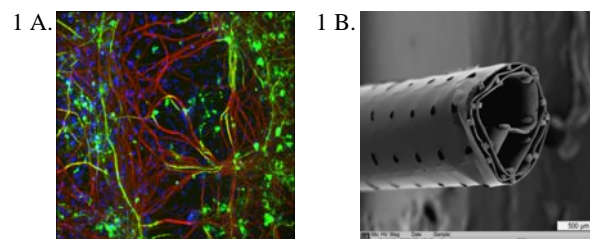


Figure 1. 1A is a representative image of an unaligned mixed spinal cord culture. Axons are immunolabelled red, myelin sheaths and myelinating oligodendrocytes are green, whilst nuclei are stained blue with DAPI. 1B illustrates the concept of the 3D construct prior to cell seeding, visualised with scanning electron microscopy.

REFERENCES: Sørensen A, Alekseeva T, Katechia K, Robertson M, Riehle M.O, Barnett SC. *Biomaterials* 2007 **28** (36):5498-5508.

Seunarine K, Gadegaard N, Tormen M, Meredith D, Riehle M.O, Wilkinson C.D.W. *Nanomedicine* 2006 **1**(3): 281-296.

* Both authors contributed equally.

PLGA Hollow Fibre Membrane Scaffolds and Serum Protein Interactions

RJ Shipley^{1,2} & MJ Ellis³

¹Christ Church, ²Oxford Centre for Industrial and Applied Mathematics, University of Oxford, UK

³[Department of Chemical Engineering](#), University of Bath, UK

INTRODUCTION: To enable tissue engineering systems to be viable on a clinical and industrial scale, there is a need to bridge recent developments in scientific knowledge with engineering and technical procedures. Hollow fibre membrane bioreactors (HFB) are an ideal cell culture environment for tissue engineering on an industrial scale. The use of PLGA to manufacture the hollow fibres allows for the regeneration of tissue, as careful selection of the monomer ratio will mean that once the fibres have completed their role of cell support and pseudovascularisation, their degradation will leave only the remodelled tissue. Several cell types have been cultured in HFBs including those of particular interest to this group, hepatocytes¹⁻⁴ and progenitor cell populations^{4, 5}. However, only the work by Wolfe et al³ combines theory and experiment by comparing the empirical permeability of membranes to theoretical values. We present a combined mathematical modelling and experimental approach to determine PLGA HFB operating conditions.

METHODS: Fibres were prepared using wet spinning^{6, 7}. Two dopes were used, 20% (w/w) PLGA in NMP and 5%-15% (w/w) PVA-PLGA in NMP, and water was used as the non-solvent. Mean pore size was measured using gas permeation, tensile strength analysed using a tensiometer and morphological analysed by SEM. Single-fibre modules were operated in a cross flow configuration. The protein solutions (containing individual or mixtures of BSA, IgG, HGF) were pumped through the lumen of the fibres for a range of conditions, of varying flow rate, pH and ionic strength, with particular focus on physiological conditions (pH 7, 0.15 M NaCl). Pressures were recorded at the inlet, lumen outlet and extracapillary space (ECS) outlet, and retentate and permeate collected for analysis at various time points. Protein content was measured using the Bradford assay and a material balance performed over the module.

RESULTS & DISCUSSION: PLGA HF membranes had a mean pore size of 0.5µm and PVA-PLGA HF membranes had a mean pore size of 1.0µm. While both these pore sizes should allow both hydraulic permeation, flux was only obtained

with PVA-PLGA fibres in the cross flow configuration. This was attributed to the hydrophobicity of PLGA HF, which cannot be wetted using standard ethanol wetting protocols due to deformation⁶, while the addition of the PVA overcomes this issue. PVA-PLGA HF showed zero rejection of 0.1 g/L BSA, and no fouling was observed such that there was a change in hydraulic flux or mean pore size of the membranes, tested after permeation studies. BSA is recognised to cause fouling in microfiltration membranes at this concentration, which has been described by the standard blocking filtration law⁸, resulting in BSA flux decrease but no electrolyte decrease. Furthermore, HGF permeation was achieved but the protein was found to degrade over time in the system, with and without BSA present.

CONCLUSIONS: The addition of PVA to PLGA membrane spinning dopes allows wetting of the fibres without the need for ethanol. Permeation of the growth factor HGF was achieved, and BSA flux and hydraulic flux were maintained in the PVA-PLGA HF system suggesting the presence of BSA in serum will not effect the transport, via fouling, in a PVA-PLGA hollow fibre membrane bioreactor.

REFERENCES:

1. Nguyen, D.T. et al. *Biotechnology Letters* 27, 1511-1516 (2005).
2. Nyberg, S.L. et al. *Annals of Surgery* 220, 59-67 (1994).
3. Wolfe, S.P. et al. *Biotechnology and Bioengineering* 77, 83-90 (2002).
4. Sardonini, C.A. & Wu, Y.J. *Biotechnology Progress* 9, 131-137 (1993).
5. Morgan, S.M. et al. *Biomaterials* 28, 5332-5343 (2007).
6. Meneghello, G. et al. *J. Membr. Sci.* submitted (2009).
7. Ellis, M.J. & Chaudhuri, J.B. *Biotechnology & Bioengineering* 96, 177-187 (2007).
8. Bowen, W.R. & Gan, Q. *Biotechnology & Bioengineering* 38, 688-696 (1991).

ACKNOWLEDGEMENTS: Work funded by Christ Church, University of Oxford and EU Marie Curie Fellowships in Early Stage Research Training; with thanks to Fernando Acosta for technical assistance in the lab.

FLUID FLOW INHIBITS EXPRESSION OF MARKER GENES FOR HUMAN MESENCHYMAL STEM CELL DIFFERENTIATION

J R Glossop & S H Cartmell

Institute for Science and Technology in Medicine, Guy Hilton Research Centre, University of Keele, Stoke-on-Trent, Staffordshire, UK.

INTRODUCTION: The ability of human bone marrow-derived mesenchymal stem cells (MSCs) to differentiate along multiple lineages, including the osteogenic, chondrogenic and adipogenic lineages [1], makes them ideal candidates for use in tissue engineering and regenerative medicine. Mechanical forces such as fluid-flow, mediated through the process of mechanotransduction [2], are important factors influencing MSC activity and responses. However, there is insufficient data detailing how these forces may influence the differentiation of MSCs. In this study we have subjected primary human MSCs to long-term (14 days) fluid flow-induced shear stress to investigate how fluid-flow exposure may regulate the differentiation of MSCs.

METHODS: Bone marrow-derived human MSCs (Lonza) at passage 5 were cultured in monolayer on prolectin-coated glass slides. Fluid flow-induced shear stress of 1 dyn/cm² was applied to cells for 1 hour/day for 14 consecutive days using a Streamer Fluid Shear Bioreactor (Flexcell). A static control was performed in conjunction with the fluid flow condition. Experiments were performed once. Preliminary determination of MSC differentiation along the osteogenic, chondrogenic and adipogenic lineages was assessed by gene expression analysis of marker genes using Taqman based (Applied Biosystems) quantitative real-time RT-PCR (Table 1). Real-time data were normalised to 18S and differential gene expression between the fluid-flow and static conditions was determined using the delta-delta Ct method and Student's T-Tests.

RESULTS: In comparison with static control cells, long-term application of fluid flow to MSCs (1 dyn/cm², 1 hour/day, 14 days) resulted in the decreased expression of marker genes used to identify osteogenesis, chondrogenesis and adipogenesis (Figure 1). The down-regulation observed was significant for all 3 lineages tested ($p < 0.005$), although not for every marker gene assessed. In particular, fluid-flow inhibited the expression of both adipogenic marker genes (14-23-fold reduction, $p < 0.015$).

Table 1. Marker genes for the determination of MSC differentiation along the osteogenic, chondrogenic and adipogenic lineages.

	Gene symbol	Gene name
Osteogenic	ALPL	Alk. Phosphatase
	BGLAP	Osteocalcin
Chondrogenic	COL2A1	Collagen type II
	ACAN	Aggrecan
Adipogenic	LEP	Leptin
	ADIPOQ	Adiponectin

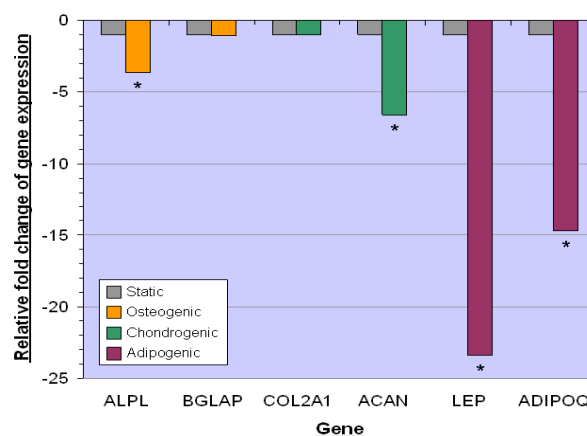


Fig. 1: Gene expression of markers for osteogenic, chondrogenic and adipogenic differentiation in human MSCs exposed to fluid flow.

DISCUSSION & CONCLUSIONS: Exposure of human MSCs to fluid flow over a 14 day period significantly down-regulated expression of marker genes indicative of osteogenic, chondrogenic and adipogenic differentiation. Our data suggest that application of fluid flow in the described regime inhibits the differentiation of MSCs along these lineages. Fluorescence immunocytochemistry is being used to confirm our gene expression data.

REFERENCES: ¹ M. Pittenger, M.F. Mackay, A.M. Beck, et al (1999) *Science* 284:143-7. ² H. Huang, R.D. Kamm, and R.T. Lee (2004) *Am. J. Physiol. Cell Physiol.* 287:C1-11.

ACKNOWLEDGEMENTS: We wish to thank Mr. Brian King for designing the slide chambers for cell lysis. This work was supported by a research grant (BB/D000548/1) from the BBSRC.

DEVELOPMENT AND CHARACTERISATION OF A TISSUE ENGINEERED OESOPHAGUS

[N Green](#)¹, Q Huang¹, L Khan², G Battaglia¹, B Corfe³, S MacNeil¹ & J Bury³

¹ *Kroto Research Institute, University of Sheffield, UK.* ² *Sheffield Teaching Hospitals, NHS Foundation Trust, UK.* ³ *University of Sheffield Medical School, UK.*

INTRODUCTION: There is demand for a reliable 3D tissue engineered model oesophagus to provide an experimental platform for investigating oesophageal disorders. A number of models have been described in the literature but there is little systematic comparison of the different approaches, making selection of a preferred platform complex.

AIM: To compare two different scaffolds, acellular de-epithelialised pig oesophageal (DEO) matrix and collagen I gel, analyzing their impact on normal human oesophageal fibroblast penetration and epithelial cell adherence, growth and maturation.

METHODS: Oesophageal tissue samples were obtained with informed consent from patients undergoing gastric or oesophageal surgery, with appropriate ethical approvals (SSREC 165/03 & 07/1309/138). Human oesophageal squamous epithelial (HOS) cells and oesophageal fibroblasts (HOFs) were isolated using methods described for the isolation of keratinocytes and fibroblasts from human skin [1]. HOFs were cultured on the scaffolds for a week prior to addition of epithelial cells. Composites were grown in a series of media optimized for oesophageal cell proliferation and differentiation [2]. After 4 days submerged growth the composites were raised to the air/liquid interface for a further 10 days.

The resulting models were formalin fixed and evaluated using haematoxylin and eosin staining. Those displaying the clearest oesophageal morphology were further characterized with immunohistochemistry for cell proliferation (Ki67), differential cytokeratin expression (CK14 & CK4), involucrin and collagen IV. Comparative work with a transformed epithelial cell line (Het-1A) was also undertaken on some scaffolds.

RESULTS: HOS cells produced a mature, stratified epithelium on both scaffolds. However the collagen gel gave a poorly attached epithelium while the pig oesophageal matrix yielded an oesophageal epithelial model comparable to a normal epithelium as shown by Ki67, CK4, CK14 and involucrin staining (Figure 1). Het-1A cells formed a hyper proliferative epithelium with no evidence of differentiation on any of the scaffolds.

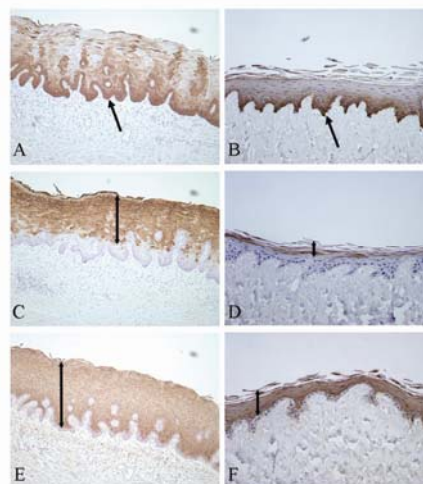


Fig. 1: IHC staining of normal oesophagus (left) and HOS cells on DEO (right) for CK14 (A,B), CK4 (C,D) and involucrin (E,F). Arrows indicate areas of positive staining

DISCUSSION & CONCLUSIONS: Our systematic comparison of some of the major variables for producing a tissue engineered model of a normal oesophagus shows that this can be achieved using human oesophageal epithelial cells and fibroblasts on an acellular pig oesophageal scaffold.

Collagen gel was less satisfactory and the Het-1A cells produced a highly abnormal epithelial layer. These data allow us to propose HOS cells seeded onto pig oesophageal matrix as the preferred model of normal human oesophagus.

REFERENCES: ¹ D.R. Ralston, C. Layton, A.J. Dalley et al (1997) *B J Plast Surg* **50**:408-15. ² C.D. Andl, T. Mizushima, H. Nakagawa et al (2003). *J Biol Chem* **278**:1824-30.

ACKNOWLEDGEMENTS: We thank Roger Ackroyd, Andrew Wyman and Chris Stoddard, Consultant Surgeons, Sheffield Teaching Hospitals NHS Foundation Trust, for help in acquiring oesophageal tissue samples. This study was supported by grants from the Bardhan Research and Education Trust (BRET) and Yorkshire Cancer Research (YCR)

Topographic Patterning of 3D Collagen Scaffolds: From Surface to Interface Engineering

E.Hadjipanayi,¹ T.Alekseeva¹, L.Bozec² and R.A.Brown¹

¹ UCL, Tissue Repair and Engineering Centre, Division of Surgical and Interventional Sciences, Institute of Orthopaedics and Musculoskeletal Sciences, London, HA7 4LP, UK

²UCL Eastman Dental Institute - 256 Gray's Inn Road - London - WC1X 8LD, UK

INTRODUCTION: Topographic patterning provides a useful tool for regulating cell function, such as adhesion, proliferation, differentiation and contact-guidance. While current (e.g.lithographic) techniques allow precise control of topographic pattern (anisotropic vs isotropic) and scale (nano- vs micro-topography)¹, they are only applicable to 2D surface patterning, which compromises their relevance to 3D tissue engineering. In this study we developed a novel method for rapid fabrication of micro-textured 3D collagen scaffolds.

METHODS: The two-step fabrication process involved, firstly, plastic compression of collagen hydrogels to remove interstitial fluid and increase matrix stiffness (from 42.2 ± 22 to 1805 ± 214 KPa)², followed by embossing a customizable template of parallel-aligned phosphate-based glass-fibers (35 or 55 μ m fiber diameter with 100 μ m inter-fiber spacing) on the scaffold's surface. Groove width and depth was measured by SEM and AFM, respectively. For 2D culture, HUVECs were cultured on smooth or micro-textured collagen scaffolds for 48hrs to test cell alignment and morphology. Cell attachment was tested by washing scaffolds with PBS 4hrs post-seeding and counting the number of adherent cells with a phase-contrast microscope. For 3D culture, human dermal fibroblasts (HDFs) were seeded within smooth or micro-textured scaffolds, with keratinocytes seeded on top. Constructs were cultured submerged for 2 days, before being raised to the air-liquid interface and cultured for an additional 12 days. Constructs were H&E stained at 2weeks and epidermal thickness was quantified by image analysis.

RESULTS: SEM showed a regular pattern of parallel grooves and ridges (Fig.1). Groove width was $30.5\pm 3.3\mu$ m and $49.5\pm 11.6\mu$ m for 35 μ m and 55 μ m diameter fibers, respectively. Groove depth was $0.95\pm 0.49\mu$ m and $1.55\pm 0.31\mu$ m, respectively. 2D culture of HUVECs on micro-textured collagen substrates showed preferential cell adhesion on 30 μ m-wide grooves compared to 50 μ m-wide grooves or smooth surfaces. Groove width also affected cell alignment and morphology, with 66% of cells aligning along groove direction on 30 μ m-

wide grooves (cell elongation-index= 3.1 ± 1.9), compared to 7.3% of cells on 50 μ m-wide grooves (cell elongation-index= 1.35 ± 0.23) (Fig.2). 3D culture of HDFs within micro-textured scaffolds, with keratinocytes seeded on top, indicated that the micro-topography of the dermo-epidermal interface influenced the rate of keratinocyte stratification, since epidermal thickness decreased from $40\pm 14\mu$ m for smooth interfaces to $14\pm 6\mu$ m for grooved interfaces.

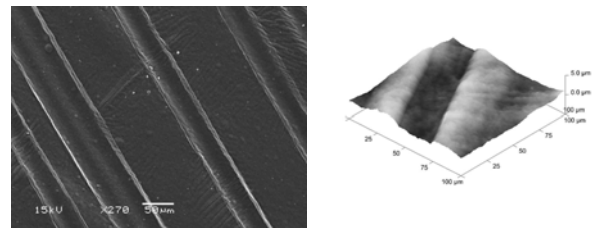


Fig. 1: SEM (left) and AFM (right) images of micro-textured collagen scaffolds

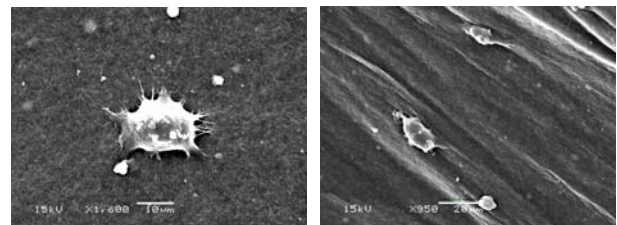


Fig. 2: Endothelial cells on smooth (left) and 30 μ m-wide grooved (right) collagen scaffolds.

DISCUSSION & CONCLUSIONS: We report on a novel method for topographic patterning of 3D biomimetic collagen scaffolds. The versatile applicability of this technique to 2D and 3D culture makes it a promising tool for investigating cell behavior on both 2D surfaces and 3D interfaces, where cell-cell interactions could critically influence cell function.

REFERENCES: ¹J.Y.Lim and H.J.Donahue (2007) *Tissue Engineering* **13**, 1879-1891. ²R.A.Brown, M.Wiseman, C.B.Chuo, U.Cheema, S.N.Nazhat(2005)*AdvancedFunctionalMaterials***15**, 1762-1770.

Perfusion Bioreactor For Bone Tissue Engineering: Experimental Parameters For A Lattice-Boltzmann Mathematical Model

[L.A.Hidalgo-Bastida](#)¹, [T.J. Spencer](#)², [I. Halliday](#)², [C. Care](#)² & [S.H. Cartmell](#)¹

¹*Institute for Science and Technology in Medicine, Keele University, UK*

²*Materials and Engineering Research Institute, Sheffield-Hallam University, UK*

INTRODUCTION: Bone tissue engineering is an emerging therapy for treating patients undergoing orthopaedic trauma or disease. One of the important factors in bone tissue engineering is the configuration of placing the cells onto a porous 3D scaffold at the start of the culture period to create the tissue-engineered construct. Mathematical modeling offers to scientists great assistance with regards to reducing the number physical laboratory experiments needed for the optimisation of cell seeding. Lattice Boltzmann equation (LBE) allows a complex model which can accommodate as many equations (parameters) as needed. This work aims to optimise dynamic perfusion bioreactor cell-seeding methods on porous 3D constructs, using a lattice Boltzmann (LB) mathematical modelling technique employing the real experimental geometries.

METHODS: A first approach was to use microCT images of a PLA scaffold to generate the 3D structure for a LBE model. The first codes were designed to model the scaffold hydrodynamics without cells. The models were obtained using a parallel code to model one quarter of the symmetrical geometry (cylinder) to reconstruct the full scaffold. At the same time, experimental work was conducted to assess the cell adhesion in simple 3D configuration. This approach would mimic the cell distribution/contact in open porous media (scaffolds) to provide data on cell deposition under flow. This was achieved by seeding hMSCs into ECM-coated tygon tubing ($\odot=1.02$ mm) shaped into 90° turns. Cells were seeded by perfusion at 0.01 ml/min for 2 hours before analysing them in a microCT (Scanco).

RESULTS: The LBE code developed for this perfusion system was able to produce models for pressure profile, mass transport and shear stress for a cylindrical scaffold placed in the bioreactor chamber (Figure 1). A reduced computing time was achieved by running parallel codes of 1/4 of the chamber. Tygon tubing was successfully immobilised at 90° using fittings. MicroCT scans after sample staining revealed internal structure of the conduit with a difference of density between the surface and the interior of the wall. Scans also showed deposition of cells inside the tubing (Figure 2).

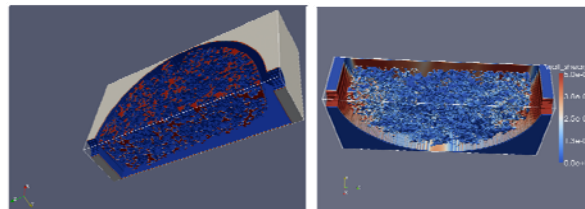


Figure 1. Models of (A) serial code (1 cpu) for 1/4 bioreactor of the scaffold hydrodynamics highlighting the pores that will be obstructed following cell seeding/deposition and (B) bulk shear stress distributions in 1/4 of the bioreactor chamber with $Q = 0.035$ ml min⁻¹.

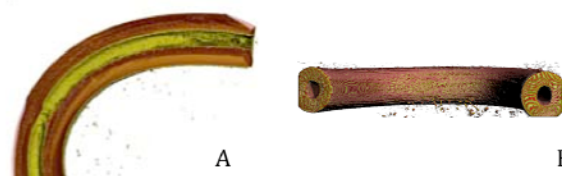


Figure 2. MicroCT images of (A) internal section of the tygon tubing showing the internal channel and the wall and (B) lateral view of the tubing.

DISCUSSION & CONCLUSIONS: Cell deposition scans provided data to model cell stagnation areas in porous media. Models have been also developed for flow/stress, oxygen concentration and carbon dioxide concentration at constant cell concentration. Further validation of the optimized model, including flow pattern will be conducted. LBE is a flexible mathematical tool to model all the parameters of a tissue engineering system, reducing time and cost.

REFERENCES: ¹ Boschetti, F. et al. Prediction of the micro-fluid dynamic environment imposed to three-dimensional engineered cell systems in bioreactors. *J Biomech* 2006; 39(3):418-25 ² Whittaker, R. et al. Mathematical modelling of fibre-enhanced perfusion inside a tissue-engineering bioreactor. *J Theor Biol.* 2009 Feb 21;256(4):533-46

ACKNOWLEDGEMENTS: This work is being supported by the BBSRC (BB/F013892/1).

Control of human periodontal ligament cells proliferation on honeycomb-patterned films for regenerative periodontal therapy

*Nagayoshi Iwama^{1,2}, Masaru Tanaka², Hiroshi Ishihata¹, Masahiro Ara², Mitsuru Shimonishi³, Masaru Nagamine⁴, Noriaki Murakami¹, Sousuke Kanaya¹, Eiji Nemoto¹, Hidetoshi Shimauchi¹ and Masatsugu Shimomura²

¹Graduate School of Dentistry, Division of Periodontology and Endodontology, ²Institute of Multidisciplinary Research for Advanced Materials, ³Division of Comprehensive Dentistry, Tohoku University Japan, ⁴Nagamine Manufacturing Co., Ltd., Kagawa, Japan

INTRODUCTION: Tissue-engineered grafts may be useful in regeneration of periodontal ligament that the method for the proliferation of cells on porous scaffold could be applied. Three-dimensional porous scaffolds fabricated from biodegradable polymers have been applied for the tissue regeneration therapy as temporary intracellular matrices. In the process of proliferation, cell bodies tend to obtain adhesions to the extracellular matrix on starting preparation to the original external form and develop of the functions. We have found that honeycomb-patterned films can be prepared by biodegradable polymers. The honeycomb-patterned film has a horizontal micropore network modified to the intercellular matrix. The characteristic of the honeycomb structure is distribution of equalized porous sizes by a micron order. All the cells that were inoculated on the film, able to be situated on unified circumstances of the topographic condition. We have demonstrated specific behaviors of the cultured cells on the fabricated honeycomb structures *in vitro*. The present study describes the human periodontal ligament cells adhesion and proliferation on the honeycomb-patterned films.

METHODS: Self-organized honeycomb films from poly(ϵ -caprolactone) (PCL) and amphiphilic polymer were prepared with highly regular porous structure by using humid atmospheric casting method. Fibroblast-like cells derived from a periodontal membrane of extracted human molar teeth. The cells belonging experimental group were cultivated on the three kinds of honeycomb films of 5, 10 and 15 μm pore sizes for 4 hours and up to 42 days. Control group cells were cultivated on the flat PCL and glass substrate.

RESULTS & DISCUSSION: In the experimental group, histological observations of the cultured tissues for 4 to 72 hours detected orientations to produce pseudopodiums of the cell bodies to be attached to the pillars in the honeycomb structure. A certain numbers of cells were migrated their bodies into the honeycomb structural lumen through the osculum of 10 and 15 μm pores. The forms of the cell bodies were recovered orientation to the spindle shape as an ordinary on the

fibroblasts after 24 hours incubation. After 72 hours, the cells were organized in plexus which reflected the frame structure of honeycomb. In the control group, the each cell adhered in the shape of flat on the plane substrates until 24 hours. The ordinary spindle cell shapes were appeared on 72 hours cultivation stating the beginning of self-organization. The cells cultivated for 28 and 42 days of both groups were organized in a sheet-like configuration after the confluent. The experimental group were obtained formative in the multilayer condition that cells were penetrated from inside and outside of the 10 and 15 μm pored film.

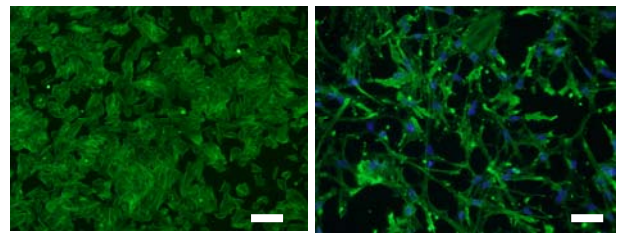


Fig. 1: Effect of honeycomb patterned scaffold on the proliferation of human periodontal ligament cells: on the glass substrate cultured 24h as control (left) and 15 μm pored honeycomb film of PCL cultured 72h (right) (Bar 10 μm).

CONCLUSIONS: The morphological effect of honeycomb-patterned film with a pillar structure was revealed that the scaffold clusteringly arrayed with modified intercellular flask, remarkably enhanced proliferation and extension of the cultured cells. The honeycomb film is applicable to the periodontal therapy as using a scaffold for the periodontal tissue regeneration.

REFERENCE: Mcmillan J.R., Akiyama M., Tanaka M., Yamamoto S., Goto M., Abe M., Sawamura D., Shimomura M., Shimizu H." Small-Diameter Porous Poly (ϵ -caprolactone) Films Enhance Adhesion and Growth of Human Cultured Epidermal Keratinocyte and Dermal Fibroblast Cells" *Tissue Engineering*, 13, 789-798, 2007.

SYNTHESIS OF NANOSCALE PHOSPHATE DEGRADABLE POLYMER COMPOSITES

S. E Kelly¹, M. J Dalby², K. E Tanner³ & D.H Gregory^{1*}

¹ *Department of Chemistry, University of Glasgow*

² *Centre for Cell Engineering, University of Glasgow*

³ *Department of Mechanical Engineering, University of Glasgow*

INTRODUCTION:

The initial aim of this project is to synthesise nanoscale phosphate degradable polymer composites for their use in biomedical applications. Due to their chemical similarity to the mineral composition of bone, hydroxyapatite (Hap, $\text{Ca}_{10}(\text{PO}_4)_6\text{OH}_2$), and tricalcium phosphate (TCP, $\text{Ca}_3(\text{PO}_4)_2$), have been widely investigated for use as bone replacement materials.¹

The current focus of our work is the synthesis and characterisation of substituted and non-substituted TCP. Our materials design strategy is then to synthesise these bioactive calcium minerals controlling size and shape at the nanoscale, and then to integrate them within a polymer matrix to create new composites. In vitro testing of the novel composites will also be investigated; cell cultures will assess the likely biological response to the material.

METHODS:

Various techniques for the synthesis of calcium phosphate minerals have been documented. Mg-substituted calcium phosphate, Mg-TCP, was synthesised using an aqueous precipitation method involving calcium hydroxide, magnesium chloride, and orthophosphoric acid.² Characterisation was investigated using Powder X-ray Diffraction (PXD), Scanning Electron Microscope (SEM) and Energy Dispersive X-ray (EDX).

RESULTS:

Initial results from PXD indicate a strong correlation between synthesised and commercial TCP (Figure 1). Similar results have been seen for Mg-TCP. Particle size and morphology have been investigated using SEM imaging (Figure 2): micrographs show agglomerated and irregular particles formed from clusters of sub-micron particles of doped TCP.

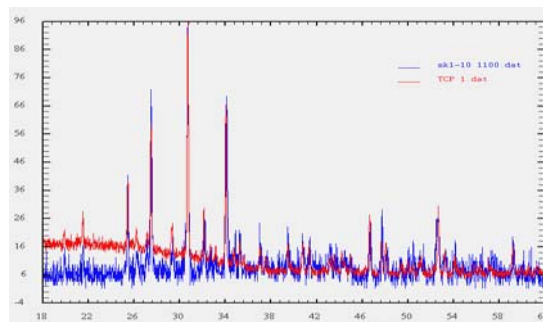


Figure 1: Powder X-ray diffraction (PXD) patterns comparing synthesised (blue) and commercial (red) TCP

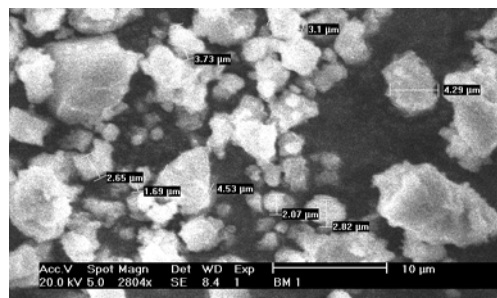


Figure 2: Scanning electron micrograph of synthesised TCP

DISCUSSION & CONCLUSIONS:

Results from synthesis are promising; next steps involve preventing agglomeration and controlling particle size and shape to produce monodisperse anisotropic nanostructures which will be used subsequently to form composites..

REFERENCES: ¹ M. Deschamps, O. Richart, P. Hardouin et al (2007) *Ceramics Int* **34**:1131-37. ² Marcia S. Sader, Racquel Z. LeGeros, Gloria A. Soares (2009) *J Mater Sci:Mater Med* **20**:521-27

ACKNOWLEDGEMENTS: This research is funded through the Kelvin/Smith Scholarship programme.

POLYMER MICROARRAYS – A HIGH-THROUGHPUT APPROACH TO THE IDENTIFICATION AND SELECTION OF TISSUE REENGINEERING SCAFFOLDS

F Khan¹, R S Tare², ROC Oreffo² & M Bradley¹

¹University of Edinburgh, School of Chemistry, West Mains Road, Kings Buildings, Edinburgh, EH9 3JJ. UK.

²University of Southampton, Bone and Joint Research Group, Southampton General Hospital, Southampton, SO16 6YD. UK.

INTRODUCTION: The pluripotent nature and proliferative capacity of stem cells make them an attractive cell source for tissue engineering and regenerative medicine [1]. However of vital importance are scaffold biomaterials that will play both a critical role in directing and controlling tissue regeneration as well as tools and devices that will allow the isolation/enrichment and controlled growth of stem cells [2-3]. Here we report on the microarray screening and analysis of some 500 biodegradable/in situ hydrolysable polymers and polymer blends for the selection and maintain of osteoprogenitors from hBMMC populations. The microarray format allowing massive parallel cellular analysis, while consuming minute amounts of cells and polymers.

METHODS: Polymer microarrays were fabricated either by contact (Genetics QArray mini: Hampshire, UK) or inkjet printing (Microdrop, GmbH, Norderstedt, Germany) with each polymer printed in quadruplicate. Analysis of the cells immobilization on the polymer microarrays was performed according to the procedures we have previously described [2, 3] using an automated high content microscope that allowed capture and analysis of the images for each polymer spot using the software Pathfinder.

RESULTS: 500 polymers or polymer blends were analysed for specific cell binding properties. Crucially different polymers were found that were able to selectively immobilize STRO-1+ osteoprogenitors from the hBMMC populations, in a highly specific manner. Different polymers were also identified that specifically bound Fetal, ATDC5, MG63 or SaOS cells. Some of the materials had gel-like properties (that offered a non-biological alternative to Matrigel) or resulted in microporous scaffolds which supported cell growth in a 3D sense [2] useful for tissue regeneration.

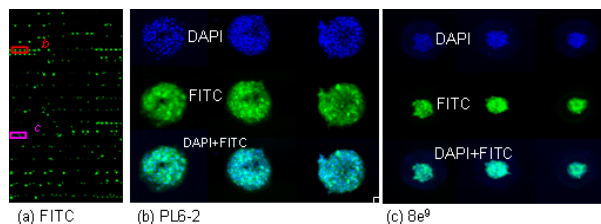


Fig. 1: STRO-1+ cells selection on a 190 member polyacrylate polymer micorarray

DISCUSSION & CONCLUSIONS: This study has shown that polymer arrays are a versatile format in allowing the high-throughput evaluation of cell binding and scaffold identification. The High-Throughput multiplexing approach allows large libraries of polymers to be screened for various cellular applications. The microarray platform here allowed the identification of new polymers for the attachment of various cell types, including adult stem cells, which are of significant interest. The microarray approach allowed the identification of cell-compatible biopolymers permissive for human skeletal stem cell growth and differentiation both in *in vitro* and *in vivo* applications, and demonstrated the potential application in tissue engineering. The high-throughput approach (can also serve as an important tool in applications where cell-selective polymers can be used to guide stem cell differentiation, to support specific cell type growth and to modulate stem cell plasticity.

REFERENCES: ¹R.O.C. Oreffo, et al (2005) *Stem Cell Reviews* **1**: 169-178. ²F.Khan et al (2009) *Angew. Chemie-Int. Edit.* **48**: 978-82. ³R.S.Tare et al (2009) *Biomaterials* **30**: 1045-55. ⁴J.-F.Thaburet et al (2004) *Macromol Rapid Commun.***25**: 366. ⁵G.Tourniaire et al (2006), *Chem Comm* (Cambridge, UK) (20), 2118.

ACKNOWLEDGEMENTS: We thank the BBSRC for funding.

Does The Thickness of Surface-Bound Hydrogel Substrate Affect Adherent Cell Behaviours?

P. Kuntanawat, C. D.W. Wilkinson & M. O. Riehle

Centre for Cell Engineering [Faculty of Biomedical and Life Sciences](#) University of Glasgow, GB.

INTRODUCTION: Surface-bound hydrogels such as polyacrylamide have been used as a versatile model of artificial extracellular matrix in cell culture. Perhaps as the cell traction field on such is in the range of a few microns, the mechanical effect of substrate thickness above tens of microns on cell behaviour was thought to be negligible¹. As the gel, on one side, is bound, we demonstrated that the gel exhibits non-uniform swelling along the gel thickness, which perhaps effectively changes the substrate's mechanics and cell behaviour when used as a cell substrate. Our preliminary biological experiment also showed the influence of the thickness on cell behaviour.

METHODS: Demonstration of the non-uniform swelling of the gel was done using a polyacrylamide rod (%bis-acrylamide = 0.13%, diameter ~10 mm) with one side attached to a glutaraldehyde-activated coverslip. The gel rods were immersed in HEPES or Medium 199-supplemented DMEM at least 7 days before swelling measuring. Freshly cast and swollen gel stiffness was also calculated using the values of given stresses and the corresponding strain obtained from a macroscopic gel stretching method.

The gel substrates for the biological experiment were prepared in the same way but were cast into a cylindrical shape with a thickness of about 60 or 2100 μm and one side bound to a 10 mm diameter glutaraldehyde-activated coverslip. The structures were then cross-linked with fibronectin using sulfo-SANPAH, followed by a set of buffer washes. After letting the gel swell fully in an environment suitable for culturing cells (complete DMEM and 5% CO_2), MG-63 (osteoblast line) cells were seeded on the structures to reach an average cell density of about 14 cells/ mm^2 . Microscopic photographing of the cells on both structures was done after 26hr of cultivation.

RESULTS: Gels exhibited a non-uniform "U" shape after immersion in the media. The rate of gel expansion away from the centre reduced, while the height away from the gel binding increased. A free gel rod could swell up to about 1.3 times its initial size. A significant 30% reduction in gel stiffness

was found in the fully swollen gel compared to the gel prior to swelling. The projected area of the cell population on the initially 60 mm thick substrate is about $1408 \pm 702 \mu\text{m}$ (average \pm SD), significantly larger than that of the 2100 mm thick one which is $780 \pm 582 \mu\text{m}$ ($p \leq 0.001$; based on 207-208 cells/treatment).

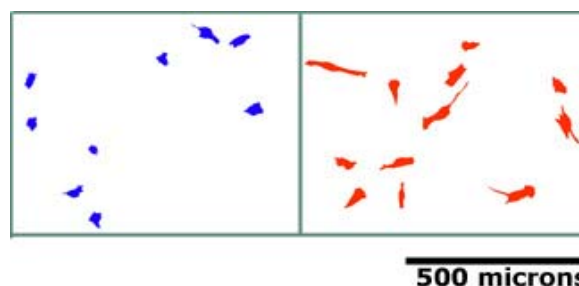


Fig. 1: Drawing of the cell samples on the surface of the surface-bound gels with different thicknesses at the time of photographing: 2100 μm thick gel (left) vs. 60 μm thick gel (right).

DISCUSSION & CONCLUSIONS: The thickness of surface-bound polyacrylamide may indirectly influence the cells adhering on the top surface of the substrate. This dimensional factor may determine a secondary inner strain pattern, stiffness or other physical property changes generated due to uneven swelling of the clamped gel bulk. Therefore it physically or mechanically affects behaviours of the cells. We are currently investigating the details of surface mechanics and physical aspects of the anisotropic swollen gels.

REFERENCES: ¹ A. J. Engler, L. Richert, J. Y. Wong, et al (2004) *Surface Science* **570**:142-154.

ACKNOWLEDGEMENTS: This project is a part of my PhD research. I would like to thank for the Royal Thai Government Scholarship and other relevant bodies for supporting my PhD education and making this project possible to be conducted in the Centre for Cell Engineering.

Scaffold Surface Processing to Enhancing Cells Colonization

Chaozong Liu^{1*}, He Liang¹, Eric W Abel²

¹ *School of Engineering, The Robert Gordon University, Aberdeen AB10 1FR, UK*

² *School of Engineering & Physical Science, Dundee University, Dundee DD1 4HN, UK*

INTRODUCTION: This paper reports the strategy for the surface processing of crosslinked collagen scaffolds by UV/Ozone processing technique to achieve an improved surface wettability. The *in vitro* performance with respect to cells' viability and colonization using human mesenchymal stem cells (hMSC) is reported.

METHODS: Collagen type I was used to fabricate the porous collagen scaffolds by freezing-drying method, followed by cross-linking by EDC method [1]. The scaffolds were characterised with respect to surface wettability, microstructure and associated dynamic mechanical property [1]. The cell viability/proliferation was evaluated *in vitro* using human mesenchymal stem cells (hMSCs).

RESULTS: Micro-CT examination revealed the resultant scaffolds have a porosity of 92%, and a mean pore size of 222 μm in the range of 100~300 μm . Scaffolds treated by EDC cross-linking shown an increased level of cross-linkage [1]. Previous study observed that the shear modulus of wet crosslinked scaffolds, tested at 37 °C, exhibited 5 times high as that of uncrosslinked one.

The examination of surface wettability revealed the crosslinking treatment reduced the surface wettability, especially for the EDC crosslinking treatment (Table 1). The water contact angle increased to about 80° from 50° for uncrosslinked sample. The UV/Ozone processing improved the surface wettability significantly. This was reflected by the reduction of water contact angle as observed in Table 1.

Table 1: Water contact angle on collagen surface

Native collagen	Crosslinked	Processed
51.7	80.6	40.2

The water contact angles reduced to about 42° after exposure the samples to UV/Ozone for only 100 seconds. The surface processing method adopted in this study can improve wettability for both the interior and exterior surface. This was well demonstrated by the water immediately diffuse into the processed scaffold (Figure 1a). In contrast, the water droplet was unable to diffuse into the unprocessed scaffold structure as observed in Figure 1b. When drop into the PBS solution, the

processed scaffold immediately sinks to the bottom, while the unprocessed scaffold float on the surface owing to its hydrophobic nature (Figure 1c).

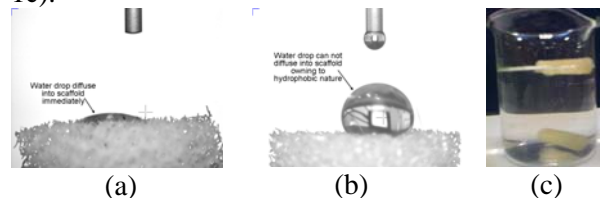
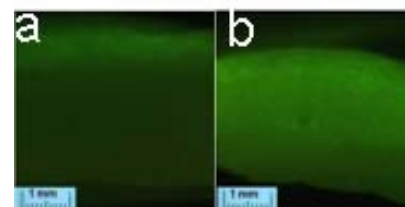


Figure 1: (a) Water drop diffuse into processed scaffold (b) water unable to diffuse into unprocessed scaffold; (c) scaffolds in PBS solution.

The *in vitro* evaluation using hMSCs revealed a poor cells migration within non-surface processed scaffolds, viable cells only limited to the top seeding layer, about 0.7 mm thick (Figure 3a). In contrast, the viable cells were observed throughout scaffolds after 1 week culture, as shown in Figure 3b. A combination of Alizarin red and Alcian blue staining revealed bone and cartilage-like tissue formed after 8 weeks culture using surface processed scaffolds.

Figure 3: GFP-labeled hMSCs cells cultured for 1 weeks *in vitro*.



CONCLUSION: The crosslinking treatment reduced the surface wettability of collagen scaffolds, while surface processing by using UV/Ozone reactor could improved their surface wettability. *In vitro* evaluation demonstrated that surface processing enhanced hMSCs migrate deep into scaffold, and proliferate and differentiate there.

REFERENCES: ¹ C Liu et al. JBMR (2008) 85B92): 519-528.

ACKNOWLEDGEMENTS: This work forms part of the Northern Research Partnership Programm sponsored Ph D studentship.

Netrin-1 promotes neurite growth of ventral midbrain dopaminergic neurons within a 3D collagen gel

Y. Liu, A. B. Jozwiak, Y. Yang & M. A. Gates

Institute for Science and Technology in Medicine (ISTM), Huxley building, Keele University

INTRODUCTION: Parkinson's disease (PD) is a neurodegenerative disease affecting 1% of the UK population¹. In PD, dopamine neurons in the ventral midbrain (VM) degenerate, effectively destroying the nigro-striatal circuit. Tissue/cells from the embryonic VM have been used to replace the dopamine neurons lost in PD, however re-growth of the nigro-striatal circuit has proven difficult. Because netrin-1² and GDNF³ are expressed within the developing nigro-striatal circuit (where they may modulate growth and / or survival of midbrain DA neurons^{2,3}), growth of VM DA neurons in a 3D collagen gel containing netrin-1 or GDNF was compared with control cultures (of collagen only) to determine how these molecules may affect DA neurite growth in a 3D collagen system. It is hoped this will unveil a new avenue for generating circuits for neural repair.

METHODS: To first determine the optimum concentration of collagen gel for DA cell growth, explants from the embryonic day 13 (E13) rat VM were cultured in different concentrations of rat tail collagen-I for 7 days. Subsequently, the growth of E13 explants / cells into an optimal concentration of collagen was compared with growth seen in collagen containing either netrin-1 (200ng/ml) or GDNF (100ng/ml). After 7 days in vitro, samples were immunostained for tyrosine hydroxylase (TH) and visualized via fluorescence secondary antibody. Neurite growth into collagen gels were counted / measured under 10x magnification using NIS-element system (Nikon).

RESULTS: Immunostaining with TH showed that VM DA neurons survived and extended neurites in all three 3D collagen gel preparations. Though neurite growth into collagen gels containing GDNF appeared similar to that seen in collagen only preps, netrin-1 containing collagen gels appeared to promote a greater number and length of neurite growth among VM DA neurons.

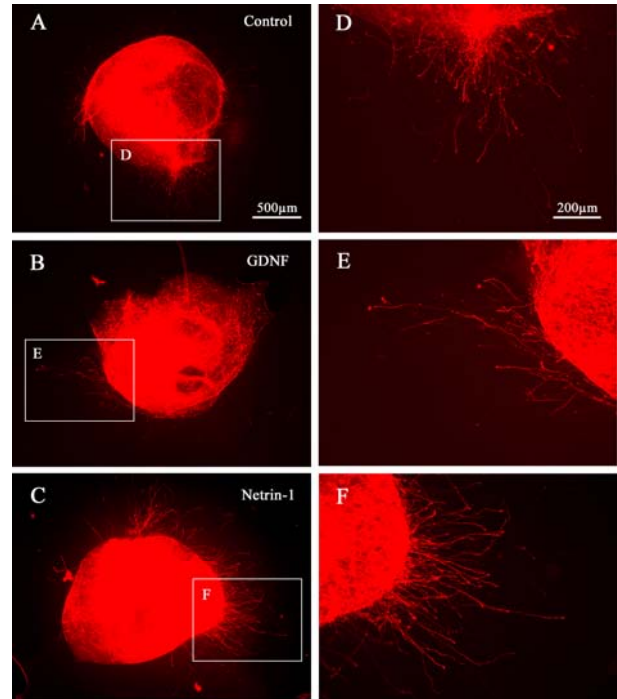


Fig. 1: Collagen embedded netrin-1 promotes greater neurite outgrowth than control (A) or GDNF (B) containing gels. Higher magnification images (D-F) illustrate neurite growth into each 3D collagen gel.

DISCUSSION & CONCLUSIONS: Adding soluble netrin-1 into collagen gels appears to enhance growth of embryonic neural tissue and cells beyond that seen in collagen-only gels. This finding, it is hoped, will enhance the potential to use collagen gels to engineer neural circuits *ex vivo* for circuitry replacement in the mammalian central nervous system.

REFERENCES: 1. Nussbaum RL, Ellis CE (2003). *N Engl J Med*; 348: 1356–64. 2. Christine Métin1 et al. (1997) *Development* 124, 5063-5074. 3. Lin LF, Doherty DH, Lile JD, Bektesh S, Collins F (1993) *Science* 260:1130–1132

ACKNOWLEDGEMENTS: The presented research was generously funded by the BBSRC

Monitoring the Effect of Silicate Substitution on Protein Adsorption/Desorption to Hydroxyapatite

M.-K. Mafina^{1,2}, A.C. Sullivan² and K.A. Hing¹

¹School of Engineering and Materials & IRC, ²School of Biological & Chemical Sciences
Queen Mary, University of London, London, E1 4NS, UK

INTRODUCTION: The aim of this study was to develop a method which would facilitate the evaluation and comparison of competitive protein adsorption on silicate-substituted hydroxyapatite (SA) and stoichiometric hydroxyapatite (HA). The initial objective was to synthesise a fluorescent label, fluorescein isothiocyanate (FITC), for covalent attachment to individual target proteins (albumin, fibronectin) and to use fluorescence to monitor competitive binding at equilibrium.

METHODS: SA and HA powders (Apatech Ltd, UK) were pressed and sintered at 1300 and 1250 °C, respectively. FITC was extended with a methyl-aminocaproate ester (Sigma-Aldrich, UK) spacer to provide covalent bonding to bovine serum albumin, BSA, (Sigma-Aldrich, UK). BSA solutions (1.5 ml in phosphate buffered saline, PBS) were placed in clean glass vials, and samples (1 dense **D** disc or 0.50 g 2-5 mm porous granules **G**, Apatech Ltd, UK) were added to analyse **adsorption**, aliquots of the solution was removed at time intervals. After 15 minutes, the materials were removed, placed in clean vials with PBS (1.5 ml) and gently agitated to remove loosely bound BSA. Test materials were then placed in fresh PBS (1.5 ml) to analyse **desorption**, aliquots were removed at time intervals. Additionally, a binding constant-type study was performed on dense SA discs, where the amount of protein adsorbed was determined for a range of equilibrium concentrations. Protein concentrations in the studies were independently analysed using the Quant-it assay (Invitrogen) and the FITC-labelled protein fluorescence intensity (excitation/emission, nm) to verify accuracy of the technique.

RESULTS & DISCUSSION: Dense SA & HA materials with densities of 98.1 and 99.1 % were formed, respectively. Analysis *via* X-Ray diffraction and FT-IR spectroscopy verified phase purity in both materials, and the presence of silicate groups in SA only, in accordance with previous findings^{1,2}. Scanning electron microscopy of surfaces demonstrated SA and HA to have similar surface morphology. Good correlation was found between Quant-it and FITC data, validating this approach as a method to quantitatively analyse an individual protein species' interaction with a bioceramic substrate. Studies confirmed that

porous specimens adsorb more BSA per μg than the dense (Fig 1a) and that BSA is more readily desorbed from HA than SA (Fig 1b)

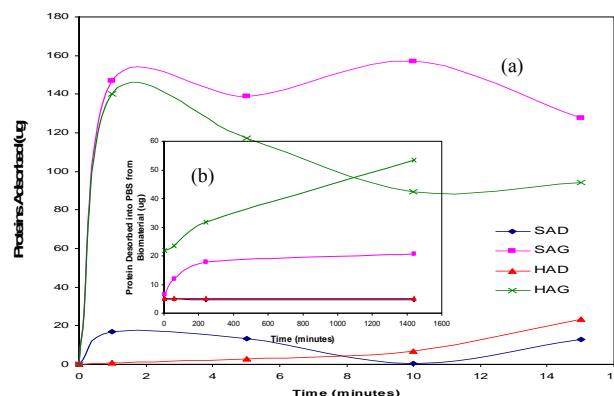


Fig. 1: (a) Adsorption and (b) desorption of BSA on dense (SAD, HAD) and porous (SAG, HAG) materials

Binding constant-type study revealed two distinct regions (Fig 2), suggesting that a monolayer-like layer may be established on SAD at an average of 1.37×10^{-14} mol/0.9 g of disc, but as the BSA solution concentration is increased a more complex multi-layer developed.

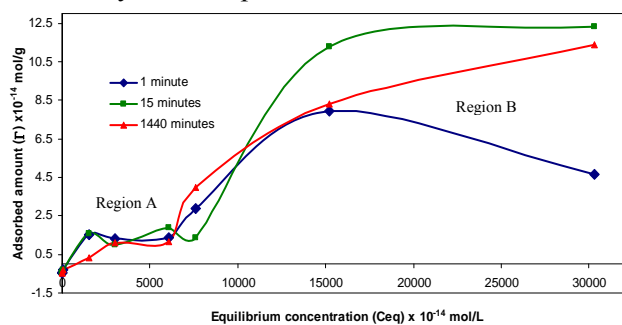


Fig 1: BSA adsorption on SAD with concentration

CONCLUSIONS Protein-surface interactions may be monitored by covalent binding of FITC to a specific target protein (BSA). Binding constant-type studies were performed. Further work will determine whether this approach will work under conditions of competitive binding.

REFERENCES: ¹I.R. Gibson, *et al.* (1999) *J. Biomed Mater Res* **44**: 422-8. ²K.A. Hing, *et al.* (2006) *Biomaterials* **27**: 5014-26.

ACKNOWLEDGEMENTS: Thank EPSRC and Apatech Ltd for funding this research.

Maintenance of Pluripotency in Human Embryonic Stem Cells Cultured on a Synthetic Substrate

[MM Mahlstedt](#)^{1,2}, D Anderson,³ JS Sharp,² MD Barbadillo Muñoz,³ LD Buttery,¹ MR Alexander,¹ FRAJ Rose,¹ & [C Denning](#)³

¹ School of Pharmacy, University of Nottingham, Nottingham, NG7 2RD, UK

² School of Physics and Astronomy, University of Nottingham, Nottingham, NG7 2RD, UK

³ School of Clinical Sciences, University of Nottingham, Nottingham, NG7 2RD, UK

INTRODUCTION: Realising the potential clinical and industrial applications of human embryonic stem cells (hESCs) is limited by the need for costly, labile or undefined growth substrates currently used in hESC culture. Here we demonstrate a novel method that maintains hESC pluripotency, equivalent to that of hESCs cultured on Matrigel, using an inexpensive and robust synthetic culture substrate.

METHODS: HUES7 and NOTT1 hESCs were trypsin-passaged for up to 50 days on oxygen plasma etched tissue culture polystyrene (PE-TCPS). This synthetic culture substrate is stable at room temperature for at least a year and is readily prepared by placing polystyrene substrates in a radio frequency oxygen plasma generator for five minutes.

X-ray photoelectron spectroscopy (XPS) and time-of-flight secondary ion mass spectrometry (ToF-SIMS) were used to evaluate any chemical changes to the polystyrene surface. Atomic force microscopy (AFM) was used to assess surface topography before and after plasma etching. Water contact angle (WCA) measurements were performed to assess surface wettability.

Pluripotency of hESCs cultured on PE-TCPS was gauged by consistent proliferation during serial passage, expression of stem cell markers (OCT4, TRA1-60 and SSEA-4), stable karyotype and multi-germlayer differentiation *in vitro*.

RESULTS: Modification of the polystyrene surface chemistry by plasma etching was confirmed by XPS and ToF-SIMS, both which identified elemental and molecular changes as a result of the treatment.

Both HUES7 and NOTT1 cultures on PE-TCPS demonstrated similar cell morphology (Fig. 1) and growth rates to Matrigel cultures. Pluripotency of PE-TCPS cultures was confirmed after a minimum of 10 consecutive passages by the expression of stem cell markers (Fig. 2) and quantified by fluorescence-activated cell sorting (FACS).

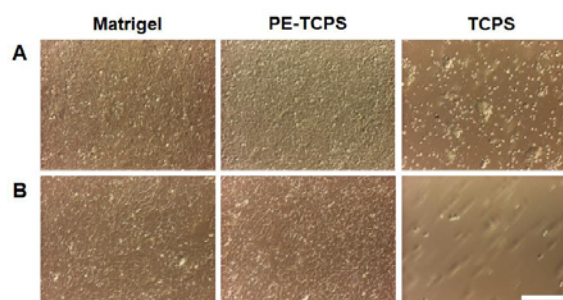


Fig. 1: Culture of hESCs on different substrates: HUES7 (A) or NOTT1 (B) cells cultured on Matrigel and on PE-TCPS show similar morphology, with high nuclear to cytoplasmic ratio and prominent nucleoli, which is distinct from the lack of attachment on TCPS. Bar = 200µm.

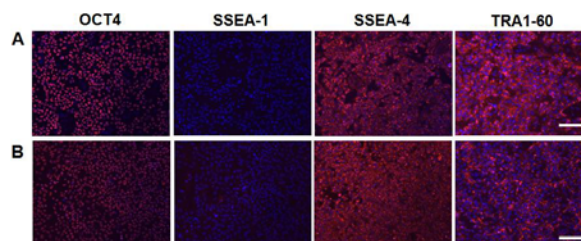


Fig. 2: Expression of stem cell markers: HUES7 (A) and NOTT1 (B) cells cultured on PE-TCPS express the hESC pluripotency markers OCT4, SSEA-4 and TRA1-60. Bar = 200µm.

DISCUSSION & CONCLUSIONS: Our work demonstrates that PE-TCPS substrates are compatible with hESC pluripotency. The generation of cost-effective, easy-to-handle synthetic, defined, stable surfaces to replace Matrigel for hESC culture will expedite stem cell use in biomedical applications.

ACKNOWLEDGEMENTS: The University of Nottingham, British Heart Foundation, BBSCR and MRC for funding.

SILICA-GELATIN HYBRID SCAFFOLDS WITH CONTROLLED DEGRADATION AND MECHANICAL PROPERTIES

O. Mahony^a, O. Tsigkou^a, C. Ionescu^b, C. Minelli^c, M.E. Smith^b, M.M. Stevens^c, J.R. Jones^a

^aDepartment of Materials^c (and Institute of Biomedical Engineering), Imperial College London, SW7 2AZ

^bDepartment of Physics, University of Warwick, Coventry, CV4 7AL, UK

Introduction: Bioactive glass scaffolds are ideal for tissue regeneration as they are osteogenic, resorbable and macroporous¹. Their limitation is that they are brittle, which restricts their load bearing applications. Composites of inorganic bioactive constituents combined with polymers have been developed to make materials with increased toughness². However this solution is not ideal as inorganic and organic phases resorb at different rates, leading to material instability. Therefore it is proposed that nanocomposite materials where the inorganic and organic are covalently linked can provide enhanced control of degradation rates and mechanical properties. This work focuses on hybrids containing silica and gelatin, covalently linked using 3-Glycidoxytrimethoxysilane (GPTMS).

Methods: A gelatin solution was functionalised by reacting with GPTMS. A sol was created by hydrolysing tetraethyl orthosilicate (TEOS) in water and 1N HCl. The two solutions were mixed and allowed to gel. Compositions of 30-60 wt % gelatin were produced with C-factors (mole ratio of GPTMS/gelatin) of 0-2000. Materials were characterised ²⁹Si MAS NMR and AFM. ICP analysis of dissolution products was also carried out. Macroporous scaffolds were produced using a novel foaming and freeze drying process. Cell response to the new materials was assessed using human mesenchymal stem cells (MSCs).

Results and Discussion: GPTMS reacted with gelatin, via opening of its epoxy ring³. In this study ²⁹Si NMR (Fig. 1) showed that GPTMS condensed with the hydrolysed TEOS as the silica network

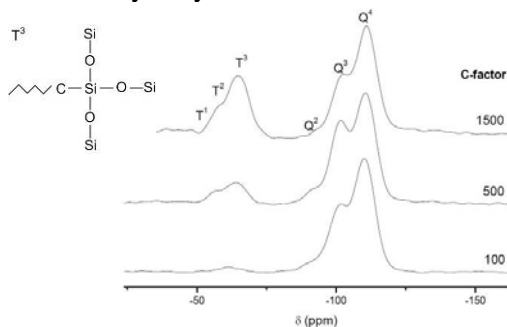


Fig. 1 ²⁹Si MAS NMR spectra of 30 wt% gelatin hybrids, C-factor 100-1500. Inset: schematic of a T³ structure

formed. Fig. 1 shows the presence of T species, which are indicative of a carbon atom bonded to a silicon atom from a silica network. The T³ species (Fig. 1 inset) increased from 10% to 26% as C-factor increased from 500 to 1500. This was

represents a reduction in the number of non-bridging oxygens. GPTMS therefore provides a covalent link between the organic and inorganic phases and increases inorganic condensation.

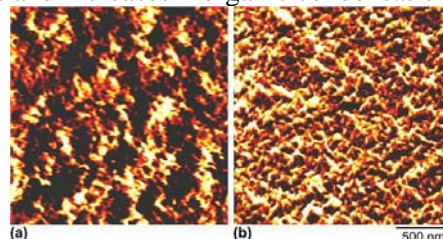


Fig. 2 tapping mode AFM showing phase images of 30 wt% hybrids with C-factor 0 (a) and 1500 (b)

Dissolution studies showed that gelatin release rate decreased as C-factor increased, with negligible release over 500h for C-factor 1500. Importantly, Si ion release followed a similar trend. For instance, silicon release from the C-factor 0 sample reached its maximum after 60 h, which was 4 times higher than the silicon release of the C-factor 1500 sample after 400 h in solution. The NMR and degradation indicate that this is a true hybrid material.

AFM phase mapping of the hybrids (Fig. 2) showed a distinct change in surface properties of the hybrids with changing C-factor. In Fig. 2 bright regions show the

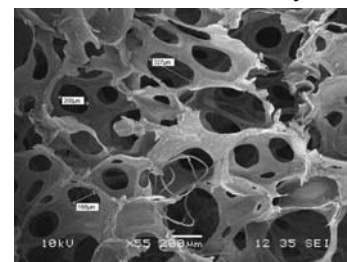


Fig. 3 SEM showing a macroporous hybrid silica-gelatin scaffold

organic phase and dark regions the inorganic phase. Fig. 2(a) shows a C-factor 0 sample that exhibited relatively large phase domains of ~87 nm, compared to C-factor 1500 (Fig. 2(b)) in which domain sizes were ~41 nm. Thus constituent phases of the hybrid had finer scale interaction as C-factor increased.

Hybrids were shown to be non cytotoxic when cultured with MSCs over 7 days. Hybrids have also been fabricated into elastic macroporous scaffolds of varying stiffness (dependent on composition). Fig 3 shows the interconnected pore network.

References ¹Jones et al. (2006). Phil. Trans. R. Soc. 364: 263-281. ²Wang (2003). Biomater. 24:133-2151. ³Ren et al. (2001). J. Sol-Gel Sci. Tech. 21:115-121

Investigation of the Impact of Wounding and Inflammation on Melanoma Migration in a 3D Skin Model

CMG Marques & S MacNeil

Tissue Engineering Group, Kroto Research Institute, North Campus, University of Sheffield, S3 7HQ, UK.

INTRODUCTION: Many studies suggest a strong association between inflammation and tumour progression. Clinical studies suggest that NSAIDs (Non Steroidal Anti-Inflammatory Drugs) provide protection against cancer. Our previous work demonstrated that inflammation (induced by TNF- α) accelerated melanoma migration and NSAIDs such as aspirin^[1] and ibuprofen^[2] reduced melanoma migration in 2D cultures.

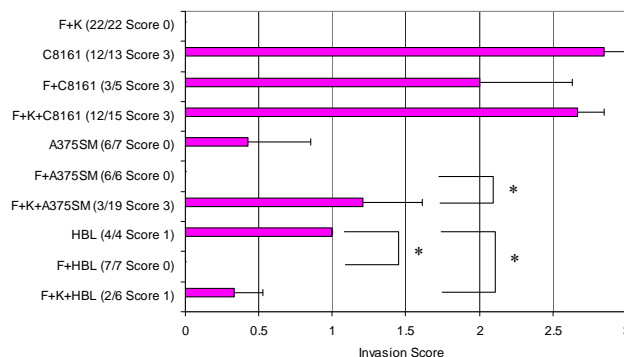
AIM: To investigate whether inflammation has an impact on wound healing and melanoma invasion using a 3D tissue engineered model.

METHODS: Tissue engineered human skin models containing 3 different melanoma cells (as described previously by Eves *et al.*^[3]) were wounded using a scalpel blade. Healing and inflammation were induced by the addition of fibrin clots and TNF- α respectively. The effect of Ibuprofen release from a hydrogel was also examined.

RESULTS: In tissue engineered human skin, melanoma cells invaded very differently. The most aggressive were C8161 followed by A373SM and then HBL cells. Fibroblasts reduced the invasion of A375SM cells ($p=0.0224$) and HBL cells ($p<0.05$), (See Figure 1). In reconstructed human skin models, full thickness wounds with melanoma cells were shown to heal *in vitro* (See Figure 2). TNF- α added to a fibrin clot reduced this wound healing but the addition of NSAID Ibuprofen incorporated into a hydrogel greatly accelerated wound healing.

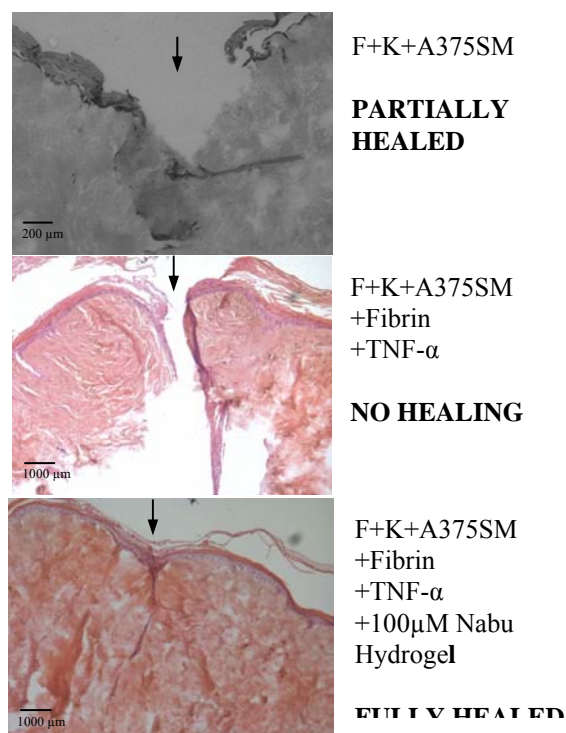
DISCUSSION & CONCLUSIONS: This work confirms the different pattern of melanoma invasion in these 3D models but also shows that fibroblasts had a suppressive effect on melanoma invasion in 2 of 3 cell lines. However the main finding was that inflammation tended to reduce healing in this 3D model while topical delivery of an anti-inflammatory (Ibuprofen) accelerated healing. This model can now be used to assess the impact of inflammation and wound healing on melanoma invasion.

Figure 1. Differences in the extent of melanoma cell invasion into the dermis. The skin composite types are described followed by the number of skin composites in which the



invasion was scored. The maximum invasion score is indicated in brackets. (The invasion score was assessed as 0 – no invasion, through to 3 – extensive invasion) The histograms show the Mean+SEM of all scores. (F=Fibroblasts; K= Keratinocytes).

Figure 2. Wounded skin composites showing the influence of



inflammation (fibrin plus TNF- α) and of a NSAID (Ibuprofen) on wound healing.

REFERENCES: ¹Katerinaki *et al.* Melanoma Res 16(1):11-22, 2006. ²Redpath *et al.* Brit J Dermatol (*in press*). ³Eves *et al.* Br J Dermatol, 142(2):210-22, 2000.

ACKNOWLEDGEMENTS: CAPES Foundation; State University of Santa Catarina - UDESC.

CHARACTERISING REGIONAL ULTRASTRUCTURE IN PERIPHERAL NERVES

S. Mason^{1,2} J. Harle² J.B. Phillips¹

¹*Department of Life Sciences, The Open University, Milton Keynes, UK.*

²*Department of Physics and Astronomy, The Open University, Milton Keynes, UK.*

INTRODUCTION: Peripheral nerve repair is often compromised by a failure to restore the biomechanical integrity of damaged nerves. Restoration of the tensile properties of nerves, in particular their ability to bend and stretch during limb movement, is an important consideration in the design of tissue engineered repair conduits and other repair approaches. An understanding of the mechanical architecture of peripheral nerves that underpins their tensile properties is therefore desirable. Previous research has identified that the stiffness of rat peripheral nerves varies longitudinally according to where they traverse joints¹. This study explores how ultrastructural features such as the size-distribution of collagen fibrils and the thickness of the perineurium vary in specific regions of rat sciatic nerves.

METHODS: Joint and non-joint regions of sciatic nerves were resected *post mortem* from 250-350 g rats. These samples were maintained at their *in situ* tension and fixed in a 2% glutaraldehyde solution in 0.1M phosphate buffer, post fixed in 1% osmium tetroxide and processed for electron microscopy. Transverse ultrathin sections were prepared and stained with uranyl acetate and Reynolds lead citrate for transmission electron microscopy (TEM). Perineurium thickness and collagen fibril diameter were measured using ImageJ (Fig 1), and joint and non-joint regions of each sample were compared.

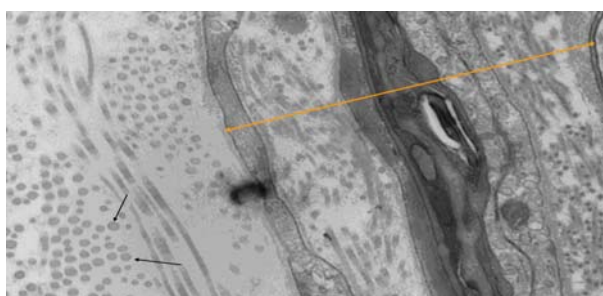


Fig 1: Representative TEM image: Line shows perineurium, arrows indicate collagen fibrils.

RESULTS: Perineurial thickness varied between the samples of rat sciatic nerve, with joint regions showing a significantly thicker perineurium than corresponding non-joint regions (Table 1). Collagen fibrils within the epineurium also varied

in size; a histogram plot showing the distribution of collagen fibril diameters is shown in Fig 2.

Table 1: Mean perineurium thickness in joint and non-joint regions of nerve \pm SEM. * $p < 0.05$

Region	n	Thickness (μ m)
joint	6	4.14 \pm 0.04
non-joint	6	3.25 \pm 0.03

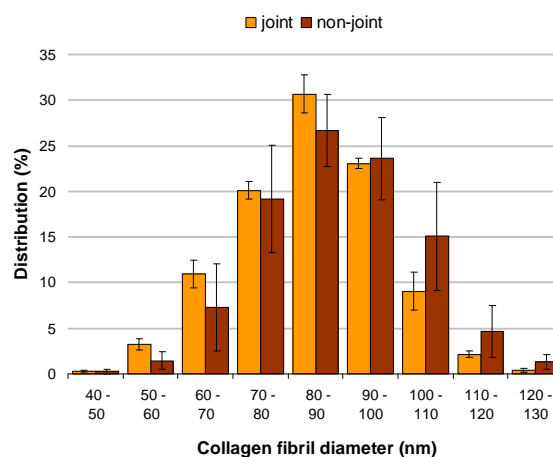


Fig 2: Collagen fibril diameter: A total of 250 fibrils were sampled from the innermost 10 μ m of the epineurium within each region (n=3).

DISCUSSION & CONCLUSIONS: Differences in the thickness of the perineurium and the size distribution of collagen fibrils in the epineurium correspond to regions known to exhibit differences in tensile properties. This study shows that ultrastructural analysis of distinct regions along the length of peripheral nerves can reveal subtle differences in structural features that may influence the ability of peripheral nerves to bend and stretch. An understanding of the cellular and extracellular factors that contribute to peripheral nerve biomechanics is likely to be essential for the successful development of future repair strategies.

REFERENCES: ¹Phillips JB, Smit X, De Zoysa N, Afoke A, Brown RA. (2004) *J. Physiol* **557**: 879-87.

ACKNOWLEDGEMENTS: Technical expertise from Heather Davies, Frances Colyer, Steve Walters and Karen Evans.

Characterisation of Hydrogels used in Regenerative Medicine

M L Mather^{1,2} & P E Tomlins¹

¹ *Biomaterials Group, National Physical Laboratory, Teddington, Middlesex, TW11 0LW, UK*

² *Applied Optics Group, Electrical Systems & Optics Research Division, University of Nottingham, Nottingham, NG7 2RD, UK*

INTRODUCTION: In regenerative medicine hydrogels are mainly used as environments to support cell growth and as cell delivery vehicles [1-3]. In these applications, the efficacy of a hydrogel typically depends on its permeability to dissolved gases, nutrients and bioactive agents as well as its ability to support: cell growth and migration; and bear mechanical load. This work outlines key factors related to hydrogel performance and discusses the need for characterisation protocols to support the translation of emerging regenerative therapies.

KEY CHARACTERISATION FACTORS:

Hydrogels are typified by high water content (~80% to 99%), structural inhomogeneities, low resilience and susceptibility to shrinkage, making them intrinsically difficult to work with. As such, special attention needs to be taken in their characterisation. A further challenge associated with hydrogels lies in translating their characteristics to performance. This can be addressed by considering some key characterisation factors which can broadly be classified as biocompatibility, kinetics, permeability and physical stability (see Table 1). Each factor can be assessed through measurement of the hydrogel attributes identified in Table 1.

CHARACTERISATION PROTOCOLS: It is important that protocols for characterisation are developed to enable consistent performance data to be obtained. Such information could be used to minimise batch-to-batch variability and to optimise hydrogel composition. Ideally characterisation protocols should: not require pretreatment of samples; use non-invasive, on-line measurements; have fast sampling rates to study the kinetics of formation; and probe material properties over a range of length scales. Additionally techniques should be insensitive to variations in sample geometry and accessible such that inter-laboratory comparisons can be carried out. For these reasons optical, ultrasonic and dielectric techniques are good candidates, which when used in combination, provide a broad spectrum of information.

Table 1. Key characterisation factors: kinetics biocompatibility, permeability, physical stability.

DISCUSSION & CONCLUSIONS: Reliable hydrogel characterisation will require the development of procedural measurement standards that will take into account the need for tight control over hydrogel preparation, measurement techniques and interpretation of results. Overall, it is concluded that improved product specification and demonstration of tighter functional control will expedite the translation of hydrogel based regenerative medicine therapies.

REFERENCES: ¹J.F. Mano, G.A. Silva, H.S. Azevedo *et al* (2007) *Journal of the Royal Society Interface* **4**, 999-1030. ² M.C. Cushing, K.S. Anseth (2007) *Science* **316**, 1133-1134. ³ M.P. Lutolf, J.A. Hubbell (2005) *Nature Biotechnology* **23**, 47-55.

ACKNOWLEDGEMENTS: This work is supported by the National Physical Laboratory Strategic Research Scheme.

Kinetics	Biocompatibility
Setting time	Cytotoxicity
Swelling rate	Sterility
Matrix degradation	Cell proliferation & Adhesion
Release rate of bioactive agents	Inflammation
Rate of change in material phase	Degradation products
Permeability	Physical Stability
Cell transport	Osmotic stability
Nutrients & waste transport	Complex modulus
Bioactive agent transport	Cell immobilisation

Effect of HINS light on the contraction of fibroblast populated collagen lattices

R McDonald¹, S J MacGregor², M Maclean², JG Anderson² & M H Grant¹

¹Bioengineering Unit, University of Strathclyde, Glasgow, G4 0NW, UK.

²The Robertson Trust Laboratory for Electronic Sterilisation Technologies, University of Strathclyde, Glasgow, G1 1XW, UK

INTRODUCTION: High intensity narrow spectrum (HINS) light has been shown to have bactericidal effects on a range of medically important bacteria[1]. HINS technology could potentially be useful as a method for disinfecting medical implants, tissue engineered constructs and wounds. The fibroblast populated collagen lattice (FPCL) was used as an in vitro model to investigate the effect of HINS light on the wound contraction phase of wound healing.

METHODS: Collagen lattices (0.3% (w/v) type I rat tail collagen) were seeded with 3T3 mouse fibroblasts cells at a density of 2.5×10^4 cells/cm² and allowed to contract freely. FPCLs were treated with HINS light at 0.1, 1, and 10mW/cm² for 1 h, equivalent to a dose of 0.36, 3.6 or 36 J/cm² respectively. The contraction of FPCLs was measured prior to, and for up to 7 days following treatment. At 24, 48 and 120 h post treatment, cells were counted using the MTT assay, after using collagenase to release the cells from the lattices. At these same time points, FPCLs were stained with propidium iodide (PI) and acridine orange (AO) to assess cell viability by fluorescence microscopy.

RESULTS: Figure 1 shows that no significant difference was observed between contraction rates of untreated FPCLs and those treated at 0.1mW/cm² and 1mW/cm². FPCLs treated at 10mW/cm² stopped contracting immediately and did not recover significantly within 7 days.

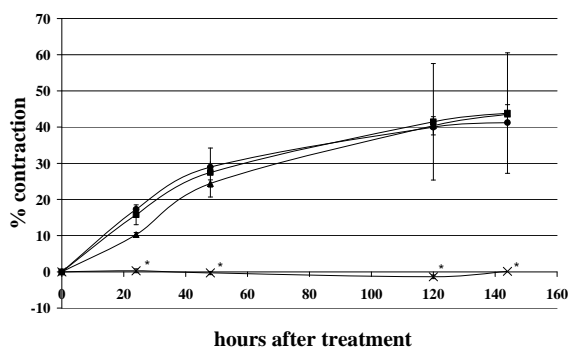


Fig. 1: Effect of HINS light on the contraction of FPCLs. Treatments were carried out, at 0.1, 1 and 10mW/cm² (squares, triangles and crosses respectively) for 1 hour. Control is indicated by circles. The percentage contraction, of the FPCL

area, was calculated from the point of treatment. *indicates significant difference from control at each time point ($P > 0.05$, ANOVA followed by Dunnett's test)

The MTT assay results show that for up to 120 h post treatment, there was no significant difference in cell number when treating FPCLs at 0.1mW/cm² and 1 mW/cm² (see Figure 2). Treatment at 10mW/cm² for 1 h caused an approximate 80% decrease in cell number after 24 h. By 120 h post treatment, cells in FPCLs treated at 10mW/cm² did not show significant recovery.

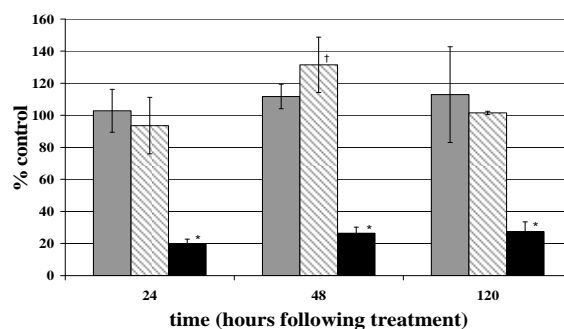


Fig. 2: MTT assay results for FPCLs treated at 0.1, 1 and 10mW/cm² (grey, shaded and black respectively) at 24, 48 and 120 hours post treatment. * $P < 0.5$, comparing between treatments at each time point, † $P < 0.5$, comparing each individual intensity over the time points (ANOVA followed by Fisher's test for both comparisons)

Microscopic assessment of cell viability using PI and AO staining confirmed these results.

DISCUSSION & CONCLUSIONS: The results show that HINS light treatment at values of 0.1 and 1mW/cm² have no detrimental effect on FPCL contraction. This technology has considerable potential to augment efforts to disinfect medical devices, tissue engineered constructs and implants.

REFERENCES: ¹ M. Maclean, S.J. MacGregor, J.G. Anderson, et al (2008) FEMS Microbiol Lett Aug;285(2):227-32

ACKNOWLEDGEMENTS: RM is supported by the ESPRC Doctoral Training Centre (DTC) in Medical Devices.

Graded Hydrogel Constructs For Cartilage Tissue Engineering

R Mcleod, G Pattappa, J Irianto, M Awan, MM Knight & DA Lee

School of Engineering and Materials Science, Queen Mary, University of London, UK

INTRODUCTION: Articular cartilage is a heterogeneous tissue with alterations in chondrocyte morphology, matrix composition and mechanical properties with depth from the articular surface^{1,2}. Most chondrocyte-seeded constructs for cartilage tissue engineering, however, fail to take account of the inherent tissue heterogeneity. This study describes a novel method for the production of cell-seeded hydrogel constructs with defined graded properties, that better replicate the heterogeneous properties of the native tissue.

METHODS: *Preparation of gradient agarose constructs:* A commercially-available gradient maker or an in-house designed system were used for the preparation of gradient agarose constructs. 2% agarose and 4% agarose solutions containing bovine chondrocytes at 4×10^6 cells.mL⁻¹ were introduced into the reservoir and mixing chambers of the gradient maker. Constructs were prepared either as a series (individual constructs are broadly homogeneous in nature but the agarose gradient is represented by a progressing alteration in properties through the construct series) or using methods where each construct exhibits the full gradient through the thickness. Cell-seeded constructs were cultured for up to 8 days.

Analysis: The permeability of individual constructs from the construct series was assessed by monitoring the diffusion of a 500 kDa FITC-dextran. The peak stress and tangent modulus at 15% strain were determined. Cell viability in gradient constructs was assessed throughout the specimen depth using calcein AM and ethidium homodimer-1 staining. The glycosaminoglycan (GAG) content was assessed using the 1,9-dimethylmethylene blue assay. Local strain and cell deformation was assessed using a microscope test rig as described previously by the group³.

RESULTS: There was a clear correlation between normalised construct position within the construct series and permeability, peak stress and tangent modulus. Cell viability was maintained at over 90% throughout the culture period. The GAG content increased significantly over time in culture, but there was no difference in the GAG content between different regions of the constructs. The local strain decreased from the 2% region and least in the 4% region of the construct. The application of compressive strain to constructs on day 1 of culture induced an alteration from a spherical

morphology to an oblate ellipsoid. This phenomenon was more pronounced for cells in the 2% region of the construct compared to the 4% region (compare Figs. 1b and 1c). With increasing time in culture there was a corresponding reduction in cell deformation on application of compressive strain (Fig. 1c,d and 1b,c).

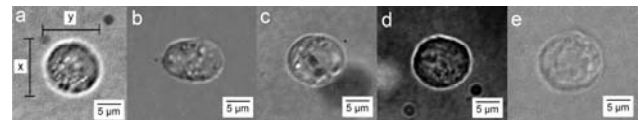


Figure 1. Representative images of cells in an unstrained construct (a) and in the 2% (b, d) and 4% regions (c, e) of a construct subjected to 20% strain on days 1 (b, c) and 8 (d, e).

DISCUSSION & CONCLUSIONS: The results clearly demonstrate the formation of a hydrogel construct with graded permeability and mechanical properties. The constructs were able to support the culture of chondrocytes, as evidenced by the retention of a high level of viability and the production of GAG-rich extracellular matrix. Cell deformation was dependent on spatial position within the construct, in a manner that recapitulates the situation in the native cartilage¹. The reduction in deformation over time is likely to be associated with the production of extracellular matrix, as reported in previous studies⁴. However, the maintenance of spatial heterogeneity of cell deformation may be important for the subsequent development of a functional cartilage neo-tissue. In this study the development of a gradient gel construct has been demonstrated using agarose. However the methods are applicable to other hydrogel systems and therefore may have widespread use for cartilage tissue engineering.

REFERENCES: ¹Guilak F et al. (1995), *J. Orthop. Res.* 13, 410-421. ²Schinagl RM et al (1997), *J. Orthop. Res.* 15, 499-506. ³ Knight et al (2002), *Biochim. Biophys. Acta.* 1570, 1-8. ⁴Lee DA & Bader DL (1995), *In Vitro Cell Dev. Biol.* 31, 828-835.

The effect of cell adhesion molecules on cellular elasticity: an AFM approach

G. M. McPhee^{1, 2}, M. J. Dalby², M. O. Riehle² & H. Yin¹

¹ Bioelectronics Research Centre, Department of Electronics & Electrical Engineering, University of Glasgow, UK.

²The Centre for Cell Engineering, University of Glasgow, UK

INTRODUCTION: It is well established that a biological cell's physical strength is conferred primarily by the actin filaments of the cytoskeleton. Using the Atomic Force Microscope (AFM) as a highly sensitive nanoindenter it is possible to characterize and quantify single cell elasticity variations induced by surface chemical changes or micro/nanotopographical features. In this study we affixed 5 μ m silica beads to tipless AFM cantilevers and probed 3T3 cells cultured on uncoated glass, Poly-L-lysine (PLL) and Fibronectin (Fn) coated glass to investigate whether these commonly used cell adhesion promoters affected cellular elasticity.

METHODS: AFM: Silica microspheres of 5 μ m diameter are affixed to the ends of tipless cantilevers (Arrow TL1, Veeco) with UV-curable glue. A grid of force-distance curves is then performed over the 3T3 cell nucleus at various speeds. No fewer than 16 curves were used to determine elasticity values at different speeds, but commonly >30 curves were averaged. The optimum indentation depth was found to be ~200nm and the Hertz model is used to fit each curve. From these measurements, an elasticity value (E) is extracted.

Sample preparation: 24mm diameter glass cover-slips were coated with 0.01% Poly-L-lysine solution (MW 70-150kDa) according to manufacturer's instructions (Sigma), or 5 μ g/cm² Fibronectin (bovine plasma) solution according to K. S. Masters *et al* [1]. Uncoated glass cover-slips were cleaned in a similar way as coated cover-slips and used as is for cell culture.

RESULTS: Analysis of the force-distance curves performed on cell nuclei highlight significant variations in cell rigidity between 3T3 cultured on PLL and uncoated glass and those cultured on Fn coated glass (Fig.1). This difference does not alter significantly with the speed of indentation, which varied between 0.25-0.5 μ m/sec for slow indentations and 3.5-5 μ m/sec for quick indentations. Using an indentation depth of ~200nm gave reproducible values and reduces the impact of the Hertz models limitations.

DISCUSSION & CONCLUSIONS: The use of AFM as a nanoindenter has previously proved a valuable tool to biologists for quantification of differences in elastic modulus. The published range of elasticity values obtained by AFM for 3T3 cells varies greatly and the values recorded here for cells on PLL or uncoated glass appear softer than recent estimates of between 0.6 and 4kPa [2, 3]. Elasticity values regularly as low as ~0.3kPa could be indicative of unhealthy cells, a sign that actin stress fibres are not properly forming due to sub-optimal culture conditions or high passage number cultures. Poly-L-lysine and Fn are commonly used for promoting cell adhesion, however, the study shown here demonstrates they might have different influences on cell cytoskeleton development, which should be taken into account when interpreting other physiological measurements. Further work on the biological mechanisms underlying this phenomenon is in progress.

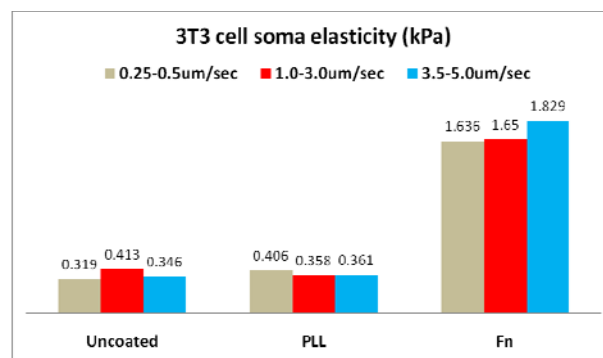


Figure 1: Young's modulus (E) values of 3T3 cells cultured for 1-3 days on PLL, Fn or uncoated glass cover-slips. Values for force-distance curves performed at 3 representative speeds are shown for each surface.

REFERENCES: 1. Masters, K.S *et al*, Journal of Biomedical Materials Research Part A, 2004.

71A (1): p. 172-180.

2. Haga H *et al*, Ultramicroscopy. 2000; **82**: 253-8.

3. Mahaffy RE, *et al*. *Biophys. J.* **86**:1777-93.

ACKNOWLEDGEMENTS: G. M. McPhee is supported by the EPSRC and H. Yin by the Royal Society of Edinburgh.

The use of aligned polymer microfibres in peripheral nerve engineering

¹C Murray-Dunning, ³S L McArthur, ²A J Ryan, ¹JW Haycock

Departments of ¹Engineering Materials and ²Chemistry, University of Sheffield, UK and
³Faculty of Engineering and Industrial Sciences, Swinburne University of Technology, Australia

INTRODUCTION: Injuries to the peripheral nervous system are common and although regeneration is possible axon damage is often to significant. Generally, surgical intervention is needed in order for any functional sensation to be regained. Although the gold standard for peripheral nerve repair is autografting there are disadvantages, including a lack of donor nerve or donor site morbidity. The high level of cell death and lack of coherent orientation of regenerating axons have lead to therapies using nerve guidance conduits (NGCs). In the simplest form NGCs are hollow tubes that act as a physical guide between the proximal and distal stumps, bridging the gap of the injury. NGCs can be made from a variety of synthetic or natural materials and incorporate cells and growth factors to improve guidance. The aim of the present study was to improve the NGC design by placing parallel degradable fibres within the NGC. Fibres are intended to support Schwann cell growth and encourage more complete axon alignment within the device.

MATERIALS & METHODS: Aligned poly L-lactide (PLLA) fibres were produced by electrospinning. Fibres were initially placed into a 2D planar model in order to investigate RN22 Schwann cell attachment and viability on PLLA fibres. Cells were analysed using a live/dead assay using Syto9/propidium iodide to measure viability. Phalloidin-TRITC, DAPI and focal adhesion point staining was also used to investigate cell attachment, alignment and structure. All cell and fibre work was imaged by confocal microscopy. The next stage of cell work focused on the introduction of a second cell type to form a coculture. For this an NG108-15 neurite cell line was used. Initial work was conducted using NG108-15 cells alone investigating viability, attachment and alignment on fibres (as for RN22 cells). To optimise cell-scaffold interactions the surface chemistry of PLLA fibres was changed by plasma polymer deposition, coating fibres with a layer of acrylic acid. Contact angle and XPS analysis was used to confirm a change in surface chemistry. A closed loop bioreactor described previously [1] was then used to further investigate cell viability, attachment and alignment under continuous flow conditions in 3D culture.

RESULTS & DISCUSSION: Initial work has showed that PLLA fibres readily sustain RN22



Figure 1: Closed loop bioreactor system. Preliminary co-culture experiments have also begun to investigate the effect of glial-neuronal cultures on different surface chemistries.

Schwann cell growth, but viability was only about 60% after 96hr culture. However, this increased significantly to 90% when the surface chemistry of fibres was modified by coating with a layer of acrylic acid. Cell number was also increased.

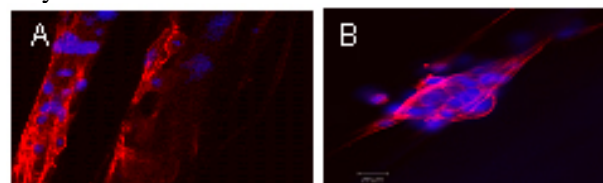


Figure 2 RN22 Schwann cell 72hr culture on: a) acrylic acid coated fibres: b) uncoated PLLA fibres. Stained with phalloidin-TRITC and DAPI NG108-15 cells were observed to show similar viability as the RN22 cells, but interestingly displayed increased dendricity when grown on surfaces coated in acrylic acid. This was evident when staining for actin filaments and focal adhesions and quantified by confocal software for measuring dendricity.

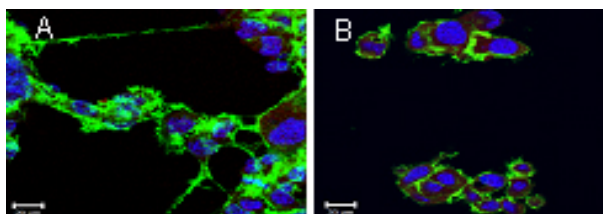


Figure 3 NG108-15 cells 72hr culture on a) acrylic acid coated coverslips and b) cultured on glass coverslips. Stained with phalloidin-FITC, DAPI and red cell tracker.

The use of a closed loop bioreactor allowed the study of cell viability and adherence in a 3D scaffold on aligned PLLA fibres. Significantly higher viability and adherence of Schwann cells was observed when cultured on fibres with an acrylic acid coating. This work forms the basis of designing 3D conduits for primary Schwann cell and stem cell delivery for PN injuries.

REFERENCES: 1. Sun T, Norton D, Vickers N, McArthur SL, MacNeil S, Ryan AJ, Haycock JW. *Biotech Bioeng* (2008) **99**(5):1250-60.

ACKNOWLEDGEMENTS: EPSRC for funding.

The influence of oxygen tension on the colony formation and proliferation of human mesenchymal stem cells

G. Pattappa, N.C. Jegard, J.D. de Bruijn & D.A. Lee

School of Engineering and Materials Science, Queen Mary University of London, London UK

INTRODUCTION: Mesenchymal stem cells (MSCs) reside *in vivo* under oxygen levels between 4-7% and have been shown to undergo greater population doublings and maintain of multipotency at later doublings upon culture under these conditions [1,2,3]. The present study investigated the effect of culture under 20%, 5% and 2% oxygen conditions on colony formation, population growth, oxygen consumption and senescence of human bone marrow derived MSCs.

METHODS: Fresh human bone marrow samples (Lonza, Wokingham UK) were aliquoted into cell culture flasks within a system permitting continuous and uninterrupted control of the oxygen environment (Biospherix, New Jersey USA). The flasks were fed with alpha-MEM + 8.5% FBS pre-equilibrated at either 20 %, 5 % or 2 % oxygen and placed into incubators set at the relevant oxygen conditions. Medium was not replenished until day 6 of culture. Thereafter, the medium was replenished every 2-3 days until confluence. The numbers of colonies (defined as a group of 16 cells) were monitored until confluence. The colony area and diameter were assessed from photomicrographs using commercial software (SigmaScan Pro, Systat software, CA., US). Population growth curves were recorded for the cells over 5 passages. Cellular oxygen consumption was assessed at passage 3 and 4 using a 384-well plate oxygen biosensor (BD Biosciences, Oxford UK). Senescence was assessed by staining for β -galactosidase activity (Sigma-Aldrich, Poole UK).

RESULTS: The number of colonies formed at 5% oxygen was significantly reduced compared with 20% and 2% oxygen for two separate donors ($p < 0.05$). The area and diameter of the colonies cultured at 2% were significantly smaller compared with oxygen in both donors ($p < 0.05$). The number of cells recovered upon first trypsinisation was greatest at 20% oxygen suggesting a greater number of cells per colony compared with 5% and 2% oxygen cultures ($p < 0.05$). The rate of proliferation for cells cultured at 20% oxygen was initially greater than the 5% and 2% conditions, however there was no significant difference in population doubling time between each oxygen condition after two passages (Fig. 1a).

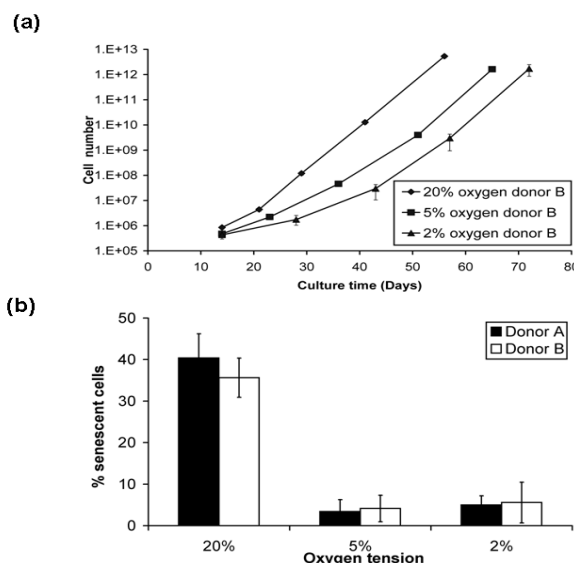


Fig. 1: (a) The proliferation growth curves for donor B and (b) the percentage of senescent MSCs grown under 20%, 5% and 2% oxygen conditions .

A significantly greater percentage of senescent cells within the 20% cell population compared with 5% and 2% oxygen cultures (Fig. 1b: $p < 0.05$). Cells cultured at 20% oxygen showed a significant increase in oxygen consumption compared with 5% and 2% oxygen, indicating a greater proportion of ATP generation through oxidative phosphorylation ($p < 0.05$).

DISCUSSION: The results of the investigation show that the oxygen tension influences the colony-forming efficiency of MSCs and may enable the selection of MSC sub-populations that have been described in previous studies [2]. Greater cell numbers were generated under 20% oxygen from initial colony formation but there was greater cellular senescence for cells grown at 20% oxygen, which may be associated with utilisation of oxidative phosphorylation leading to the generation of reactive oxygen species [1].

REFERENCES: ¹ F. Mousavvi-Harami et al (2004), *Iowa Orthop. J.* **24**: 15-20. ² G. D'Ippolito et al (2004) *J. Cell. Sci.*, **117**:2971-2981. ³ W.R. Grayson et al (2005), *J. Cell. Phys.* **207**: 331-339

ENGINEERING THE BONE-LIGAMENT INTERFACE

Jennifer Z. Paxton^{1,2}, Liam M. Grover³, Kenneth Donnelly^{1,2}, Robert P. Keatch² and Keith Baar¹

¹Division of Molecular Physiology and ²Division of Mechanical Engineering and Mechatronics, University of Dundee, DD1 5EH, ³Chemical Engineering, School of Engineering, University of Birmingham, Edgbaston, Birmingham, West Midlands B15 2TT, UK

INTRODUCTION: One of the major challenges faced in the engineering of artificial tissues for implantation is the development of a smooth transition between the artificial and native tissue. This is particularly relevant with regard to tissue engineering of musculoskeletal tissues, where the function of the tissue is to produce or transmit force. In these cases, it is essential to produce an interface that minimizes impedance mismatch between the biological and synthetic tissues and allows high fidelity force transmission while minimising strain concentrations that lead to failure of the interface. Current methods of ligament/tendon tissue engineering focus on the ligament proper, ignoring how the graft will be fixed in the body. We have directly addressed this issue and have engineered a functional bone-ligament interface between a bone mimetic (brushite cement) and tissue-engineered ligaments. This study shows the potential for engineering complete bone-to-bone grafts for future implantation.

METHODS:

Brushite cement anchor formation - Brushite cements were made by combining β -TCP (beta tricalcium phosphate) with orthophosphoric acid at specific powder to liquid ratios (P:L) and set in custom made molds .

Ligament formation - Brushite cement anchors were pinned to a Sylgard-coated 35mm petri dish and sterilised with 70% ethanol for 20 mins. 500 μ l of Dulbecco's Modified Eagle Medium supplemented with 10% FBS, 1% Penicillian/Streptomycin, 200U/ml thrombin, 2 μ l/ml Aminohexanoic acid and 2 μ l/ml Aprotinin solution was used to coat the sylgard layer. 200 μ l of 20mg/ml fibrinogen was added dropwise and the fibrin gel was left to polymerise at 37°C for 1hr. Chick tendon fibroblasts (CTFs) were seeded on top of the gel at a concentration of 100K/ml.

Measuring Interface Stress - Stress at the anchor/tissue (bone/ligament) interface was assessed by using a custom built bioinstron machine and measuring the force at which the interface failed.

Improving Interface Ability to Withstand Stress -

50uM ascorbic acid (AA), 50uM proline (P) and 2.5nM TGFbeta were added to the constructs 1 week following seeding.

RESULTS:

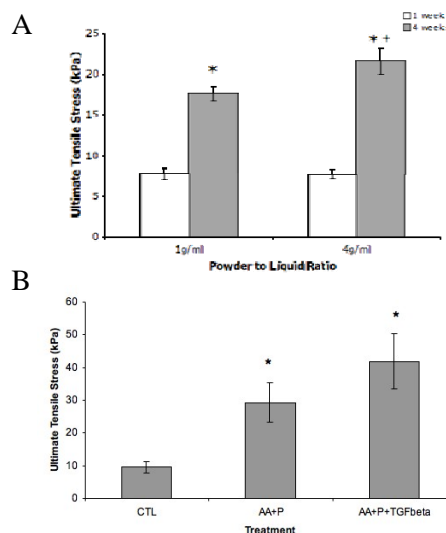


Fig. 1: A. The ability of the bone-ligament interface to withstand stress increases over time. Increasing P:L also improves interface stability. B. Treatment with AA+P for 1 week increases interface strength (increasing ultimate tensile stress) and this is further enhanced by the addition of TGFbeta.

DISCUSSION & CONCLUSIONS: An artificial bone-ligament interface has been engineered. The ultimate tensile stress of the interface increases over time from 7.8kPa \pm 0.75 kPa to 17.6 \pm 0.88 kPa (1g/ml) and from 7.7 \pm 0.59 kPa to 21.6 \pm 1.6 kPa (4g/ml). Furthermore, the addition of AA+P and TGFbeta improves the interface stability from 9.5 \pm 1.6 kPa to 29.2 \pm 5.9 kPa (AA+P) and 41.8 \pm 8.4 kPa (TGFbeta). These data strongly suggest that the integrity of the bone-ligament interface can be enhanced by material adaptations and growth factor supplementation to reach a strength suitable for future implantation.

ACKNOWLEDGEMENTS: This work was supported by a project grant from the EPSRC EP/E008925/1

Development & Characterisation of γ -PGA/Bioactive Silica Nanocomposite for Bone Regeneration

Gowsihan Poologasundarampillai & Julian R. Jones

Department of Materials, Imperial College London

INTRODUCTION: An important goal in bone tissue regeneration is to make constructs that have matching chemical, structural and mechanical properties to host bone available for implantation as soon as the need arises. Organic and inorganic materials are often used. Bioactive glasses have been shown to bond to soft and hard tissue [1] and stimulate bone growth [2]. Porous polymers can be degradable by chain scission and enzymatic action [3]. However, these two classes of materials alone are not suitable for applications that undergo cyclic loading due to poor tensile properties of glasses and because polymers easily buckle under compressive loading. Therefore a suitable bone tissue engineering construct would be a composite of the organic and inorganic constituents. In conventional composites the bioactive phase can be masked and it is difficult to match degradation rates. The aim of this work is to create new bioactive inorganic/organic hybrid scaffolds.

METHODS: The sol-gel method was used to produce class II nanocomposite monoliths and foams of Poly(γ -glutamic acid) (γ -PGA)/bioactive silica (Fig 1). The γ -PGA was first functionalised with glycidoxypropyltrimethoxy silane (GPTMS). This was then added to the inorganic sol containing hydrolysed TEOS. The solution was foamed with vigorous agitation after the addition of HF and surfactant.

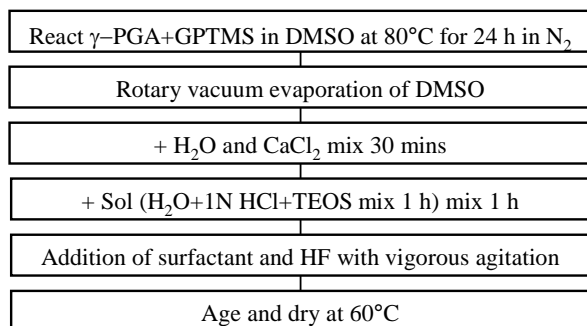


Fig 1. Flow diagram of the steps involved in synthesis of class II nanocomposite foams.

Bioactivity in simulated body fluid (SBF) and osteosarcoma cell line SaOs-2 cell attachment on the monoliths were tested. Mechanical properties of the monoliths were tested by performing compression tests. Foams were imaged in micro-

computed tomography (μ CT) and the pore network was quantified.

RESULTS: FTIR and ²⁹Si-NMR data showed the γ -PGA was successfully functionalised and crosslinked to the inorganic through Si-O-Si bonds. SEM and TEM showed nanoscale integration of the organic and the inorganic. The nanocomposite monoliths were found to deposit hydroxy carbonated apatite (HCA) layer in 24 h of immersion SBF. SaOs-2 cells were seen to populate the surface of the nanocomposite with extended filopodia indicating the materials' non-toxicity to cells.

Macroporous foams were also found to be bioactive and had modal macropores larger than 250 μ m and modal interconnects larger than 150 μ m (Fig 2).

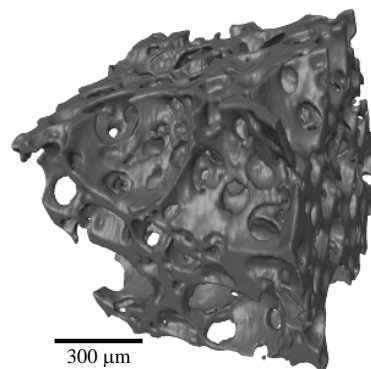


Fig 2. 3D μ CT image of nanocomposite foam.

DISCUSSION & CONCLUSIONS: Class II nanocomposites with polymer crosslinked to inorganic and both phases continuous have resulted in flexible monoliths. They were bioactive and not cytotoxic. The pore and interconnect sizes of the organic/inorganic nanocomposite foams were also calculated to be suitable for tissue regeneration.

REFERENCES: ¹L.L. Hench (1980) *Science* **208**(4446):826-31. ²I.D. Xynos, A.J. Edgar, L.D. Buttery et al (2001) *J Biomed Mat Res* **55**(2):151-7. ³M. Obst (2004) *Biomacromol*, **5**(4):1166-76.

ACKNOWLEDGEMENTS: EPSRC and RaEng for funding the project.

Combination of PDGF-BB and bFGF Reduces Differentiation but Maintains Proliferation of Human Tenocytes in Low Bovine Serum Culture *in vitro*

Yiwei Qiu, Xiao Wang, Raj Rout, Andrew J. Carr, Zhidao Xia*

Botnar Research Centre, Nuffield Department of Orthopaedic Surgery, University of Oxford, Nuffield Orthopaedic Centre, Oxford OX3 7LD, U.K.

INTRODUCTION: Degenerative tendon ruptures, such as massive rotator cuff tears are difficult to repair and the re-tear rates post surgery are high. Tissue engineering has the potential to improve the surgical outcomes of tendons repair by manipulating the cellular and biochemical processes [1, 2]. Previous work in our group has proven that combination of growth factors can promote tenocytes differentiation in 0% FBS in *in vitro* monolayer culture. The aim of this study is to utilize a fractional factorial design to optimize the culture medium with growth factors (PDGF-BB, bFGF and IGF-1) that controls tenocytes proliferation and differentiation with the lowest possible fetal bovine serum (FBS) for future tissue engineering. We hypothesize that the culture medium supplemented with combination of growth factors with minimum FBS usage will yield a satisfactory proliferation rate and maintain the tenocytes at less differentiated state.

METHODS: The tenocytes were isolated from healthy individuals. Following expansion for three passages, the tenocytes were seeded in 96 well culture plates with the initial cell number of 5×10^3 per cm^2 ; each seeded well was fed with 200 μl of the designated medium. Media were replaced twice a week. Alamar blue assays were performed according to manufacturer's protocol on day 1, 7 and 14 to examine the cell proliferation rate. Collagen synthesis was quantified by Sirius red staining and collagen synthesized per cell was calculated. Total RNA was extracted from tenocytes on day 14 and was reverse transcribed to complementary DNA (cDNA). Template cDNA was then used in gene specific PCR for Collagen I, Scleraxis, Tenomodulin and Decorin. The GAPDH was used as internal control. The procedures were performed according to manufacturer's protocol. The relative quantification of the mRNA levels of the target genes was determined by using the $2^{-\Delta\Delta Ct}$ method.

RESULTS: The results showed that 1% FBS supplemented with 50ng/ml PDGF+50ng/ml bFGF in tenocytes monolayer culture maintained high proliferation rate and inhibited differentiation in comparison to 10% FBS, as verified by collagen synthesized per cell and the mRNA expression of the tenocytes differentiation markers.

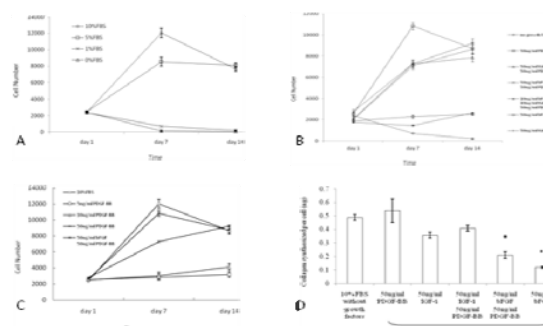


Fig. 1: Tenocytes proliferation rates in different culture medium by Alamar Blue Assay and collagen synthesized per cell by Sirius red. 10% FBS as control group. (A) 0% FBS with no growth factors, (B) 1% FBS with different concentrations of growth factors, (C) 1% FBS with different concentrations of PDGF-BB and bFGF, (D) collagen synthesized per cell by Sirius red staining of the tenocytes cultured in different culture medium supplements after 14 days.

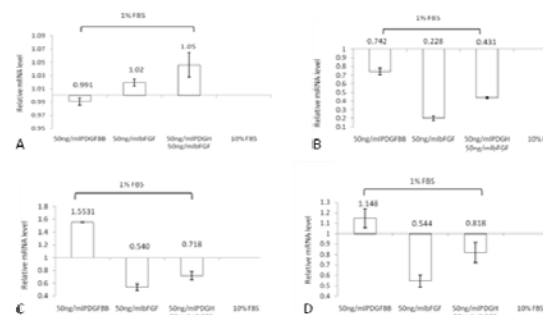


Fig. 2: Relative mRNA expression of SCX(A), COL1(B), TNMD(C) and DCN(D) by real time RT-PCR after 14 days of culture. GAPDH mRNA was used to normalize the variability in template loading. The data was presented as ratio of expression to the control group (10%FBS) whereas the expression of the control group is equal to one.

CONCLUSIONS: This work has proven that PDGF-BB is a potent stimulator in tenocytes proliferation and bFGF is a strong inhibitor in tenocytes differentiation, both growth factors act dose dependently.

REFERENCES:

- Goh, J.C., et al., *Tissue-engineering approach to the repair and regeneration of tendons and ligaments*. Tissue Eng, 2003. **9** Suppl 1: p. S31-44.
- Woo, S.L., et al., *Tissue engineering of ligament and tendon healing*. Clin Orthop Relat Res, 1999(367 Suppl): p. S312-23.

THE POTENTIAL OF SIMVASTATIN PRO-DRUG FOR OSTEOGENIC DIFFERENTIATION ON MOUSE EMBRYONIC STEM CELLS

O.Qutachi¹, K.M. Shakesheff, L.D. Buttery

Wolfson Centre for Stem Cells Tissue Engineering and Modelling, Centre of Biomolecular Sciences, School of Pharmacy, University of Nottingham, Nottingham, U.K

INTRODUCTION: Simvastatin is a pro-drug that inhibits the hepatic enzyme, 3-hydroxy-3-methylglutaryl-coenzyme A reductase which is the rate limiting step in cholesterol synthesis. Statins have been used effectively in the treatment of hypercholesterolemia. For tissue engineering purposes simvastatin show anabolic effects on bone¹. Currently most of the *in vitro* studies if not all concentrate on the active form of simvastatin. The aim of this work was to monitor osteogenesis in mouse embryonic stem cells using four different concentrations of the simvastatin pro-drug.

METHODS: An initial cytotoxicity assay for simvastatin on feeder free mouse embryonic stem cells was performed using alamar blue. Regarding osteogenic differentiation, embryonic stem cells were allowed to aggregate in a multi-well plate² then after three days embryoid bodies were disaggregated and cultured in the plate for 21 days. Four concentrations of simvastatin were tested (4 μ m, 2 μ m, 1 μ m and 0.1 μ m) against control containing no simvastatin. The media for all groups was supplemented with ascorbic acid 2-phosphate and β -glycerophosphate. Analysis was performed at three time points (day 7, 14 and 21) where alkaline phosphatase (ALP) activity in cell lysates was measured by a spectrophotometric method based on the enzymatic transformation of p-nitrophenol. Protein concentration was determined by BCA assay. Data were expressed as ALP activity per μ g protein. In addition matrix mineralization was assessed in which cells were fixed with 4% paraformaldehyde and stained with 2% alizarin red washed with water and left to dry.

RESULTS: Simvastatin concentrations higher than 4 μ m were excluded due to severe toxicity. ALP activity starts to increase from day 7 within the 0.1 and 1 μ m groups. The 2 μ m group showed a constant level between day 7 and day 14 which start to increase then after. With the 4 μ m group the level started much higher at day 7 and continue to decline. The control group showed a continuous increase until day 14 then started to decline. Matrix mineralization was obvious within the 0.1 and 1 μ m group; weak for the control; and negative for the 2 μ m and 4 μ m groups.

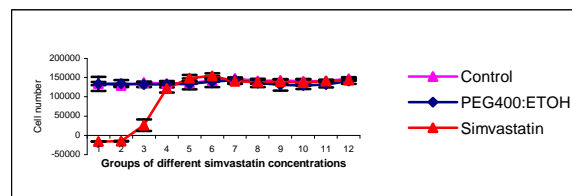


Fig. 1: Mouse ES cells after 96 hours exposure to simvastatin starting with 35 μ M per ml ending with 0.04 μ M per ml. The drug vehicle (PEG400: ETOH) at 55:45 ratio was also tested.

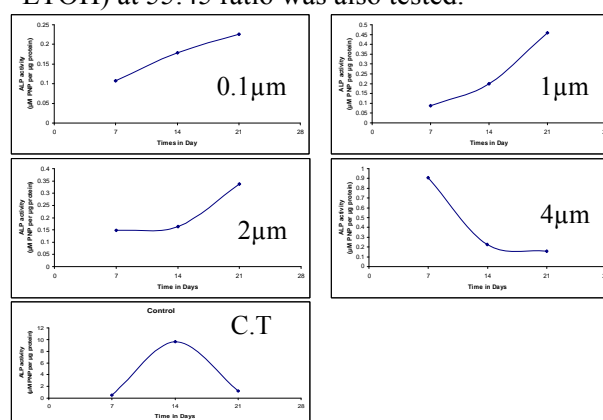


Fig. 2: ALP activity normalised against protein for different simvastatin concentrations at three time points.

DISCUSSION & CONCLUSIONS: Simvastatin pro-drug induce osteogenic differentiation and this was observed within considerably low concentration between 0.1 and 1 μ m. Some cytotoxicity observed with the 4 μ m group which might interfere with the osteogenic differentiation. Interestingly the 2 μ m group didn't show matrix mineralization; further study using PCR is needed.

REFERENCES: ¹ Mundy, G., et al., *Stimulation of bone formation in vitro and in rodents by statins*. Science, 1999. **286**(5446): p. 1946-9. ² Ezekiel, U.R., et al., *Single embryoid body formation in a multi-well plate*. Electronic Journal of Biotechnology, 2007. **10**(2): p. 328-335.

ACKNOWLEDGEMENTS: I would like to thank my family, tissue engineering group and the University of Nottingham.

DYNAMIC CULTURE OF ANTERIOR CRUCIATE LIGAMENT TISSUE ENGINEERED CONSTRUCTS

S Rathbone¹, D Healy², S Cartmell¹

¹ Institute of Science & technology in Medicine, Keele University, Hartshill, Stoke-on-Trent.

² Giltech Ltd, North Harbour Estate, Ayr, Scotland.

INTRODUCTION: Tissue engineering may offer improvements to the current surgical procedures undertaken by the 150,000 people per year¹ in the UK that need an ACL reconstruction. This study has investigated different materials and culture regimes for use in ACL tissue engineering.

MATERIALS & METHODS: Two different materials were analysed as a cell guiding conduit for primary human mesenchymal stem cells (MSCs) in this ACL tissue engineering approach – (1) A degradable glass fibre/alginate composite (Giltech Ltd, Scotland, consisting of the basic networking oxides NaO, CaO and P₂O₅, which were then combined with sodium alginate to form a composite) and (2) A porous (30-250µm in diameter) polyurethane foam (Qosina, USA). MSCs (Lonza, passage 5) were cultured on the scaffolds (strips, 1x6cm) for up to 12 days. All samples were cultured in static conditions for the first 7 days. For days 7-12 samples were either continued in static culture or were mechanically loaded (0.5Hz, 1hr/day) using a Bose ELF3200 biodynamic instrument. Glass fibre/alginate constructs were strained at 1% and PU constructs at 10% of their initial lengths using a sinusoidal waveform. A DNA assay (4hrs and 7days) and live/dead staining, scanning electron microscopy (SEM) and collagen type I and III gene expression using real time RT-PCR (7 and 12days n=5) was performed.

RESULTS: Approximately 80% of the initial cell number was seeded onto both constructs. Between 4hrs and 7d, there was no increase in cell number on either scaffold type. At 7 and 12d, live/dead staining showed viable, non-confluent cells attached to the glass fibre/alginate composite and cells appeared more spread in the glass/alginate loaded sample than in the static sample (fig 1). The cells on the PU sample appeared rounded in morphology at 7 and 12d in both static and loaded conditions. SEM images also showed sparse cell coverage, where few cells appeared to be attached in the loaded samples at 12d with small amounts of fibrous extracellular matrix (ECM) with both scaffold types (fig 1). There was no significant difference in collagen type I or III gene expression over the 12d for static or loaded samples in the PU foam. But there was a significant

down regulation in collagen type I and III after loading at 12d in comparison to 7d static culture.

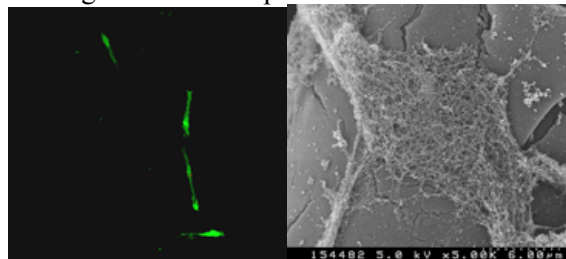


Fig. 1: 12day 1% strain glass fibre/alginate composite with live/dead stain (left) & SEM (right)

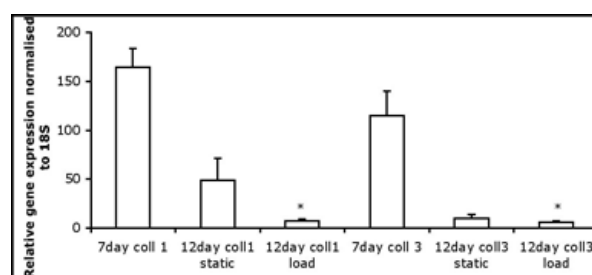


Fig. 2: Gene Expression of collagen type I & collagen type III of cells on statically cultured or mechanically strained glass fibre/alginate composite. * $p < 0.05$ of 12 day loaded sample in comparison to 7day static culture for both collagen type I and III (bars = standard error of mean).

DISCUSSION & CONCLUSIONS: Both scaffolds used showed potential with regards to low toxicity however further optimisation of the surface characteristics of both scaffolds to aid cell adhesion / proliferation over a 12 day time frame needs to be performed. The mechanical properties of the PU foam allowed more physiological loading regimes of 10% strain to be applied, however the PU foam is not degradable. The degradable glass fibre and alginate scaffold was limited in terms of elasticity and allowed loading regimes up to 1% only. We are currently investigating surface treatments of these scaffolds along with analysing fully degradable elastomeric foams that can withstand higher loading regimes such as poly((1,2-propanediol-sebacate)-citrate).

REFERENCES: ¹ J. Cooper, H. Lu, et al. (2005) *Fiber-based tissue-engineered scaffold for ligament replacement: design considerations and in vitro evaluation.* *J Biomaterials* **26**(13): 1523-1532.

ACKNOWLEDGEMENTS: This work is supported by a BBSRC CASE studentship and Royal Society.

CELL PATTERNING ON MODIFIED DIAMOND-LIKE CARBON (DLC)

EM Regan¹, JB Uney¹, AD Dick², JP McGeehan³, F Claeysens⁴, S Kelly¹

¹Henry Wellcome L.I.N.E., Clinical Sciences South Bristol, University of Bristol, BS1 3NY, UK.

²Academic Unit of Ophthalmology, University of Bristol, Lower Maudlin Street, Bristol BS1 2LX, UK.

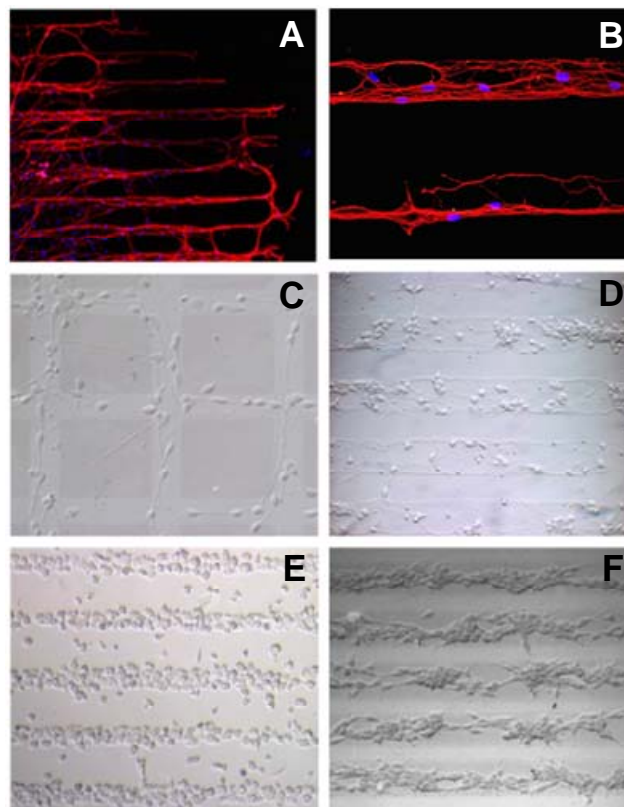
³Centre for Communications Research*, Faculty of Engineering, University of Bristol, Merchant Venturers Building, Woodland Road, Bristol BS8 1UB. ⁴Dept. of Engineering Materials, The Kroto Research Institute, North Campus, University of Sheffield, Broad Lane, Sheffield S3 7HQ.

INTRODUCTION: We have a longstanding interest in using diamond-like carbon (DLC) as a coating material for neural implantable devices (including biosensors). We have shown previously that phosphorous-doped DLC (P:DLC) improves neuron adhesion and that this can be used to produce patterned process extension between cells [1]. Here we report some recent findings that extend from our earlier work. First, we show that P:DLC can be used to pattern other neural cell types. Second, we describe how UV irradiation can be used to pattern neurons and PC12 cells differentially. Third, we highlight that the surface chemistry of DLC can be used to attach factors that can reduce glial cell adhesion.

METHODS: DLC was prepared using pulsed laser deposition [1]. Thin films of DLC and P:DLC (20% P) were deposited onto glass coverslips. Patterned P:DLC substrates were prepared by first coating glass coverslips with P:DLC. Copper transmission electron microscope (TEM) grids were placed onto substrates and held in place using a spot of silver dag. The exposed areas of the grid were then coated with DLC. UV:DLC samples were subjected to 18hrs of UV exposure (patterns were made by placing the grid between the light source and the sample).

Dissociated cortical neurones and dorsal root ganglion explants were cultured from E18 wistar rats on substrates using standard tissue culture protocols [1]. Prior to plating, substrates were sterilised in ethanol and coated with poly-D-lysine (70,000–150,000 MW). Patterned polyethylene glycol (PEG) patterns were produced by incubating poly-D-lysine coated P:DLC/DLC micropatterned substrates with TM-PEG-NHS (Pierce) for 12h. U-87 astroglial cells were grown in DMEM media containing 10% FCS, L-Glutamine and penicillin/streptomycin.

RESULTS: Figure 1 highlights some of the cell patterning achieved on P:DLC and UV:DLC. In A & B dorsal root ganglia neurons and their processes extend along P:DLC channels in (red = beta-III-tubulin). In C human neural progenitor cells can be seen to travel along P:DLC channels (lighter lines). In D cortical neurons adhere and



extend processes preferentially along UV:DLC channels. This is reversed in E where PC12 cells adhere to non-UV:DLC lines (i.e., standard DLC). In F astroglia cells do not adhere to PEGylated channels (light lines).

DISCUSSION & CONCLUSIONS: Our data highlight that DLC is a modifiable substrate suitable for coating brain implants. We describe patterned growth of several neural cell types on P:DLC & UV:DLC. We also show preliminary data showing an approach that could reduce the brains inflammatory response to brain implants.

REFERENCES: ¹Regan EM et al. *Biomaterials* (2008) 29(17):2573-80.

ACKNOWLEDGEMENTS: ER would like thank Micron Foundation for provision of a scholarship.

OPTIMISING CONDITIONS FOR HUMAN MESENCHYMAL STEM CELL DIFFERENTIATION TO CHONDROCYTE-LIKE CELLS FOR TISSUE ENGINEERING OF THE DEGENERATE INTERVERTEBRAL DISC

SM Richardson¹, R Ulijn², AJ Freemont¹ & JA Hoyland¹

¹ *Tissue Injury and Repair, University of Manchester, Manchester, M13 9PT, UK*

² *Laboratory for Biomolecular Nanotechnology, The University of Strathclyde, G1 1XL, UK*

INTRODUCTION: During intervertebral disc (IVD) degeneration the nucleus pulposus (NP) is damaged, leading to spinal instability and low back pain. Current clinical interventions cannot repair the IVD matrix; therefore our aim is to use a tissue engineering approach to regenerate the NP¹. Due to changes in their behaviour NP cells cannot be used, therefore we have focused on the use of human mesenchymal stem cells (MSCs) for our IVD tissue engineering strategies. However, in order to develop a successful strategy a number of issues must be considered. This includes the identification and efficacy testing of an ideal biomaterial and the optimisation of conditions for differentiation on MSCs into NP-like cells. Importantly, any implanted cells must be capable of surviving within the harsh physiochemical environment of the degenerate IVD and we have developed an *in vitro* loading bioreactor in order to test MSC survival, differentiation and matrix formation under conditions similar to those experienced within the human IVD.

METHODS: Human MSCs were seeded in a range of biomaterials to test their ability to maintain MSC viability, allow or support lineage-specific differentiation to NP-like cells and permit or promote matrix synthesis and deposition. These biomaterials included chitosan/glycerophosphate (C/Gp) hydrogels², type I collagen hydrogels and self-assembling dipeptide hydrogels³, which are all capable of gelation *in vivo* following implantation into the IVD. A range of variables were also tested, including cell density, culture in standard and differentiating medias, and culture in normoxic and hypoxic conditions with and without the application of mechanical (compressive or hydrostatic) load. Following culture phenotype was assessed using real-time quantitative PCR and matrix synthesis assessed using histological staining, immunohistochemistry, and DMMB and Sircol assays for proteoglycans and collagens respectively.

RESULTS: C/Gp hydrogels demonstrated MSC differentiation in standard medium and increasing cell density from 1×10^6 to 4×10^6 /ml (equivalent to *in vivo* NP cell density) improved PG production over collagen and importantly was more influential than the addition of growth factors. MSCs cultured in type I collagen gels demonstrated more rapid differentiation when cultured in hypoxic conditions and exposed to daily mechanical (compressive) loading. Noatably, these cells failed to demonstrate either hypertrophic or osteoblastic marker genes when cultured under hypoxic loaded conditions. When MSCs were cultured in self-assembling peptide gels they rapidly differentiated into NP-like cells without the need for differentiating medium and varying the peptide composition of these hydrogels altered the gene expression profiles of the differentiated cells.

DISCUSSION & CONCLUSIONS: We have analysed a number of biomaterials and combined this with studies into the effects of cell seeding density and humoral environment to ascertain the optimal conditions for MSC differentiation and appropriate matrix formation. The results demonstrate the importance of identifying the correct biomaterial and conditions for MSC differentiation to NP-like cells if a successful tissue engineering strategy is to be identified for regeneration of the degenerate human IVD.

REFERENCES: ¹S.M. Richardson, A. Mobasher, et al (2007) *Histol Histopathol.* **22**:1033-41. ²S.M. Richardson, N. Hughes, et al. (2008) *Biomaterials.* **29**:85-93. ³V. Jayawarna, S.M. Richardson, et al. (2009) *Acta Biomater.* **5**:934-43.

ACKNOWLEDGEMENTS: This work was funded through grants from the ARC, BBSRC, MRC, EPSRC, NWDA and RCUK.

Concentration-Dependent Effects of Magnesium Ions on MG63 Cells

Z Robertson¹, B. Annaz¹ & I.R. Gibson¹

¹ School of Medical Sciences, [Institute of Medical Sciences](#), University of Aberdeen, UK.

INTRODUCTION: Calcium phosphate-based ceramics, such as porous hydroxyapatite (HA), can play a prominent role in bone repair in orthopaedic, dental and maxillofacial surgery. Preliminary studies have shown that manipulating the surface chemistry of HA implants, by ion-substitution could provide an effective way of stimulating bone repair¹. One type of substituted material that has been chemically synthesized is magnesium-substituted HA². Magnesium (Mg²⁺) is the most abundant intracellular divalent cation in the body and plays an important role in many biological processes³. The aim of this study was to determine the effect of Mg²⁺ on osteoblast-like cell behaviour *in vitro*.

METHODS: The osteoblast-like cell line (MG63) was cultured using DMEM supplemented with 10% FBS on 24 well plates (2.5x10⁴ cells/well). Following 24 hour incubation, medium was replaced with ion-supplemented DMEM (1mM-50mM) using MgCl₂ as a source of magnesium ions. Intracellular metabolic activity was determined using the alamarBlueTM continuous assay. Cell morphology was observed and cell number was counted. Using cell lysates, DNA was measured using the Picogreen assay and alkaline phosphatase (ALP) activity was determined using the p-nitrophenol method.

RESULTS: MG63 cells showed a general increasing trend in metabolic activity with time for all Mg²⁺ concentrations. No significant changes were observed at days 3 and 5. In contrast, both the 25 and 50mM concentrations showed a significant decrease when compared to the control at days 7 and 10 (P<0.01). Cells showed no change in morphology after incubation in the presence of Mg²⁺ between 1 and 25mM, but cells incubated at concentrations of 50mM were sparse and showed an elongated fibroblast-like morphology. All culture conditions showed an overall temporal increase in cell number and DNA from day 4 to 10. At days 4, 7 and 10, the 50mM concentration showed a significant decrease in cell number when compared to the control (P<0.05;P<0.01). The 25mM concentration also showed a significant decrease at day 10 (P<0.05). The 50mM concentration showed a significant decrease in DNA at days 4 (P<0.05) and 7 (P<0.01) compared

to the control. A trend of decreasing ALP activity over time was observed for all Mg²⁺ concentrations. At each time point ALP activity increased with increasing ion concentrations. For all time points studied a significant increase in activity was observed with both the 25mM and 50mM (see Figure 1).

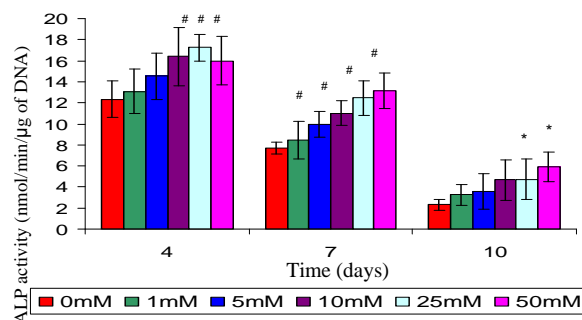


Fig. 1: Effect of magnesium ions added to the culture medium of MG63s on ALP activity

DISCUSSION & CONCLUSIONS: Results showed that magnesium ions can alter the intracellular metabolic activity, proliferation and ALP activity of MG63 cells, depending on the concentration. Despite an overall increasing temporal trend with all ion concentrations, an increase in Mg²⁺ concentration from 1mM to 50mM caused a decreasing trend in metabolic activity, cell number and DNA at each time point. In contrast, a significant increase in ALP activity was seen at all time points with the highest Mg²⁺ concentration. Together this data suggests that high concentrations of Mg²⁺ can reduce cell growth and stimulate MG63 differentiation.

REFERENCES: ¹ I.R. Gibson, K.A. Hing, P.A. Revell, et al (2002) *Key Eng Mater* **218-220**: 203-206. ² E. Landis, A. Tampieri, M. Mattioli-Belmonte, et al (2006) *J Euro Ceram Soc* **26**: 2593-2601. ³ F.I. Wolf and A. Cittadini (2003) *Mol Aspects Med* **24**:3-9.

ACKNOWLEDGEMENTS: The authors would like to thank the University of Aberdeen for a PhD studentship (ZR) and EPSRC for an Advanced Research Fellowship (IRG).

Development of an *in vitro* model of spinal cord injury using microfabrication

L Ross¹, S Boomkamp², M Riehle¹, S Barnett², N Gadegaard¹

¹ Centre for Cell Engineering, University of Glasgow, G12 8QQ, UK.

² Glasgow Biomedical Research Centre, University of Glasgow, G12 8QQ, UK

INTRODUCTION: Damage to the central nervous system (CNS) causes highly debilitating injuries to victims due to the loss of motor control and sensory data from, potentially, large areas of the body. The lack of growth factors and the formation of a scar consisting of densely packed glial cells prevents severed spinal axons, whose cell bodies survive, from re-growing past the site of injury thus almost always making the damage permanent. Currently the most widely used method to study spinal cord injury (SCI) is to directly wound animals; this is technically demanding, time consuming and expensive. Large numbers of animals are also required to give statistical significance to the data. Development of an *in vitro* model for SCI will, firstly, reduce the number of animals required for studies as they will only be needed for the harvesting of neuronal cells. Secondly, the animals used will not be exposed to the long term suffering caused by *in vivo* experiments of the kind needed. Finally, the complexity of the experimental procedure will be reduced, as no animals will be directly used for experiments. This project aims to development an *in vitro* model which will have to fulfill three roles: providing a hospitable environment for the growth of neurons, contain the neurons soma to an area to prevent them migrating around the device and, finally, provide guidance cues to the axons so that they can be patterned out on the device (Fig. 1a).

METHODS: A device was designed to find the optimal ridge dimensions for axonal guidance (Fig. 1b). Photolithography mask plates were designed in Tanner L-Edit for 100 mm wafers. Chrome masks were created with a Vistec VB6 UHR EWF electron beam lithography tool. Ferric copies of the masks were then made using a SUSS MicroTec MA6 mask aligner. Layers of SU-8 3000 photoresist were spun onto the wafers and exposed using the ferric masks. Three layers in total were used: a sacrificial layer, 13mm disk layer and a ridge layer. Unexposed SU-8 was then developed off using EC solvent and isopropanol.

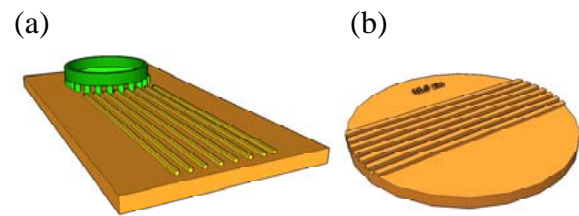


Fig. 1: (a) A possible layout for the final device. The green area will contain the soma while allowing the axons to project out. The ridges will provide guidance to pattern out the axons. (b) A device for finding the optimal ridge dimensions. It consists of a 13 mm disk, which can fit into cell culture wells, with ridges covering ~50% of its surface. The un-patterned areas provide a built in control. The ridges are 12.5, 25 or 50 μm wide and 5, 10, 15 or 20 μm deep. The range of sizes used are based on previous work by this group¹. Note that these device sketches are not to scale.

RESULTS: Due to over exposure of the disk layer, the sacrificial layer was exposed and thus the devices failed to lift off from the substrate. Under exposure of the ridges resulted in some of them peeling away from the disks.

DISCUSSION & CONCLUSIONS: The problems experienced with the first set of devices are due to the exposure times used. Exposure doses will have to be adjusted until stable ridges can be fabricated reproducibly. The problem with the sacrificial layer could also be solved via the use of a different polymer for the layer. Once these problems are resolved, seeding of CNS cultures onto the devices will be performed so that their response to the different topographies can be assessed. Also, a device will be designed to find the optimal method of soma containment.

REFERENCES: ¹ Sorensen A, Alekseeva T, Katechia K, Robertson M, Riehle MO, Barnett SC (2007) *Biomaterials* **28**(36): 5498-5508.

ACKNOWLEDGEMENTS: L Ross is a member of the Doctoral Training Centre in Cell and Proteomic Technologies and is funded by the EPSRC. We also thank the NC3Rs for there support of this work.

Si ion concentration affects osteoblast gene expression

J. Ruangsuriya, Z. Robertson, B. Annaz & I.R. Gibson

School of Medical Sciences, *Institute of Medical Sciences*, University of Aberdeen, UK.

INTRODUCTION: A number of scaffold materials used for tissue engineering, including silicate-substituted hydroxyapatite, Bioglass and Si-containing organic-inorganic hybrids, release various concentrations of silicon (Si) ions in culture. Silicon ions, or more correctly the monomeric silicic acid, $\text{Si}(\text{OH})_4$, has been shown to stimulate osteoblast (OB) gene expression as part of dissolution products from Bioglass [1]; the dissolution products also result in appreciable concentrations of Ca^{2+} and Na^+ and a change in pH, in addition to high levels of silicon (15-200ppm, or 500 μM -7mM). Silicic acid has also been added to OB cultures at low concentrations (0.3-1.4ppm, or 10-50 μM) and has been shown to increase ALP and osteocalcin gene expression [2]. This study looks at the effect of low (20 μM) and high (500 μM) concentrations of Si ions on gene expression of OB cells, under conditions of controlled pH.

METHODS: MG63 and primary human osteoblast (HOB) cells (Promocell) were grown in 6-well plates without osteogenic supplements. Si ions were added to the culture medium at concentrations of 0, 20 and 500 μM using a 1000ppm standard silicon solution (VWR); the pH of the media were adjusted to pH 7.4 with 1M HCl. Cells were cultured for 4, 7 and 10 days and RNA was extracted and purified using established protocols. Gene expression was quantified using qRT-PCR (LightCycler® 480, Roche) with GAPDH employed as a house-keeping gene. The effect of Si additions on cell morphology (SEM) and growth (total DNA, Picogreen assay) were also assessed.

RESULTS: Additions of up to 500 μM Si did not affect the morphology of MG63 or HOB cells during the various culture periods. Total DNA showed an increase with increasing culture time, but no significant differences between the different Si concentrations were observed at any of the culture periods.

Of the genes studied here (ALP, PHOSPHO-1, OCN, COLL-1a1, COLL-1a2, OPN), the most significant effect of Si concentration was a large 2-3 fold increase in COLL-1a1 gene expression for both MG 63 cells (at day 4) and HOB cells (at both

days 4 and 7) with 500 μM Si, compared to both 0 and 20 μM Si. A significant but smaller increase in gene expression was also observed for COLL-1a2, and a small increase in ALP gene expression was observed for MG63 cells at 4 days of culture with 500 μM Si concentrations compared to 0 and 20 μM . Osteocalcin gene expression of HOB cells showed a significant increase with high Si concentration at prolonged culture periods (days 14 and 21 days).

DISCUSSION & CONCLUSIONS: Many studies have reported how the ionic dissolution products from Bioglass can affect gene and protein expression of osteoblasts [1,3], but the mechanisms have been difficult to establish due to the complexity of the medium containing the ionic dissolution products, and the effect that the Bioglass has on increasing the pH of the culture medium. The results described here where the only variable was an increase in Si concentration of the culture medium, supports findings for the Bioglass studies where an increase in collagen-1 gene expression was observed. The results for high concentrations of Si in this study are also in contrast to those of Reffitt et al [2], who did not observe changes in collagen type I gene expression for Si concentrations of 0-50 μM , but did observe increases in collagen type I protein expression. Si ions can clearly play an important role in OB behaviour, and their addition to OB cultures is a potentially simple method of altering ECM production.

REFERENCES: ¹ I.D Xynos *et al*, (2001) *J. Biomed. Mater. Res.* **55**: 151-157. ² D.M. Reffitt *et al*, (2003) *Bone* **32**: 127-135. ³ T. Gao *et al* (2001) *Biomaterials* **22**:1475-1483.

ACKNOWLEDGEMENTS: The authors would like to thank the Royal Thai Government (JR), the University of Aberdeen and EPSRC for an Advanced Research Fellowship (IRG).

CRYOPRESERVATION OF CELLS ENCAPSULATED IN 3D CONSTRUCTS

[S Sambu](#)¹, [X Xu](#)¹, Y Liu¹, [ZF Cui](#)¹

¹*Institute of Biomedical Engineering, Old Road Campus Research Building, University of Oxford, Old Road Campus, Headington, Oxford OX3 7DQ, UK*

INTRODUCTION: Cryopreservation of cells in suspension has long been the practice within the field of cryopreservation. While this procedure has had clear utility in the research and clinical arenas, there are challenges in scarcity of storage facilities and the maintenance of viability and cell-specific characteristics when these protocols are scaled up. Furthermore, in anticipation of the need for off-the-shelf availability of functional tissues, the pursuit of 3D cryopreservation techniques has intensified. The purpose of this study was to investigate the effect of 3D encapsulation on cell viability during cryopreservation.

METHODS: Separately, bovine articular chondrocytes or mouse embryonic stem cells (mESCs) were embedded in alginate (1.2 %). Using DMSO at the concentration of 2, 4, 6, 8 and 10 % (v/v), cells in alginate and in suspension were cryopreserved at various cooling rates (1, 5 and 10 °C/min) and preloading times (15, 30, 45 and 60 minutes at 40 °C). Cell viability was evaluated after thawing and DMSO removal using Trypan blue or Calcein-AM and propidium iodide staining methods. To empirically investigate the association between CPA concentration and spatial distribution of cell survival in 3D constructs, cell viability was monitored using multiphoton microscopy. To understand the underlying physical processes, transient DMSO concentration inside 3D alginate beads with 1 mm diameter was simulated using mathematical modelling.

RESULTS: Cell survival rate for chondrocytes after cryopreservation in suspension was 3.67±0.58%, 87.33 ±3.05, 79.93±4.65, 71.83±8.18, 14.27±5.90% for the preloading time 0, 15, 30, 45, and 60 at a cooling rate of 1 °C/min. Cell survival rate for chondrocytes after cryopreservation in beads was 3.37±0.46%, 16.00±5.20%, 57.67 ± 8.14, 38.33±2.31, 22.47±10.12% for the preloading time 0, 20, 30, 45, and 60 at the cooling rate of 10 °C/min. Mouse ESCs cryopreserved in suspension recorded a survival rate of 73.44±6.25 %; those cryopreserved in alginate beads recorded 29.54±5.82 % survival. These results were consistent with simulation results. The diffusion models showed that with the preloading time of 30 min, the cells throughout the 3D construct were exposed to 10 % DMSO. In contrast, a preloading time of 15 min was not long enough to allow the

diffusion of DMSO throughout the beads. Finally, when the preloading time was extended to 60 minutes, the cells were damaged due to toxicity caused by excessive exposure to DMSO.

DISCUSSION & CONCLUSIONS: These results show much promise for cells cryogenically preserved in 3D. Moreover, they show that cell viability after cryopreservation in 3D constructs is dependent on the cell-type. Further work may help elucidate the impact of cell-matrix interaction on the post-thaw maintenance of cell phenotype.

ENGINEERED CRANIOFACIAL MUSCLE CONSTRUCTS EXPRESS MARKERS OF MUSCLE DIFFERENTIATION

R.Shah, J.C.Knowles, N.P.Hunt, M.P.Lewis

Division of Biomaterials and Tissue Engineering, UCL Eastman Dental Institute, U.K.

INTRODUCTION: Tissue engineering has the potential to serve as an alternative to surgical tissue transfer for the management of soft tissue defects. The perceived advantages include reduced donor site morbidity and restoration of function and aesthetics to ideal. Degradable scaffolds are utilised in the early stages of cell growth and development with the advantage of eventual elimination to leave space for the engineered tissue and a reduced chance of rejection.

METHODS: Cells were extracted and characterised from human masseter muscle biopsies obtained from healthy consented adult patients. Ethical approval had been obtained. Immunofluorescent markers to desmin and α -sarcomeric actin confirmed myogenicity. Degradable iron-phosphate glasses were produced in disk and fibre form. The disks were coated with collagen and the fibres were aligned and coated with a thin layer of collagen or encased within a collagen gel. Cells were seeded on these scaffold combinations and a collagen gel was used as a control. Cell attachment, survival, alignment, differentiation and maturation over time were assessed using the CyQUANT assay, light and modulation contrast microscopy, immunofluorescence and RT-PCR.

RESULTS:

Disk Biocompatibility: There was good cell attachment and survival on collagen-coated disks. myoD and myogenin gene expression increased over the 14-day experimental period. Furthermore, there was an increase in the embryonic and neonatal myosin heavy chain gene expression by day 14 and variable expression of all other myosin heavy chains.

Biomimetic Scaffold Response: Interestingly, cell orientation was unidirectional on the glass fibre and glass fibre-collagen scaffolds analogous to native skeletal muscle; this was in contrast to the collagen gel controls where the cell direction was random. The gene expression of myoD and myogenin was highest on the glass fibre scaffolds initially, however by day 21, the other scaffolds had greater expression ($p < 0.05$). This was also the finding for all myosin heavy chains gene expression ($p < 0.05$).

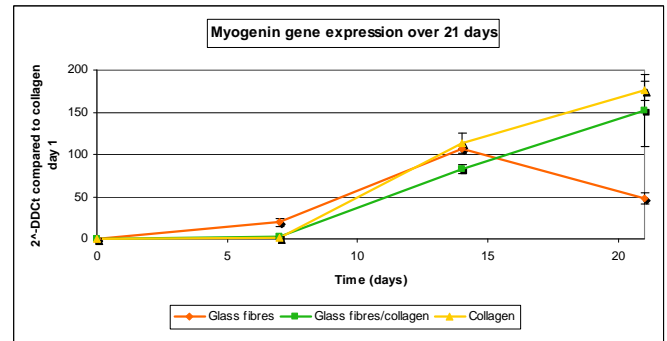


FIGURE ONE: Expression of myogenin transcripts by skeletal jaw muscle constructs (determined by quantitative PCR). After 21 days in culture, the glass fibre-collagen composites show comparative performance to collagen gels alone. Both are superior to glass fibres alone.

DISCUSSION & CONCLUSIONS: There was good cell biocompatibility with degradable iron-phosphate glass disks. The creation of a biomimetic scaffold enabled orientation of the cells into the same direction to produce architecture similar to native skeletal muscle. Although the control collagen gels demonstrated evidence of muscle cell differentiation and maturation, as did the glass fibre scaffolds, these scaffolds may not be ideal for implantation: in particular, the collagen gels contracted uncontrollably. The glass fibre-collagen gel scaffolds provided a much more manipulable system and have the potential to provide a suitable hard-soft tissue interface.

REFERENCES: Lewis, M.P., Mudera, V., Cheema, U., Shah, R. (2009). Muscle Tissue Engineering. in Meyer, U., Meyer, Th., Handschel, J., Wiesmann, H.P., (ed.) Fundamentals of Tissue Engineering and Regenerative Medicine. Heidelberg: Springer. pp. 243-254; Shah, R., Sinanan, A.C.M., Knowles, J.C., Hunt, N.P and Lewis, M.P. (2005) Craniofacial muscle engineering using a 3-dimensional phosphate glass fibre construct. Biomaterials. 26: 1497-1505.

ACKNOWLEDGEMENTS: The patients who donated muscle biopsies.

Enhancing the mechanical properties of collagen by photo-chemical cross-linking

S.A. Shahban¹, R.A. Brown¹, L. Bozec², U. Cheema¹

¹University College London (UCL), Tissue Repair and Engineering Centre, Institute of Orthopaedics, Stanmore Campus, London, HA7 4LP, UK

²Division of Biomaterials & Tissue Engineering, Eastman Dental Institute (EDI), London WC1X 8LD, UK

INTRODUCTION: Cell survival within mechanically strong scaffolds is critical in the design of tissue engineered constructs. Collagen type I gels tend to be mechanically weak due to the low percentage of collagen with limited orientation and crosslinking. To enhance the properties of collagen type I gels we used the following approaches: a) plastically compress the collagen gel to increase the density and b) photochemically crosslink the gel using riboflavin as a photoinitiator and high intensity blue light. Following plastic compression both the collagen density and cell number increase 58-fold¹. This study aims to assess mechanical properties and the degree of cell viability in different areas of the compressed gel following cross-linking. Patterns of cross-linking were also applied to induce anisotropic features to the gels (*fig.1*).

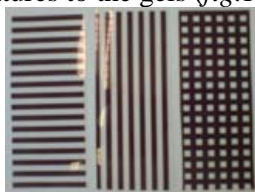


Figure 1: The negative image created by the mask indicates where light penetrates the gel and thus where cross-linking is encouraged, creating gels that are cross-linked horizontally, vertically and with a grid pattern.

METHODS: Collagen gels were manufactured through combining 4ml of type I collagen, 0.5ml of 0.25mM riboflavin, 0.5ml Dulbecco's MEM and 0.5ml HDFs cell suspension. Once set, the gel was compressed for five minutes using a 120g weight, 2 sheets of absorbent paper and nylon mesh². Masks were used to encourage cross linking in specific areas of the gel when placed under high intensity blue light (465nm in wavelength and 4680mW intensity). Mechanical properties were assessed using a tensile tester and the dynamic mechanical analyser (DMA) and cell viability was visualised using calcein AM and ethidium homodimer (EthD-1) under a fluorescence microscope.

RESULTS: Tensile testing showed that the collagen sample with crosslinks running horizontally had a higher Force at Failure (mN) than that of the samples which had been cross-

linked without a mask, with a vertical mask and with a gridded mask ($p < 0.05$). The horizontal mask was applied over a collagen gel containing 2×10^6 HDFs, and after 3 days of incubation at 37°C, a visible pattern of live and dead cells could be seen under a fluorescence microscope (*fig.2*).

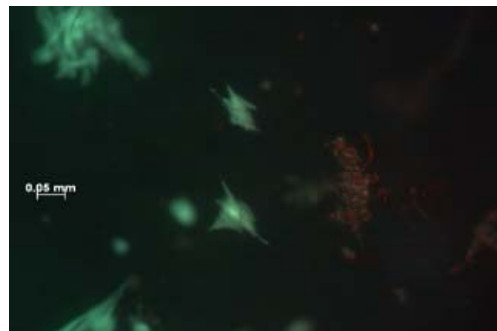


Figure 2: Image of a cell seeded collagen gel at day 3 which had had a horizontal mask covering before being exposed to blue light. This border of live and dead cells indicates the masked and unmasked regions of the gel, respectively.

DISCUSSION & CONCLUSIONS: Mechanical integrity and cell viability are both of great importance in the design of tissue engineered scaffolds. The ability to transform native collagen gels to increase their mechanical strength (using photoinitiated riboflavin) whilst maintaining cell viability (with the use of a mask) shows the exciting potential for designing mechanically stable biomimetic structures for implantation at muscle-tendon interfaces.

REFERENCES:

- ¹Cheema U, "Spatially defined oxygen gradients and vascular endothelial growth factor expression in an engineered 3D cell model," *Cellular and Molecular Life Sciences* **65**(1), 177 (2008).
- ²Brown RA, "Ultra-rapid engineering of biomimetic tissues%3A A plastic compression fabrication process for nano-micro structures," *Advanced Functional Materials* **15**, 1762 (2005).

ACKNOWLEDGEMENTS: This work was funded by the Tissue Repair and Engineering Centre, as part of UCL.

The influence of nanofibre orientation on keratinocyte and fibroblast behaviour

JR Sharpe¹, J Roxburgh¹, Y Dong², J Ong^{1,2}, K Jubin¹ & MM Stevens²

¹ *Blond McIndoe Research Foundation, Queen Victoria Hospital, East Grinstead, West Sussex.* ² *Department of Materials and Institute of Biomedical Engineering, Imperial College London, United Kingdom*

INTRODUCTION: If an open wound is left to heal without treatment it contracts and shrinks in size forming scar tissue which adversely affects appearance and function. Wound contraction can be reduced by the use of skin grafts, however, the availability of graft donor sites is limited. Artificial skin substitutes and skin cells sprayed onto wounds have been shown to reduce wound contraction [1] although these fail to reproduce the high quality wound repair achieved following skin grafting.

Electrospinning allows fibrous materials to be generated with a high degree of control over their nanoscale architecture. Recent studies have demonstrated the potential for electrospun nanofibres to act as artificial skin substitutes [2] which are capable of modulating contraction [3].

By gaining an understanding of the precise differences in the contractile behaviour of skin keratinocytes and fibroblasts in response to nanofibre arrays with different orientations and structures we hope to be able to develop wound repair materials designed specifically to reduce wound contraction. These studies set out to investigate the orientation of actin filaments within human skin keratinocytes and fibroblasts in response to nanofibre constructs with either aligned or randomly oriented fibres.

METHODS: Human keratinocytes and fibroblasts were isolated from skin obtained following surgery with patient consent and cultured using standard cell culture methodology. Following treatment with trypsin, a cell suspension of either keratinocytes or fibroblasts was seeded onto aligned or randomly oriented PLLA nanofibres at a density of 2×10^5 cells/cm². Cells were incubated on nanofibres for 5 days, fixed, stained with phalloidin (Alexa fluor 488 phalloidin, Invitrogen, UK) and visualized by fluorescence microscopy.

Nanofibre arrays were electrospun from 6.5%(w/v) PLLA solution in hexafluoroisopropanol (HFIP) at the electrospinning laboratory (Institute of Biomedical Engineering, Imperial College, London) onto either aluminium foil or BioPrepNylon™ (Fisher, UK) 50µm nylon mesh and sterilized by gamma irradiation prior to use.

RESULTS: Keratinocytes and fibroblasts assumed an aligned morphology on aligned nanofibres and

the actin filaments were oriented along their length (Figure 1, a & b). In random nanofibre scaffolds both cell types assumed a random orientation and actin filaments assumed a similarly random distribution (Figure 1, c & d). In aligned nanofibre constructs both keratinocytes and fibroblasts rarely bridged the gaps between the fibres whereas in randomly orientated constructs cells regularly bridged between fibres due to their more interwoven nature.

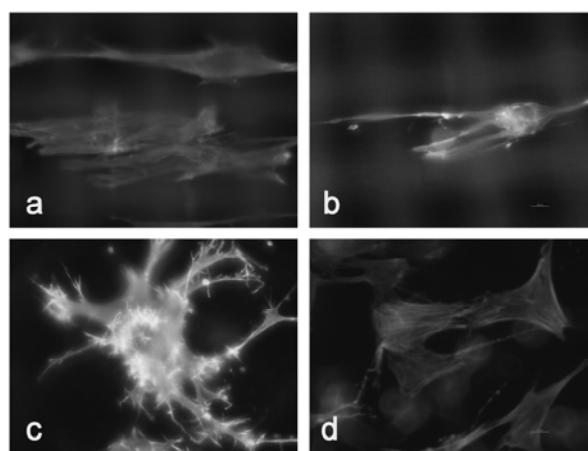


Fig. 1: Alignment of actin filaments within keratinocytes (a, c) and fibroblasts (b, d) on aligned (top) and randomly oriented (bottom) electrospun PLLA nanofibres.

DISCUSSION & CONCLUSIONS: These findings demonstrate that actin, which is responsible for cell contraction and motility becomes oriented to the direction of nanofibres in keratinocytes and fibroblasts. Further work is required to investigate the relationship between nanofibre alignment and cell mediated contraction of the matrix. The analysis of SM α -actin expression by fibroblasts will provide a measure of fibroblast contractile phenotype in response to nanofibre constructs with differing properties.

REFERENCES: ¹ MacNeil S, (2007) *Nature* **445**, 874-880. ² Powell HM et al (2008) *Biomaterials* **29**:834-843. ³ Pan, H., et al (2006), *Biomaterials* **27**: 3209-3220.

USE OF A TISSUE ENGINEERED MODEL OF BACTERIAL INFECTION OF HUMAN SKIN TO DEVELOP RESPONSIVE POLYMERS TO REDUCE BACTERIAL BURDEN OF INFECTED WOUNDS

J. Shepherd^{1,2}, P. Sarker³, S. Rimmer³, L. Swanson³, I. Douglas¹, & S. MacNeil²

¹Departments of Oral Pathology¹, Engineering Materials² and Chemistry³,
The University of Sheffield, Sheffield, UK

INTRODUCTION: Our aim was to synthesize polymers to which antibiotics could be coupled, which would specifically bind to bacteria and collapse around them to assist in their removal from infected skin wounds.

METHODS: We synthesised the polymer branched poly(isopropylacrylamide), BPNIPAM, using reversible addition-fragmentation chain transfer (RAFT) polymerisation. We then coupled acid ended branched PNIPAM with the antibiotics vancomycin (BPNIPAM-VAN) and polymyxin-B (BPNIPAM-PMX-B). Vancomycin binds Gram-positive bacteria (such as *Staphylococcus aureus*) and polymyxin-B binds Gram-negative bacteria (such as *Pseudomonas aeruginosa*). We have recently developed a 3D model of bacterial infected human skin [1] and used this to study the capacity of the polymer to bind to bacteria in the wound. BPNIPAM-PMX-B in solution (5mg/ml) was applied to skin which had been infected with *P.aeruginosa* (1×10^7 cfu) for 24h. After 1h incubation at 37°C, the polymer was washed off in PBS. Viable numbers of bacteria in both tissue and supernatant were counted, and tissue formalin fixed, embedded in paraffin, sectioned and Gram stained to reveal bacteria.

In addition, we bound BPNIPAM-VAN to a hydrogel membrane and applied this to skin samples which had been infected with 1×10^7 cfu *S.aureus*. Skin samples were examined for numbers of viable bacteria as above, and bacteria adherent to the membranes were counted by hand.

RESULTS: When applied to *P.aeruginosa* infected skin in solution for 1 hour, BPNIPAM-PMX-B bound bacteria and removed them from the skin when washed away. Viable numbers of bacteria in the skin were greatly reduced in samples treated with polymer compared with those treated with PBS as control, and the reduction in bacteria was visible by Gram-staining sections of infected skin (Fig.1). Also, when BPNIPAM-VAN bound to a hydrogel membrane was applied to

S.aureus-infected skin samples there was a decrease in numbers of viable bacteria remaining in the skin compared to control samples, and numbers decreased further with repeated applications and removal of the membrane. The number of bacteria adherent to the VAN-membrane were higher than those adherent to the control membrane.

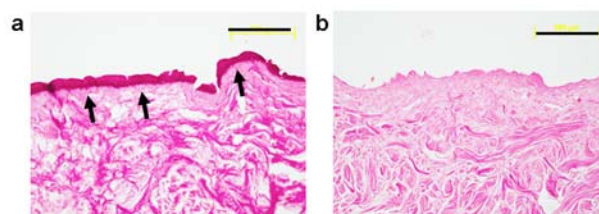


Fig. 1: Gram stained sections of *P.aeruginosa* infected skin samples incubated for one hour either with PBS (a) or BPNIPAM-PMX-B polymer (b). Large numbers of bacteria are visible in the control sample (stained dark pink, arrows) which are not present in the polymer-treated sample. Scale bar = 200µm.

DISCUSSION & CONCLUSIONS: BPNIPAM-VAN and -PMX-B are novel branched polymers sensitive to the presence of Gram-positive and Gram-negative bacteria respectively. These polymers can effectively reduce the bacteria in infected tissue engineered human skin by simple application and removal of the polymers, either in soluble form or coated onto a hydrogel membrane.

REFERENCES: ¹ J. Shepherd, I. Douglas, S. Rimmer, L. Swanson, and S. MacNeil (2009) *Tissue Engineering Part C*, In Press.
ACKNOWLEDGEMENTS: This work was funded by grants from the DSTL and EPSRC.

MICRO THERMAL ANALYSIS: A NOVEL METHOD OF DETERMINING THE EXTENT OF COLLAGEN CROSS-LINKING WITHIN A COLLAGEN CONSTRUCT- APPLICATIONS FOR TISSUE ENGINEERING

¹A.Shepherd, ¹R.Brown & ²L.Bozec

¹Institute of Orthopaedic Science, Stanmore (UCL) ²Eastman Dental Institute, London (UCL)

INTRODUCTION: Increasingly complex designs of collagen scaffolds used in tissue engineering require more accurate and sensitive methods of testing. A new proposal to create cross-linked tunnels within a collagen scaffold for use in vascular and nerve studies will require a novel method of assessing the extent of cross-linking within the walls of the tube- to ensure maximal strength for matrix viability. To date this method has not yet been investigated.

Aim: this study will investigate ways to differentiate between cross-linked and native collagen using melting characteristics found by Micro thermal analysis at point regions throughout the construct to give a detailed intra-matrix map.

METHODS: Three samples were made for testing: native (control), cross-linked with glutaraldehyde (control) and photochemically cross-linked with riboflavin and blue light (436nm wavelength)- the method under test. Differential scanning calorimetry (DSC) and a Mettler FP Hot Stage (heating rate 10C/min from 20-80°C) investigations were conducted for macro-level testing. Comparison studies were then performed using MicroThermal Analysis (Micro TA) (heating rate 25°C/sec). The MicroTA combines the imaging ability of the Atomic Force Microscope and the thermal characterization of temperature modulated DSC to estimate the point deterioration of collagen when exposed to heat¹. Data collected included temperature of onset (change in slope of sensor corresponding to melting temperature) and sensor derivative peaks.

RESULTS: DSC and Hot stage thermal analysis (fig.1) showed the controls (native and glutaraldehyde cross-linked collagen) to have expected melting temperatures² in hydrated (58°C and 78°C respectively) and dehydrated states as did the Micro TA. However, the macro analysis did not accurately differentiate between the native and test collagen using melting temperatures. The MicroTA data showed marked differences in the sensor derivative peaks of all collagen forms (fig. 2) as well as identifying other characteristics such as swelling temperatures in cross-linked samples.

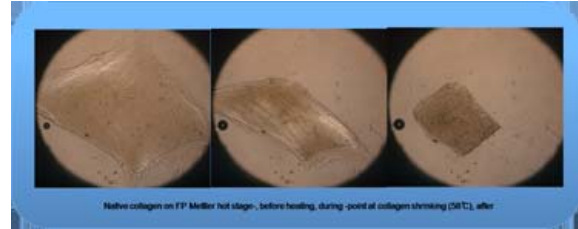


Fig. 1: Hydrated native collagen- hot stage, before heating (left), during heating- shrinking at 58°C (centre) and after heating (right).

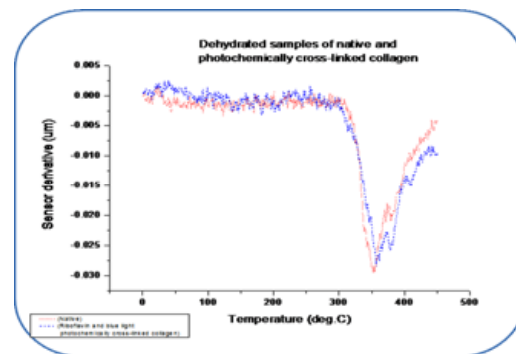


Fig.2: Sensor derivative data for dehydrated collagen. Native collagen red, photochemically cross-linked collagen blue.

DISCUSSION & CONCLUSIONS: This study has found that MicroTA can successfully identify the individual denaturing characteristics of collagen after each treatment, allocating a 'fingerprint' to each as a means of recognition when analysing collagen. This is not only useful for differentiating between cross-linked and noncross-linked locations in collagen but also to further assess the extent of cross-linking by each treatment.

REFERENCES: 1. Nguyen A et al (1974) The Dynamic Mechanical, Dielectric, and Melting Behavior of Reconstituted Collagen. May;13(5):1023-37. 2. Comparative Performance of Electrospun Collagen Nanofibers Cross-linked by Means of Different Methods. Torres-Giner. S et al. ACS Appl. Mater. Interfaces, 2009, 1 (1), pp 218-223

MIMICKING THE BODY- A NOVEL METHOD OF CROSS-LINKING COLLAGEN TO CONTROL SCAFFOLD DESIGN- IMPLICATIONS ON HUMAN TISSUE ENGINEERING

¹A.Shepherd, ¹R.Brown & L. Bozec²

¹ Institute of Orthopaedic Science, Stanmore (UCL) ² Eastman Dental Institute, London (UCL).

INTRODUCTION: Scaffold design is an essential part of tissue engineering. Cross-linked collagen matrices are often used to increase the mechanical strength of scaffolds. The ability to create and control different patterns of cross-linking within a collagen matrix would allow manipulation of scaffold characteristics (e.g. anisotropy, strength and shape) in order to tailor the design of the scaffold more appropriately to different applications. Photochemical crosslinking using Riboflavin and blue light¹ has the potential to create patterns of crosslinking throughout a matrix. If successful, it can have applications in more sophisticated scaffold creation such as crosslinked tubular structures for nerve and vascular engineering. This study will assess the suitability of this method for such an application.

METHODS: Collagen (type 1) gels were made using standard techniques and plastically compressed for five minutes. Some of the gels were treated with riboflavin before setting, to be crosslinked after compression. Using a masking technique which only permitted blue light (436nm) to enter and crosslink those gels in certain directions, varying patterns of crosslinked gels were produced- fully crosslinked, vertically crosslinked, horizontally crosslinked and native. The extent of crosslinking was measured in dry and hydrated states through thermal analysis (DSC and Mettler FP Hot stage analysis) and anisotropy was measured using dynamic mechanical analysis (DMA) and tensile testing¹. Further investigation using micro thermal analysis (MicroTA)² on the individual characteristics of collagen crosslinked in this manner were used to create a melting 'fingerprint'- which can be used to recognise such cross-linked areas later on.

RESULTS: There were differences in the break stresses of vertically crosslinked collagen- 0.25MPa (± 0.01) compared to a fully crosslinked - 0.16MPa(± 0.01) (table1.). The melting temperature of photochemically crosslinked collagen compared with native collagen was unremarkable in the DSC and Hot Stage data. However MicroTA data showed marked differences in the sensor derivative data (fig.1).

Table 1. DMA results for relative break stresses of collagen under varying treatments- different patterns of cross-linking

Collagen samples	Stress at Failure(Mpa)
Fully Cross-linked	0.32 (± 0.04)
Vertical anisotropy	0.25 (± 0.01)
Horizontal anisotropy	0.37 (± 0.04)
Native	0.14 (± 0.01)

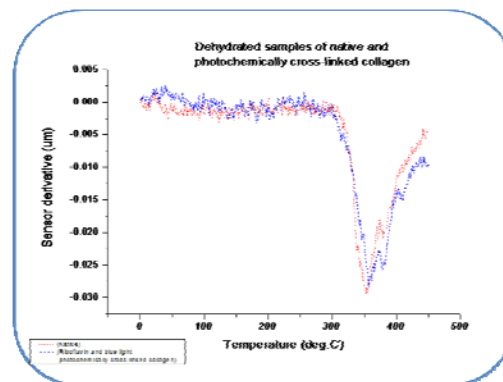


Fig.1: Sensor derivative data for dehydrated collagen. Native collagen red, photochemically cross-linked collagen blue

DISCUSSION & CONCLUSIONS: This study has shown that photochemically cross-linking collagen can be successfully manipulated to recreate anisotropy. However, there is controversy over the nature of the anisotropy, as unlike our findings, the gels should have a higher break stress in the vertical direction- the direction in which the DMA was assessing strength. This could be due to the masking technique allowing less light in the vertical direction therefore allowing less area of those samples to be cross-linked. The different denaturing characteristics highlighted by the MicroTA are promising in identifying individual 'fingerprints'. This is another desirable trait of photochemical cross-linking which can be used as a basis for recognition in more complex future scaffolds.

REFERENCES: 1. Torres-Giner, S. et al. Comparative Performance of Electrospun Collagen Nanofibres Cross-linked by Means of Different Methods. ACS Appl. Mater. Interfaces, 2009 1(1) pp 218-223. 2 Nguyen A et al (1974) The Dynamic Mechanical, Dielectric, and Melting Behavior of Reconstituted Collagen. May;13(5):1023-37.

Extra-cellular Diffusion Imaging

P. Shields^{1,2}, M.O. Riehle², D.R.S. Cumming¹

¹Microsystem Technology Group, *Department of Electronics and Electrical Engineering, University of Glasgow, UK*

²Centre for Cell Engineering, *Faculty of Biomedical & Life Sciences, University of Glasgow, UK*

INTRODUCTION: This paper reports progress towards a micro-fluidic device for extra-cellular ionic diffusion imaging. The bench-top device integrates multi-channel micro-fluidics – patterned in SU-8 photoresist – with existing CMOS pH sensing technology [1] to form an enclosed cell-culture structure.

METHODS: Two patterned substrates are used to package the CMOS device: one PCB board; and one quartz square. A microfluidic channel flows between the PCB and the quartz square, allowing cells to be introduced into a region directly above the 16x16 ISFET array of the chip. It is hoped that from the 256 time-domain traces obtained, the position of any ionic emitter above the array may be inferred.

The chip is recessed and bonded onto the PCB using an automated bonding machine typically capable of bonds heights of 150um to 200um. These bond wires – and a 5cm square region surrounding the chip – are encapsulated in a single layer of SU-8 2050 photoresist. Out of this resist, the microfluidic channels are developed. Three microfluidic inlet ports and one outlet port are attached to the underside of the PCB, to allow the introduction of suspended MDCK epithelial cells via standard PEEK tubing.

An array of 4x4 platinum electrodes – along with breakout tracks – are patterned onto the quartz square by evaporation. These electrodes will be used to create a controlled source of H⁺ ions used to calibrate the system in anticipation of the monitoring of biological ionic emissions.

By considering appropriate boundary conditions, Fick's second law of diffusion (eq 1) yields a two dimensional solution – in 1-D space and time – (eq 2) for the evolution of ionic concentration along a 1-D path. By parameterizing all 256 datasets from the CMOS chip it is hoped the 3-D position of ionic emitters may be inferred.

$$\frac{\partial \phi}{\partial t} = D \frac{\partial^2 \phi}{\partial x^2} \quad (1)$$

$$\phi(x, t) = a_0 A \frac{1}{\sqrt{t - T}} e^{-\frac{(x-b)^2}{2(c_0 C \sqrt{t-T})^2}} \quad (2)$$

RESULTS: Initial modelling has shown that the time, strength and distance of an ionic emission can be inferred from ionic concentration variation at a single probe. Large scale bench tests have also backed up this assumption – although some further linear calibration is needed.

Previous fabricated versions of the device have proved leaky. It is hoped that the latest version – which uses a flat quartz square coated in SU-8 – will provide a seal tight enough for long-term cell culture.

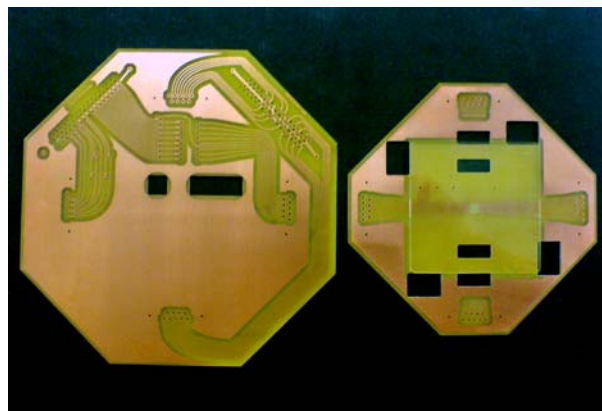


Fig. 1: Motherboard and Module Board.

DISCUSSION & CONCLUSIONS: While we have developed a method of predicting the position of ionic emitters on the large scale, it remains to be seen whether ionic diffusion behaves similarly on the micro-scale. We hope to have results from the integrated micro-scale device within the next few months.

REFERENCES: ¹ M.J. Milgrew, M.O. Riehle, D.R.S. Cumming (2005) A large transistor-based sensor array chip for direct extracellular imaging *Sens. Actuators B Chem.* **111**: 347-353.

ACKNOWLEDGEMENTS: This work is funded by Research and Enterprise at the University of Glasgow under the Kelvin-Smith scholarship scheme.

Freeform Fabrication of Scaffold for Bone Tissue Engineering Applications

L Shor¹, S Güçeri², W Sun²

¹ School of Engineering and Material Science, Queen Mary University of London.

² Computer-Aided Tissue Engineering Lab, Drexel University, USA

INTRODUCTION: For scaffold-guided tissue engineering, the design of an effective scaffold requires a greater understanding of how the micro environment influences cellular activity. Solid freeform fabrication (SFF) techniques have been investigated for their ability to create constructs of a well defined microstructure^{1,2}. In this study, a novel SFF system was used to fabricate polycaprolactone scaffolds with a controlled pore size of 350 μm . A cell-scaffold interaction study was then conducted for a period of 21 days.

METHODS: PCL (Sigma Aldrich Inc, Milwaukee, Wisconsin) in the form of pellets was used as the scaffold material. The scaffolds were fabricated through a SFF technique, Precision Extruding Deposition (PED), developed at Drexel University. **Construct Characterization:** The microstructure of the fabricated scaffold was evaluated by micro-CT. A SkyScan 1172 (Kontich, Belgium) micro-CT desktop scanner was used to scan the internal architecture of the scaffold. These sliced images were analyzed in SkyScan's CTAN software. Volume fraction and surface per unit volume were determined using the 3D analysis function. **Cell-Scaffold Interaction:** A 21 day study was conducted with scaffolds of dimensions 14mm x 14mm x 3mm, porosity of 65%, and pore size of 350 μm , which were seeded with primary fetal bovine osteoblast cells. Calcium levels were measured in the cell-scaffold constructs with a Calcium Test Kit (Stanbio Laboratories, Boerne, TX) on days 7, 14, and 21. Cell morphology was evaluated by SEM on days 14 and 21.

RESULTS: Micro-CT analysis showed the scaffolds to be $64.72 \pm 0.84\%$ porous with near 100% interconnectivity. These results show little variation between samples, illustrating the repeatability of the process. Mineralization of bone formed on the scaffolds was measured by calculating the amount of calcium produced by cells on days 7, 14, and 21. A steady increase in the amount of calcium produced by cells throughout the cultured time was observed (Fig. 1). The morphology and extent of mineralization on the PCL surfaces were assessed using SEM on days 14 and 21. The SEM images show mineralization of the scaffold by day 14 (Fig. 2A)

and the entire scaffolds were covered by mineralized matrix by day 21 (Fig. 2B).

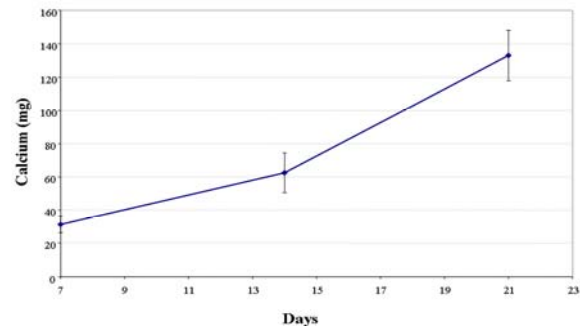


Fig. 1: Calcium production by osteoblasts seeded on PCL scaffolds

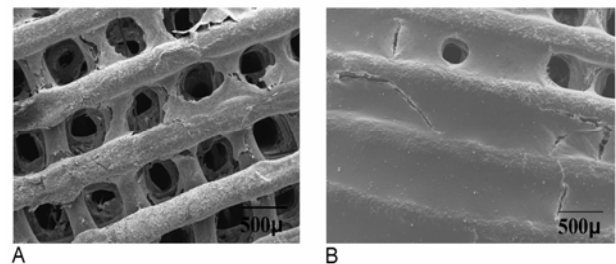


Fig. 2: SEM images showing mineralized matrix on PCL scaffolds on day 14 (A) and day 21 (B).

DISCUSSION & CONCLUSIONS: The ability to fabricate PCL scaffolds using the PED system was demonstrated. Results of the characterization demonstrated the accuracy of PED fabrication on the control of microstructure and pore size. A cell-scaffold interaction study demonstrated the biocompatibility of the process and material. No adverse cytotoxic effects were observed with these scaffolds. With this technique, scaffolds with complex internal geometries can be studied with the ultimate goal of generating structures optimized for bone tissue ingrowth.

REFERENCES: ¹ M Sachlos, JT Czernuszka (2003) *Eur Cell Mater.*;5:29-39, ² W Sun, B Starly, et al, (2004) *JBiotechnol Appl Chem* 39:49-58.

ACKNOWLEDGEMENTS: Support from NSF grant NSF-0427216 .

Anodized titania nanopillars for control of cell development on Ti surfaces

T Sjöström¹, J Mansell¹ & B Su¹

¹ Department of Oral and Dental Science, University of Bristol, Bristol UK.

INTRODUCTION: Modification of Ti surfaces has long been used to improve bone bonding to implant surfaces. Recently surface nanotopography has been shown to influence *in vitro* cell response. Little is however known about the exact mechanisms behind nanotopography influence on cell behaviour. In order to gain a better understanding of nanotopography-cell interactions it is desirable to work with well defined and tuneable nanotopography features on clinically relevant materials.

We have previously shown that a through-mask anodization technique can be used to pattern bulk Ti surfaces with nanodot and pillar structures with tuneable dimensions [1]. In this work we examined the initial adhesion of MG63 osteoblast-like cells to Ti surfaces with titania nanopillar structures of varying heights in the sub-100 nm range.

METHODS: Ti surfaces were mechanically polished to a mirror surface where after a thin Al film was deposited on the Ti. The samples were anodized in a 0.3 M oxalic acid electrolyte to create a porous alumina mask on top of the Ti which was subsequently used for through-mask anodization of the Ti. Different anodization voltages were used to create titania nanopillars with 15, 55 and 100 nm heights. To reveal the anodic titania structures the alumina mask was removed in a H₃PO₄/CrO₃ selective chemical etch solution.

MG63 cells were cultured on the anodized Ti for 2 and 24 h and then fixed with Glutaraldehyde. Polished Ti surfaces were used as control. The morphology of the cells was analyzed using SEM and cross-sections of the cell/surface interface were achieved using FIB milling.

RESULTS: The cells adhered well and conformed to the 15 nm high structures. On the higher structures cell spreading was reduced after 24 h incubation and the cells appeared heavily elongated on the 100 nm high structures. Cross-section imaging of the cell/substrate interfaces revealed that the higher pillar structures left voids in between the cell and the Ti substrate while the cells appeared to conform closely to the 15 nm structures. The SEM images further revealed that the pillar features appeared to be imprinted in the cell membranes both on the 55 and 100 nm

surfaces.

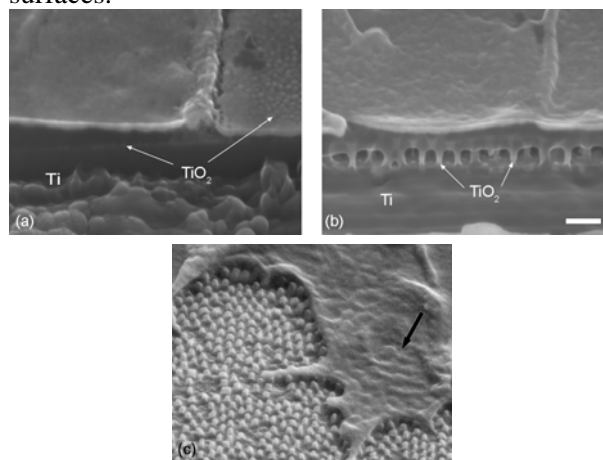


Fig. 1: Cross-sections of cells on a) 15 nm and b) 100 nm high titania structures. c) 100 nm high pillars imprinted in the cell membrane.

DISCUSSION & CONCLUSIONS: The initial adhesion of cells to a substrate is of high importance for later cell development. The results in this study showed that titania nanopillar structures can be used to control the cell response on Ti surfaces, with 15 nm high structures improving the cell-surface response. The results agree with our previous studies using hMSCs on the same nanopatterned Ti substrates where spreading, adhesion and matrix deposition was reduced with increasing topography feature height [2]. The fact that the higher topography features appeared imprinted in the cell membranes may explain the different cell response to the different surfaces. It has been suggested that imprinting of topography into the cell membrane may disrupt the cytoskeletal development and thereby impair cell signalling and later cell development events [3].

REFERENCES: ¹T. Sjöström, N. Fox and B. Su (2009) *Nanotechnology* **20**:135305. ²T. Sjöström, M. Dalby, A. Hart, et al (2009) *Acta Biomater* In Press doi:10.1016/j.actbio.2009.01.007. ³A. Curtis, M. Dalby and N. Gadegaard (2006) *J R Soc Interface* **3**:393-398.

ACKNOWLEDGEMENTS: The authors would like to thank Neil Fox for the Al film deposition and Georgi Lalev for the FIB milling.

Nuclear Localisation of Magnetic Nanoparticles Using HIV-1 tat and Magnetic Fields

C Smith¹, M Mullin² & CC Berry¹

¹Centre for Cell Engineering, FBLs, University of Glasgow, UK

²Integrated Microscope Facility, Division of Infection & Immunity, FBLs, University of Glasgow, UK

INTRODUCTION: Magnetic nanoparticles (mNPs) can be functionalised with specific ligands for various clinical applications including MRI, drug and gene delivery (magnetofection). Due to their nm small size, they can penetrate most tissues, however historically a major problem has been achieving sufficient cell and nuclear uptake due to the impermeable nature of both the plasma and nuclear membranes. Current methods to overcome this to date all have their specific limitations. One of the more promising approaches is conjugating NPs to cell penetrating peptides that can cross the plasma membrane due to the presence of a protein transduction domain (PTD). In this study fibroblasts were challenged in culture with mNPs coated with a thin layer of gold and functionalised with the HIV1-tat peptide PTD, in the presence and absence of an 8mT magnetic field (mNPs size ~7 nm).

METHODS: Fibroblasts were seeded on 13mm glass coverslips at a density of 1×10^4 cells per disk in 1ml of complete medium. Cells were incubated at 37°C with a 5% CO₂ atmosphere for 24 h (for immunofluorescence and SEM), or 5 days (for TEM). At this point cells were incubated in complete medium containing 20µg/ml mNPs for 30min, with/without a magnetic field.

Immunostaining After incubations the cells were fixed in 4% formaldehyde/PBS with 1% sucrose at 37°C for 15min. The samples were then stained with with phalloidin (actin) and antibodies against tubulin, clathrin and caveolin respectively before viewing by fluorescent microscopy.

SEM Samples were fixed with 1.5% glutaraldehyde buffered in sodium cacodylate for 1h at 4°C, then prepared for SEM analysis prior to examination with a Hitachi S800 field emission SEM at an accelerating voltage of 10keV.

TEM Samples were fixed as for SEM then prepared for TEM analysis prior to examination with a Zeiss 902 electron microscope at 80kV.

Microarrays RNA was collected, amplified and hybridised, with gene changes detected using a 32,000 gene transcript affymetrix microarray.

RESULTS: The TEM images clearly show that there is nanoparticle uptake into both the cell and the nucleus both \pm the magnetic field (fig 1).

Uptake appears to be *via* a variety of endocytic pathways (clathrin and caveolin-mediated).

Cells indicated differing levels of uptake in the presence and absence of a magnetic field, with microarray analysis clearly highlighting different gene sets being activated in each case.

Finally, cells were also observed in the early stages of aligning with the magnetic field when examined using fluorescence microscopy and SEM, which is rarely reported with such short exposures.

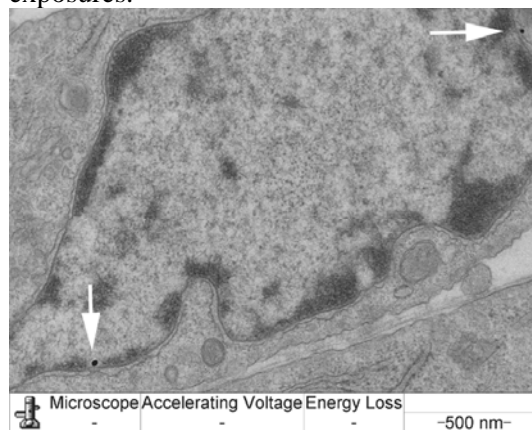


Figure 1. TEM indicating tat functionalised mNPs localised in the nucleus. Cells challenged with mNPs for 30 mins under a 8mT field.

DISCUSSION & CONCLUSIONS: This study documents the synthesis of ~7 nm mNPs functionalised with a cell penetrating peptide. Results showed clear cell and nuclear uptake, both with and without a magnetic field. Such mNPs would benefit all current mNP applications, by enhancing cell and nuclear uptake.

The gene changes and cell alignment observed under the magnetic field indicate that the cells are clearly influenced by the 8mT field for 30 minutes, something which should be borne in mind when routinely using fields in delivery and magnetofection techniques.

REFERENCES: Kamei, K., Y. Mukai, et al. (2009). *Biomaterials* **30**(9): 1809-14.
de la Fuente, J. M. and C. C. Berry (2005). *Bioconjug Chem* **16**(5): 1176-80.

ACKNOWLEDGEMENTS: Dr L. Tetley, Integrated Microscope Facility, & Sir Henry Wellcome Functional Genomics Facility (SHWFGF), University of Glasgow

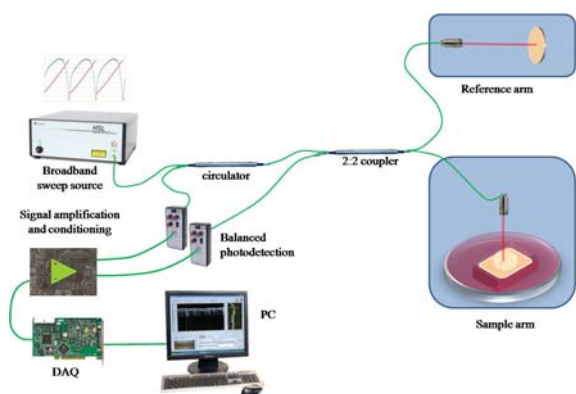
Exploring the use of optical coherence tomography in the non-invasive imaging of tissue engineered skin.

L.E. Smith¹, M. Bonesi¹, R. Smallwood², S. Matcher¹ and S. MacNeil¹

¹ Department of Engineering Materials, Kroto Research Institute, University of Sheffield, North Campus, Broad Lane, Sheffield, S3 7HQ, UK. ² Department of Computer Science, University of Sheffield, Regent Court, 211 Portobello, Sheffield S1 4DP, UK.

INTRODUCTION: The demand to non-invasively monitor the development of tissue engineered constructs is growing. Current imaging techniques are generally invasive and/or destructive, making the measurement unrepeatable. Lab monitoring techniques include histology, which remains the gold standard, light microscopy, fluorescent or confocal laser scanning microscopy. These techniques involve sacrificing the sample or part of the sample (for histology, immunohistology or SEM) and usually involve the staining of cells and/or extracellular matrix. To monitor evolution in time of engineered constructs, a non-destructive, non-invasive imaging technique is desirable. Here we report on the use of Optical Coherence Tomography (OCT), an optical interferometric imaging technique, for the non-invasive imaging of tissue engineered skin.

METHODS: Tissue engineered skin was produced as previously reported [1]. Briefly de-epithelialised acellular dermis (DED) was seeded with human dermal fibroblasts or a co-culture of human dermal fibroblasts and human keratinocytes. All composites were cultured in Green's medium. Imaging was performed with the skin, at air-liquid interface (ALI) sealed inside a 6-well plate using a Swept-Source OCT (SS-OCT) system. A diagram of the SS-OCT imaging setup is shown in Figure 1. It makes use of a 1300 nm central wavelength swept

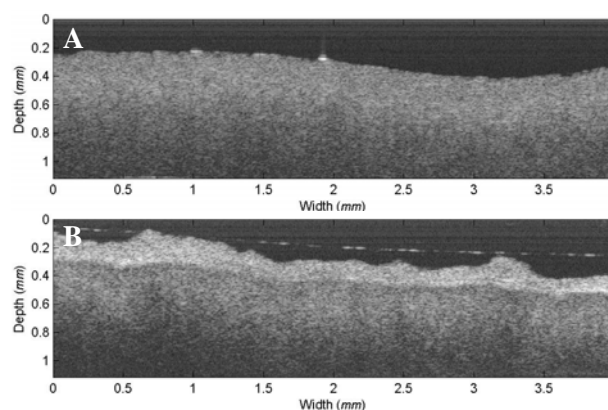


laser source, which offered a depth imaging resolution of about 5 μm .

Fig. 1: Schematic diagram of the SS-OCT imaging setup.

RESULTS: We were successfully able to differentiate between acellular DED, DED with

fibroblasts and DED with fibroblasts and keratinocytes. Also we could regularly monitor the development of the neoepidermis over a period of 3 weeks from being raised to the air-liquid interface. Examples of this are illustrated in Figure 2, showing the monitored engineered tissue at day 1 and day 22, by which time the development of a second, more scattering layer on the top of the DED



can be seen. This was confirmed to be epidermis using conventional histology.

Fig. 2: SS-OCT images of the reconstructed skin composite at A) ALI day 1 and B) ALI day 22.

DISCUSSION & CONCLUSIONS: OCT is being used increasingly to non-invasively image tissue engineered constructs such as tissue engineered tendons [2] and the development of human skin equivalents formed from amorphous collagen gels [3 and 4]. The latter two studies were able to successfully differentiate between the epidermal and dermal regions with OCT. However to the best of our knowledge this is the first time OCT has been used to image tissue engineered skin based on natural human dermis.

In conclusion we would suggest that OCT shows great promise for the non-invasive imaging of optically turbid tissue engineered constructs, including tissue engineered skin and reveals itself as a valid support for tissue engineering developing techniques.

REFERENCES: ¹Harrison, C.A. *et al.*, (2006) *Tissue Eng.* **12**(11) 3119-3133. ²Bagnaninchi, P.O. *et al.*, *Tissue Eng.* (2007) **13**(2)323-331. ³Spöler, F. *et al.*,(2006) *Skin Res. Tech.* **12**(4) 261-267. ⁴Yeh, A.T. *et al.*, (2004) *J. Biomed Optics* **9**(2) 248-253.

ACKNOWLEDGEMENTS: The authors would like to thank the BBSRC for funding and Dr Nikola Krstajić for many useful discussions.

Impact of Varying Intensities of Blue-Light Exposure on 3T3 cells

S. Smith¹, M Maclean², SJ MacGregor², JG Anderson² & MH Grant¹

¹ Bioengineering Unit and ² Robertson Trust Laboratory for Electronic Sterilisation Technologies, University Of Strathclyde, Glasgow, UK

INTRODUCTION: There is the need to develop a compatible sterilisation method for hybrid biomaterials. High-intensity blue light in the 405 nm region has been shown to be an effective bacterial decontamination method [1], to cause no noticeable damage to the gross structure of type-I collagen monomer (when treated at 10 mW/cm²) [2], and to have no noticeable effect on 3T3 cell viability, growth rate, redox state or lactate dehydrogenase (LDH) leakage (at 1.0 mW/cm²) [2]. The purpose of this research was to investigate the effect of varying the blue-light intensity on the 3T3 cell response parameters.

METHODS: 3T3 cells, at a seeding density of 2 x10⁴ cells/cm², were exposed to the blue-light source at intensities of 10, 1 and 0.1 mW/cm², for 1 hour. Cell responses were measured for up to 4 days post treatment using the MTT and neutral red (NR) microplate assays, LDH leakage and the intracellular levels of reduced glutathione (GSH) and protein.

RESULTS AND DISCUSSION: At treatment intensities of 0.1 and 1 mW/cm² there was no significant negative effect on any of the response parameters. For example, MTT was 150 ±4% of control cells, NR was 102 ±1%, LDH leakage 70 ±4% and GSH 112 ±8% 1 day after treatment with blue-light at 0.1 mW/cm². Figure 1 shows that, in contrast, treatment with 10 mW/cm² had a negative effect on cell responses 1 day after treatment.

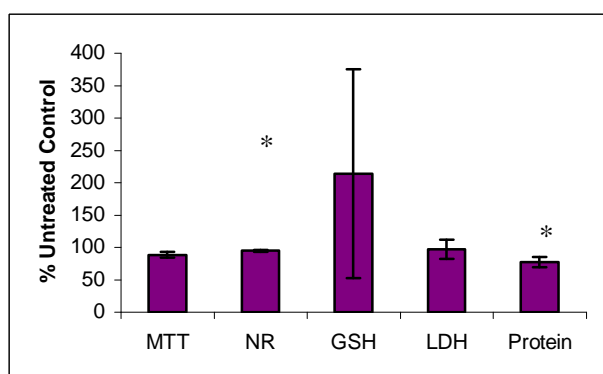


Fig. 1: Effect of blue-light treatment at 10 mW/cm² on 3T3 cell response parameters at 1 day post-treatment. Statistical analysis was carried out using ANOVA followed by Dunnett's test, at the 95% level.

A small drop in viability after 1 day was observed but was found only to be significant using the NR assay. Treatment at 10 mW/cm² had no significant effect on LDH leakage, therefore it does not appear to compromise cell membrane integrity. The most notable effect of blue-light treatment at 1 day was on intracellular levels of GSH, where an increase was observed (0.030 ±0.022 GSH/mg protein compared to 0.014 ±0.004 GSH/mg protein for the untreated control). It is known that blue-light causes excitation of endogenous porphyrins, generating light-induced reactive oxygen species (ROS). The increased GSH levels observed suggest that the blue-light at 10 mW/cm² results in the production of ROS and induces a state of oxidative stress within the cells. This effect was reversible, and by 2 days post treatment the GSH levels were comparable to those of the untreated control (0.038 ±4 and 0.044 ±4 GSH/mg protein, respectively), providing evidence of recovery. The cell growth rate also showed evidence of recovery post-treatment with all control and treated cultures reaching confluence at day 3.

CONCLUSION: Blue light treatment at intensities of 1 mW/cm² and lower has no significant affect on 3T3 cell response parameters. This finding together with the lack of effect on type I collagen suggests that blue light shows excellent potential to be utilised as a sterilisation method for hybrid biomaterials.

REFERENCES: ¹ M. Maclean, S MacGregor, J Anderson et al (2008) *FEMS Micro Let* **285**(2): 227-232. ² S. Smith, M. Maclean, S. MacGregor et al. (2009) *IFMBE Proceedings* **23**: 1352-1355.

ACKNOWLEDGEMENTS: SS is funded by EPSRC Doctoral Training Centre (DTC) in Medical Devices.

*Creating viable muscle-motor neurone synaptic interactions in an *in vitro* 3D collagen co-culture gel model.

AST Smith¹, A Patel¹, B Kalmar², L Greensmith², V Mudera³ and MP Lewis¹

¹ Department of Biomaterials and Tissue Engineering UCL Eastman Dental Institute.

² Department of Motor Neuroscience and Movement Disorders UCL Institute of Neurology.

³ Division of Surgical and Interventional Sciences UCL Institute of Orthopaedics and Musculoskeletal Sciences.

INTRODUCTION: The ability to generate biomimetic 3D skeletal muscle tissues *in vitro* would have important implications for both cell biology and medicine. To that end, a significant body of work has recently been published detailing the efforts of various groups to synthesise such a model. These protocols involve the seeding of muscle derived cells (MDCs) within a biomimetic scaffold of extra cellular matrix proteins and rely on the ability of MDCs to self-orientate between two fixed points. The contractile ability of our collagen based 3D model, constructed in such a way, is well established¹ and our goal now is towards making the model more biomimetic. Since denervated muscle quickly undergoes atrophy, it is likely that the introduction of a neural input will significantly improve the maturation of MDCs within our culture system, as well as establish a complex 3D co-culture model that better mimics *in vivo* conditions that exist within innervated muscle. Furthermore, the possibility of neuromuscular junctions (NMJs) formation *in vitro* opens the door to future research testing the effects of neuromuscular agents in culture, which may help to minimize the need for *in vivo* testing of such agents. Here we present our data characterising the development and maturation of this 3D co-culture system, compare results with both 2D and *in vivo* controls and discuss the implications for the future of skeletal muscle tissue culture techniques.

METHODS: MDCs isolated from P1 neonatal rat pups were seeded, at a density of 10^6 cells per ml, in neutralised type-1 rat tail collagen and plated, in 3 ml quantities, into standard dimension chamber slides (TTP Lab Tech). The slides each held a custom built (by engineers at the Eastman Dental Institute) floatation bar (termed “A-frame”) at either end. Once the collagen gelled, it was cut away from the sides of the chamber and suspended in growth medium (20% fetal calf serum in low glucose DMEM). This provided only two focal attachment points for the gel so that, as the cells attached and contracted lines of isometric tension developed along the long axis of the gel. This tension provided sufficient mechanical stimulus to promote the alignment and fusion of the MDCs.

The result was a 3D tissue possessing uniaxially aligned and fully differentiated myotubes capable of directed contraction. These models were cultured for 7 days before plating primary rat motor neurones, derived from E14 embryos, on top at a density of 4×10^5 cells per gel. The gels were then cultured a further 7 days before being either stained for myogenic and neuromuscular junction markers or prepared for qPCR analysis.

RESULTS: Preliminary data demonstrated (i) the alignment of viable cells over the *in vitro* culture period (Fig. 1) and (ii) the ability of primary motor neurones to remain viable in this *in vitro* system when co-cultured with MDCs.

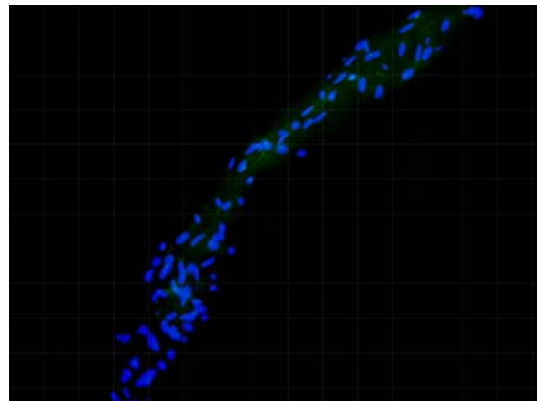


Figure 1: x20 image of cells within a 30 μ m slice of an *in vitro* collagen matrix. Gels were stained for Desmin expression (green) and Nuclei (Blue).

DISCUSSION & CONCLUSIONS: We have demonstrated for the first time the ability to co-culture primary motor neurones with mature myotubes in a 3D biomimetic culture system. We observed a significant improvement in muscle maturation in these 3D cultures compared to that previously reported for muscle cells *in vitro*. Although we have yet to establish the presence of functional NMJs, our results show that motor neurons are able to survive within the collagen 3D cultures.

REFERENCES: ¹ M. Brady, M.P. Lewis, and V. Mudera (2008) *J Tissue Eng Regen Med* 2:408-417.

ACKNOWLEDGEMENTS: AST Smith is in receipt of an MRC studentship.

Phosphatase Induced Stiffness Control in a Self-Assembled Peptide Hydrogel

K. Thornton^{1,2}, A. Smith,^{1,2} C. L. R. Merry¹ & R. V. Ulijn^{*3}

¹ Material Science Centre, University of Manchester, Grosvenor Street, Manchester, M1 7HS

² Manchester Interdisciplinary Biocentre, University of Manchester, 131 Princess Street, Manchester, M1 7DN

³ WestCHEM, University of Strathclyde, Cathedral Street, Glasgow, G1 1XL

* Corresponding authors

INTRODUCTION: A recent study detailed that the mechanical properties of materials have a direct effect on the differentiation pathways chosen by mesenchymal stem cells [1]. The ability to predetermine and efficiently control mechanical properties would therefore be beneficial for the 3D culture of stem cells. This can be particularly difficult in hydrogel systems and is dependant on the initiator of self assembly. Enzyme-initiated self assembly operates under constant conditions and has greater control over the reaction kinetics in comparison to those methods where self-assembly is initiated by a change of environmental conditions.

Yang et al (2007) recently demonstrated a relationship between enzyme concentration and the mechanical properties of hydrogels [2]. Here we report on the use of alkaline phosphatase to produce hydrogels from Fmoc-tyrosine(phosphate)-OH of varying mechanical properties.

METHODS: Fmoc-tyrosine(phosphate)-OH was dissolved in an alkaline phosphate buffer and the pH adjusted to neutral by the addition of concentrated hydrochloric acid or sodium hydroxide. Alkaline phosphatase was required to initiate the self assembly process, Figure 1. The hydrogels produced were characterised by HPLC, TEM, Cryo-ESEM, rheology, CD and fluorescence spectroscopy.

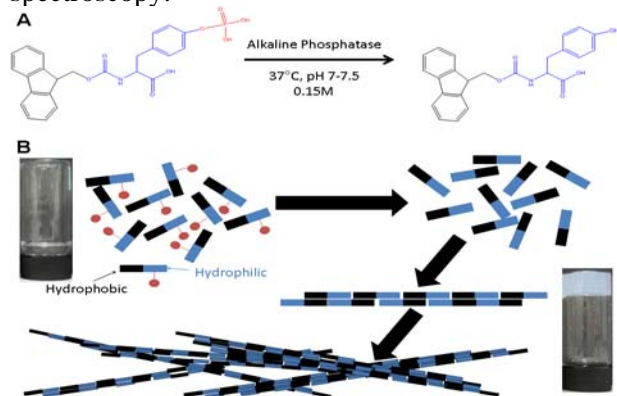


Figure 1. The reaction schematic and proposed method of self assembly.

RESULTS: The hydrogels formed on addition of alkaline phosphatase exhibited a dependence on the enzyme concentration for their gelation time and mechanical properties, Table 1. The fibre size, determined by TEM, was found to be independent of the enzyme concentration. The molecular order within the fibre structures was also found to be dependant on the concentration of enzyme.

Table 1. The effect of enzyme concentration on gelation times, fibre size and mechanical properties. Enzyme units 1 U hydrolyses 1 μ mole 4-nitrophenyl phosphate per minute at 37 °C and pH 9.8)

Enzyme concentration (U per μ l)	Gelation time (mins)	Fibre size (nm)	G' (kPa)
10	60-120	31.0 \pm 13.3	34 \pm 13
3	60-120	24.9 \pm 8.2	16 \pm 7
1	120-240	33.0 \pm 11.0	9 \pm 8
0.1	>1440	34.3 \pm 10.3	12 \pm 6

DISCUSSION & CONCLUSIONS: We have shown that we can produce hydrogels with varying mechanical properties from the same substrate by varying the enzyme concentration used. The enzyme concentration also effected the gelation and molecular order but had no effect on the fibre size. The suitability of these hydrogels for three dimensional cell culture will be investigated using embryonic stem cells to monitor the effect on cell fate decision.

REFERENCES:

- Engler, A.J., et al., *Matrix elasticity directs stem cell lineage specification*. Cell, 2006. 126(4): p. 677-689.
- Yang, Z.M., et al., *In vitro and in vivo enzymatic formation of supramolecular hydrogels based on self-assembled nanofibers of a beta-amino acid derivative*. Small, 2007. 3(4): p. 558-562.

Attachment and Proliferation of Tenocytes /Macrophages on Silks with Different Treatments

Xiao Wang, Yiwei Qiu, Andrew J. Carr, Zhidao Xia*

Botnar Research Centre, Nuffield Department of Orthopaedic Surgery, University of Oxford, Nuffield Orthopaedic Centre, Oxford OX3 7LD, U.K.

INTRODUCTION: It is reported that more than 330 000 tendon repair procedures annually in the US.[1] Currently, four major methods[2], which are surgical techniques using sutures, biological grafts, permanent artificial prostheses and tendon tissue engineering are used to repair tendon lesions. However, the outcomes of the former three methods still possess inferior functionalities compared with those of uninjured tendons. Tendon tissue engineering aims to repair the lesions by integrating engineered substitutes with their native counterparts *in vivo*, thereby restoring the defective functions. For such a purpose, appropriate materials are crucial. Due to superior biologic and mechanic properties, silk has been a promising candidate for tendon engineering. Therefore, the aim of this study is to screen suitable silk materials and degumming methods and to test attachment and proliferation of tenocytes and macrophages on these materials.

METHODS: Silks from different species (A: Bombyx; B: Pernyi; C: Gonomete) were degummed by different treatments (A0, B0, C0: No Treatments; A1, B1: Treatment 1 (4h); B2: Treatment 2; B3: Treatment 1 (16h); C1: Treatment 3 (4h); C2: Treatment 1 (4h) + Treatment 3 (4h)). After degumming the silk fibroins were then cut into 0.4 cm segments and put into centrifuge tubes. Macrophages and tenocytes were cultured in α MEM, supplemented with 10% FBS and harvested when getting 75% confluence. Macrophages and tenocytes were seeded separately on silks in centrifuge tubes with seeding densities of 2×10^6 and 5×10^4 respectively and rolled on a rock-and-roll device at 37°C for 2 hours. The silks with cells attached were then moved from centrifuge tubes to 48 well plates and fed with α MEM, 10% FBS. Cell numbers on silks and left in centrifuge tubes were estimated by Alarma Blue assay on Day 1 and 7.

RESULTS: The results showed that tenocyte proliferation on degummed silks were significantly higher than that on undegummed silks. Degummed

silks also showed lower attachment of macrophages.

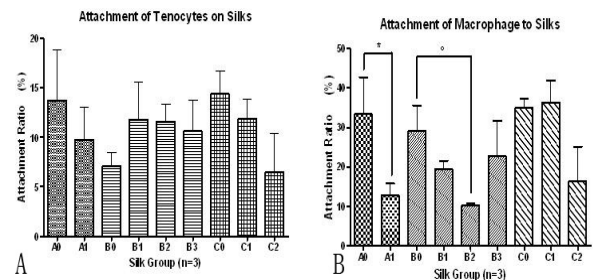


Fig. 1: Attachment Ratio of tenocytes and macrophages on silks on day 1 by Alamar Blue. (A) No statistical significances observed in tenocyte group, (B) A1 was significantly lower than its control A0. B2 was statistically lower than B0, their respective control in macrophage group.

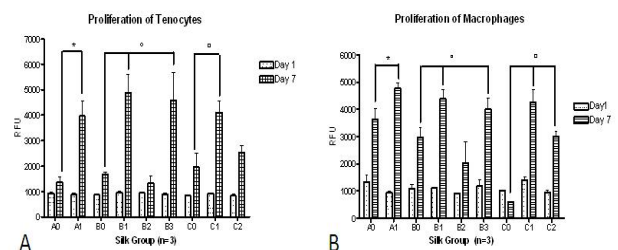


Fig. 2: Proliferation of tenocyte and macrophages on silks from day 1 to day 7. (A) In tenocyte group, A1, B1, B3, C1 were significantly higher than their respective control. (B) In macrophage group, A1, B1, B3, C1 were also significantly higher than their respective control.

CONCLUSIONS: The degummed silks showed superior proliferation in tenocyte group and moderate attachment in macrophage group *in vitro*. However, further *in vivo* tests are needed to test the effects of degumming methods on host tissue inflammatory and immune responses.

REFERENCES:

1. Langer, R. and J.P. Vacanti, *Tissue engineering*. Science, 1993. **260**(5110): p. 920-6.
2. Liu, Y., H.S. Ramanath, and D.A. Wang, *Tendon tissue engineering using scaffold enhancing strategies*. Trends Biotechnol, 2008. **26**(4): p. 201-9.

DEVELOPMENT OF A CELL POPULATION MIGRATION ASSAY

A. Whitton,¹ R. A. Black¹ & D. J. Flint²¹Bioengineering Unit, University of Strathclyde, Glasgow, UK²Strathclyde Institute of Pharmacy and Biomedical Sciences, University of Strathclyde, Glasgow, UK

INTRODUCTION: Cellular migration is central to many physiological and pathological processes, from wound healing and the immune response to cancer cell invasion. Many *in-vitro* assays have been developed to study these processes and can be classified by the nature of the assay, for example migration of single cells or entire populations, as well as migration on a planar surface or through a 3D structure.

This work concerns the development of an assay to study the migration of whole populations of cells across a deformable planar substratum, which may be coated in adsorbed adhesion molecules. The technique detailed below was developed from the Teflon fence assay.¹

METHODS: QSil216 silicone elastomer (ACC Silicones Ltd, UK) was cast into a mould to yield optically clear membranes, each containing a 0.5cm² square hole. The deformable substrates were made of polyurethane (PU) (grades Z1A1 and Z3A1, Biomer Technology Ltd., Runcorn, Cheshire, UK), cast from solution (10% in DMF), from which discs with a diameter of 15mm were punched. The latter were secured in the bases of 24-well tissue culture plates (Sigma). Solutions of adhesion molecules, such as fibronectin, were applied to the discs as required for the adsorption of the protein to the PU surface and then subsequently washed. Square wells were created by placing the silicone membrane onto the PU discs. Into these square wells 150µl suspensions of human aortic smooth muscle cells, at a concentration of 5x10⁵ ml⁻¹ in medium 231 supplemented with SMGS (Invitrogen, UK), were placed. Within 24-48 hours the cells had attached to the PU surface and migrated and proliferated to completely cover the base of the square wells. Upon removal of the silicone membrane the cells started to migrate and populate the cell-free area. Phase-contrast images of each well were captured at regular intervals using an AxioImager Z1 microscope (Zeiss) to record the motion of the cells as they migrated into the unpopulated regions. The “Mark and Find” function of the microscope software was used to track cell motion at specific locations in each sample whereas the image analysis software ImageJ (NIH, USA) was used to determine average rates of migration. The latter were determined by measuring the mean

displacement of all cells at each time point relative to the initial boundary.

RESULTS: The Figure below shows a sequence of graphically-enhanced phase-contrast images of a representative sample area of cells migrating into the adjacent cell-free area over a period of 72 hours in culture. The rate of migration over this time period was relatively constant and the leading edge of cells uniform along the perimeter of the initial cell confinement area.

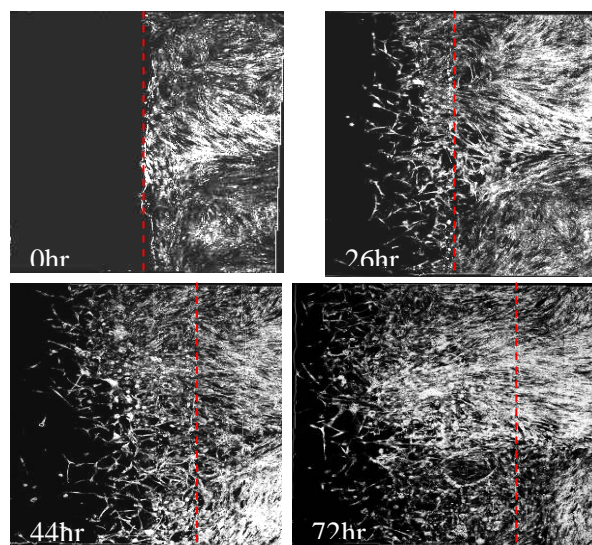


Figure 1: Representative phase-contrast images of the migration of cell population after the removal of the constraint at t=0 hours.

DISCUSSION & CONCLUSIONS: The assay developed here builds on the original Teflon fence assay for the purpose of providing a robust and reproducible method of measuring cell population migration rates on compliant substrates coated in adsorbed proteins. The circular fence of the original assay was replaced by a square one to aid in the processing of data while the Teflon construction material was replaced with a silicone elastomer. This allowed for a better contact with the PU, preventing cells “escaping” under the barrier before the start of the experiment in more samples. The optical clarity of the silicone allowed the determination of such a breach of the barrier and the sample to be discarded.

REFERENCES: ¹ Pratt, B. M. et al. *A. Am. J. Pathol.* 1984, 117 (3), 349-354.

Study of the surface properties of electrospun nanomats

I. Wimpenny¹, N. Ashammakhi^{1,2}, Y. Yang¹

¹Institute of Science and Technology in Medicine, Keele University, UK.

²Institute of Biomaterials, Tampere University of Technology, Tampere, Finland

INTRODUCTION: Nanofibrous materials are common components of native extracellular matrix (ECM). It is possible to manufacture ECM-like structures from biodegradable materials using electrospinning. Electrospun nanofibers have been shown to be suitable as tissue engineering scaffolds for a variety of cell types¹. The aim of this study is to investigate the physical properties of electrospun nanofibres, in particular the wettability of the nanofibres. This can then enhance our understanding how and why cells have a preference for different nanofibrous surfaces in the field of tissue engineering.

METHODS:

Electrospinning:

Poly L,D lactic acid (PLDLA); 96%L, 4%D (96/4), and poly lactic-glycolic acid (PLGA) 80% lactide (96/4), 20% glycolide were dissolved in a mixture of chloroform and dimethylformamide (Sigma, UK) at a ratio of 7:3. The solutions were then electrospun to coverslips at 15cm, 6kV, 0.025ml/min. PLDLA and PLGA polymers were also dissolved in chloroform and cast to form films. The test groups are expressed in Table 1.

Blank Coverslip	PLDLA		PLGA	
	Film	Nanofiber	Film	Nanofiber
N=9	N=9	N=9	N=9	N=9

Table 1. Experimental setup for electrospun polymers

Contact angle analysis:

10µl of ultra pure H₂O was applied to coverslips using a Hamilton syringe, at 22°C, 35% humidity. An image of the resulting droplet was taken after 20 seconds using a CCD camera (XC-ST50CE, Sony, Japan). The images were then assessed using the 'drop_snake' Image J plug-in, courtesy of Stalder *et al.* (2006)².

RESULTS:

Water contact angles on PLDLA films were comparable to control coverslips, however, PLDLA nanofibers appeared to be considerably more hydrophobic (Figure 1).

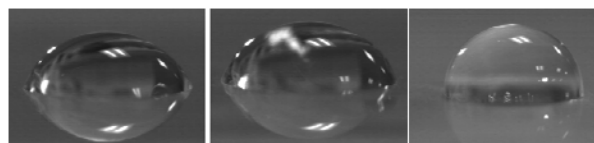


Figure 1. Comparison of contact angle of a 10µl droplet of H₂O on a different surfaces; from left to right, blank coverslip, PLDLA film, PLDLA nanofiber coated coverslip, imaged 20 seconds after droplet deposition.

Contact angles on PLGA films were again comparable to that of the glass coverslip. Electrospun PLGA fibers were marginally less hydrophobic than PLDLA fibers. A comparison of contact angles on all surfaces is demonstrated in figure 2. It was important to note that the droplets on coverslips appeared to spread more rapidly than on cast films or nanofibers.

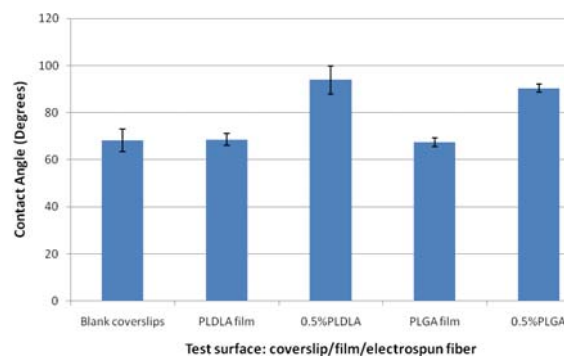


Figure 2. Contact angles of droplet on the different test surfaces after 20 seconds.

DISCUSSION & CONCLUSIONS: The use of nanofibres may influence the surface properties of materials, affecting behaviour of fluid contact. This was attributed to the dramatic increase in surface area of nanofibrous materials. PLGA nanofibres are more hydrophilic than PLDLA nanofibres and are therefore likely to be a preferable surface for cell attachment and subsequent tissue engineering applications.

REFERENCES:

- Ashammakhi N, Ndreu A, Nikkola L, Wimpenny I, Yang Y. Advancing tissue engineering by using electrospun nanofibers. *Regenerative Medicine* 2008;3(4):547-574.
- Stalder AF, Kulik G, Sage D, Barbieri L, Hoffmann P. A snake-based approach to accurate determination of both contact points and contact angles. *Colloids and Surfaces A: Physicochemical and Engineering Aspects* 2006;286(1-3):92-103.

ACKNOWLEDGEMENTS: Funding by BBSRC CASE Studentship award.

Regenerative Capacity of Cultured Neurons Following Photodynamic Therapy in a 3D Collagen Gel Culture System

[K E Wright](#) and [J B Phillips](#)

Life Sciences Department, The Open University, Milton Keynes, U.K.

INTRODUCTION: Photodynamic therapy (PDT) is a promising treatment modality for cancer which involves administration of a photosensitising agent that can be activated subsequently within a patient's cells, resulting in cell death from oxidative damage. Peripheral nerve sparing has been reported following PDT with the photosensitiser *meta*-(tetra-hydroxyphenyl) chlorin (mTHPC) [1 & 2]. Dorsal root ganglia (DRG) neurons have been shown to be relatively insensitive to mTHPC-PDT doses that killed other cell types in a 3D collagen culture system [3]. The aim here was to determine the extent to which 'surviving' neurons were able to sprout neurites as an indication of functional recovery following PDT.

METHODS: Mixed cultures of dissociated neurons and satellite glia were prepared from the DRGs of 250-300 g rats and maintained within thin 3D collagen gels for 4 days. Cultures were exposed to 4 and 10 $\mu\text{g/ml}$ mTHPC for 4 h, then illuminated at a fluence rate of 1.6 mW/cm^2 for 10 min, giving a total light dose of 1 J/cm^2 [3]. After a latency period of 24 h, during which time a substantial number of satellite glia died, surviving neurons were extracted by digesting gels with 0.125 % collagenase for 30 min. PDT treated cells were collected and combined with untreated satellite glia then further cultured in monolayer on 20 $\mu\text{g/ml}$ PLL-coated 19 mm diameter coverslips for 2 days. The ratio of β III-tubulin immunoreactive neurons with or without new neurite growth, and the lengths of neurites were assessed using fluorescence microscopy and digital image analysis.

RESULTS: Fig 1 shows the proportion of neuronal cell bodies that showed neurite growth. Neurons treated with 3 & 4 $\mu\text{g/ml}$ mTHPC-PDT showed no difference to untreated and light only controls in their ability to produce neurites. Fig 2 shows length of neurite outgrowth was not significantly different between control and light only and 3 & 4 $\mu\text{g/ml}$ mTHPC-PDT treated cells. Only 10 $\mu\text{g/ml}$ mTHPC-PDT treated cells showed significantly reduced neurite lengths in comparison to light only control (* $P < 0.05$; 1-way ANOVA with Dunnett's post test).

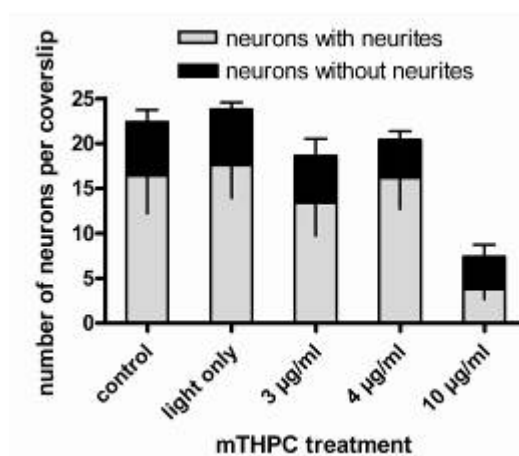


Fig. 1: Neurons showing neurite outgrowth

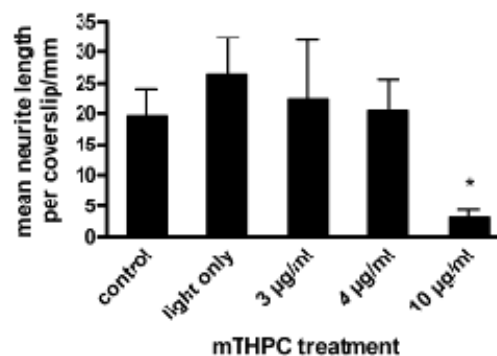


Fig 2: Length of neurite outgrowth

DISCUSSION & CONCLUSIONS: The ability of neurons treated with mTHPC-PDT to extend neurites in this model system acts as an indication that they remain functionally active in terms of regenerative capacity. This is an important finding since identifying PDT conditions that enable neurons to survive while tumor cells are destroyed may be of particular benefit for treating cancers within or adjacent to the nervous system.

REFERENCES: ¹C.M. Moore, T.R. Nathan, W.R. Lees et al. (2006) *Lasers Surg Med* 38(5):356-63. ²CS Betz, HR Jäger HR, et al. (2007) *Lasers Surg Med* 39(7):571-82. ³K.E. Wright, A J MacRobert, & J B Phillips (2008) *European Cells and Materials* Vol. 16. Suppl. 3:13.

ACKNOWLEDGEMENTS: With thanks to the BRU staff. Funded by the Open University.

Cryopreservation of Adherent Human Mesenchymal Stem Cells 2

Xia Xu, Yang Liu, Zhanfeng Cui

Institute of Biomedical Engineering, Department of Engineering Science, University of Oxford, Oxford, OX1 3PJ

Introduction: Since mesenchymal stem cells (MSCs) have a capacity of self-renew and ability of differentiation into different cell types, MSCs have become a potential cell source for regenerative medicine to treat degenerative disease or injured organs/tissues. During expansion of MSCs, it is crucial for cells to attach on a solid surface to maintain viability, growth and undifferentiated status. Hence, cryopreservation of adherent MSCs can reduce time between cell storage and use in the subsequent experiments. In this study, we investigated the freezing rate and coating materials on cell viability and recovery after cryopreservation.

Materials and Methods: Human MSCs (Cell line) were maintained using α MEM containing 10% Fetal Bovine Serum (FBS) and 1% pen/strep. The cells were plated on the coverslips, which were coated with gelatin or matrigel in advance, in the 24-well plates. 2 days later, the cells were cryopreserved using 10 % dimethylsulfoxide (DMSO) in culture medium at different freezing rates, 1, 5 and 10 °C/min using programmable freezer until -80°C. Cell viability was assayed using Calcein-AM and propidium iodide staining methods. Cytoskeleton labeled with rhodamine phalloidin, was monitored using a fluorescence microscope. Cell recovery was assessed after 1 day of subsequent culture after cryopreservation.

Results: The greatest cell viability was achieved after cryopreservation using freezing rate of 10 °C/min. In contrast, the lowest viability was obtained with freezing rate of 1 °C/min. The cells closed to the edge of coverslips had higher viability than the cells around the centre. Change in cytoskeleton was observed when the cells were adherent to the gelatin coated coverslips. However, it is interesting to observe a good recovery when the cells were cryopreserved on the gelatin-coated plates.

Conclusions: Cryopreservation of adherent MSCs is freezing-rater related. Cell viability and cell

recovery after cryopreservation is dependent on the properties of coated materials. Furthermore, cytoskeleton change during cryopreservation may play a role in cell recovery.

Acknowledgements: This research was supported by the Biotechnology & Bioengineering Science Research Council (BBSRC) of the UK (BB/D014751/1).

Cryopreservation of Adherent Human Mesenchymal Stem Cells

Xia Xu, Yang Liu, Zhanfeng Cui

Institute of Biomedical Engineering, Department of Engineering Science, University of Oxford, Oxford, OX1 3PJ

Introduction: Human embryonic stem (hES) cells have enormous potential for clinical applications. However, one of challenges is to achieve high cell recovery rate after cryopreservation. Understanding how the conventional cryopreservation protocol fails to protect the cells is a prerequisite for developing efficient and successful cryopreservation methods for hES cell line and banks.

Materials and Methods: HUES 2 cell line was used. Two culture methods were used: feeder-dependent and feeder-independent culture. hES cells were dissociated and cryopreserved using 10% dimethylsulfoxide (DMSO) at 1°C/min to -80°C. The cells were kept in LQ until use. The cells were thawed and then recovered in the absence of ROCK inhibitor or in the presence of ROCK inhibitor, or the combination of ROCK inhibitor and p53 inhibitor at the first day of culture. Cell viability and apoptosis was analyzed using Annexin V- Propidium Iodide (PI) staining method. Cell recovery rate was evaluated for regular passage, after DMSO exposure only, and after cryopreservation. We also measured activity of caspas-8, caspase-9 and level of intracellular reactive oxygen species (ROS). F-actin and p53 were assessed. hES cell colonies were immunocytochemically characterized.

Results: Around 80 % of cells were survival immediately after thawing, but around 30 % of cells were undergoing early apoptosis 2 h after thawing. Cell recovery rate after freezing was lower than after regular passage and after DMSO exposure only. The level of reactive oxygen species (ROS) is significantly increased after

freezing. Caspase-8 and caspase-9 were activated after cryopreservation. F-actin content and distribution was altered, also p53 was activated.

Conclusions: Activation of caspase-8 and caspase-9 indicates that apoptosis after cryopreservation is induced by the intrinsic and extrinsic pathway. We propose that ROS production, ROCK activation, change in F-actin and activation of p53 together work as a network and contribute to the induction of apoptosis in cryopreservation. However, what causes activation of the extrinsic pathway is still unclear and deserves further investigation.

Acknowledgements: This research was supported by the Biotechnology & Bioengineering Science Research Council (BBSRC) of the UK (BB/D014751/1), the Wellcome trust, and the John Fell OUP Research Fund. We thank to Maud Thio for maintenance of HUES-2 hES cell lines.

Generation Of Protein Micropattern By Piezoelectric PrintingA. Zarowna¹, E. Gu^{1*}, E.O. McKenna³, M.D. Dawson¹, A. Pitt³, J.M. Cooper², H.B. Yin^{2*}¹*Institute of Photonics, University of Strathclyde, Glasgow, UK*²*Bioelectronics Research Centre, University of Glasgow, Glasgow, UK*³*Faculty of Biomedical & Life Sciences, University of Glasgow, Glasgow, UK*

INTRODUCTION: It is well known that living cells can recognise and preferentially attach to the natural extracellular matrix (ECM) proteins, such as collagen or poly-L-lysine. Thus, the employment of these types of proteins to promote specific cell attachment in particular locations becomes an attractive approach to create a cell pattern. A cell pattern with arbitrary arrangement ranging from tens to hundreds of microns allows flexible manipulation of cell numbers, which is essential in many quantitative studies.

Several methods for the generation of high resolution protein patterns have been developed, such as photolithography and micro-contact printing [1,2]. However, often they involve multi-step processes and harsh conditions. Inkjet printing is a simple, high throughput alternative technique for the generation of small biomolecule (e.g. DNA, protein or aptamer) microarrays, which avoids exposure to denaturing factors. In this study we exploit inkjet printing to generate collagen and poly-L-lysine micropatterns of resolution down to tens of microns, with the aim of developing a robust, flexible and non invasive method for subsequent cell pattern formation and cell based toxicity analysis.

METHODS: A stock solution of collagen was prepared by dissolving dry collagen (calf skin, type I, Sigma) in 0.1M acetic acid. The pH was adjusted to a physiological level of 7.4 with NaOH solution. The stock solution was further diluted with phosphate buffered saline (PBS) to concentrations of interest. Poly-L-lysine solution from Sigma (0.01% (w/w) in DI water) was used directly for the printing.

Protein solutions were printed using either a Dimatix® ©FUJIFILM inkjet printer or PerkinElmer® Piezorray™ microarray spotter. Dimatix® allows precise deposition of 10 pl volume of a solution, whilst a PerkinElmer® system, is capable of using a minimum printing volume of 330 pl.

RESULTS & DISCUSSION: Using the Dimatix® system, uniform arrays of 30µm dots have been generated with 0.1 mg/ml collagen solution with added surfactants, 0.01% Tween 20 or 0.1% Tween 80. Surfactants reduce surface tension of the collagen solution, which was beyond the operation range for the Dimatix® system. Printing of poly-L-lysine solution, without the need of surfactants, resulted in 10 µm

dots. A further adjustment of protein density within each spot has been achieved through multilayer printing on the same dot (Figure 1). By adjusting the volume of the printed solution to 330 pl using the PerkinElmer® spotter system, a precise 100 µm collagen spot is formed.

Preliminary study of cell culture using 3T3 fibroblasts showed specific cell attachment on the collagen or poly-L-lysine patterns, giving rise to distinctive cellular patterns (Figure 2).

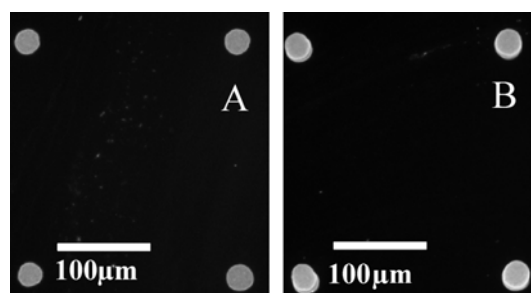


Fig. 1 Fluorescence image of collagen pattern formed by (A) one layer and (B) 5 layers printing.

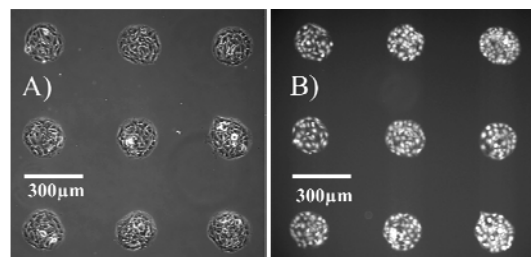


Fig. 2. 3T3 fibroblasts on collagen patterns after 24 hour of culture (A) phase contrast image (B) fluorescence image of calcein staining.

CONCLUSION: We present a simple and robust method to prepare highly uniform collagen / poly-L-lysine micropatterns of dimensions ranging from tens to hundreds of microns using commercial piezoelectric systems. The protein patterns have been shown to be suitable for generation of well-defined cellular patterns.

REFERENCES: ¹D.I. Rozkiewicz, Y. Kraan, M.W.T. Werten, et al (2006) *Chem.-Eur. J.* **12**:6290-6297. ²E.E. Hui, S.N. Bhatia (2007) *Langmuir* **23**:4103-4107.

ACKNOWLEDGEMENTS: This work has been supported by SFC, BBSRC and EPSRC through funding of the SCIMPS and RASOR projects. HY is supported by the Royal Society of Edinburgh.